1992

Structure elucidation of alkaloids from Philippine flowering plants

Maribel G. Nonato
University of Wollongong

STRUCTURE ELUCIDATION OF ALKALOIDS FROM PHILIPPINE FLOWERING PLANTS

A Thesis Submitted in Fulfillment of
the Requirements for the Award
of the Degree

of

DOCTOR OF PHILOSOPHY

from

The University of Wollongong

by

MARIBEL G. NONATO, M.Sc.

Department of Chemistry
January 1992

DECLARATION

This is to certify that the work described in this thesis has not been submitted for a higher degree at any other university or institution.

M. G. NONATO

To Papa and Eddie

This fulfillment is shared with you in life much more in death.

TABLE OF CONTENTS

Acknowledgements i

Abstract iii

List of Figures v

List of Schemes ix

List of Tables xi

List of Diagrams xiv

List of Structures xv

List of Abbreviations xx

CHAPTER 1: GENERAL INTRODUCTION

1.1 Introduction 1

1.1.1 Primary Role of Secondary Metabolites 2

1.2 Alkaloids in Plants 3

1.2.1 Screening of Alkaloids 5

1.3 Natural Product Chemistry in the Philippines 7

CHAPTER 2: ISOLATION AND STRUCTURE ELUCIDATION OF ALKALOIDS FROM *OPHIORRHIZA ACUMINATA*

2.1 Introduction 9

2.1.1 β-Carboline Alkaloids 10

2.1.2 Monoterpenoid-Derived Indole Alkaloid 14

2.1.3 Genus *Ophiorrhiza* 21

2.1.4 *Ophiorrhiza acuminata Linnaeus* (Rubiaceae) 27

2.2 Results and Discussion 28

2.2.1 Tertiary Alkaloid, Oa-3A (Harman) 28

2.2.2 Isolation and Structure Elucidation of Glucoindole Alkaloids 29

2.2.2.1 Structure Elucidation of Oa-4A-1 31

2.2.2.2 Structure Elucidation of Oa-4A-2 50

2.2.3 Isolation of the Glucoindole Alkaloids as Methyl Ester Derivatives 58
2.2.3.1 Structure Elucidation of Oa-WS-Me-I 60
2.2.3.2 Structure Elucidation of Oa-WS-Me-II 66
2.2.4 Synthesis of β-Carboline Derivatives 70
2.2.4.1 1,9-Dimethyl-β-carboline 70
2.2.4.2 1,9-Dimethyl-β-carboline N-oxide 72
2.2.4.3 1-Acetoxymethyl-9-methyl-β-carboline 72
2.2.4.4 1-Hydroxymethyl-9-Methyl-β-carboline 73
2.2.4.5 1-Methyl-β-carboline N-oxide 73
2.2.4.6 1-Acetoxymethyl-β-carboline 74
2.2.4.7 1-Hydroxymethyl-β-carboline 74
2.2.4.8 1-Methyl-9-acetyl-β-carboline 75
2.3 Summary and Conclusion 76
CHAPTER 3: ISOLATION AND STRUCTURE ELUCIDATION OF *TALAUMA GITINGENSIS* ALKALOIDS
3.1 Introduction 79
3.1.1 Synthesis of Aporphine Alkaloids 81
3.1.2 Biosynthesis of Aporphine Alkaloids 83
3.1.3 Pharmacology 85
3.1.4 Oxoaporphine Alkaloids 86
3.1.5 Genus *Talauma* 88
3.1.5.1 *Talauma mexicana* 89
3.1.5.2 *Talauma hodgsoni* 89
3.1.5.3 *Talauma obovata* 89
3.1.5.4 *Talauma ovata* 90
3.1.5.5 *Talauma gitingensis* 91
3.2 Results and Discussion 92
3.2.1 Isolation and Structure Elucidation of Tg-3A-1 92

3.2.2 Isolation of the N-Acetyl Derivatives of the Noraporphine Alkaloids 95
3.2.2.1 Structure Elucidation of N-Acetyl-Tg-3A-2 95
3.2.2.3 Structure Elucidation of N-Acetyl-Tg-3A-3 104
3.3 Summary and Conclusion 106
CHAPTER 4: FALSE-POSITIVE ALKALOID FROM *GRAPTOPHYLLUM PICTUM*
4.1 Introduction 107
4.1.1 *Graptophyllum pictum* (L.) Griff. 107
4.2 Results and Discussion 109
4.3 Summary and Conclusion 113
CHAPTER 5: ISOLATION AND STRUCTURE ELUCIDATION OF ALKALOIDS FROM *PANDANUS AMARYLLIFOLIUS*
5.1 Introduction 114
5.1.1 *Pandanus amaryllifolius* Roxb. 116
5.2 Results and Discussion 118
5.2.1 Pandamarilactone-1 (Pa-3A-1) 118
5.2.2 Pandamarilactone-32 (Pa-3A-32) 124
5.2.3 Pandamarilactone-31 (Pa-3A-31) 131
5.2.4 Pandamarilactone-2 (Pa-3A-2) 134
5.3 Summary and Conclusion 136
CHAPTER 6: BIOSYNTHESIS OF *IPOMOEA MURICATA* INDOLIZIDINE ALKALOIDS
6.1 Introduction 138
6.1.1 *Ipomoea muricata Jacq. (Linn.)* 143
6.2 Results and Discussion 144
6.2.1 Incorporation of [2-^{14}C]Acetate 145
6.2.2 Incorporation of [U-^{14}C]Tyrosine 148

CHAPTER 7: EXPERIMENTAL

7.1 General Procedures 151
7.1.1 Solvents 151
7.1.2 Chromatography 151
7.1.3 Melting Points 152
7.1.4 Optical Rotations 152
7.1.5 Ultraviolet (UV) Spectra 152
7.1.6 Circular Dichroism 152
7.1.7 Infrared (IR) Spectra 152
7.1.8 Mass Spectra (MS) 152
7.1.9 ^{1}H and ^{13}C Nuclear Magnetic Resonance (NMR) Spectra 153
7.2 Experimental Section for Chapter 2 154
7.2.1 NMR Spectroscopy 154
7.2.1.1 2-D NMR Experiments 154
7.2.2 MS Analysis by Smith-Kline Beecham Pharmaceutical Groups for Oa-4A-1, Oa-4A-2, Oa-4A-Me-1 and Oa-WS-Me-I 155
7.2.3 Plant Description 156
7.2.4 Extraction of the Alkaloids from *Ophiorriza acuminata* 157
7.2.4.1 Purification of Oa-3A 157
7.2.4.2 Spectroscopic Data of Oa-3A 158
7.2.5 Isolation and Purification of the Water-Soluble Alkaloids 159
7.2.5.1 Purification by High Pressure Liquid Chromatography 159
7.2.5.2 Purification by Gel Chromatography on Sephadex LH-20 160

7.2.5.3 Enzyme Hydrolysis of Oa-4A-1 162
7.2.5.4 Spectroscopic Data for Oa-4A-1 163
7.2.5.5 Spectroscopic Data for Oa-4A-2 164
7.2.6 Isolation of Oa-WS-Me-I and Oa-WS-Me-II 165
7.2.6.1 Spectroscopic Data for Oa-WS-Me-I 166
7.2.6.2 Spectroscopic Data for Oa-WS-Me-II 166
7.2.7 Synthesis of β-Carboline Derivatives 167
7.2.7.1 1,9-Dimethyl-β-Carboline 167
7.2.7.2 1,9-Dimethyl-β-Carboline N-oxide 169
7.2.7.3 1-Acetoxymethyl-9-methyl-β-Carboline 170
7.2.7.4 1-Hydroxymethyl-9-methyl-β-Carboline 171
7.2.7.5 1-Methyl-β-Carboline N-oxide 172
7.2.7.6 1-Acetoxymethyl-β-Carboline 173
7.2.7.7 1-Acetoxymethyl-9-methyl-β-Carboline 174
7.2.7.8 1-Hydroxymethyl-β-Carboline 175
7.2.7.9 1-Methyl-9-acetyl-β-Carboline 175
7.3 Experimental Section for Chapter 3 177
7.3.1 NMR Spectroscopy 177
7.3.2 Collection of Sample 177
7.3.3 Plant Description 177
7.3.4 Extraction and Isolation of Alkaloids 178
7.3.4.1 Spectroscopic Data for Tg-3A-1 178
7.3.5 Isolation of the Noraporphine Alkaloids 179
7.3.5.1 Spectroscopic Data for N-Acetyl Tg-3A-2 179
7.3.5.2 Spectroscopic Data for N-Acetyl-Tg-3A-3 180
7.4 Experimental Section for Chapter 4 181
7.4.1 Collection of Sample 181
7.4.2 Plant Description 181
7.4.3 Isolation of Gp-78 181

7.4.3.1 Spectroscopic Data for Gp-78 182
7.5 Experimental Section for Chapter 5 183
7.5.1 NMR Spectroscopy 183
7.5.2 2-D NMR Experiments 183
7.5.3 Isolation of Alkaloids 185
7.5.3.1 Purification and Spectroscopic Data for Pandamarilactone-1 (Pa-3A-1) 187
7.5.4 Purification of Pa-3A-3 187
7.5.4.1 Spectroscopic Data for Pandamarilactone-31 (Pa-3A-31) 188
7.5.4.2 Spectroscopic Data for Pandamarilactone-32 (Pa-3A-32) 188
7.5.5 Pandamarilactone-2 (Pa-3A-2) 189
7.6 Experimental Section for Chapter 6 190
7.6.1 Cultivation of the *Ipomoea muricata* Plant 190
7.6.2 Incorporation Time Determination 190
7.6.3 Administration of Acetate-Labelled Precursor to *I. muricata* 190
7.6.4 Extraction of Ipalbidine and Ipomine from *I. muricata* 191
7.6.5 Radioactivity Measurements 192
7.6.6 Administration of [U-^{14}C]Tyrosine to *I. muricata* 192
APPENDIX 1: TWO DIMENSIONAL NMR SPECTROSCOPY
A1.1 Double Quantum Filtered (DQF) COSY 2-D NMR 194
A1.2 Triple Quantum Filtered COSY 194
A1.3 Relay COSY 194
A1.4 Double Relay COSY 196
A1.5 Total Correlation Spectroscopy (TOCSY) 197

A1.6 Nuclear Overhauser Enhancement Spectroscopy (NOESY) and Rotating-Frame Overhauser Enhancement Spectroscopy (ROESY) 151

A1.7 Inverse-Detection Direct Heteronuclear Multiple Quantum Coherence (HMQC) 199

A1.8 Inverse-Detection Long Range Heteronuclear Multiple Bond Correlation (HMBC) 200

A1.9 Attached Proton Test (APT) 201

APPENDIX 2

A2.1 ^{1}H-^{1}H COSY NMR Spectrum of Oa-4A-1 203

A2.2 2RCOSY NMR Spectrum of Oa-4A-1 204

A2.3 TOCSY NMR Spectrum of Oa-4A-1 205

A2.4 NOESY NMR Spectrum of Oa-4A-1 206

A2.5 ROESY NMR Spectrum of Oa-4A-1 207

A2.6 ^{1}H-^{1}H COSY NMR Spectrum of Oa-WS-Me-II 208

A2.7 TOCSY NMR Spectrum of Oa-WS-Me-II 209

A2.8 ROESY NMR Spectrum of Oa-WS-Me-II 210

A2.9 ^{1}H NMR Spectrum of Pandamarilactone-1 211

A2.10 TOCSY NMR Spectrum of Pandamarilactone-32 212

A2.11 ROESY NMR Spectrum of Pandamarilactone-32 213

APPENDIX 3 214

REFERENCES 215

PUBLICATIONS AND CONFERENCES 230

Acknowledgements

I like to give my sincere thanks to my supervisors, Dr. Mary J. Garson for her continuous guidance, support and understanding during the past years, and Dr. Roger J. W. Truscott, for his encouragements and kind advices during the course of this study.

Thanks are extended to the Australian International Development Assistance Bureau (AIDAB) for this fellowship.

A warm thanks to Dr. John Carver for sharing with me the wonders of Nuclear Magnetic Resonance Spectroscopy.

The University of Santo Tomas Research Centre for the Natural Sciences for giving their trust in me to carry out this study which is a part of the on-going research program on Natural Product Chemistry and for providing the plant samples used in this investigation.

My utmost thanks to the following people who in one way or another had extended their kind assistance in the completion of this work:

- Assoc. Prof. Jack R. Cannon, for inspiring me to undertake this challenge on Natural Product Chemistry.

- Prof. John Coll, for trusting in me and supporting me for this fellowship.

- Smith Kline and Beecham People: Dr. Brad Carte, for the HRFABMS of the *Ophiorrhiza acuminata* glucoindole alkaloids; M. Bean for the HRFAB and MS/MS data; M. Mentzer for scanning HRDCI data and M. Hemling for the LRFAB and LRDCI.

- Dr. John Macleod, Research School of Chemistry, Australian National University, for the HRMS.

- Dr. Bob Vagg (Macquarie University) and Miss Yolanta Sztaba (University of Sydney) for the circular dichroism measurements.

- Peta Simmond (Australian National University) for some NMR spectra of the *Pandanus amaryllifolius* alkaloids.

- Steve Pople and Wayne of the Wollongong Botanic Garden for the cultivation of the *Ipomoea muricata* seeds for the biosynthetic study; Graham Kohler for the assistance in the maintenance of the *I. muricata* plants.

- my good friend, Grace Benavente, not only for her kind help in the drawings, corrections and compilation of this thesis but most of all for her warm friendship for the past four years.

- to you Dorothy for always being there to understand and comfort me.

- to Ellen Manning for her kind assistance with the NMR spectrometer (especially whenever the spectrometer breaks down).

- to all my friends who have been my family here in Wollongong for their care and support which enable me to cope up during the past years.

- to a very special friend who had provided me the challenge and determination in the pursuit of this endeavour.

- and most importantly to my family for putting up with me through laughters and tears during the past years.

ABSTRACT

This work forms part of growing studies on Natural Product Chemistry in the Philippines. Alkaloid field screening conducted by the University of Santo Tomas Research Centre provided the opportunity to carry out this study on five endemic Philippine plants. Structural elucidation of the alkaloids present in three of these plants was obtained largely by physical methods, most importantly by the use of sophisticated NMR techniques which are described in detail in the text.

Talauma gitingensis of the family Magnoliaceae afforded the oxoaporphine liriodenine and two noraporphine alkaloids, anonaine and xylopine, both of which were characterised as their N-acetyl derivatives. The existence of conformational isomerism for the N-acetyl derivatives was described for the first time together with a complete ^{1}H NMR characterisation of the compounds using 1-D decoupling experiments, nOe enhancement and 2-D COSY spectroscopy. This was also the first reported isolation of anonaine in the genus *Talauma*.

The species *Ophiorrhiza acuminata* belonging to the family Rubiaceae gave the β-carboline alkaloid, harman, and the glucoindole monoterpenoid alkaloid, lyalosidic acid. Three other glucoindole alkaloids were isolated, two of which were characterised as their methyl esters. Our isolation of Oa-4A-2 is the first reported isolation of a palicoside epimer at C-3 in nature. The other two methyl ester glucoindole alkaloids were identified as the C-20 epimer of lyaloside, a methyl ester of lyalosidic acid, and a C-3 epimer of dolichantoside.

Four alkaloids were isolated from the leaves of *Pandanus amaryllifolius* (Pandanaceae). The novel structures of three of these alkaloids were determined using inverse 2-D NMR techniques such HMQC and HMBC, and named Pandamarilactone-1, Pandamarilactone-31 and Pandamarilactone-32. A fourth alkaloid proved difficult to purify and was found to be unstable. This prevented the definite elucidation of its structure although partial characterisation is reported.

During the course of this work on alkaloids, an example of a false-positive alkaloid was isolated from a plant identified as *Graptophyllum pictum* of the family Acanthaceae. This compound reported for the first time as being present in the family Acanthaceae and the genus *Graptophyllum* was identified as vomifoliol A, previously isolated from *Rauwolfia vomitoria* of the family Apocynaceae.

In parallel with these structural elucidation studies of alkaloids, a preliminary investigation of the biosynthesis of indolizidine alkaloids from *Ipomoea muricata* was undertaken. The *Ipomoea* indolizidine alkaloids are the only alkaloids known to occur in nature with a methyl substituent on the indolizidine nucleus. Since these alkaloids are biologically active, a closer investigation of their biogenetic origin was undertaken. The precursors [2-^{14}C]acetate and [U-^{14}C]tyrosine were found to be incorporated into the intact plant of *I. muricata* at a low level however insufficient labelled alkaloids were available for chemical degradation studies which would have established the sites of labelling.

LIST OF FIGURES

No.		Page
1	Map of the Philippines with the Geographical Location of Plants Investigated in this Study	7
2	^1H NMR Spectrum of Oa-4A-1 [400 MHz, CD_3OD, referenced at δ3.35]	31
3	Double-Quantum Filtered COSY (DQF COSY) NMR Spectrum of Oa-4A-1 [400 MHz, CD_3OD, referenced at δ3.35]	36
4	Triple-Quantum Filtered (TQF) COSY NMR Spectrum of Oa-4A-1 (Region between 3.0 - 4.0 ppm) [400 MHz, CD_3OD, referenced at δ3.35]	37
5	Relay COSY (RCOSY) NMR Spectrum of Oa-4A-1 [400 MHz, CD_3OD, reference at δ3.35]	38
6	RCOSY NMR Correlations in the $C_8H_8O_3$ unit of Oa-4A-1	39
7	2RCOSY NMR Correlations for the $C_8H_8O_3$ unit of Oa-4A-1 [400 MHz, CD_3OD, reference at δ3.35]	40
8	Lyaloside, 15α, 20β, 21α	41
9	NOESY/ROESY NMR Correlations at C-15, C-21 and C-21	44
10	Possible Conformation of Oa-4A-1 by Molecular Modelling Obtained from the ALCHEMY Program	44
11	Mechanism for the Formation of Harman from Lyalosidic Acid by Enzyme Hydrolysis Proposed by N. Aimi	48
12	Another Possible Mechanism for the Formation	

	of Harman from Oa-4A-1 by Enzyme Hydrolysis	49
13	^{1}H NMR Spectrum of Oa-4A-2[400 MHz, CD_3OD, referenced at δ3.35]	51
14	^{1}H-^{1}H COSY NMR Spectrum of Oa-4A-2 [400 MHz, CD_3OD, referenced at δ3.35]	52
15	^{1}H NMR Spectrum in DMSO-d_6 of Oa-4A-2 [400 MHz, referenced at δ2.00]	53
16	Possible Conformation of Oa-4A-2 based on Molecular Modelling using ALCHEMY Program with Energy Minimisation	56
17	MS Fragmentation Pattern of Oa-4A-2	58
18	MS Fragmentation of Oa-WS-Me-I	61
19	^{1}H NMR Spectrum of Oa-WS-Me-I [400 MHz, CD_3OD, referenced at δ3.35]	60
20	^{1}H-^{1}H COSY NMR Spectrum of Oa-WS-Me-I [400 MHz, CD_3OD, referenced at δ3.35]	61
21	Four Possible Structures of the Monoterpernoid Unit of Oa-WS-Me-I Based on the Observed Coupling Constants	63
22	Possible Conformation of Oa-WS-Me-1 Based on Molecular Modelling using ALCHEMY Program with Energy Minimisation	65
23	^{1}H NMR Spectrum of Oa-Ws-Me-II [400 MHz, CD_3OD, referenced at δ3.35]	67
24	Aporphine Nucleus	79
25	Stereochemical Arrangements of Aporphine Alkaloid	80
26	^{1}H NMR Spectrum of Tg-3A-1 [400 MHz, $CDCl_3$, referenced at δ7.25]	92

27. ^{1}H NMR Spectrum of N-Acetyl-Tg-3A-2 [400 MHz, $CDCl_3$, referenced at δ7.25].....95

28 Partial ^{1}H NMR Assignments for N-Acetyl-Tg-3A-2.....97

29 ^{1}H-^{1}H COSY NMR Spectrum of N-Acetyl-Tg-3A-2 [400 MHz, $CDCl_3$, referenced at δ7.25].....97

30 The Two Rotational Isomers of N-Acetyl-Tg-3A-2.....102

31 ^{1}H NMR Spectrum of N-Acetyl-Tg-3A-3 [400 MHz, $CDCl_3$, referenced at δ7.25].....103

32 Quinazoline Nucleus.....107

33 Structure of Gp-78.....109

34 ^{1}H NMR Spectrum of Gp-78 [400 MHz, $CDCl_3$, referenced at δ7.25].....109

35 *Pandanus amaryllifolius (Pandanaceae)* Plant.....116

36 ^{1}H-^{1}H COSY NMR Spectrum of Pandamarilactone-1 [400 MHz, $CDCl_3$, referenced at δ7.25].....119

37 Expanded Regions of Inverse-Detection (^{1}H-^{13}C) Heteronuclear Multiple Quantum Coherence (HMQC) NMR Spectra of Pandamarilactone-1 [500 MHz, $CDCl_3$, referenced at δ7.25 (^{1}H) and δ7.70 (^{13}C)].....120

38 Expanded Regions of Long-Range Heteronuclear Multiple Bond Correlation (HMBC) NMR Spectra of Pandamarilactone-1 [500 MHz, $CDCl_3$, referenced at δ7.25 (^{1}H) and δ7.70 (^{13}C)].....121

39 ^{1}H NMR Spectrum of Pandamarilactone-32 [400 MHz, CDCl3, referenced at δ7.25].....125

40 ^{1}H-^{1}H COSY NMR Spectrum of

Pandamarilactone-32 [400 MHz, $CDCl_3$, referenced at δ7.25]....126

41 Expanded Regions of Heteronuclear Multiple Quantum Coherence (HMQC) NMR Spectra of Pandamarilactone-32 [500 MHz, $CDCl_3$, referenced at δ7.25(^1H) and δ77.0 (^{13}C)]....127

42 Expanded Regions of Long-Range Heteronuclear Multiple Bond Correlation (HMBC) NMR Spectra of Pandamarilactone-32 [500 MHz, $CDCl_3$, referenced at δ7.25(^1H) and δ77.0 (^{13}C)]....128

43 ^1H NMR Spectrum of Pandamarilactone-31 [400 MHz, $CDCl_3$, referenced at δ7.25]....130

44 Expanded Regions of Heteronuclear Multiple Quantum Coherence (HMQC) NMR Spectra of Pandamarilactone-31 [500 MHz, $CDCl_3$, referenced at δ7.25(^1H) and δ77.0 (^{13}C)]....132

45 Expanded Regions of Long Range Heteronuclear Multiple Bond Correlation (HMBC) NMR Spectra of Pandamarilactone-31 [500 MHz, $CDCl_3$, referenced at δ7.25(^1H) and δ77.0 (^{13}C)]....133

46 Indolizidine nucleus....138

47 *Ipomoea muricata* Plant....142

48 *Ophiorrhiza acuminata* Plant....155

49 *Talauma gitingensis* Plant....177

50 *Graptophyllum pictum (Acanthaceae)* Plant....180

LIST OF SCHEMES

No.		Page
1	Possible Pathway for the Biosynthesis of Eleagnine **9** and Harman **10**	12
2	Classification of Indole Alkaloids by Kompis, Hesse and Schmid	14
3	Transformation of Geraniol **36**/Nerol **37** into Loganin **38**	16
4	Biosynthesis of Vincoside **23** and Strictosidine (Isovincoside) **22**	19
5	Sequence of Formation of the Five Bases as Categorised by Dalton	20
6	Flowchart for the Fractionation and Isolation of the *O.acuminata* alkaloids	27
7	Proposed Synthesis of 1-Methylharman Glucoside	69
8	Proposed Synthesis of Harman Glucoside	70
9	Aporphine Synthesis via Condensation of *o*-Nitrophenylacetylchloride with Phenylethylamine	80
10	Synthesis of Glaucine	81
11	Aporphine Synthesis by Based-Catalysed Condensation of *o*-Nitrotoluene with Isoquinolinium salt	82
12	Biosynthetic Conversion of Reticuline to Isoboldine	83
13	Biosynthesis via Formation of Dienone	83
14	Biosynthesis of Aporphine Alkaloid by Coupling to Neoaporphines	84

18 Schematic Diagram for the Isolation and Purification of the *Pandanus amaryllifolius* Alkaloids....117

19 Proposed Biosynthetic Pathway for the Conversion of Leucine to 2-carboxylic acid-4-methyl-oxacyclopent-3-ene-5-one....136

20 Biosynthesis of Tylophorine....139

21 Biosynthesis of Indolizidine Alkaloids via Pipecolinic acid....140

22 Biogenetically Based Synthesis of Ipalbidine....142

23 Proposed Kuhn-Roth Degradation of Labelled Alkaloids....147

24 Possible Biosynthetic Fate of Acetate in the Indolizidine Alkaloid....148

LIST OF TABLES

No.		Page
1	Some Monoterpene Indole Alkaloids of Pharmacological Significance	13
2	^{1}H and ^{13}C NMR Assignments for Oa-3A [CD_3OD, referenced at δ3.35 (^{1}H) and δ49.0 (^{13}C)]	28
3	Accurate Mass Measurements of Oa-4A-1 Fragment Ions with their Corresponding Possible Elemental Composition	30
4	^{13}C NMR Assignments of Oa-4A-1 Sugar in Comparison with the Literature Values	32
5	^{1}H and ^{13}C NMR Data for Oa-4A-1 [CD_3OD, referenced at δ3.35 (^{1}H) and δ49.0 (^{13}C)]	34
6	Correlation of the Observed Dipolar Interactions (NOESY/ROESY) with the Bond Distances Measured from the ALCHEMY Molecular Modelling	46
7	^{1}H NMR Chemical Shift Differences Between Oa-4A-1 and Lyalosidic Acid on Selected Protons (CD_3OD, 400 MHz, referenced relative to CD_3OD at δ3.35)	46
8	^{13}C NMR Data for Oa-4A-1 and Lyalosidic Acid on Selected Carbons (CD_3OD, Varian 400 MHz, referenced relative to residual CH_3OH at δ3.35)	48
9	Accurate Mass Measurements of Oa-4A-2 Fragment Ions With Their Corresponding Possible Elemental Compositions	49
10	^{1}H NMR Assignments for Oa-4A-2 (CD_3OD, Varian 400 MHz, referenced relative to CD_3OD at δ3.35)	50

11 Comparison of Percentage Intensity of Observed Fragment Ions for Oa-WS-Me-I and Oa-4A-1-Me.....59

12 ^{1}H NMR Assignments for Oa-WS-Me-1 [CD_3OD, 400 MHz, referenced relative to residual CH_3OH at δ3.35 (^{1}H) and δ49 0(^{13}C)].....62

13 Chemical Shift Differences of Selected Protons Between Oa-WS-Me-I and Oa-4A-Me-I. [CD_3OD, 400 MHz, referenced relative to residual CH_3OH at δ3.35].....62

14 Correlation of Observed nOe Responses with the Measured Bond Distances from the Energy Minimised Structure (ALCHEMY) of Oa-WS-Me-I.....65

15 ^{1}H NMR Assignments for Oa-WS-Me-II.[CD_3OD, 400 MHz, referenced relative to the residual CH_3OH at δ3.35].....66

16. ^{1}H and ^{13}C NMR Assignments for Harman **10** and 1,9-Dimethyl-β-carboline **55** [CD_3OD, 400 MHz, referenced relative to residual CH_3OH at δ3.35 (^{1}H) and δ49.0 (^{13}C)].....71

17 ^{1}H NMR Assignments for the Z and E Isomers of N-Acetyl-Tg-3A-2.....102

18 ^{13}C NMR Assignments for the Z and E Isomers of N-Acetyl-Tg-3A-2.....103

19 ^{1}H and ^{13}C NMR Assignments for Pandamarilactone-1 [500 MHz, $CDCl_3$, referenced relative to residual $CHCl_3$ at δ7.25 (^{1}H) and δ77.0 (^{13}C)].....118

20 ^{1}H and ^{13}C NMR Assignments for Pandamarilactone-32 (Pa-3A-32) [$CDCl_3$, 400 MHz, referenced relative to the residual signals

for $CHCl_3$ at δ7.25 (^1H) and δ77.0 (^{13}C)].....124

2 1 ^1H and ^{13}C NMR Assignments for Pandamarilactone-31 (Pa-3A-31) [$CDCl_3$, 400 MHz, referenced relative to the residual signals for $CHCl_3$ at δ7.25 (^1H) and δ77.0 (^{13}C)].....131

2 2 Level of ^{14}C Radioactivity in Different Solvent Extracts of *I.muricata* seeds ([2-^{14}C]acetate).....145

2 3 Radioactivity Counting of the [2-^{14}C]Acetate Labelled Alkaloids.....145

2 4 Level of ^{14}C Radioactivity in the Different Solvent Extracts of *I. muricata* seeds Labelled with [U-^{14}C]Tyrosine.....148

2 5 Incorporation of the [U-^{14}C]Tyrosine into Ipalbidine and Ipomine.....148

LIST OF DIAGRAMS

No.		Page
1	Pulse Sequence for DQF COSY	194
2	COSY 90 Pulse Sequence	195
3	Relay COSY Pulse Sequence	195
4	Double Relay COSY Pulse Sequence	196
5	Total Correlation Spectroscopy Pulse Sequence	197
6	NOESY Pulse Sequence	198
7	ROESY Pulse Sequence with spin-locking	199
8	HMQC Inverse-Detection Pulse sequence	199
9	HMBC Inverse-Detection Pulse Sequence	201
10	Attached Proton Test with Delayed Acquisition	202

LIST OF STRUCTURES

No.	Name of Compounds
1	Gibberellic Acid
2	Indoleacetic Acid
3	Cytokinin
4	Abscisic Acid
5	Reserpine
6	Tubocurarine
7	Codeine
8	Morphine
9	Eleagnine
10	Harman
11	Harmine
12	Norharman
13	1-Hydroxymethyl-β-carboline
14	3-Methoxy-carbonyl-1-methyl-β-carboline
15	1-(1',2'-dihydroxy)ethyl-4-methoxy-β-carboline
16	4,8-Dimethoxy-1-vinyl-β-carboline
17	Harmaline
18	Harmalol
19	Tryptophan
20	Tryptamine
21	Secologanin
22	Strictosidine
23	Vincoside
24	Ajmalicine
25	Secodine
26	Vincamine

27 Vindoline

28 Fructicosine

29 Catharanthine

30 Yohimbine

31 Ajmaline

32 Strychnine

33 Quinine

34 Tabersonine

35 Mevalonic Acid

36 Geraniol

37 Nerol

38 Loganin

39 Hydroxyloganin

40 Camptothecin

41 10-Methoxycamptothecin

42 Ophiorine A

43 Ophiorine B

44 Lyaloside

45 Lyalosidic Acid

46 10-Hydroxylyalosidic Acid

47 6-Hydroxyharman

48 9-Methoxycamptothecin

49 10-Hydroxyharman

50 Pumiloside

51 Deoxypumiloside

52 Chaboside

53 Inamoside

54 Palicoside

55 Dolichantoside

56 1,9-Dimethyl-β-carboline

57 1,9-Dimethyl-β-carboline N-oxide

58 1-Acetoxymethyl-9-methyl-β-carboline

59 1-Hydroxymethyl-9-methyl-β-carboline

60 1-Methyl-β-carboline N-oxide

61 1-Acetoxymethyl-β-carboline

62 1-Acetoxymethyl-9-acetyl-β-carboline

63 1-Hydroxymethyl-β-carboline

64 1-Methyl-9-acetyl-β-carboline

65 Morphine

66 Apomorphine

67 Glaucine

68 Corytuberine

69 Corydine

70 Isocorydine

71 Bulbocapnine

72 *o*-Nitrophenylacetylchloride

73 *o*-Nitrotoluene

74 Isoquinolinium salt

75 Reticuline

76 Isoboldine

77 Orientaline

78 Orientalinone

79 Orientalinol

80 Isothebaine

81 1,2-Methylenedioxyapomorphine

82 Boldine

83 Alkaloid PO-3

84 Corunnine

85 Liriodenine

86 Ushinsunine

87 Roemerine

88 Lanuginosine

89 Xylopine

90 Anonaine

91 Aztequine

92 Anolobine

93 Asimilobine

94 Costunolide

95 Vomifoliol

96 Theaspirone

97 Inamoside

98 Ionone

99 (2S,4R)-4-Hydroxy-4-methylglutamic acid

100 (2S,4S)-4-Hydroxy-4-methylglutamic acid

101 2-Acetyl-1-pyrroline

102 4-Hydroxyglutamic acid

103 Glutamic acid

104 Pandamarine

105 Tylophorine

106 Swainsonine

107 Slafranine

108 Ipalbidine

109 Ipalbine

110 Ipomine

111 Isoipomine

112 Methoxyipomine

113 Dimethoxyipomine

114 Ipohardine

115 Ipoharine

LIST OF ABBREVIATIONS

^{1}H NMR	Proton Nuclear Magnetic Resonance
^{13}C NMR	Carbon Nuclear Magnetic Resonance
IR	Infrared
UV	Ultraviolet
CD	Circular Dichroism
$[\alpha]_D$	Specific Optical Rotation
ε	Extinction Coefficient
HRMS	High Resolution Mass Spectrometry
LRMS	Low Resolution Mass Spectrometry
CIMS	Chemical Ionisation Mass Spectrometry
EIMS	Electron Impact Mass Spectrometry
DCIMS	Desorption Chemical Ionisation Mass Spectrometry
FABMS	Fast Atom Bombardment Mass Spectrometry
OCS	Organic Counting Scintillant
DPM	Disintegration per minute
HPLC	High Pressure Liquid Chromatography
PTLC	Preparative Thin Layer Chromatography
TLC	Thin Layer Chromatography
APT	Attached Proton Test
BIRD	BIlinear Rotation Decouling
CAMELSPIN	Cross-relaxation Appropriate for Minimolecules Emulated by Locked SPIN
COSY	COrrelation SpectroscopY
DQF	Double-Quantum Coherence
TQF	Triple-Quantum Coherence
NOESY	Nuclear Overhauser and Exchange SpectroscopY

2RCOSY	Double Relayed Coherence Transfer
TOCSY	TOtal Correlation SpectroscopY
HMQC	Heteronuclear Multiple Quantum Correlation
HMBC	Heteronuclear Multiple Bond Correlation
ROESY	Rotating-Frame Overhauser Enhancement SpectroscopY

CHAPTER 1

GENERAL INTRODUCTION

1.1 INTRODUCTION

Plants can be considered as the most prolific laboratory for their remarkable capacity to produce and elaborate organic compounds of nearly every conceivable structural class; the study of which provides a fascinating and fruitful area for scientific investigations. Primarily, the plant produces a pool of organic compounds such as carbohydrates, common sugars, low molecular weight acids, amino acids, proteins and fats. This array of compounds is widely distributed in plants and is considered to be essential in life processes. Hence they are called primary metabolites. In contrast with the intermediates of primary metabolism which are ubiquitous, complex compounds like alkaloids, terpenes, mycotoxins, phenols, polyenes, and polyacetylenes, occur sporadically throughout Nature.[1] These compounds which are formed by specific, enzyme-catalysed reactions, often with primary metabolites serving as their starting materials appear to have no explicit role in the economy of the organism that produces them.[2-5] This distinction among natural products has long been recognised, and substances in this second category are commonly referred to as secondary metabolites. This myriad of compounds have been used by humans as drugs, stimulants, dyes, and for many other purposes since prehistoric times. In spite of the many new synthetic drugs available, some of our most valuable medicinal agents remain the ones discovered by primitive man.

Secondary metabolites unlike primary metabolites, have a restricted distribution, being found mostly in plants and microorganisms although they occur in great numbers throughout the plant kingdom. They are often characteristic of individual

genera, species, or strains and they are biosynthesised along specialised pathways from the primary metabolites.

The great interest in secondary metabolites has stemmed from several factors, (1) the search for chemicals from natural resources as curative agents; (2) an increased interest in the chemical compounds in plants from the viewpoint of pure science; (3) studies on biogenetic of essential plant constituents involving secondary constituents; and (4) interest in the use of chemical constituents as an aid to plant taxonomy, so called chemical taxonomy.

1.1.1 Primary Role of Secondary Metabolites

Secondary substances in plants seem to perform many functions. Interactions between these substances and various other plants and animals in the environment is indeed very complex in some instances. Numerous views concerning the roles of secondary compounds in plants and their interactions with organisms have been proposed in both the chemical and biological literature of the past century.[6-8] Secondary metabolites have been considered to be without functions, i.e. they represent end products of metabolism which plants store or excrete by various mechanisms, or that they are detoxification products of simple products or plant metabolism. It is generally acknowledged now however that these secondary metabolites are involved in the defense of the plant against animals, fungi, bacteria, and other plants.[8]

Results of feeding experiments into plant systems provided data supporting the proposal that secondary metabolites exist in a state of dynamic equilibrium and are not static end products of metabolism.[9-13] Pulse radioactive tracer studies have established

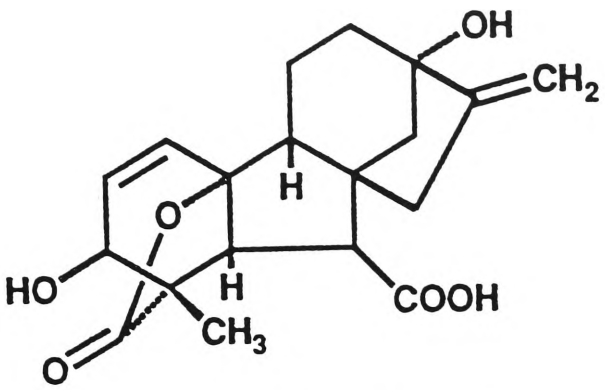

Gibberellic Acid 1

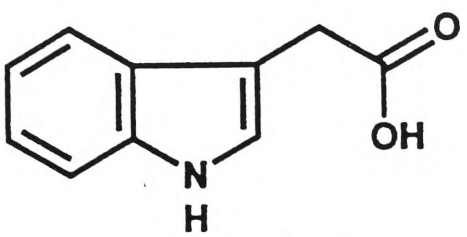

Indoleacetic acid 2

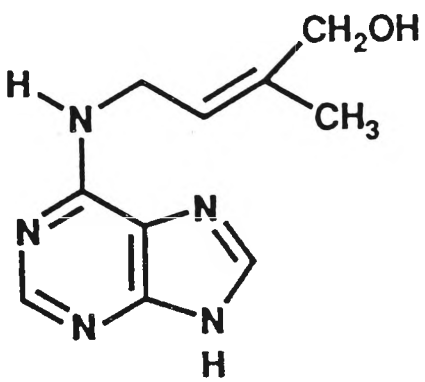

Cytokinin 3

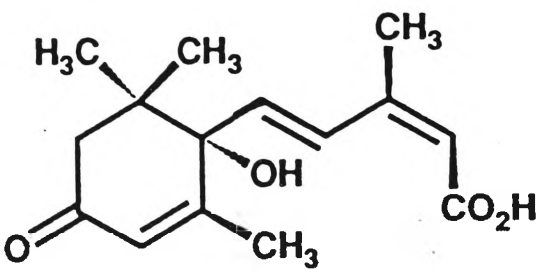

Abscisic acid 4

that, for various plant and microbial phenols and for some alkaloids, both synthesis and turnover occur, and they are simultaneous.[14] This turnover suggests that the secondary metabolic products are closely involved with primary metabolic functions in the plants.

Secondary chemicals may also act as important regulators of biochemical processes. Gibberellic acid **1**, indoleacetic acid **2**, cytokinin **3** and abscisic acid **4** are well known for their capacity of altering plant growth.[15]

One of the secondary metabolites whose functions are still a matter of controversy are the alkaloids. Alkaloids have been regarded as by product of plant metabolism and as reserve material for protein synthesis[16]; as protective substances discouraging animal or insect attacks[17]; as plant stimulants or regulators similar to hormones[18], or simply as detoxification products.[19] However, the dynamic nature of alkaloid formation, and degradation has been well demonstrated, and this has led to the concept that alkaloids are not merely a "metabolic sludge".

1.2 Alkaloids in Plants

Alkaloids can be defined as basic, nitrogen-containing heterocyclic compounds derived from higher plants. The basic nitrogen of alkaloids may be either primary, secondary, tertiary, or quaternary and can exist as an amine oxide. The search for new alkaloids is continuing and the use of modern chromatographic separations and new and powerful analytical techniques such mass, NMR and IR spectroscopy has enabled chemists to isolate and characterise alkaloids even when they are present in plants in only trace amounts. The sources for new alkaloids include both

previously investigated species and those from which alkaloids had earlier been separated by chemical means.

Alkaloids have been detected in more than 100 plant families and the vascular plants which have so far been investigated have been found to contain more than 2000 individual alkaloids. Most of the alkaloids are found in dicotyledons, with some in monocotyledons. Gymnosperms, Pteridophytae, and with the exception of two families, fungi are apparently devoid of them.[20]

Alkaloids are found in various parts of a mature plant including seeds (*Strychnos*, *Delphinium* and *Cola*); roots (*Baptesis* and *Aconitum*); rhizomes (*Sanguinaria*); leaves (*Belladonna*, *Boldus*, and *Stramonium*); fruits (*Capsicum*, *Piper* and *Conium*); and bark (*Cinchona*, *Granatum*, *Xanthoxylum*).[21]

The same plant can sometimes produce alkaloids in more than one organ, such is the case in *Belladonna* where alkaloids are found in the leaves and roots. Manske[22] observed that an enormous number of alkaloids in biennials and perennials are found in the roots, with the exception of *Dicentra*, *Aconitum*, and *Delphinium*, which produce more alkaloids in the aerial portions. In annual plants the localisation of alkaloids in particular organs is not as pronounced. Wounded tissue as well as regenerated tissue after removal of the bark (*Cinchona*) is often rich in alkaloids.

Secondary plant metabolites are in a constant dynamic state of change and interchange during plant growth. The appearance and disappearance of alkaloids, for instance, poses questions as to whether they were translocated from another site, broken down *in situ*, exhaled, or leached out. This has been clearly demonstrated in tobacco where the alkaloid nicotine is synthesised in the root and translocated to the leaf. Alkaloids in living cells are usually found in

the cell vacuole in the form of water-soluble salts of such organic acids as malic, citric, oxalic, succinic, or tannic acid.

In plants, alkaloids are synthesised almost exclusively from a restricted group of α-amino acids - ornithine, lysine, phenylalanine, tyrosine and tryptophan. In spite of their great structural diversity, a few principles may be discerned which govern the synthesis of alkaloids *in vivo*. The C-N framework of the heterocyclic ring of many alkaloids is almost always generated by the initial condensation of an aldehyde and a primary amine.[2-5, 23] Both aldehyde and amine may be derived from the same amino acids. The initial condensation product may then be involved in either intramolecular or intermolecular reactions. The great variety of alkaloids is then derived by different chemical transformations of these initial condensation products.

1.2.1 Screening of Alkaloids

Screening programs have been particularly stimulated by the pharmacological properties that many alkaloids possess. Thus a great number of screening programs are currently underway in many parts of the world to evaluate the local flora; to study medicinal folklore with modern techniques; to check herbarium collections for useful drugs; to explore toxic or poisonous plants; or to survey plants for particular pharmacological properties. Aside from isolation and structural studies, the interest of phytochemists is also centred on finding the function of alkaloids in the plants, their site and mechanism of synthesis, their metabolism; or their importance in taxonomy.

There are several approaches that have been employed for selecting investigational plants having a drug potential. The most

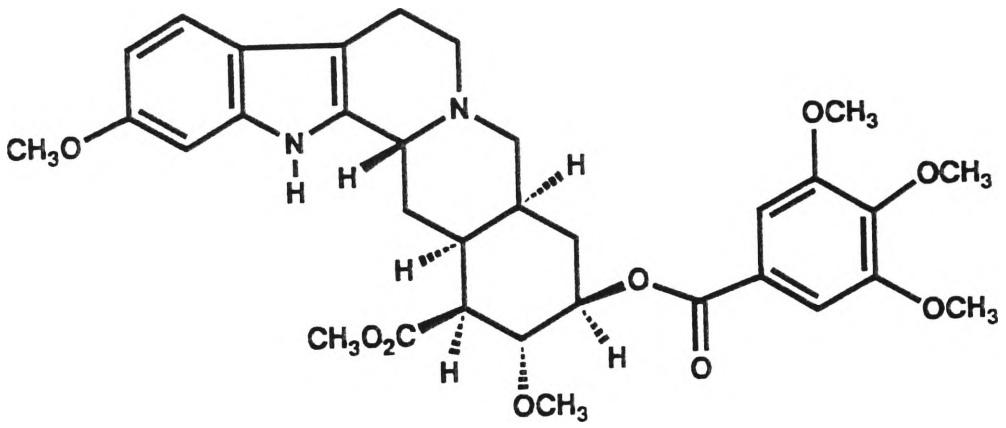

Reserpine 5

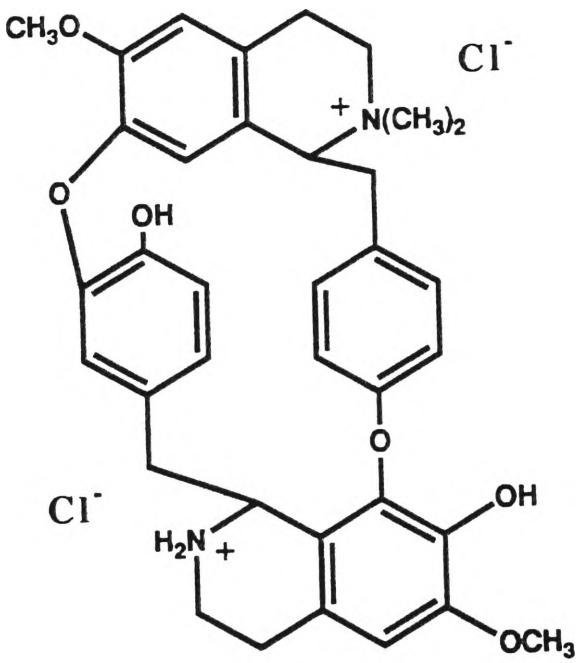

Tubocurarine 6

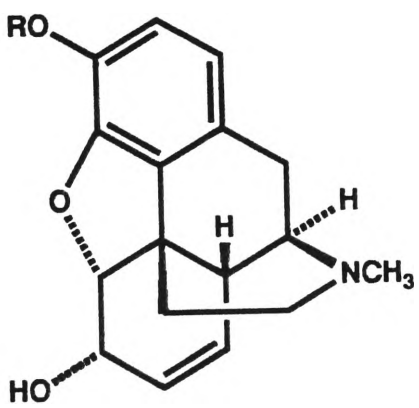

R = CH_3 Codeine 7
R = H Morphine 8

basic of which is the selection of plants known to have a medicinal folkloric background, including those selected from field studies in ethnobotany. Some outstanding examples that support the value of investigating folkloric medicinal plants are *Rauwolfia serpentina* which yielded the hypotensive alkaloid reserpine **5**; the curare plant from which the muscle relaxant *d*-tubocurarine **6** was found and the analgesic codeine **7** and morphine **8** from Opium poppy.

Another approach is the random or discrete selection of large numbers of plants followed by phytochemical screening to establish the presence of particular chemical groups that are usually associated with specific types of biological activity. Screening of randomly selected plants from one or more types of biological activity is another approach that is becoming popular amongst phytochemists.

In screening crude plant extracts for alkaloids one has to be aware of the false positive reaction obtained with some commonly used alkaloid reagents, such as Mayer's, Silicontungstic acid, Dragendorff's or Wagner's reagent. For instance, proteins and other substances can cause precipitates with reagents containing heavy metals. Artifacts giving a positive alkaloids test can be created by interaction of NH_4OH and acetone in plant extracts, or by action of an NH_3 in nonalkaloidal precursors of "alkaloids". Farnsworth[24] had reviewed false-positive and false-negative alkaloids reactions.

Present day research in Natural Products Chemistry ranges from the search for drugs or other compounds with practical uses, and even beyond the challenge presented by an unknown structure of a new compound. The structure of naturally occurring compounds are often a reflection of genetic individuality, and many of them are now recognised as valuable indicators of the

relationships between the living organism from which they are derived and of the chemical transformations that take place in the cell.

1.3 Natural Product Chemistry in the Philippines

For the past years, natural product chemistry in the Philippines had gained recognition for its continuous research on the isolation of biologically active compounds from endemic plants. The government, aware of its rich flora, have always encouraged and supported research aimed at investigating the potential of indigenous Philippine plants. Folklore medicine had long been a practice in several areas of the country and still is popular in some distant areas where more modern medical practices are unavailable. Information acquired from the folklore archives has been a constant guide in the search for plants that could be a potential source of novel biologically important secondary metabolites.

Several private universities and governments institutions have conducted phytochemical surveys in different areas of the country. These phytochemical surveys have been well documented in the literature.[25,26]. Cooperative work with foreign universities provides essential aids to facilitate research on these plants.

The University of Santo Tomas Research Centre has been conducting alkaloid field screening in different localities of the Philippines for the past ten years. The isolation and structural elucidation of alkaloids and other biologically active compounds has been the top priority of its long range program on natural products. This work which is parallel to the on-going natural products research at the UST Research Centre has the main objective of

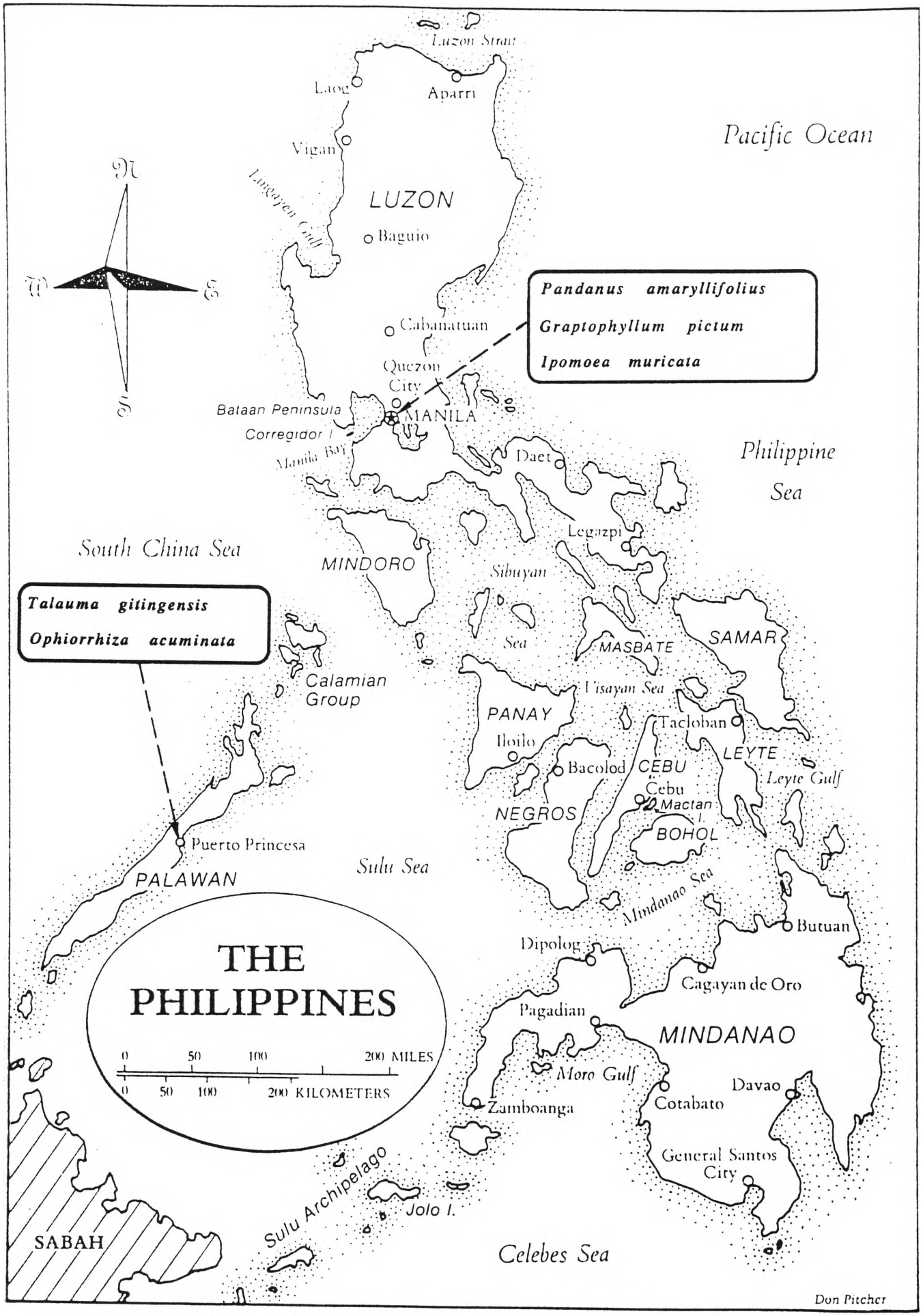

Figure 1. Map of the Philippines with the Geographical Locations of the Plants Investigated in this Study.

isolating and establishing the structures of alkaloids from Philippine plants that give positive responses with the Culvenor-Fitzgerald alkaloid field screening tests. Plants were collected from the different areas surveyed by the UST group which comprises a team of chemists, botanists and foresters. Close coordination between chemists and botanists play an important role in the success of this type of work. Geographical locations of the habitat of the plants investigated in the study are indicated in Figure 1. It was the aim of this work to elucidate the structures of the alkaloids contained in these plants. Whenever possible, these alkaloids can serve as a model compound for either further biosynthetic works or characterisation of biological activities.

CHAPTER 2

ISOLATION AND STRUCTURE ELUCIDATION OF ALKALOIDS FROM *OPHIORRHIZA ACUMINATA*

2.1 INTRODUCTION

Living plants produce a rich variety of chemical substances, of which some have proved the delight (and the frustration!) of organic chemists for the challenges in structural and synthetic chemistry which they offer. One group of alkaloids that has caught the interest of chemists because of their complex and diverse structures, is the indole alkaloids.

Indole alkaloids are most widely distributed among flowering plants as most alkaloids generally are. The great majority of simple indole alkaloids are confined to the dicotyledons. It is also logical then, that the more complex indole alkaloids also mainly inhabit the dicotyledons. Moreover, as pointed out by Le Men and Taylor[27], they occur most frequently in the Apocynaceae, Loganiaceae and Rubiaceae plant families. A few representatives of this remarkable group of alkaloids have also been found in phylogenetically more remote families such as Annonaceae, Euphorbiaceae, and Sapotaceae. Alangiaceae and Icacinaceae are the most recent additions to the list of plants which contain complex indole alkaloids. Simple indole alkaloids basically contain the tryptamine unit derived from tryptophan. Complex indole alkaloids, on the other hand, feature in their structures the tryptamine unit, which is usually unmodified, together with C_9-C_{10} units, which initially offered puzzling problems in the definition of their biosynthetic origin, until it was recognised that they resemble naturally occurring cyclic monoterpenes.

A number of reviews[28,29] suggest that chemotaxonomic considerations in this area have been aided by the rapid progress made in the chemistry and biosynthesis of the various indole alkaloids. Furthermore, the latter two disciplines have benefited

from a chemotaxonomic understanding in the search of new alkaloids and in the elucidation of biosynthetic pathways.

Over 2000 indole alkaloids are known at present. These include compounds with the true indole chromophore and those derived from it. Furthermore, the indole alkaloids are subdivided according to structural and biogenetic considerations. Only the class of indole alkaloids relevant to discussion of *Ophiorrhiza acuminata* alkaloids will be reviewed at this point.

2.1.1 β-Carboline Alkaloids

The β-carboline alkaloids constitute a group of alkaloids derived from simple variations in the oxidation state of the β-carboline ring system. These alkaloids, of which eleagnine **9** and harman **10** are the simplest members of the series, occur in various plant families, e.g. Leguminoseae and Rubiaceae. Cordell[30] had classified indole alkaloids with β-carboline ring system as Harmala alkaloids.

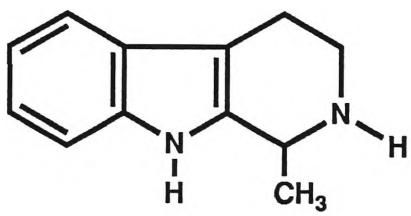

Eleagnine 9

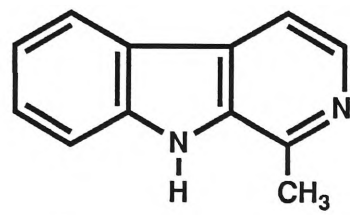

Harman 10

In β-carboline itself, the pyridine nitrogen is weakly basic but in the tetrahydroderivatives, the piperidine nitrogen is quite strongly basic. The indole NH is acidic in both cases. Most of the Harmala alkaloids are substituted at C-1 by a methyl group and the parent compound having this structure is known as harman.

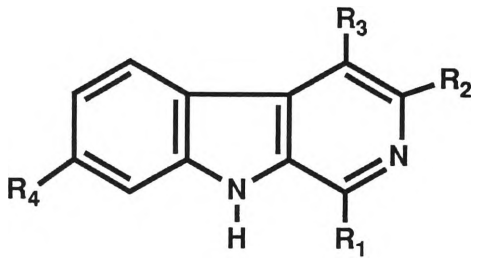

R_1	R_2	R_3	R_4	
CH_3	H	H	OCH_3	Harmine 11
H	H	H	H	Norharman 12
CH_2OH	H	H	H	1-hydroxylmethyl-β-carboline 13
CH_3	$COOCH_3$	H	H	3-methoxy-carbonyl-1-methyl-β-carboline 14
$CH(OH)-CH_2OH$	H	OCH_3	H	1-(1',2'-dihydroxy)-ethyl-4-methoxy-β-carboline) 15
$CH=CH_2$	H	OCH_3	H	4,8-dimethoxy-1-vinyl-β-carboline 16

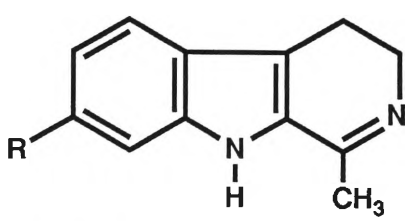

R

OCH_3 Harmaline 17

OH Harmalol 18

The β-carbolines, simple in structure as they may seem, have been reported to exhibit a wide range of pharmacological activities. Eleagnine **9** and harmine **11** were once used for treatment of tremors in Parkinson's disease.[31] A study made by Ohmoto and Koike[32] showed that some β-carbolines, unlike other herpes drugs which are nucleic acids, are potential inhibitors of herpes virus. Those found to be effective against HSV-1 are the alkaloids norharman **12**, harman **10**, 1-hydroxylmethyl-β-carboline **13**, 3-methoxy-carbonyl-1-methyl-β-carboline **14**, 7-methoxy-methyl-β-carboline (harmine) **11**, 1-(1', 2'-dihydroxy)ethyl-4-methoxy-β-carboline **15** and 4,8-dimethoxy-1-vinyl-β-carboline **16**.

Al-allaf and his group[33] found that a range of novel complexes of Platinum and Palladium with β-carboline alkaloids harmaline **17**, harmalol **18**, harmine **11** and harman **10**, exhibit some antitumour activity. Some β-carbolines were able to potentiate mutagenecity of benzo[α]pyrene, but they themselves were not mutagenic.[34,35] Rashan[36] found harmine **11** and harmaline HCl to exhibit antiviral activity against *Herpes virus hominis* type I, with harmalol found to be inactive.

A number of β-carbolines have been found to be potent inhibitors of the monoamine oxidase enzyme with the aromatic β-carbolines found to be better inhibitors than their corresponding tetrahydroderivatives. Alkylation at N-9 nitrogen increased the activity quite remarkably[37] while substitution of N-2 nitrogen of the β-carbolines by CH completely supressed monoamine oxidase inhibitory activity.[38]

As a result of the reported biological activities observed for this class of indole alkaloid, several groups examined aspects of the synthetic chemistry. Synthesis of β-carbolines was initiated by

Kernack[39] in 1921 when the condensation product of tryptophan **19** with acetaldehyde in the presence of acid was oxidised with $K_2Cr_2O_7$. The resulting base was found to be harman **10**, identical to the base obtained by Hopkins *et al*[40] in 1903 by the oxidation of tryptophan **19** with ferric chloride in the presence of ether.

Harman **10**, which was first prepared as a degradation product of harmine **11**[41], also occurs in Nature. The alkaloids, loturine[42] and aribine[43], isolated from *Symploccus racemosa* Roxb and *Arariba rubia* Mart, respectively, were found to be identical to harman **10**.

Early syntheses of β-carbolines involve two general reactions: (a) ring closure of various acid amides of tryptophan **19** with the aid of P_2O_5 in boiling xylene giving rise to dihydroharman or its derivatives.[44,45] Subsequent dehydrogenation with Pd black yielded harman **10**[46]; (b) the condensation of tryptamine **20** with paraldehyde giving the tetrahydroharman.[47] The alkaloid eleagnine **9** was shown to be the racemic form of tetrahydroharman.[48]

At present, in the syntheses of β-carbolines, the Pictet-Spengler condensation is the most widely used reaction, carried out in a protic solvent, which most likely resembles the *in vivo* conditions.[49]

The carbolines have long been a subject of biosynthetic speculations with the farsighted proposal by Perkin and Robinson[50] in 1919, that they arise *in vivo* from a Mannich condensation between a tryptamine derivatives and acetaldehyde. So far, few studies have provided data on carboline alkaloid biosynthesis.

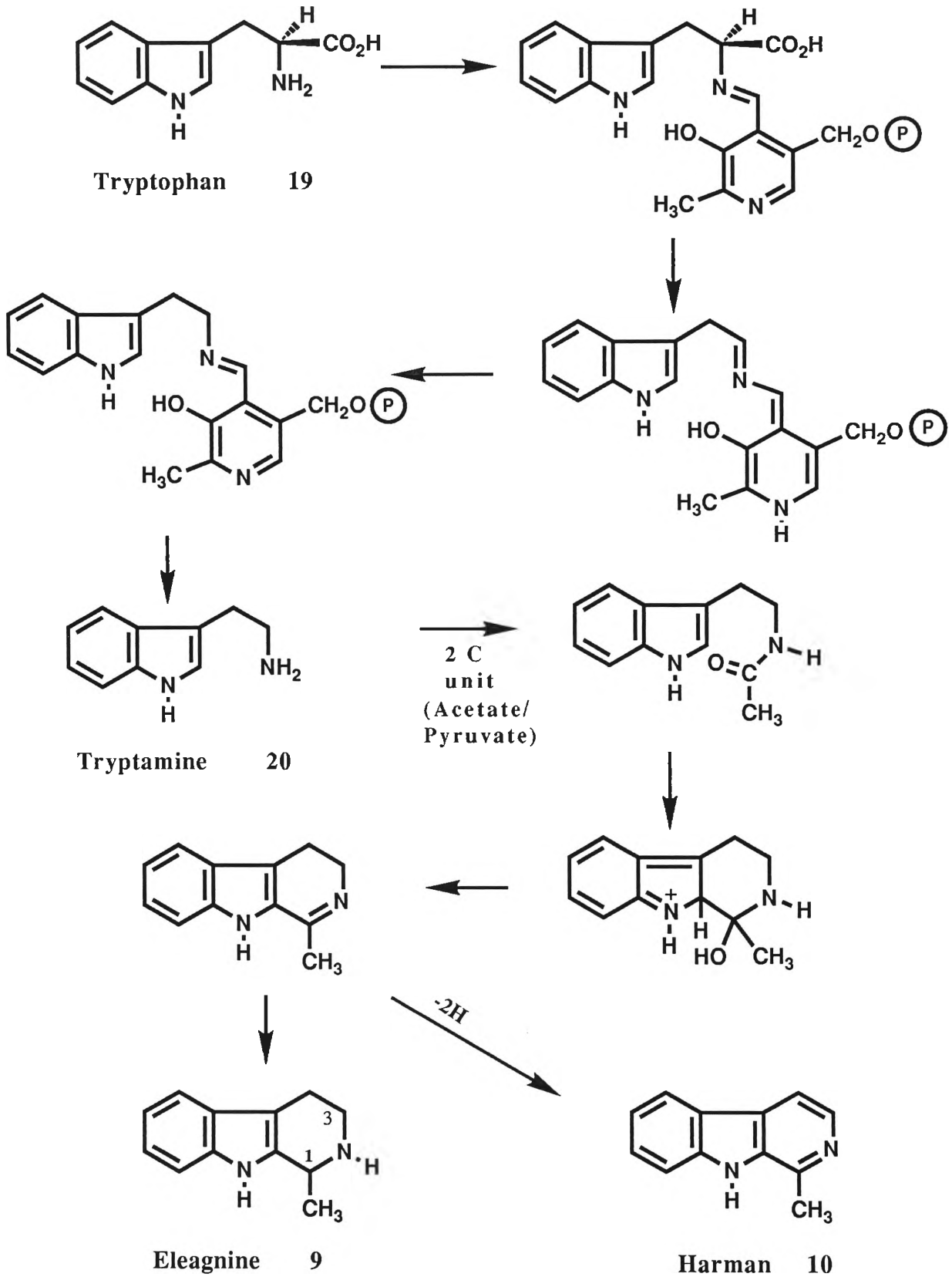

Scheme 1. Possible Pathway for the Biosynthesis of Eleagnine **9**[51] and Harman**10.**[52]

O'Donovan and Kenneally[51] examined the formation of eleagnine **9** in *Elaeagnus angustifolia*. Feeding experiments with [2'-^{14}C]-DL-tryptophan and sodium [1-^{14}C]acetate yielded a radioactive alkaloid, labelled exclusively at C-3 and C-1 respectively, in support of the Perkin-Robinson proposal. Surprisingly though, the extent of incorporation of the two precursors was low (0.01% C-3 and 0.003% C-1).

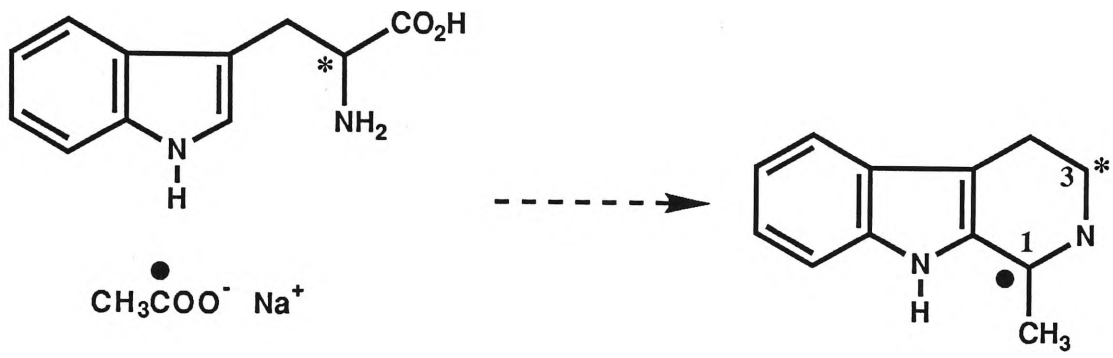

Scheme 1 shows a possible pathway for the biosynthesis of eleagnine **9** based on the above feeding experiments. A pyridoxyl phosphate-catalysed decarboxylation yields tryptamine **20** which condenses with acetyl coenzyme A or some other suitable 2C donating species, to ultimately produce eleagnine **9**.

A thorough study of the biosynthesis of harman **10** in *Passiflora edulii* was reported by Slaytor and Macfarlane[52] (Scheme 1). Evidence that tryptamine **20** and N-acetyltryptamine are intermediates in the tryptophan **19** to harman **10** conversion were presented. N-acetyl-[2'-^{14}C]-tryptophan was shown not to serve as a precursor for harman **10**, while [1'-^{14}C]-tryptamine and N-acetyl-[1'-^{14}C]-tryptamine were both utilised to form specifically the labelled alkaloids. Free tryptamine **20** was detected in the plant, however the presence of N-acetyltryptamine could not be

Table 1. Some Monoterpene Indole Alkaloids of Pharmacological Significance.

Compounds	**Sources**	**Pharmacological Activity**
Ajmalicine	*Catharanthus roseus*	hypotensive
Ajmaline	*Rauwolfia sp.*	antirythmic
Camptothecin	*Campthotheca acuminata*	anticancer
Deserpidine	*Rauwolfia carescens*	hypotensive
Ibogaine	*Tabernanthe iboga*	psychotomimetric
Leurocristine	*Catharanthus roseus*	anticancer
Quinidine	*Remijia sp.*	cardiac depressant
Quinine	*Cinchona sp.*	antimalarial
Rescinnamine	*Rauwolfia sp.*	hypotensive
Reserpine	*Rauwolfia vomitoria*	hypotensive
Strychnine	*Strychnos mux vomica*	CNS depressant
Vincaleukoblastine	*Catharanthus roseus*	anticancer
Vincamine	*Vinca major*	hypotensive

directly established. Stolle and Groger[53] in their study of the biosynthesis of harmine **11**, showed that the two carbon-unit of the β-carboline ring system is generated either from acetate or pyruvate.

2.1.2 Monoterpenoid-Derived Indole Alkaloids

This is the major group of indole alkaloids and numbers over 700 members of widely differing structure and pharmacologic activity. Representative alkaloids of this group are listed in Table 1 together with their therapeutic importance and sources.

Biosynthetic experiments have established that the fundamental building blocks for monoterpene indole alkaloids are tryptamine (derived from tryptophan) and the iridoid secologanin **21**.

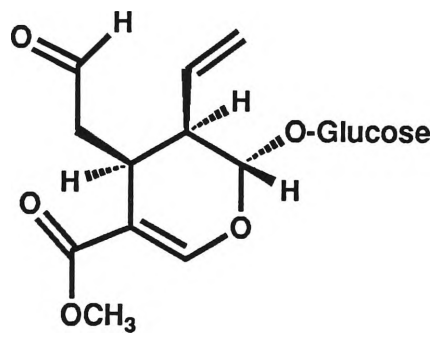

Secologanin 21

Condensation of these two compounds forms (*in vivo*) strictosidine **22** (formerly named isovincoside) and its epimer vincoside **23**, the nitrogenous glycosides which are the key intermediates in the biosynthetic elaborations of the indole alkaloids.

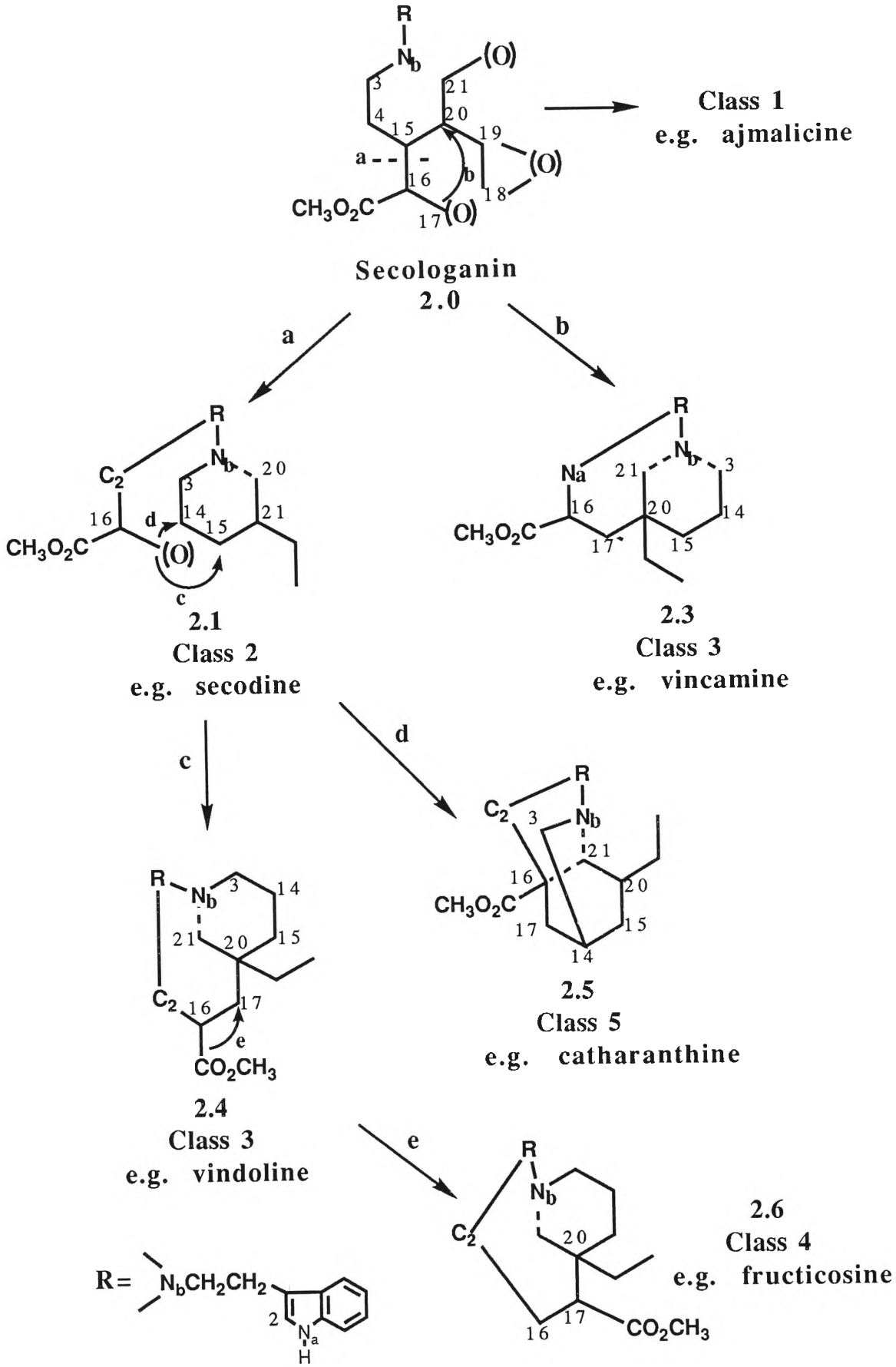

Scheme 2. Classification of Indole Alkaloids by Kompis, Hesse and Schmid.[54]

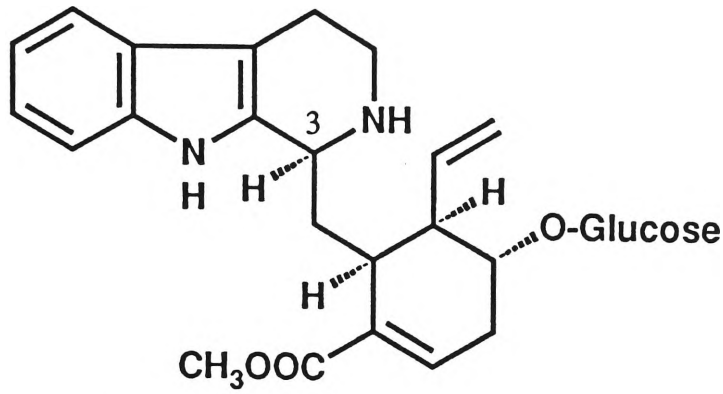

Strictosidine 22

Vincoside (C-3 epimer) 23

Because the building units for the indole alkaloids have already been established, a secure foundation through which a biogenetically based system for the classification of these bases can be constructed. Thus, in 1971, Kompis, Hesse and Schmid[54], presented a new approach to the classification of indole alkaloids based on the structural framework established by biosynthesis studies (Scheme 2).

According to Scheme 2, the indole alkaloids can be divided into 5 major classes, as follows: (1) Class 1, represented by ajmalicine **24**, contains the non-rearranged secologanin unit, (2) Class 2, which arises from pathway **a** as shown in Scheme 2, is typified by secodine **25**, (3) Class 3, such as vincamine **26**, involves process **a** and a rearrangement via **b**; vindoline **27** is also typical of Class 3 which arises from the rearrangement of skeleton 2.3 via process **c**, (4) Class 4, of which fructicosine **28** is typical, involves rearrangement of the structural unit of Class 3 via pathway **e**; and (5) Class 5 which includes catharanthine **29** involves the attachment of C-17 to C-14 via route **d** as shown in the scheme. These classifications may be of use in the field of chemotaxonomy of indole alkaloid-bearing plants.

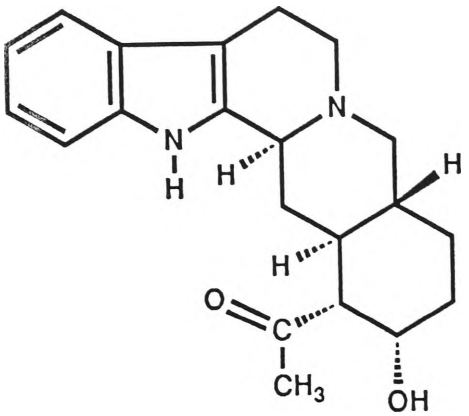

Yohimbine 30

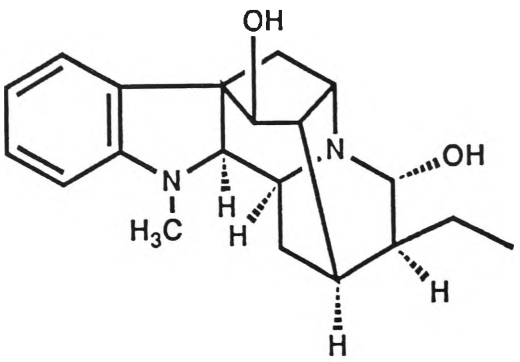

Ajmaline 31

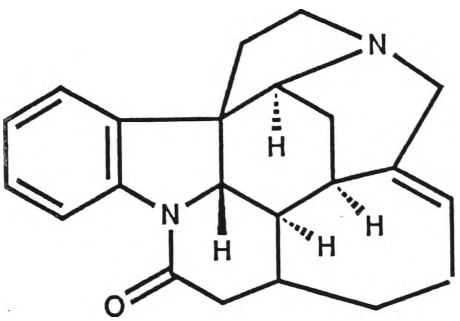

Strychnine 32

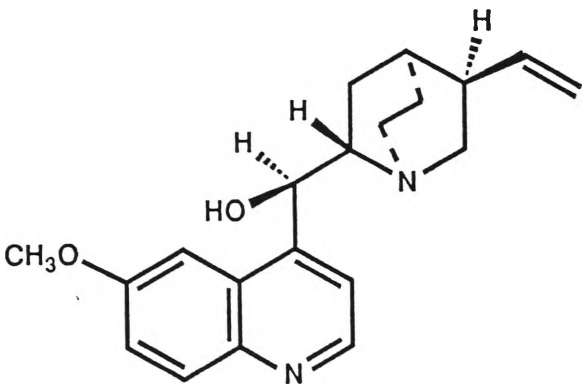

Quinine 33

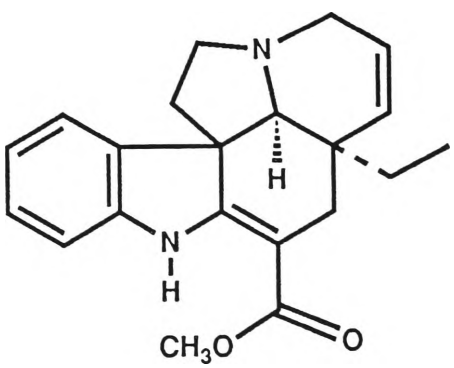

Tabersonine 34

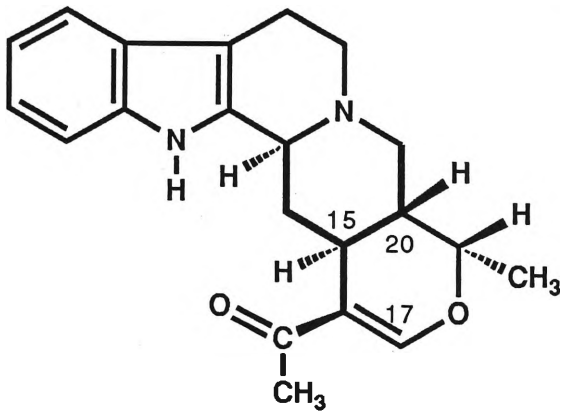

Ajmalicine 24

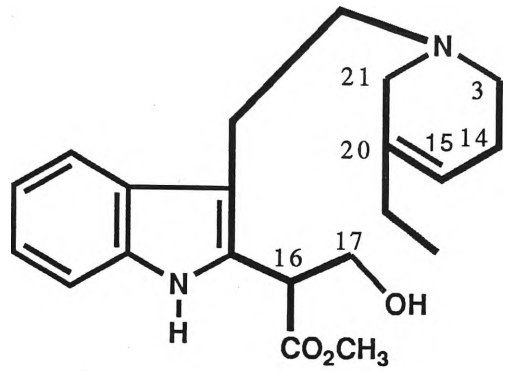

Secodine 25

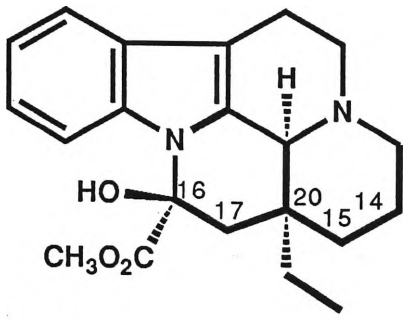

Vincamine 26

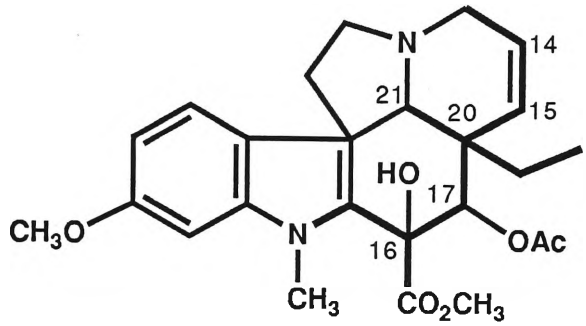

Vindoline 27

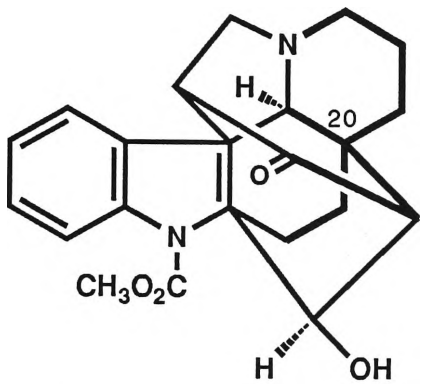

Fructicosine 28

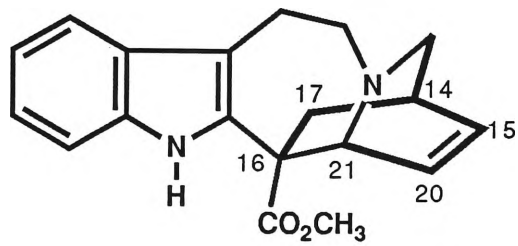

Catharanthine 29

Dalton[31], in his review on the biosynthesis of monoterpenoid indole alkaloids, had renamed the above classes into five widely recognised categories: namely, (1) Corynanthe-Strychnos bases as represented by ajmalicine **24**, yohimbine **30**, reserpine **5**, ajmaline **31** and strychnine **32**; (2) the Cinchona alkaloids, of which quinine **33** is typical; (3) the Iboga alkaloids such as catharanthine **29**; (4) the Aspidosperma bases as typified by tabersonine **34** and (5) the

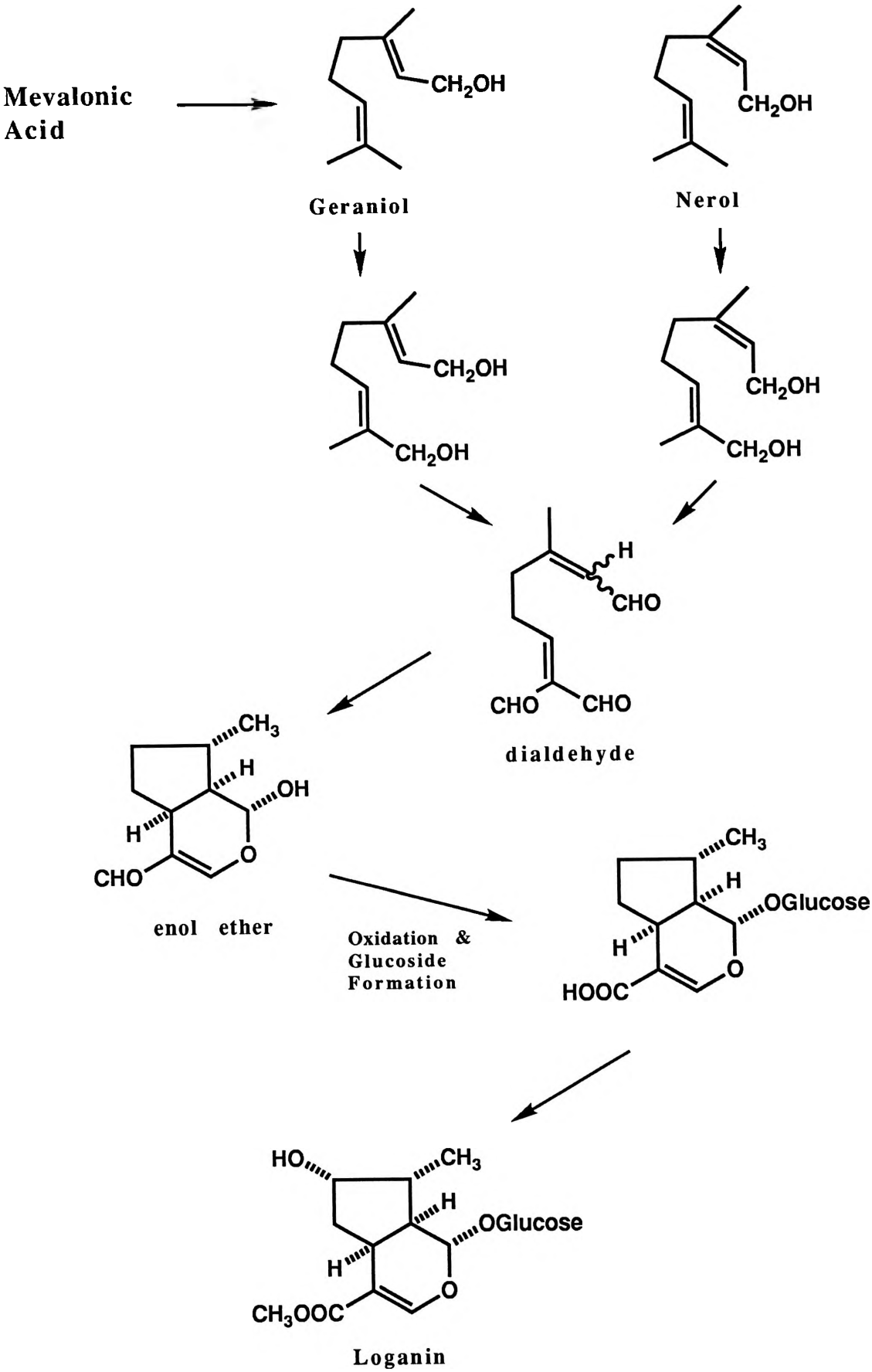

Scheme 3. Transformation of Geraniol 36/Nerol 37 into Loganin 38

Eburna family, which includes vincamine **26**. These categories have since been widely used in discussions of monoterpenoid indole alkaloids.

Secologanin **21** has been established to be the source of the C_9-C_{10} unit of monoterpenoid indole alkaloids. Several studies have proved that the secologanin unit did not come from phenylalanine, tyrosine, malonate, acetate and formate[55,56]; shikimic acid[57]; methionine[58]; or glycine.[59] Instead, based on the investigations conducted independently by Battersby[60], Scott[61], Arigoni[62] and their co-workers, on a single plant *Vinca roseus*, the C_9-C_{10} unit as represented by the Corynanthe-Strychnos, Aspidosperma and Iboga skeletons, is derive from two molecules of mevalonic acid **35**.

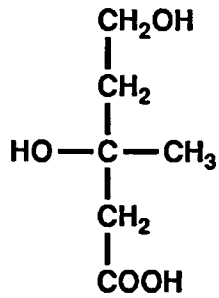

Mevalonic Acid 35

The conversion of mevalonic acid to secologanin **21** involves 3 distinct transformations: (a) the conversion of mevalonate to geraniol **36** and its trans isomer nerol **37**; (b) the transformation of geraniol **36** and/or nerol **37** into loganin **38** (Scheme 3), and (c) the cleavage of loganin to secologanin **21**.

The transformation of geraniol or nerol involves the conversion of a dialdehyde to an enol ether into the intermediate deoxyloganic acid and eventually to loganin. Loganin is a key intermediate on the biosynthetic pathway to the complex indole

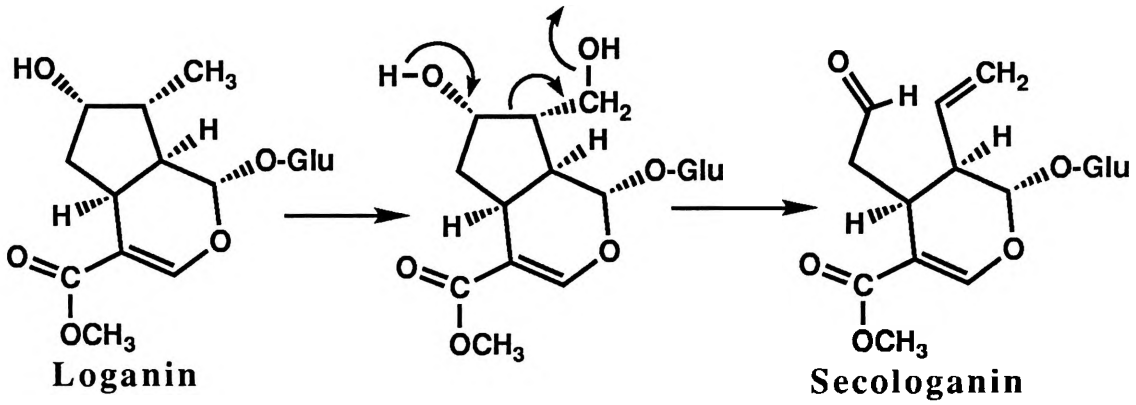

Equation 1

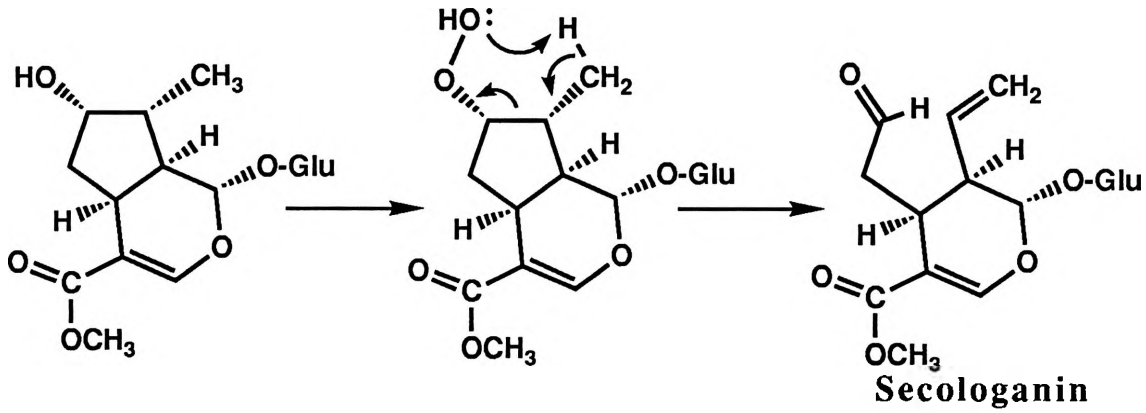

Equation 2

alkaloids and its transformation from geraniol and nerol is very critical in the stereochemical evaluation of the secologanin unit of the monoterpenoid indole alkaloids. The trans isomer nerol **37** and its hydroxyderivative are incorporated slightly better than is geraniol.[31]

Several possible pathways have been postulated for the conversion of loganin **38** to secologanin **21.**[31] One possible pathway is the oxidation of loganin **38** to the unknown hydroxyloganin **39** and a cleavage reaction leading to secologanin (Equation 1). Another possible route is the introduction of a suitable leaving group onto the hydroxyl (e.g., as a peroxide) and cleavage in the opposite way to route (a) (Equation 2).

The condensation of tryptophan and secologanin leads to the formation of isovincoside, now called strictosidine, **22** and its C-3 epimer vincoside **23** (Scheme 4). Initially, it was believed that Corynanthe-Strychnos, Aspidosperma and Iboga alkaloids were derived from vincoside which was considered to be the product of the reaction between tryptamine and secologanin.[63] However, biosynthetic studies on *Catharanthus roseus* cell cultures showed that the sole product of the condensation between tryptamine and secologanin is strictosidine.[64-67] The confusion on the stereochemistry of the C-3 position was eventually cleared up with biosynthetic studies conducted on cell-free extracts of *C. roseus.* Strictosidine was transformed to ajmalicine, vindoline and catharanthine and negligible incorporation of vincoside into these alkaloids were found.[64, 65, 68-70]

A summary of further elaborations of strictosidine into the major class of monoterpenoid alkaloids is shown in Scheme 5.

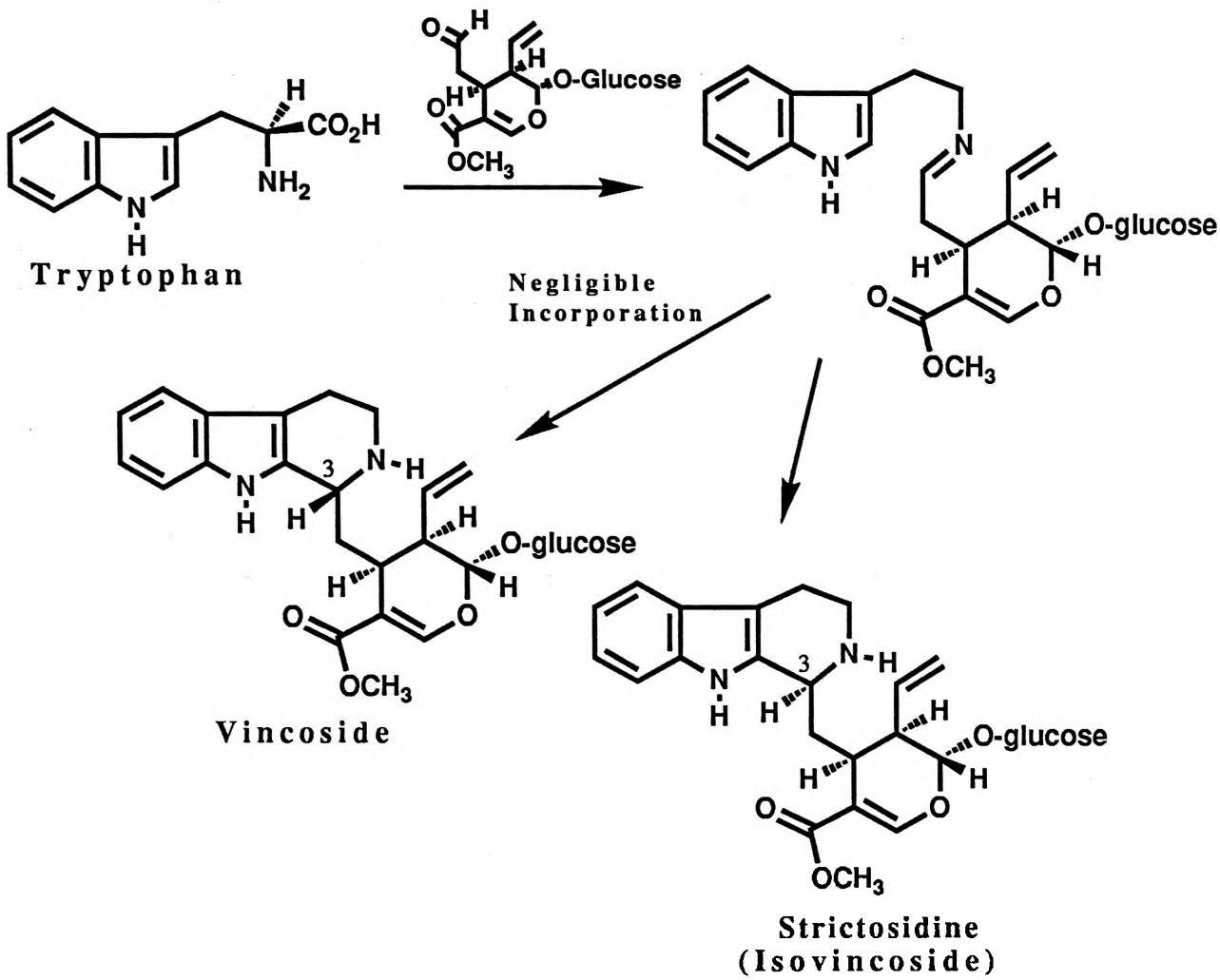

Scheme 4. Biosynthesis of Vincoside **23** and Strictosidine (Isovincoside) **22**.

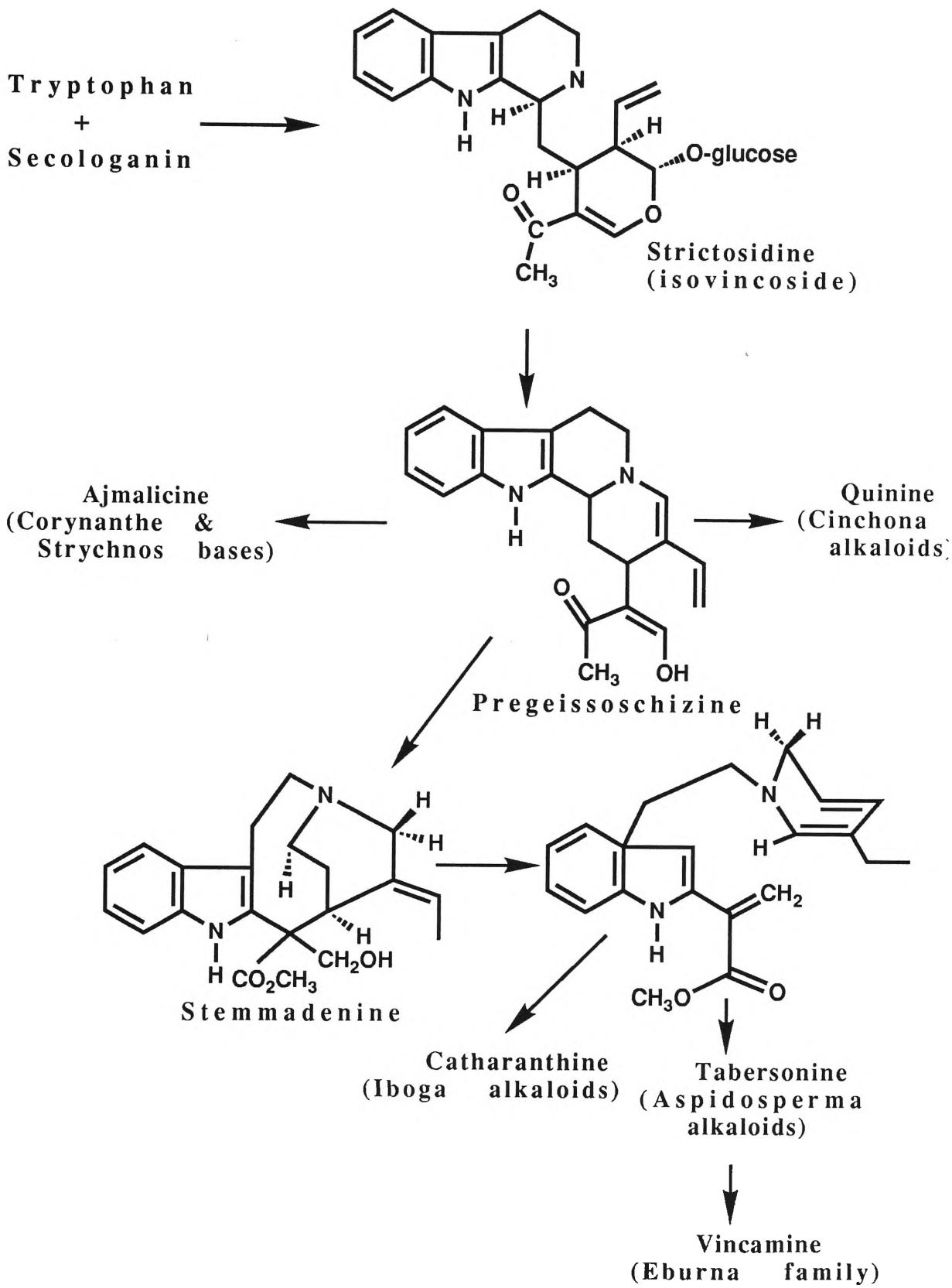

Scheme 5. Sequence of Formation of the Five Bases as Categorised by Dalton.[31]

2.1.3 Genus *Ophiorrhiza*

Since the first reported literature on the Genus *Ophiorrhiza* in 1959, only four species have been reported namely, *Ophiorrhiza mungos*, *Ophiorrhiza japonica*, *Ophiorrhiza kurowai* and *Ophiorrhiza pumila*.

Ophiorrhiza mungos Linn. is a small herbaceous shrub indigenous to southeast Asia and South India. Ethnomedical information reveals the roots, which are bitter, to be useful for the treatment of snake bites and rabies. Another report states that this plant is useful in the treatment of cancer.[71,72] Preliminary chemical examination of the roots showed the presence of β-sitosterol, 5α-ergost-7-ene-3β-ol and 5α-ergost-8-(14)-en-3β-ol (as an ester).[71] In a routine screening for antiviral activity conducted by Tafur *et al*[72], the alcoholic extract of *O. mungos* leaves, roots and stems was shown to be a potent inhibitor of herpes virus. Two active compounds identified as camptothecin **40** and 10-methoxycamptothecin **41** were isolated from the leaves of *O. mungos* by a bioassay-directed fractionation method.[73] Both compounds were found to be active using a plaque reduction assay for herpes virus.

Camptothecin and 10-methoxycamptothecin were first isolated by Wall *et al*[73] from the rare chinese tree *Camptotheca acuminata* (Nyssaceae) in small yield. Recently, *Mappia foetida* has been reported to be a rich source of these compounds.[74]

Camptothecin **40** is a potent antileukemic and antitumor agent in experimental animals.[75] While 10-methoxycamptothecin **41** has not been reported as an inhibitor of herpes virus, it has been shown to fragment DNA.[76] However with the plaque reduction

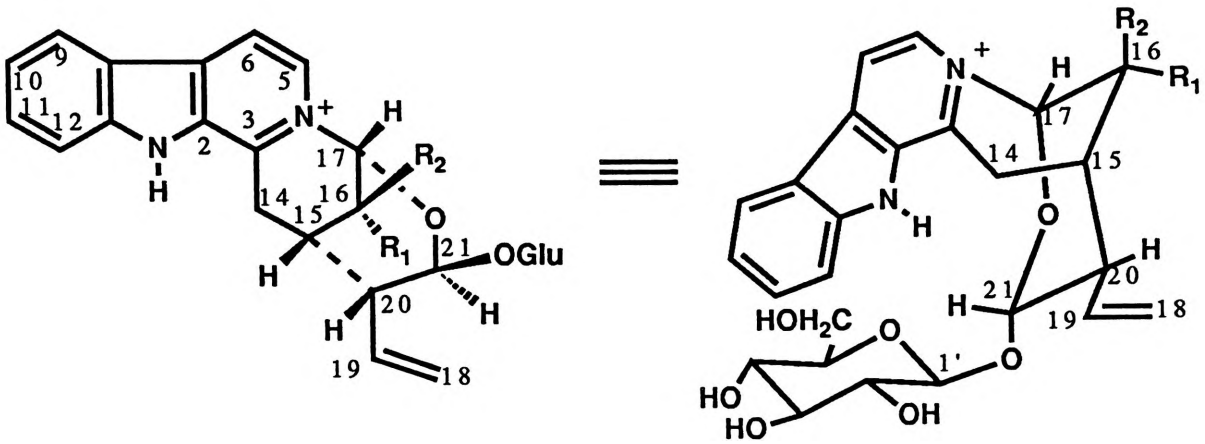

R_1 = H , R_2 = COO^- Ophiorine A 42

R_1 = OCH_3, R_2= H Ophiorine B 43

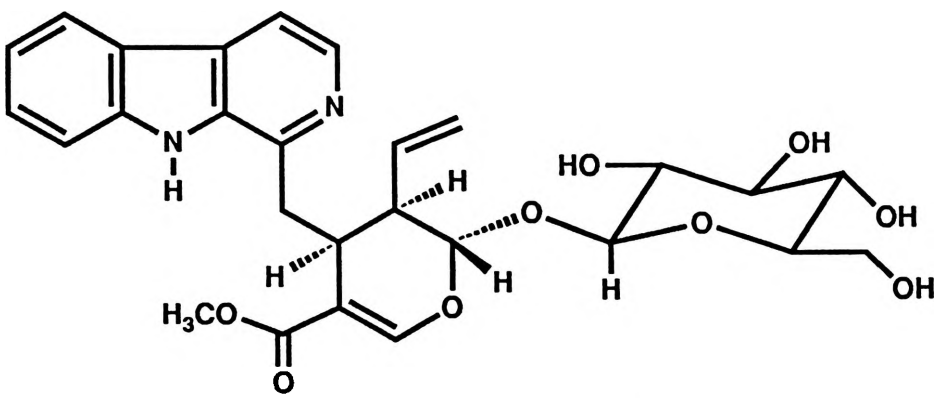

Lyaloside 44

assay, the methoxy analog is about 8 times more potent than camptothecin **40** as a herpes virus inhibitor.[72]

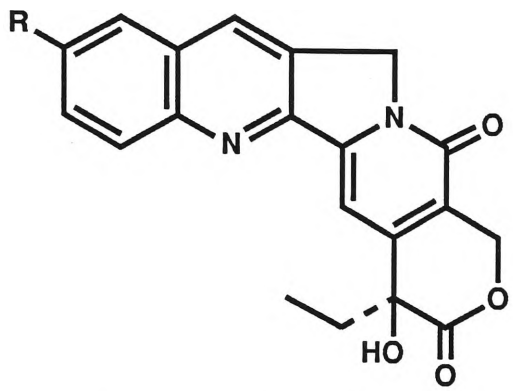

R = H Camptothecin 40

R = OCH_3 10-Methoxycamptothecin 41

A study made on the constituents of *O. japonica* Bl. by Fujita and Sumi[77] showed the ethereal extract to contain the β-carboline alkaloid harman **10**, friedelin and β-sitosterol. The methanolic extract gave harman as the sole alkaloid.

With the report on the isolation of campthothecin from this genus, Aimi and his group took a closer look at the constituents of *O. japonica*. In 1985, he reported the isolation of two novel betaine type indole alkaloids, Ophiorines A **42** and B **43** from the water layer obtained from the alcoholic extract of the leaves of *O. japonica*.[78] Both compounds were identified by chemical and spectroscopic methods. On methylation of Ophiorines A and B with CH_2N_2 in CH_3OH, retro Michael reaction was observed to occur yielding the known glucoindole alkaloid lyaloside **44**.[79]

This observation together with the ^1H and ^{13}C chemical shift arguments allowed the deduction of the stereochemical configuration of Ophiorines A and B at C-15 (and therefore, C-17), C-20, and C-21. Of the more than 20 glucoindole alkaloids found in

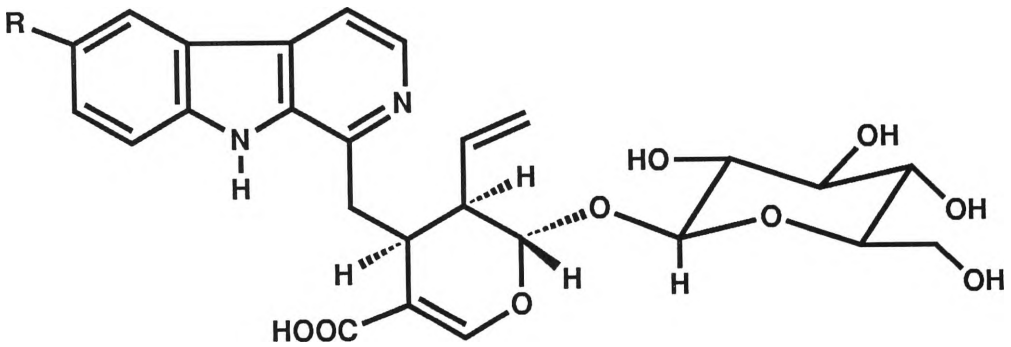

R = H Lyalosidic Acid 45
R = OH 10-Hydroxylyalosidic Acid 46

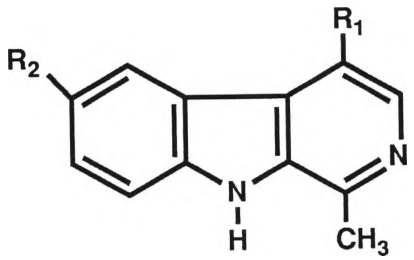

R_1 = OH R_2 = H 6-Hydroxyharman 47

R_1 = H R_2 = OH 10-Hydroxyharman 49

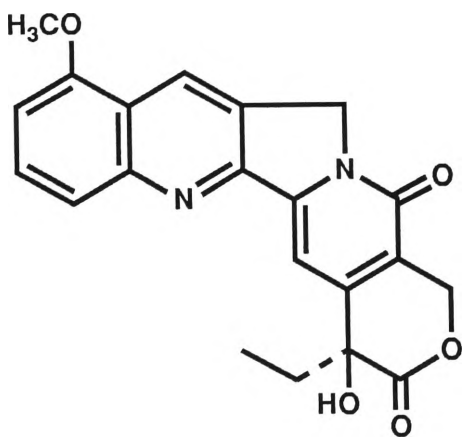

9-Methoxycamptothecin 48

nature,[78] Ophiorines A and B are unique for possessing $N_{(b)}$-C_{17} linkage and β-carbolinium type structure. The same alkaloids, Ophiorines A and B, together with several other constituents were also found in *O. kurowai* which grows in Ishigaku and other south-west islands of Okinawa Prefecture.[79]

A year later, Aimi and his group reported the isolation of two more new glucosidic alkaloids namely, lyalosidic acid **45** and 10-hydroxylyalosidic acid **46**, together with a known β-carboline alkaloid, 6-hydroxyharman **47** from *O. japonica*.[79] Lyalosidic acid, together with harman, camptothecin **40**, 9-methoxycamptothecin **48** and 10-methoxycamptothecin **41** were also isolated from *O. kurowai*.[80]

The alkaloid 6-hydroxyharman **47** is the second simple β-carboline found in genus *Ophiorrhiza* since Fujita and Sumi isolated harman from the same plant.

Enzymatic hydrolysis of the glucosidic linkage of lyalosidic acid **45** and 10-hydroxylyalosidic acid **46** yielded harman **10** and 10-hydroxyharman **49** instead of the desired aglycone which was intended to serve as the starting material for biomimetic chemical conversion. These results, together with the isolation of a simple β-carboline like 6-hydroxyharman **47** and harman **10** and their corresponding glucoalkaloids in the same plants, strongly suggested a close relationship between these two types of constituents.

The wide distribution of harman, accompanying monoterpenoid indole alkaloids has been noted in Rubiaceous plants.[81,82] In some plants, like *O. japonica*, the coexistence of simple β-carbolines with their corresponding glucoindole alkaloids has been demonstrated, e.g. harman and palinine in *Palicourea alpa*[83], and 3-methoxycarbonylharman[84], and desoxycordifolinic

acid[85] in *Nauclea diderichii.* Hence, Aimi and his group proposed a new mechanism for harman formation which operates, probably secondarily, in *Ophiorrhiza* and other related Rubiaceous plants. It is based on the observed facile fragmentation of some β-carboline type monoterpenoid glucoindole alkaloids induced by enzymatic cleavage of the glucosidic bonds.

This mechanism for the formation of harman presents a striking contrast to the normal biosynthetic pathway of the harman class of alkaloids, in which a two-carbon unit (C_1-C_{10}) originates from acetate or pyruvate and the remaining part comes from tryptophan **19** through tryptamine **20**, as proven in Zygophyllaceae, Elaeagnaceae, Passifloraceae and other plant families.[86]

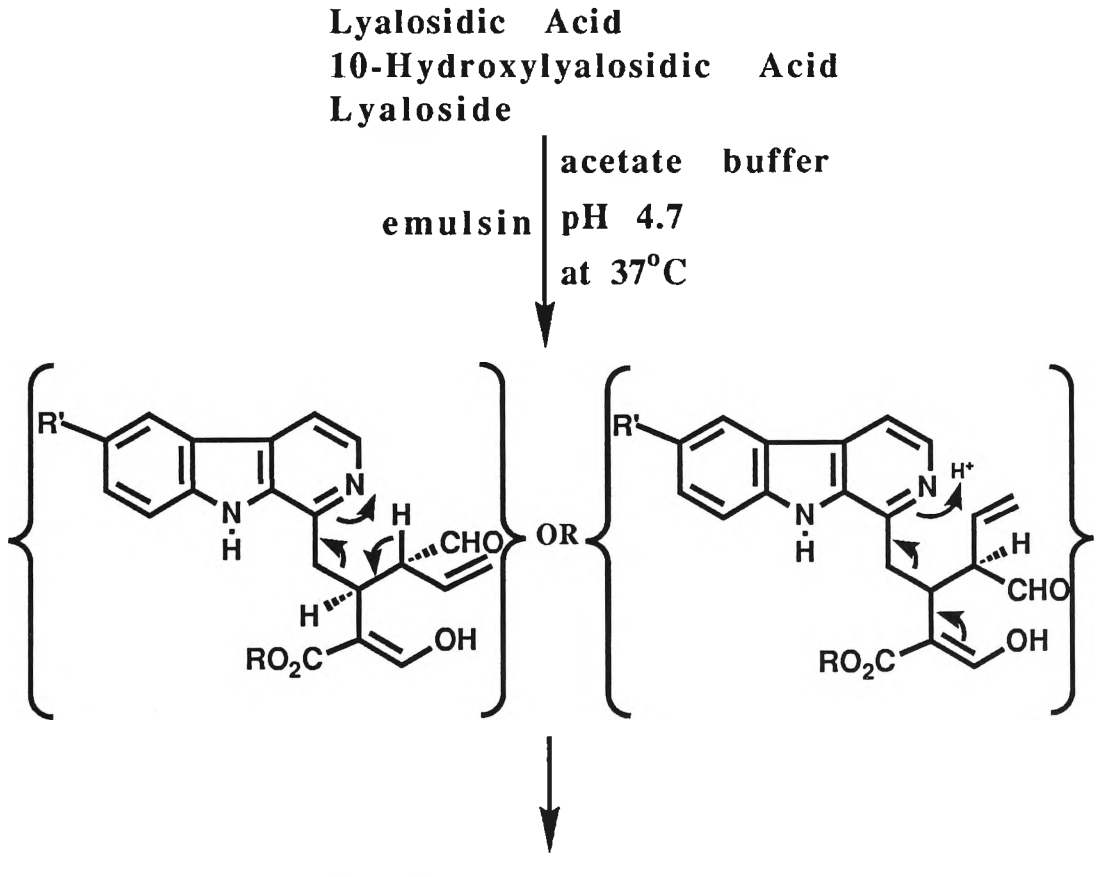

In 1989, Aimi and his group reported the isolation of two novel glucosidic alkaloids, pumiloside **50** and deoxypumiloside **51** from *O. pumila*.[87] These alkaloids are related in structure to camptothecin **40** and have previously been suggested to be plausible intermediates in camptothecin biosynthesis.[88] Their isolation therefore had shed light over camptothecin formation process in living plants.

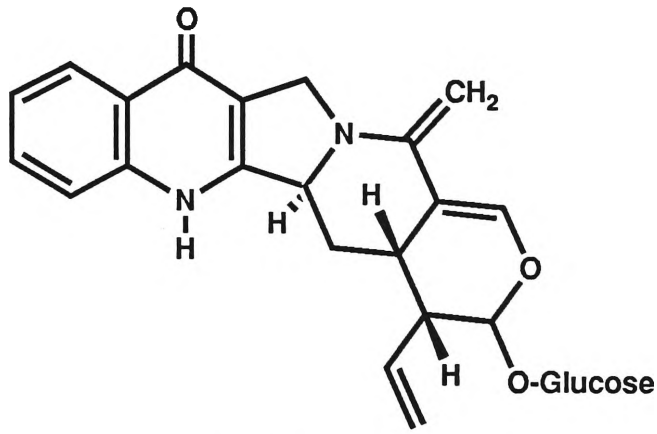

Pumiloside 50

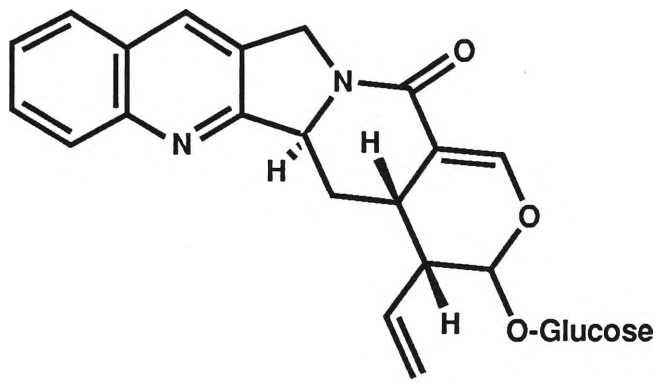

Deoxypumiloside 51

It is interesting to note that *O. pumila*, which also contain camptothecin, showed no trace of harman **10**, lyaloside **44** and other member of β-carboline derivatives which were found in other species of *Ophiorrhiza*.

After Aimi's reported isolation of pumiloside **50** and deoxypumiloside **51**, a joint research group by Smith Kline Beecham and a group at Virginia University reported the presence of pumiloside in *Camptotheca acuminata*.[89]

Because of the interesting findings in *O. pumila*, Aimi and his group continued their study on the said plant. This, eventually led to the isolation of the first natural glycocamptothecin alkaloid named chaboside **52**[90] This compound carries 2 oxygen atoms on the ring A. Recently, synthesis of camptothenoid glycosides were reported[91] and these were found to be pharmacologically active.

From the same plant, a new ionone glucoside, inamoside **53**, related in structure to Blumenol A, was obtained.[92]

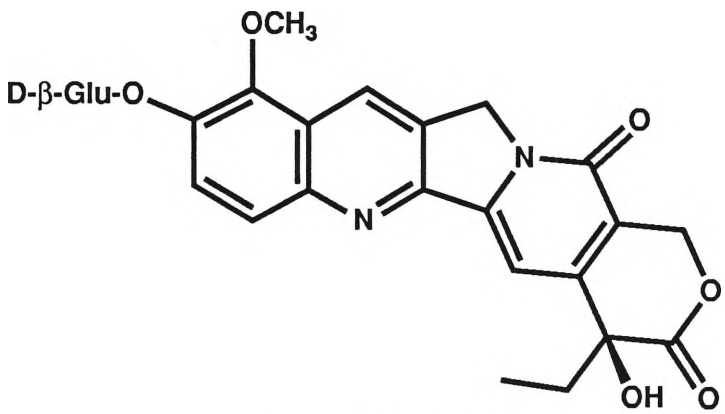

Chaboside 52

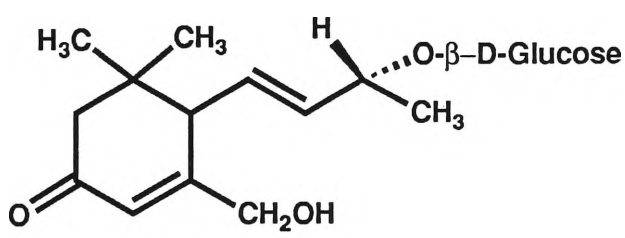

Inamoside 53

2.1.4 *Ophiorrhiza Acuminata* Linnaeus (Rubiaceae)

Ophiorrhiza acuminata , code REB 034, was identified by Mrs. Rose Madulid and Dr. Domingo Madulid from the National Museum, Philippines. This was collected in 1988 in the forest of northwest Palawan near Port Barton facing the China Sea during alkaloid field screening conducted by the University of Santo Tomas Research Centre at the Island of Palawan. A herbarium specimen of the plant is kept at the University of Santo Tomas Research Centre, Manila, Philippines.

O. acuminata, locally known as Payang-payang-gubat (Tagalog) or mongoose plant (English) is found from the Bataan and Babuyan Islands and northern Luzon to Palawan and Mindanao, in thickets and forests at low altitudes. It also occurs in India to Malaya.

No chemical examination on this plant has been reported in the literature to date. This, together with the isolation of biologically active alkaloids from this genus, prompted us to undertake a detailed chemical study of this plant.

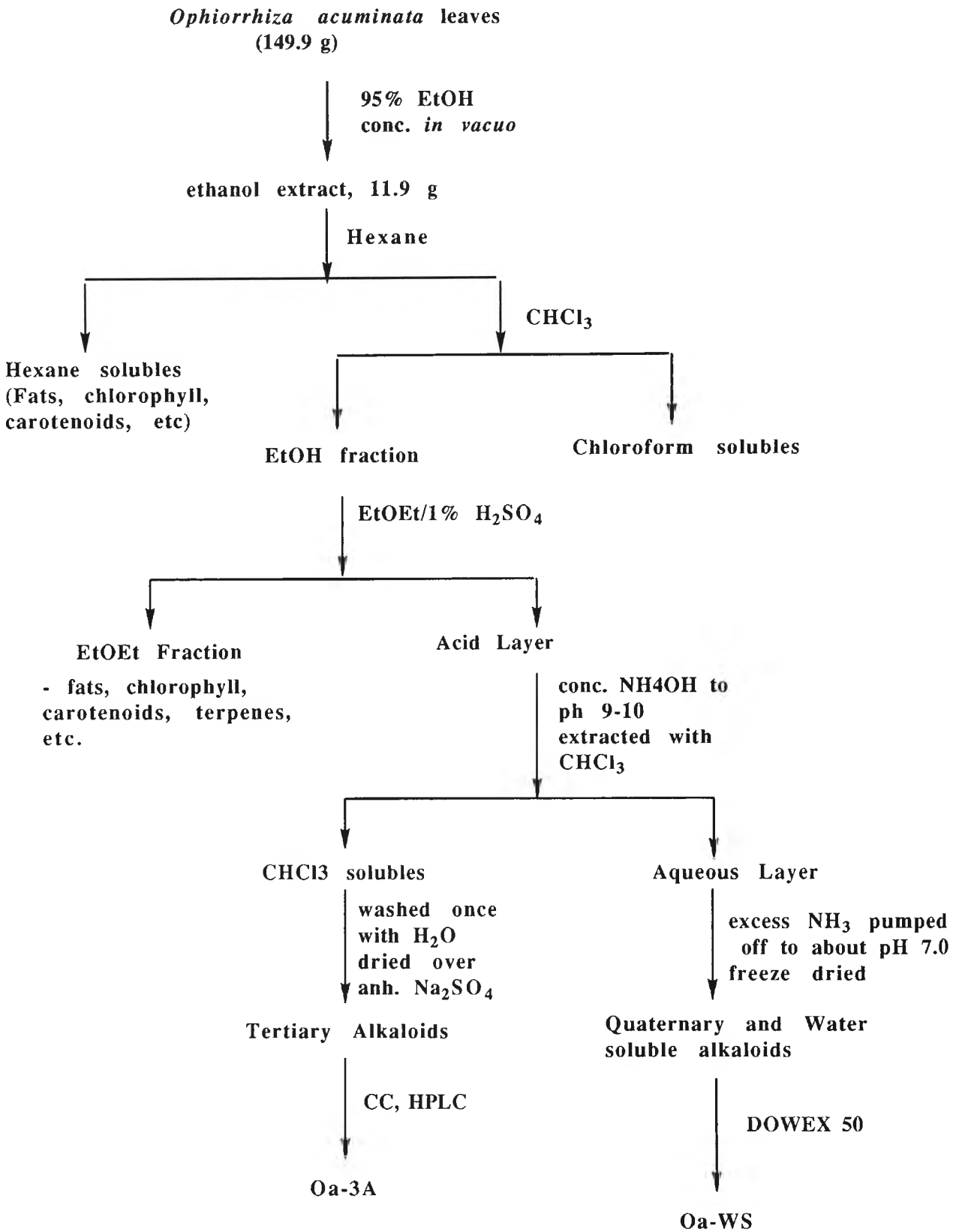

Scheme 6. Flowchart for the Fractionation and Isolation of *O. acuminata* Alkaloids.

2.2 RESULTS AND DISCUSSION

Ophiorhhiza acuminata leaves, 149.9 g, yielded 11.94 g of ethanolic extract. The crude ethanolic extract was fractionated by sequential solvent extraction which led to a hexane-soluble oil fraction, a chloroform-soluble fraction, and a green resinous EtOH fraction. Alkaloid extraction on the semi-purified ethanolic fraction was achieved following a standard acid-ether extraction procedure shown in Scheme 6. Repeated chromatographic purifications gave three alkaloids, harman, lyalosidic acid and Oa-4A-2.

2.2.1 Tertiary Alkaloid, Oa-3A (Harman)

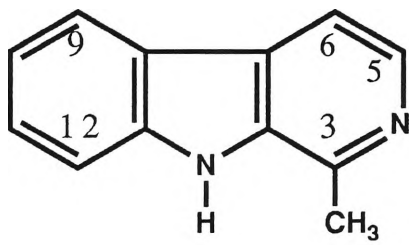

Oa-3A

Oa-3A was obtained as light yellow crystals on recrystallisation from chloroform, m. pt. >195°(dec). The UV spectrum in CH_3OH showed absorption indicative of a highly conjugated system, λ 348.4, 335.2, 287.6, 235.6, 217.4 nm. The infrared spectrum showed a weak absorption for the NH group of the indole ring. The HREIMS gave a *m/z* at 182.0829 consistent with $C_{12}H_{10}N_2$ indicating that the compound contained 9 double bond equivalents. Therefore, the molecule was clearly aromatic as evidenced from the ^1H NMR spectrum which showed 6 aromatic protons, one exchangeable proton (D_2O) and a methyl singlet. These data suggested that the structure of Oa-3A was

Table 2. ^{1}H and ^{13}C NMR Assignments for Oa-3A [CD_3OD, referenced at δ3.35 (^{1}H) and δ49.0 (^{13}C)].

Carbon	^{13}C, δ[a]	^{1}H, δ [integration, multiplicity, J in Hz][b]
2	134.5	
3	141.7	
5	138.8	8.36 (1H, d, 5.2Hz)
6	112.9	7.76 (1H, d, 5.2Hz)
7	128.2	
8	121.8	
9	122.1	8.12 (1H, dd, 8.0Hz)
10	120.2	7.31 (1H, ddd, 8.0, 2.0Hz)
11	128.3	7.54 (2H, m)
12	111.5	7.54 (2H, m)
13	140.0	
14	20.2	2.83 (3H, s)
NH		8.65 (1H, s)

[a] assigned by comparison with referenced to Welti.[94]

[b] assigned by selective 1D decoupling experiments and by comparison with those from the literatures.[96-98]

that of harman **10** for which detailed ^{13}C NMR data have been reported by Welti[93] using the 2-D INADEQUATE NMR technique. More recently, harman has been used as a model compound to investigate a 1-D inverse detection method for the measurement of long-range heteronuclear couplings (**S**elective **I**nverse **M**ultiple **B**ond **A**nalysis).[94] Proton and ^{13}C NMR data for our isolated harman, Oa-3A, are summarised in Table 2 and serve as model data in the assignments of other *O. acuminata* alkaloids. Harman **10** occurs widely in plants and has been previously isolated from another species of the genus *Ophiorrhiza*, *O. japonica*[77].

2.2.2 Isolation and Structure Elucidation of Glucoindole Alkaloids

Preliminary purification of the aqueous fraction was done by ion exchange chromatography using DOWEX 50 which yielded a brown vermiculite-like solid labelled as Oa-WS, 540 mg. The TLC chromatogram [C18 TLC plate, n-Butanol:Acetic Acid:H_2O (4:2:1)] showed a major band with Rf=0.68 that gave a positive colouration with Dragendorff reagent. This same compound also gave a positive response (violet colouration) with α-naphthol-sulfuric acid indicating the presence of a sugar in the molecule. The UV spectrum in CH_3OH of Oa-WS gave an absorption identical to that obtained for Oa-3A suggesting a similarity in the molecular chromophore. These data suggested a glycoside derivative of the isolated tertiary alkaloid, harman.

Other chromatographic methods tested to isolate and purify the constituent glycosides included High Pressure Liquid Chromatography (HPLC) and Gel Filtration (gel permeation)

Chromatography. Reversed Phase HPLC using gradient elution with acetonitrile or methanol in water proved to be a better solvent system for isolating the glycoalkaloids. Preliminary purification by gel permeation chromatography which works on the principle of molecular sieving using Sephadex LH-20 with elution with either H_2O or CH_3OH afforded the glycoalkaloids based on their observed UV absorption spectra and ^1H NMR spectra. Details of these purification methods are included in the experimental section.

Eventually combined gel permeation chromatography and HPLC were used to isolate and purify the water soluble alkaloid. The Oa-WS was chromatographed twice on Sephadex LH-20 with CH_3OH. Two separate bands were obtained: one a yellow and the other a pale brown coloured band. Both gave UV spectra consistent with a β-carboline ring system. Preparative thin layer chromatography (PTLC) on SGF_{254} developed in 75% CH_3OH/H_2O afforded two glycoalkaloids, a major one (39.12 mg) which appeared as a bright blue band under UV light at 254 and 365 nm and a minor glycoalkaloid (20.75 mg) absorbing as a dark blue band at UV_{254}. Purification of these isolated glycosidic alkaloids was achieved by HPLC on a reversed phase column. Two alkaloids were eluted with 60% CH_3OH/H_2O at 1.0 ml/min with UV detection at 254 nm. The first alkaloid, labelled as Oa-4A-1, eluted after 5.8 mins and the second alkaloid, Oa-4A-2, with retention time of 6.25 min.

Table 3. Accurate Mass Measurements of Oa-4A-1 Fragment Ions with Their Corresponding Possible Elemental Composition.

Found (Calculated)	Composition	Double Bond Equivalent	Possible Fragment Ions
513.187600 (513.187306)	$C_{26}H_{29}N_2O_9$	13.5	$M^+ + H$
307.144900 (307.144653)	$C_{19}H_{19}N_2O_2$	11.5	$MH\text{-}CO_2\text{-}C_6H_{10}O_5$
289.132500 (289.134088)	$C_{19}H_{17}N_2O$	12.5	$MH\text{-}CO_2\text{-}C_6H_{12}O_6$
263.117500 (263.118438)	$C_{17}H_{15}N_2O$	11.5	$MH\text{-}CO_2\text{-}C_6H_{12}O_6\text{-}C_2H_2$
219.02197 (219.092223)	$C_{15}H_{11}N_2$	11.5	
182.084300 (182.084298)	$C_{12}H_{10}N_2$	9.0	[Harmane]$^{+\cdot}$

2.2.2.1 Structure Elucidation of Oa-4A-1

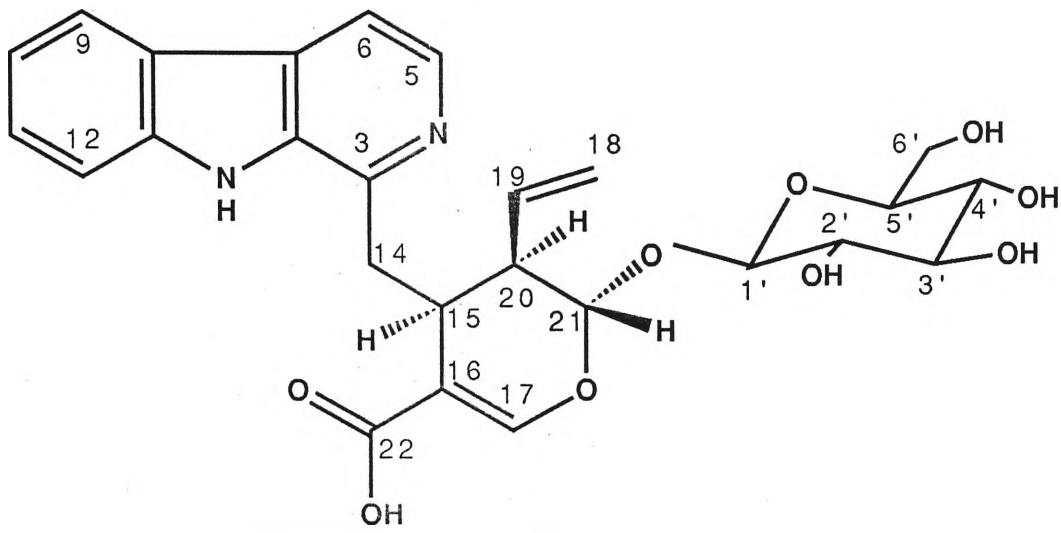

Oa-4A-1

The major alkaloid, Oa-4A-1, was obtained as a pale yellow amorphous solid, and appeared as a bright blue band on tlc under 254 and 365 nm UV light. The UV spectrum in CH_3OH showed absorbance at 351.4 nm. These data, which were identical with those for Oa-3A strongly indicated a highly conjugated system arising from $n \rightarrow \pi$ and $\pi \rightarrow \pi^*$ transitions and are clearly consistent for a β-carboline ring system in the molecule. A violet colouration with α-naphthol-H_2SO_4 upon heating was observed indicating the presence of a sugar unit. LRFABMS in glycerol gave a *m/z* at 512. A *m/z* of 513.1876 (M + H) was observed by HRDCIMS (High Resolution Desorption Chemical Ionisation Mass Spectrometry). This established the molecular formula of $C_{26}H_{29}N_2O_9$ with 14 double bond equivalents. The fragment ions were measured by scanning HRDCIMS with possible elemental compositions presented in Table 3. The base peak was observed at 351 which may arise to MH-162 (hesoxyl) fragmentation. After accounting for the hexose and harmane in

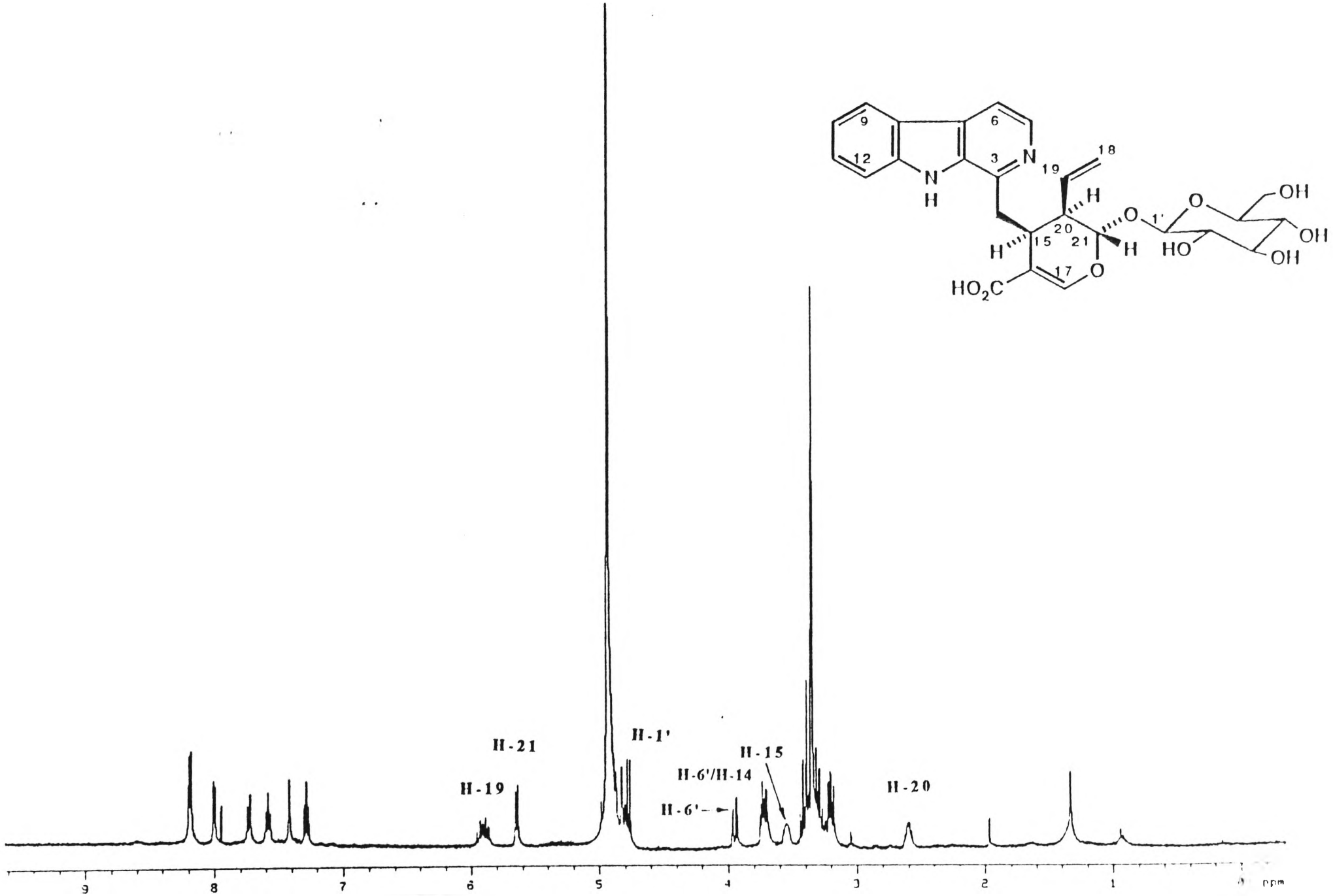

Figure 2. ^1H NMR Spectrum of Oa-4A-1 [CD_3OD, referenced at δ3.35].

the compound, the residual portion of the molecule has a composition of $C_8H_8O_3$. There was a strong tendency to lose CO_2 from this portion of the molecule as evidenced by ions corresponding to MH-hexose-CO_2 at m/e 289 in the DCI spectrum and to a lesser extent in the MS/MS spectrum. The MS/MS spectrum also showed the loss of 18 mass unit corresponding to loss of H_2O, followed by decarboxylation (M^+ - CO_2). This, being a typical fragmentation process for a carboxylic acid.

The ^1H NMR spectrum in CD_3OD (Figure 2) showed 7 aromatic proton resonances similar in pattern to Oa-3A, and complex signals at δ3.0-4.0 ppm arising from the sugar proton signals.

Structure elucidation of Oa-4A-1 was attempted following the usual procedure for glycoside identification, that is, to hydrolyse the molecule into its aglycone and its sugar unit. Enzyme hydrolysis with β-glucosidase is the most common way of cleaving off the sugar unit to yield the aglycone.

Enzyme hydrolysis of Oa-4A-1 with β-glucosidase provided some interesting results. The yellow reaction mixture at pH 5.0 rapidly changed to a pink-coloured solution which darkened with time. After work up, two reaction products were observed on tlc (SGF_{254}, CH_3OH, UV_{254} and Dragendorff) with a bright blue band at Rf=0.53 responding positively with Dragendorff reagent. No trace of the starting material was observed. The isolated hydrolysis product co-chromatographed on tlc with standard harman **10** and both its ^1H NMR spectrum and MS fragmentation were identical with harman **10**. Similar observations were obtained when the enzymatic hydrolysis was carried out in acetate buffer (0.2 M, pH 5.0). These results were very

Table 4. ^{13}C NMR Assignments of Oa-4A-1 Sugar in Comparison with the Literature Values.[76]

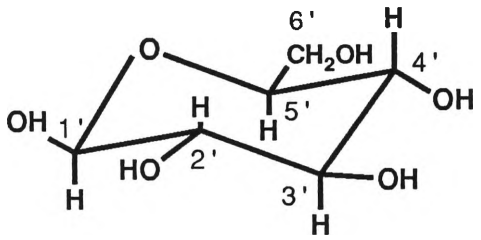

Carbon	Oa-4A-1	β-anomer	α-anomer
1	δ101.1	δ97.1	δ93.3
2	δ75.4	δ75.6	δ73.1
3	δ78.7	δ77.3	δ74.4
4	δ72.4	δ71.2	δ71.2
5	δ79.2	δ77.3	δ72.9
6	δ63.7	δ62.4	δ62.4

interesting since initially harman was not expected to be isolated as the hydrolysis product of Oa-4A-1. However, the enzyme hydrolysis proved that the aglycone after hydrolysis, could further breakdown into several products of which harman is the major product. Since Oa-4A-1 has a β-carboline ring system, it seemed probable that the molecule could be a glycoside derivative of harman.

The sugar unit was identified by comparison on tlc with different standard sugars and by its ^{1}H and ^{13}C NMR chemical shifts. The freeze dried isolated sugar co-chromatographed on tlc with glucose and galactose. Based on most glucoindole alkaloids reported in the literature, glucose was the most likely sugar unit. The ^{1}H NMR spectrum of Oa-4A-1 (Figure 2) strongly supports glucose for its chemical shifts correlates well with those in the literature thus eliminating galactose.[95] The doublet at δ4.78 (1H, J10.Hz) was assigned to the β-anomeric proton of glucose. The ^{13}C NMR assignments of Oa-4A-1, shown in Table 4, are also consistent for the β-anomer structure of D-glucopyranose unit.[96].

The detailed proton NMR assignments for glucose will be discussed later in relation with the analyses of the intact molecule using 2-D NMR techniques.

The above results established that the two following fragments below were found to be part of the Oa-4A-1 molecule.

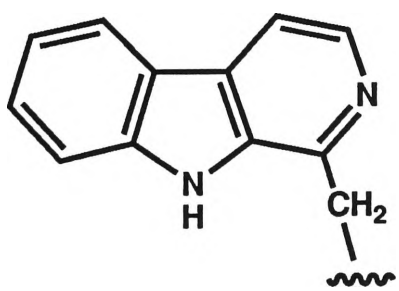

Fragment A

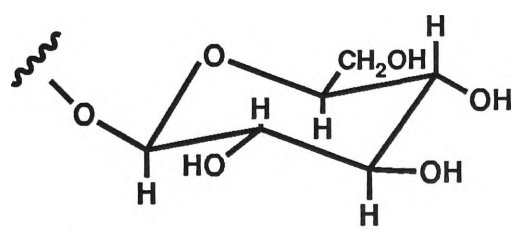

Fragment B

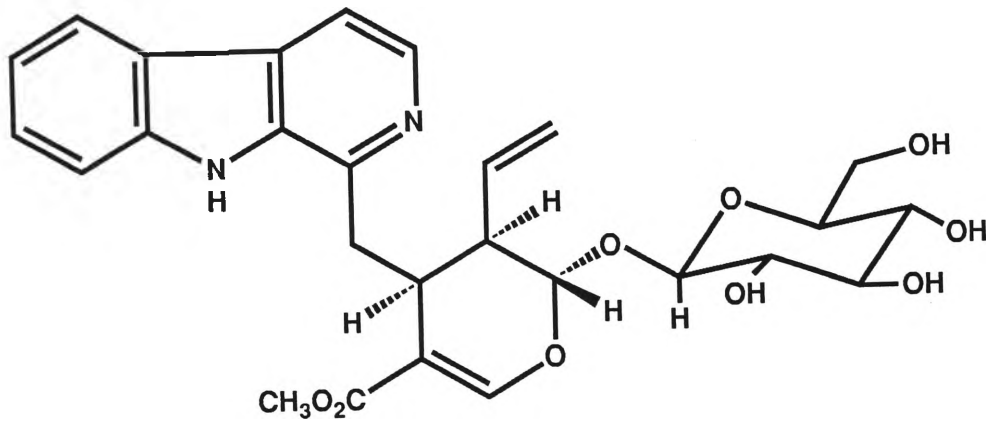

Lyaloside **44**

At this stage, it appears that Oa-4A-1 is most likely to have the same structure to a monoterpenoid indole alkaloid, lyalosidic acid **45**, isolated from *Ophiorrhiza japonica* by Aimi and his group in 1986.[79]

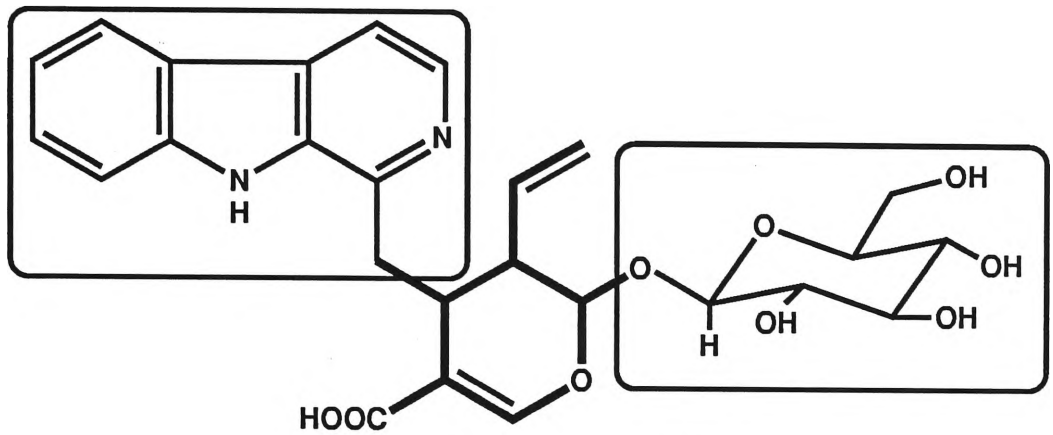

Lyalosidic Acid 45

Lyalosidic acid was not fully characterised by Aimi et al as only its ^{13}C NMR data were reported in the literature. He prepared the methyl ester of lyalosidic acid and compared it with the known compound lyaloside **44** previously isolated by Levesque from *Pauridiantha lyalii* (Rubiaceae).[97] Up until 1982, lyaloside was the only known representative of a structural family chracterised by a sequence: alkaloid-monoterpene-sugar (C_6-C_3) acid. Unfortunately, Aimi did not indicate in the paper what physical methods he used for comparison. Subsequently, through personal communication he advised us that he compared the ^{1}H and ^{13}C NMR data of his sample to those of lyalosidic which he acquired from Prof. Cave. These incomplete data reported in the literature for lyalosidic acid prompted us to carry out full characterisation of Oa-4A-1 and to look carefully at its stereochemistry. The important questions to address were: Is Oa-4A-1 identical to lyalosidic acid? and how do the ^{1}H and ^{13}C

Table 5 ^{1}H and ^{13}C NMR Data for Oa-4A-1 [CD_3OD, referenced at 3.35 (^{1}H) and 49.0 (^{13}C)]

Carbon	^{1}H, δ (multiplicity, integration, J in Hz)[a]	^{13}C, δ[b]
2		136.8
3		146.6
5	8.19/8.18 (m, 2H)	137.1
6	7.98 (d, 1H, 5.6Hz)	114.1
7		131.2
8		123.1
9	8.19/8.18 (m, 2H)	123.5
10	7.28 (t, 1H, 8.0Hz)	121.6
11	7.59 (t, 1H, 7.0 Hz)	130.6
12	7.74 (d, 1H, 8.0Hz)	114.1
13		143.6
14	3.71 (dd, 1H, Hz), 3.18 (dd, 1H, Hz)	36.6
15	3.57 (m, 1H)	37.8
16		115.4
17	7.41 (s, 1H)	151.4
18	4.91 (d, 1H, 17Hz), 4.83 (d,1H,10.0Hz)	119.4
19	5.92 (ddd, 1H, 17.0,10.0,9.0Hz)	137.2
20	2.64 (m, 1H)	47.2
21	5.65 (d, 1H, 7.0Hz)	97.9
1'	4.77 (d, 1H, 8.0Hz)	101.0
2'	3.20 (t, 1H, 8.0Hz)	75.4
3'	3.25 (t, 1H, 9.0Hz)	78.7
4'	3.40 (t, 1H, 9.0Hz)	72.4
5'	3.32 (qt, 1H, 9.0Hz)	79.2
6'	3.74 (m, 1H), 3.92 (dd, 1H, 12Hz,1.0Hz)	63.7
22		170.0

[a] assigned based on 1-D and 2-D NMR Experiments.

[b] assigned by DEPT 135 and by comparison with Aimi's reported data as well as the 2-D inadequate data for harman reported by Welti.[93]

NMR data of Oa-4A-1 fit the structure of lyalosidic acid proposed by Aimi?

Several model compounds were synthesised in the hope of establishing a basis for comparison of the proton signals of Oa-4A-1. This synthetic aspect of the work will be discussed towards the later part of this chapter.

It was clear that there was insufficient Oa-4A-1 for structure elucidation by chemical methods. With the rapid development of NMR spectroscopy, this technique has become a powerful tool for the structure elucidation of secondary metabolites which are often, as not, obtained in milligram quantities. Thus, utilisation of physical methods in particular NMR spectroscopy, was used to elucidate fully the structure of Oa-4A-1. Table 5 presents the summary of the ^{1}H and ^{13}C NMR assignments for Oa-4A-1.

Several 1-D and 2-D NMR techniques were utilised in further structure analyses of Oa-4A-1 with a closer look at the $C_8H_8O_3$ unit which the mass spectrum suggested contained a -COOH unit.

The ^{1}H NMR assignments for the β-carboline unit of the molecule was established from the combined information obtained from 1-D selective decoupling experiments and the 2-D ^{1}H- ^{1}H COSY[98,99] experiment. A two spin (H-5 and H-6) and a four spin system (H-9, -10, -11, -12) were observed from the aromatic region of the ^{1}H NMR spectrum (Figure 2) in Oa-4A-1. The overlapping resonances at δ8.19/8.18, integrating for 2H, were assigned to H-5 and H-9, respectively. These overlapping signals showed COSY crosspeaks (Appendix 2) to the doublet signals at δ7.98 (J5.6 Hz) assigned to H-6 and the triplet signal at

δ7.28 assigned to H-10. Furthermore, this signal at δ7.28 showed a COSY crosspeak to the signal at δ7.58 (H-11) which showed connectivity to the doublet signal at δ7.75 (H-12). The singlet at δ7.38 (H-17) was assigned to an isolated olefinic proton in the $C_8H_8O_3$ fragment.

The analyses of the $C_8H_8O_3$ unit started off with the ddd signal at δ5.92 (H-19) which showed crosspeaks to the signals at δ4.83 (1H, J10.0Hz,), δ4.89 (1H, J17.0Hz) and the multiplets at δ2.64 (H-20). Both the doublet signals at δ4.89 (H-18) and δ4.83 (H-18) showed COSY crosspeaks only between each other and to the signal at δ5.92 for a three spin system. The 17.0Hz coupling between δ5.92 and δ4.89 and the 10.0Hz coupling between δ5.92 and δ4.83 are typical for a vinylic group. Together with the multiplet at δ2.64, the signals at δ5.92, δ4.89 and δ4.83 comprise an AA'BX spin system.

The multiplet at δ2.64 (H-20), integrating for one proton showed crosspeaks to the doublet signal at δ5.65 (H-21) and to the multiplets at δ3.51 (H-15). This one proton signal at δ3.51 showed a further COSY crosspeak to the overlapping resonances centered at δ3.18. The anomeric proton at δ4.77 (d, 1H, J8.0Hz, H-1') showed a COSY crosspeak to the overlapping signals at δ3.18-3.44.

The region between 3.18-3.44 arose from the resonances of mutually coupled protons that have closely similar chemical shifts. In the COSY spectrum, the crosspeaks of these protons appeared very near the diagonal line and was obscured by overlap of the diagonal line. In our case, the CH_3OH signal from the solvent at δ3.35 contributed to the difficulty in assigning the spin systems involved in the region δ3.18-3.44. It is with this

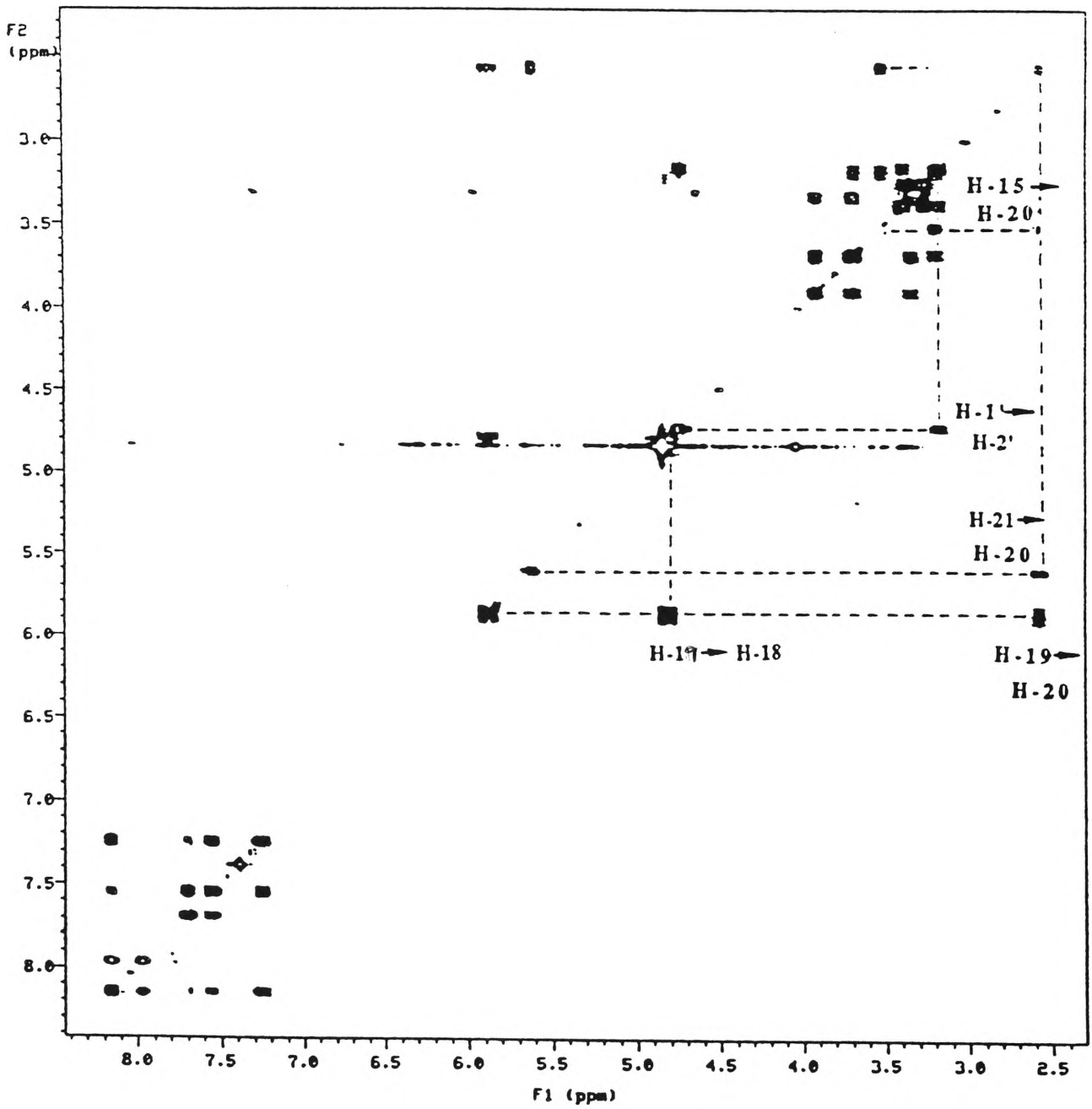

Figure 3. Double-Quantum Filtered (DQF) COSY NMR Spectrum of Oa-4A-1 [400 MHz, CD_3OD, referenced at δ3.35].

type of problem where one of the shortcomings of the ^{1}H-^{1}H COSY NMR experiment is pronounced.

Further improvement though can be achieved with the use of the so-called double-quantum filtered phase-sensitive COSY 2-D NMR technique. Double Quantum Filtered ^{1}H-^{1}H COSY (DQF COSY) filters the magnetisation through double quantum transitions and hence filters out single signals in the spectrum.[100,101] The large -OH resonance in CD_3OD is thereby minimised and a cleaner spectrum results. The DQF COSY spectrum of Oa-4A-1 (Figure 3) was acquired in the phase-sensitive mode leading to a better resolution compared with the absolute value COSY spectrum

The doublet at δ3.92 (1H, J12.0Hz, H-6') showed COSY crosspeak to the overlapping signals at δ3.71/3.74 (H-6', H-14) which was established to be δ3.74 (d, 1H, J12.0Hz).by selective decoupling experiment Furthermore, the signal at δ3.92 (H-6') was coupled to δ3.32 (H-5') whose crosspeak was still obscured by other proton resonances around the region. The doublet at δ3.71 (H-14) showed connectivity with the signal at δ3.18 (H-14) and 3.51 (H-15). The 12Hz coupling for the signals at δ3.74 and δ3.71 are typical of a vicinal coupling for protons that have a fixed conformation. Freely rotating vicinal protons show coupling close to 7Hz. [96] From all the correlations obtained from the COSY and DQF COSY, fragments B and C were established.

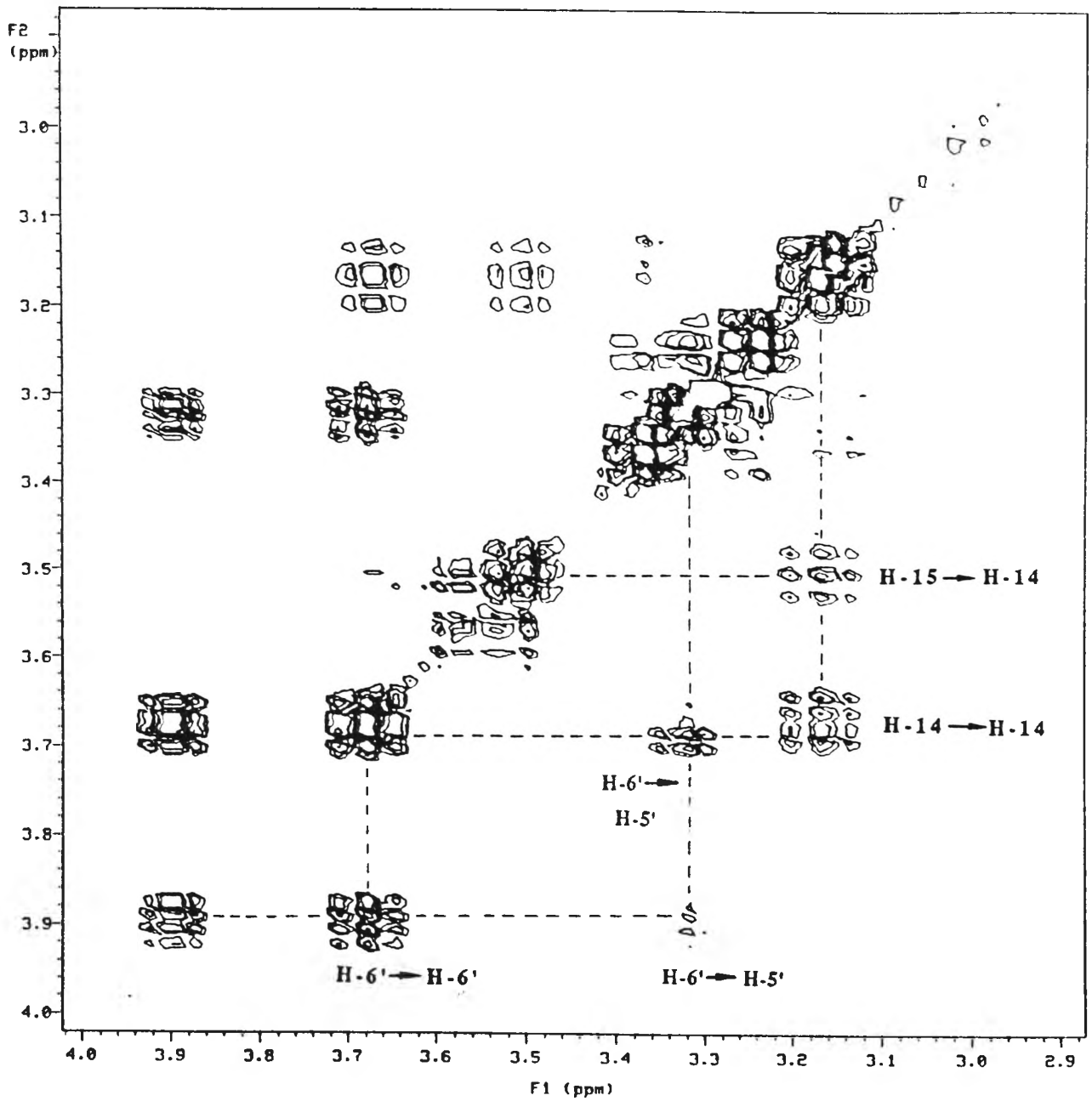

Figure 4. Triple-Quantum Filtered (TQF) COSY NMR Spectrum of Oa-4A-1 (Region between 3.0-4.0 ppm) [400 MHz, CD_3OD, referenced at δ3.35].

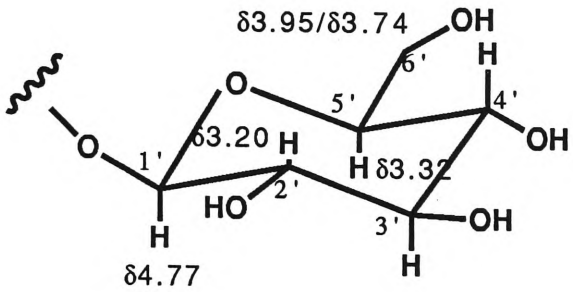

Fragment B

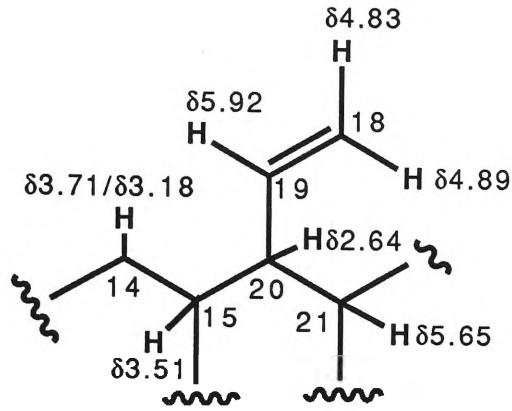

Fragment C

The 3-spin systems for H-5' and H-6', H-19 and H-18 and H-14 and H-15 were all confirmed using Triple Quantum Filtered COSY (TQF COSY).[104] This 2-D NMR technique eliminates not only the singlets but all AB and AX systems producing a much simpler spectrum of only three spin system. Figure 4 shows the TQF COSY of Oa-4A-1.

The TQF COSY spectrum (Figure 4) showed distinctly the 3-spin system for H-19, H-18_{cis} and H-18_{trans}. These are marked with dotted lines on the spectrum. The doublet at δ3.92 (H-6') showed a crosspeak to the signal at δ3.74 which showed a crosspeak with δ3.32 (H-5'). The H-14 proton at δ3.71 correlated with the triplet at δ3.18 which also showed a crosspeak with the δ3.51 multiplet.

However, after the COSY, DQF and TQF COSY experiments, the connectivity for H-4' and H-3' of the sugar moiety and H-17 and H-21 of the $C_8H_8O_3$ unit were still not clear.

Another 2-D NMR experiment that compliments all of the above 2-D experiments is Relay COSY (RCOSY).[102] This provides ^1H-^1H correlation beyond a pair of directly coupled spins to the next nearest neighbour through transfer or relay magnetisation. Eich, Bodenhausen and Ernst[103] have been credited for the

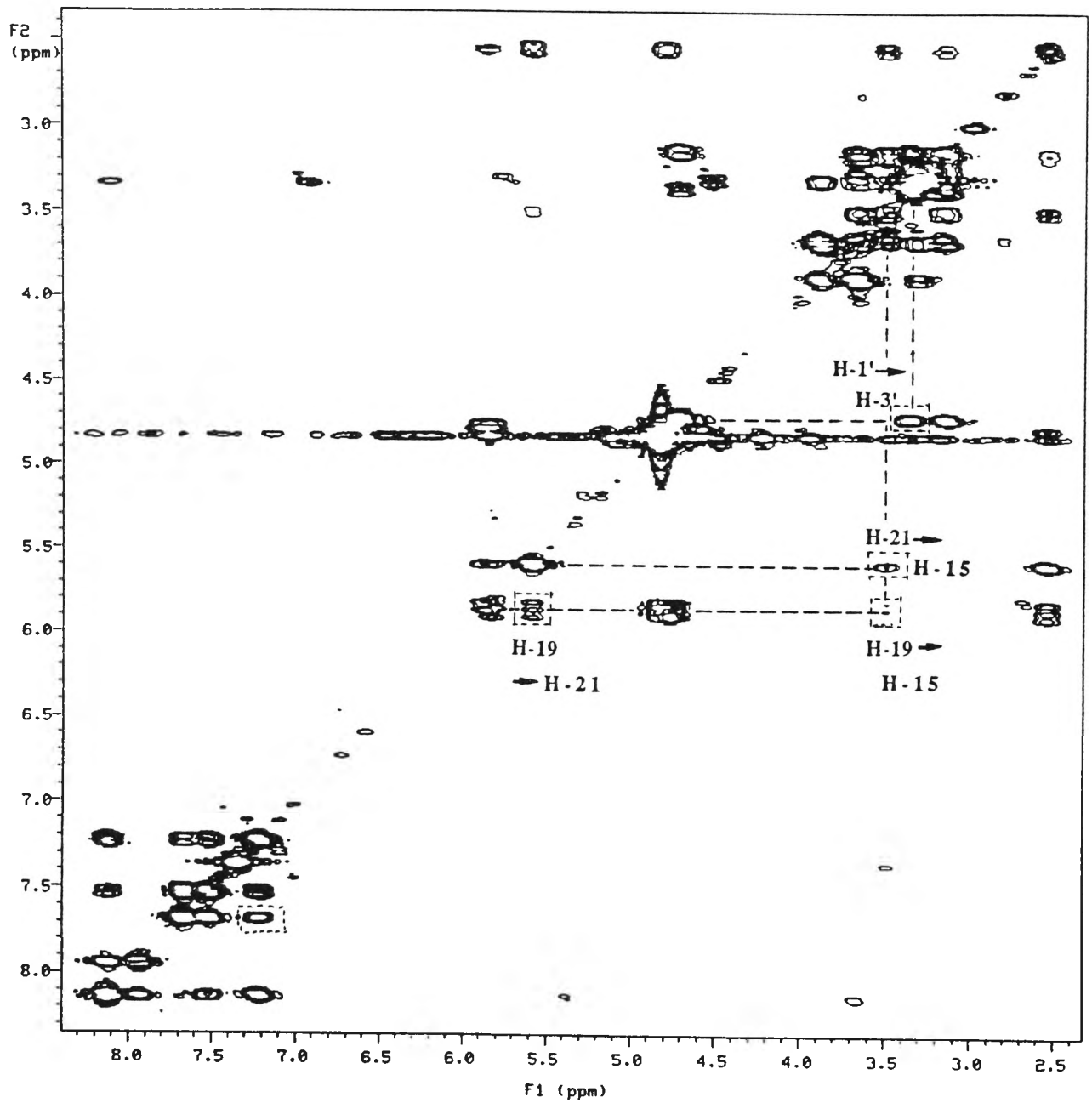

Figure 5. Relay COSY (RCOSY) NMR Spectrum of Oa-4A-1 [400 MHz, CD_3OD, referenced at $\delta 3.35$].

original concept of relayed coherence. A RCOSY experiment of Oa-4A-1 is shown in Figure 5.

Interpretation of the RCOSY spectrum is facilitated by comparison with the COSY spectrum. Thus, it is very important to acquire initially a COSY spectrum before a RCOSY. To facilitate easy analysis, the additional crosspeaks are encircled on the RCOSY spectrum shown in Figure 5.

The RCOSY spectrum confirmed the proton assignments for fragments B and C. The doublet at δ5.65 (H-21) only showed relay crosspeaks to δ5.92 (H-19) and δ3.51 (H-15) which agreed with its assignment in fragment C for a methine proton adjacent to oxygen. H-15 did not show any other RCOSY crosspeaks other than those observed from the DQF and TQF COSY spectra Summary of RCOSY correlations at the $C_8H_8O_3$ unit are illustrated in Figure 6.

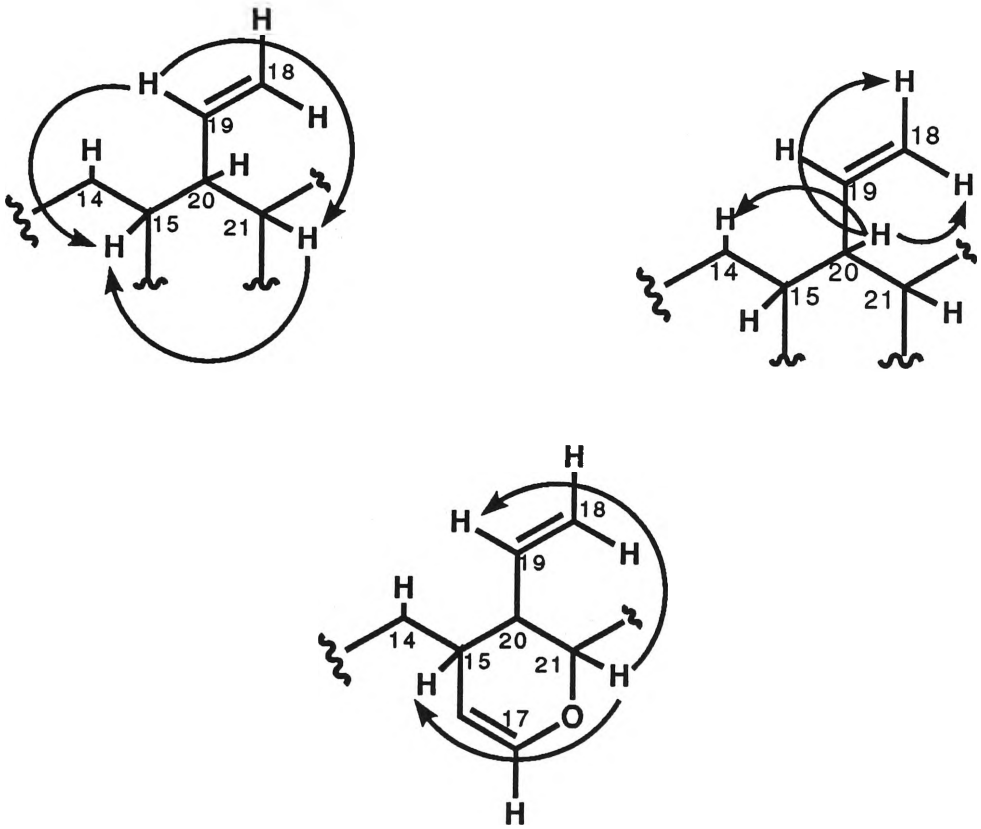

Figure 6. RCOSY NMR Correlations in the $C_8H_8O_3$ unit of Oa-4A-1.

The anomeric proton of the sugar unit at δ4.77 (H-1') showed relayed crosspeaks to the signal at δ3.25 (H-3') which in turn showed a relayed crosspeak to H-5'. The observed relay crosspeak between H-6' protons at δ3.95 and δ3.74 to the overlapping resonances at δ3.36-3.44 suggested that the chemical shifts for H-5' and H-4' were similar to each other. After a closer look at the expanded spectrum and selective decoupling experiment in which δ3.32 (H-5') was irradiated the signal centred at δ3.40 corresponded to H-4'.

At this stage, it is most likely that C-17 is attached to the oxygen adjacent to C-21 to form the monoterpenoid unit of Oa-4A-1 with the -COOH group attached to C-16.

Other 2-D scalar NMR techniques such as Double Relay COSY (2RCOSY) and TOCSY were used primarily to confirm the ^1H assignment for the monoterpenoid ring and the sugar unit. Double Relay COSY NMR spectroscopy or a 2RCOSY[102] experiment involves the transfer of magnetisation beyond four bonds. The 2RCOSY spectrum (Appendix 2) was obtained for Oa-4A-1 with a τ_m of 30 ms. A summary of the 2RCOSY corrrelations are presented in Figure 7.

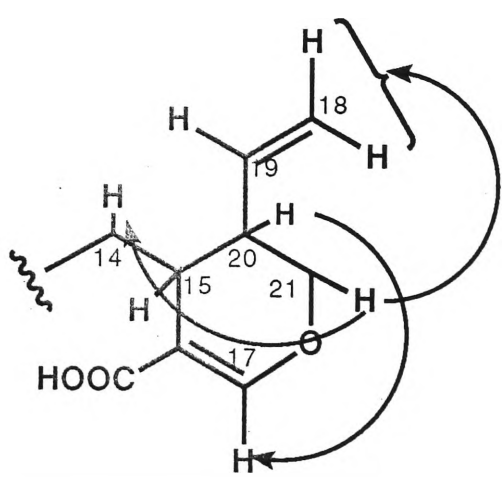

Figure 7. 2RCOSY NMR Correlations for the $C_8H_8O_3$ unit of Oa-4A-1.

The last of the 2-D scalar correlation experiments that was acquired was TOCSY or Total Correlation Spectroscopy.[104] As the name implied, this technique provides the overall correlation between protons in the molecule. The TOCSY spectrum for Oa-4A-1 (Appendix 2) was acquired with a mixing time of 75 ms showing additional information arising from the TOCSY correlations. The correlation between H-21 and H-14 protons (δ3.71 and δ3.18), not observed in the RCOSY and 2RCOSY spectra, was very distinct in the spectrum. Furthermore, the anomeric proton showed crosspeaks arising for all the other sugar protons, H-2', H-3', H-4', H-5' and H-6'. Thus, from the TOCSY spectrum, all the sugar resonances were assigned unequivocally.

From the above analyses of the 2-D scalar NMR techniques the three fragments of Oa-4A-1 were established unambigously.

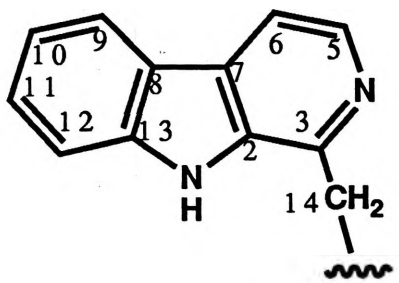

Fragment A

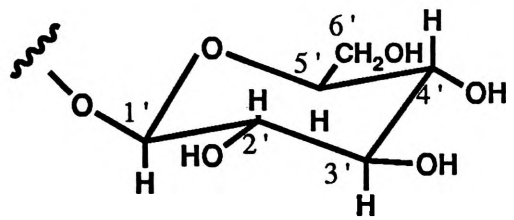

Fragment B

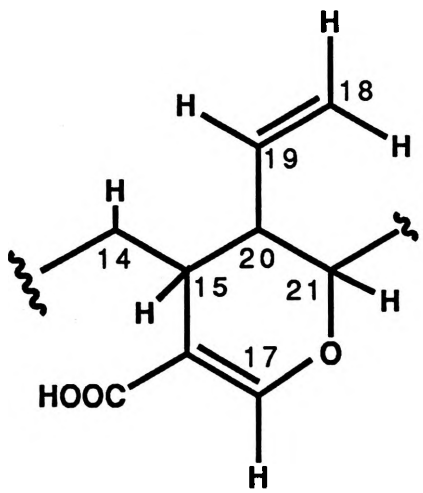

Fragment C

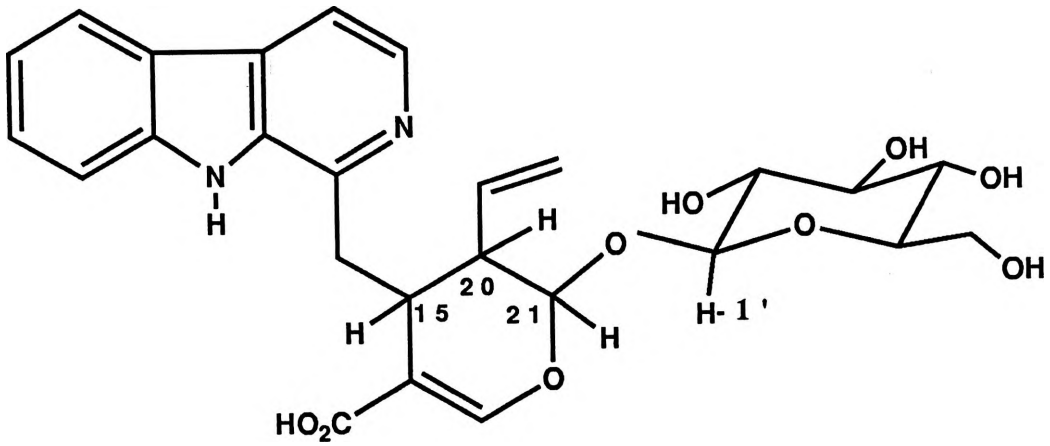

Oa-4A-1

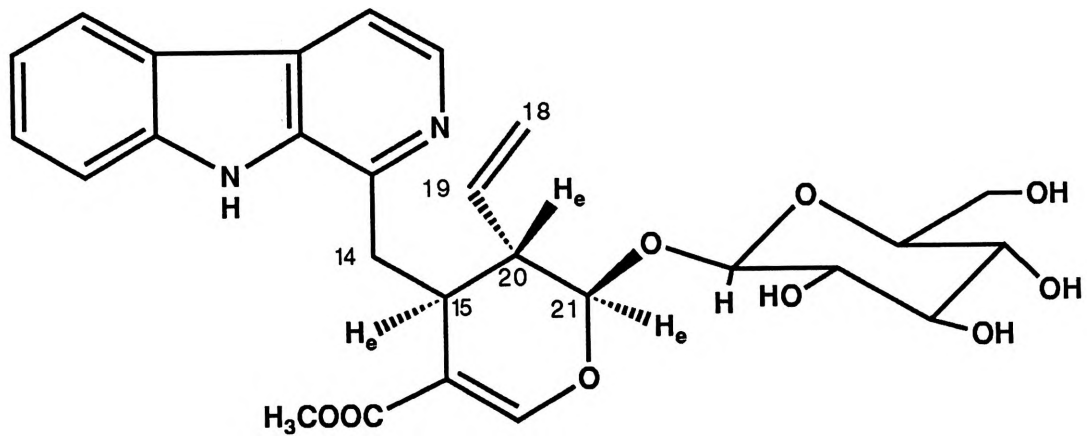

Figure 8. Lyaloside, 15α, 20β, 21α

To establish the linkages between the 3 major fragments of the molecule, that is, the β-carboline ring system, the sugar moiety and the monoterpenoid unit, dipolar correlations were utilised; i.e., interactions though space. Difference nOe (nuclear Overhauser effect) spectroscopy and a 2-D NOESY (Nuclear Overhauser Enhancement Spectroscopy)[105] spectroscopy showed a dipolar interaction between H-21 and H-1' establishing the linkage between the monoterpenoid unit and the sugar. The structure of Oa-4A-1 was thus established to have the same structure as lyalosidic acid **45** although its stereochemistry has yet to be addressed.

As mentioned earlier, Aimi did not provide evidence to confirm the stereochemistry at C-15, C-20 and C-21. The assignments were based on comparison with those for lyaloside **44**. Levesque argued that the stereochemistry of lyaloside **44** based on the coupling constants $J_{15\text{-}20}$ = 3.5 Hz and $J_{20\text{-}21}$ = 5 Hz favored 3 equatorial protons in the monoterpenoid ring, and thus all the bulky susbtituents are axially disposed, corresponding to an α, β, α arrangements for H-15, H-20 and H-21 (Figure 8). Subsequently, Levesque[106] corrected his assignments to α, α, β which was more logical on the basis of the biosynthetic origin of the monoterpenoid unit derived from tryptamine and secologanin. The corrections were made on the basis of the observed coupling constants ($J_{15\text{-}20}$ = 3.5 Hz and $J_{20\text{-}21}$ = 5 Hz) and by comparison of the ^{13}C NMR data of lyaloside with those for the iridoids which provided confirmation that the stereochemistry of lyaloside at C-15, C-20 and C-21 was definitely α, α, β.

These ambiguities and the lack of evidence in the literature regarding the stereochemistry of lyalosidic acid were now addressed for Oa-4A-1. Since then work on more sophisticated NMR methods have been introduced which could provide evidence for the stereochemical assignments at C-15, C-20 and C-21 of lyalosidic acid. The observed coupling constants, 1-D and 2-D nOe experiments such as NOESY and ROESY (Rotating-frame Overhauser Enhancement Spectroscopy)[107,108] provided the information to establish the stereochemistry at the chiral centres.

H-15 shows a 5.0 Hz coupling with H-20 characteristic for an axial-equatorial or equatorial-equatorial orientation. A coupling constant of 7.2 Hz between H-21 and H-20 is quite big when compared with the usual 1-5Hz coupling characteristic for axial-equatorial or equatorial-equatorial relationships and small for an axial-axial disposition. Lack of W coupling between H-15 and H-21 from the COSY spectrum suggested that these two protons have different dispositions. Difference nOe spectra showed enhancement to H-15 (δ3.51) when H-20 (δ2.60) was irradiated. Irradiation of the signal at δ5.65 (H-21) showed no observed nOe onto H-20 and H-15. To obtain more conclusive evidence to establish the stereochemistry at C-15, C-21 and C-21, 2-D NMR experiments such as NOESY and ROESY were used.

A NOESY spectrum provides information on dipolar or spatial relationships between protons. However, occurrence of crosspeaks arising from scalar correlations are often observed which may led to misinterpretation of the observed crosspeaks. This happens because the NOESY pulse sequence was the same as the DQF-COSY aside from the introduction of τ_m. In comparison, a ROESY experiment, also showed occurrence of crosspeaks arising

from COSY and TOCSY (HOHAHA) coherence transfer however, these crosspeaks could be differentiated from the nOe crosspeaks since they appeared on the opposite phase from the enhancement signal. Thus, the ROESY experiment supports the assignments of the NOESY crosspeaks.

Data information obtained from the NOESY and ROESY NMR experiments (Appendix 2) showed a strong crosspeak between H-15 (δ3.51) and H-20 (δ2.60). No observed crosspeak between H-20 (δ2.60) and H-21 (δ5.65) was evident on either NOESY or ROESY spectra. H-21 showed a crosspeak with H-1' (δ4.77) arising from the proximity of this proton with the anomeric proton, hence the observed linkage. A strong dipolar correlation was observed between one of the H-14 protons at δ3.18 and H-21. This suggested a possible half-chair orientation of the terpenoid ring. H-19 showed a dipolar interactions with H-15. These observed dipolar correlations are all summarised in Figure 9.

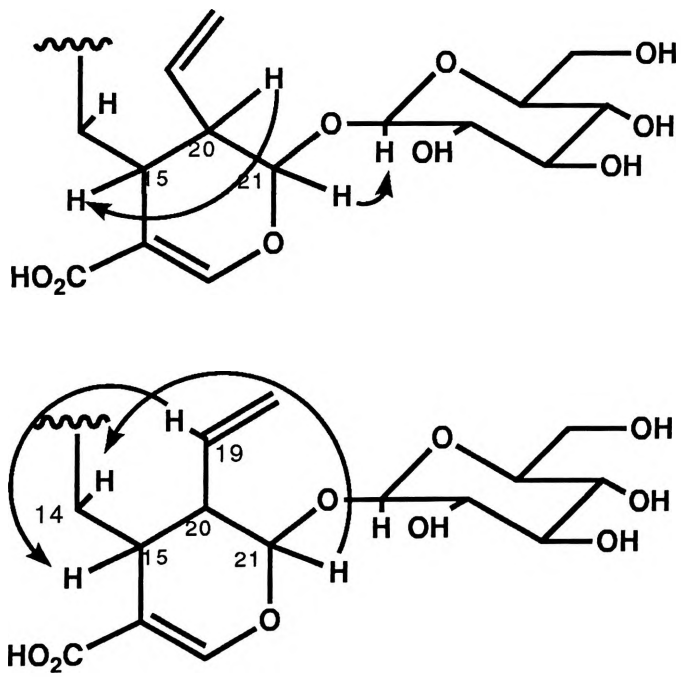

Figure 9. NOESY/ROESY NMR Correlations at C-15, C-21 and C-21.

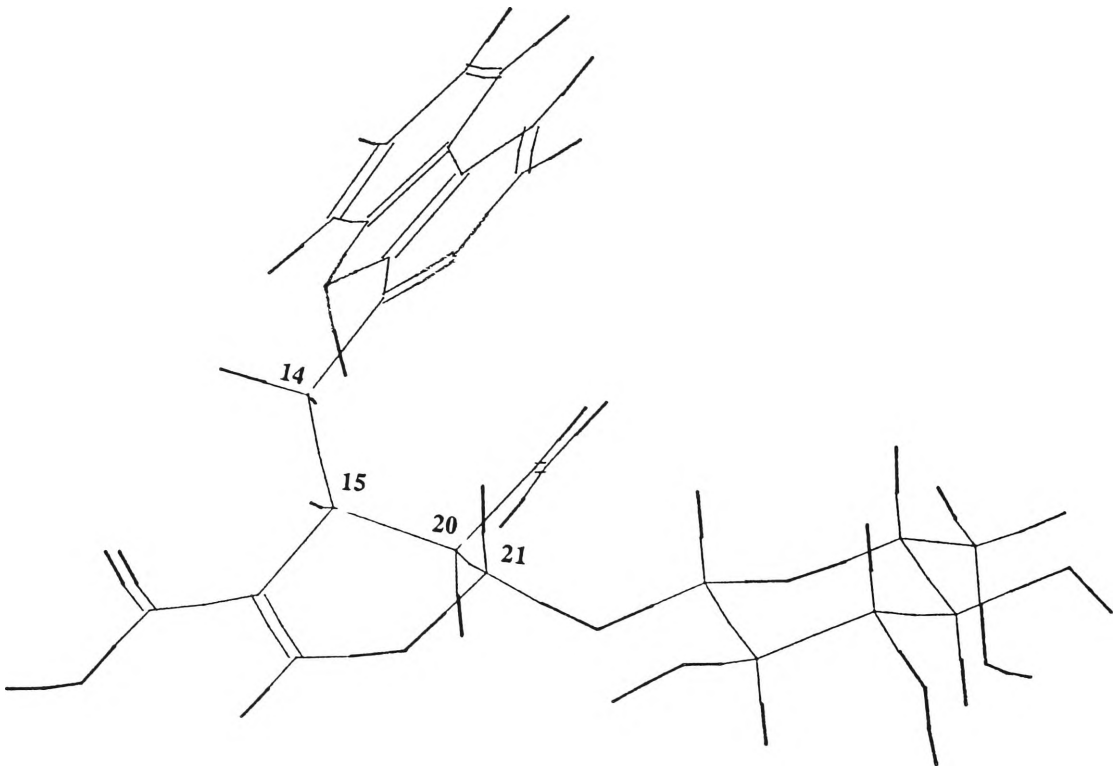

Figure 10. Possible Conformation of Oa-4A-1 by Molecular Modelling Obtained from the ALCHEMY Program.

All these data fit well with an α, α, β orientation for H-15, H-20 and H-21 respectively as illustrated below.

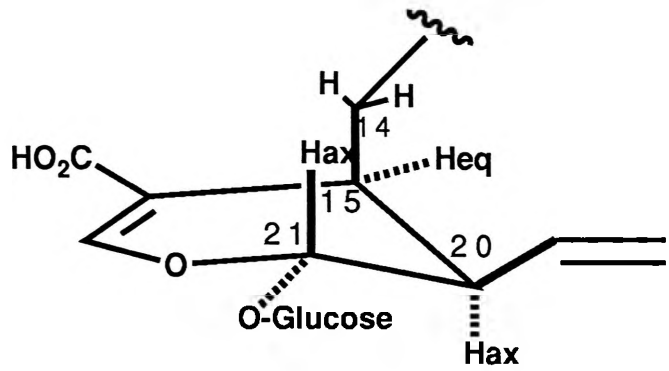

The proposed stereochemistry was verified by correlating the observed NOESY and ROESY responses with the bond distances between the proton of interest by molecular modelling using the ALCHEMY software. The proposed structure of Oa-4A-1 was fed into the ALCHEMY software and minimisation gave the most stable conformation for Oa-4A-1 as shown in Figure 10. With the obtained conformation, the different bond distances between the protons of interest were measured. The comparison of the measured values and the observed nOe responses is shown in Table 6.

Table 6. Correlation of the Observed Dipolar Interactions (NOESY/ROESY) with the Bond Distances Measured from the ALCHEMY Molecular Modelling.

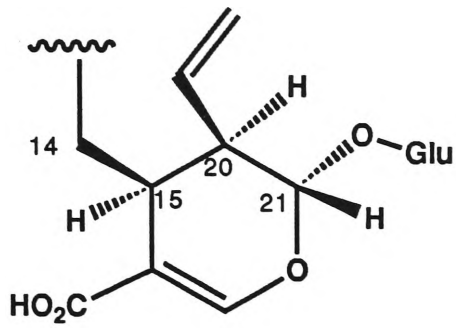

15S (α), 20R (α), 21S (β)

	Bond Distance, A°	Observed nOe
H_{15} - H_{20}	2.347	strong nOe (+++)
H_{15} - H_{21}	3.706	no. nOe.(n.o)
H_{15} - H_{19}	3.755	no nOe (n.o.)
H_{20} - H_{21}	3.057	no nOe (n.o.)
H_{21} - H_{14}	2.583/3.866	nOe (+)
H_{21} - $H_{1'}$	2.542	nOe (+)

(+++) Large nOe (+) Small nOe (n.o) not observed.

There are a number of considerations, both practical and theoretical[109] which affect the magnitudes of nOe's. Because of these, it was considered impractical to accurately measure nOe enhancements. Large or small nOe's were determined by visual inspection.

The measured bond distances are in agreement with the observed qualitative nOe responses. This establishes the stereochemistry of Oa-4A-1 to have a relative configuration of 15S(α), 20R(α) and 21S(β) as shown in proposed structure of Oa-4A-1. These observed stereochemistries correspond

Table 7. ^{1}H NMR Chemical Shift Differences Between Oa-4A-1 and Lyalosidic Acid on Selected Protons (CD_3OD, 400 MHz, referenced relative to CD_3OD at δ3.35).

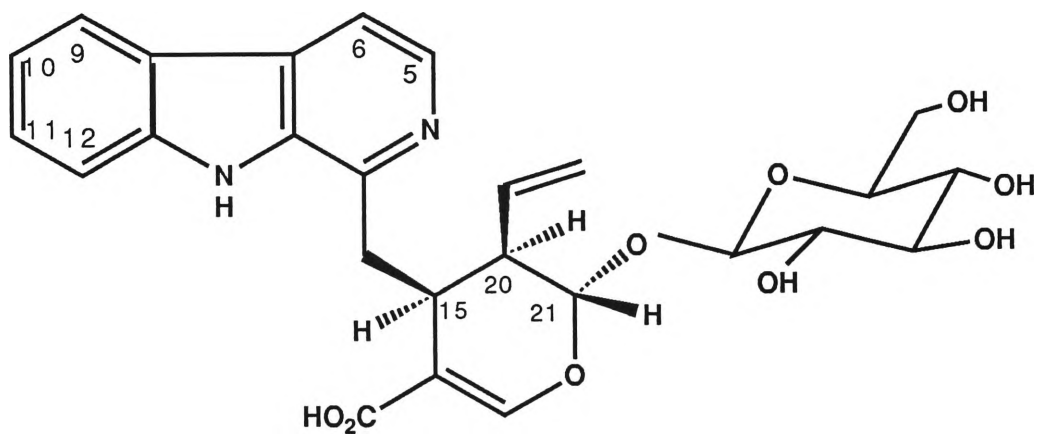

	Oa-4A-1	Lyalosidic acid
H-5	δ8.19	δ8.27
H-6	δ8.01	δ8.18
H-9	δ8.19	δ8.27
H-10	δ7.28	δ7.36
H-11	δ7.59	δ7.67

reasonably well with the α, α, β stereochemistry generally observed with this type of compounds.

Personal communication with Prof. Norio Aimi enabled us to obtain an authentic sample of lyalosidic acid **45** together with a recently acquired ^{1}H NMR spectrum in CD_3OD on their Jeol 270 MHz NMR spectrometer. On comparison with Oa-4A-1 ^{1}H NMR spectrum, slight chemical shifts differences for some protons were observed. Spectra for both Oa-4A-1 and Aimi's lyalosidic acid obtained on the same Varian 400 MHz spectrometer still exhibited the slight chemical shifts differences as presented in Table 7.

The proton chemical shifts for Oa-4A-1 occured more upfield than those for Aimi's lyalosidic acid. However spectra acquired using equal concentrations provided identical chemical shifts values which cleared up the ambiguity. This, we feel was substantial evidence and avoided having to do doing NMR experiments where Oa-4A-1 was spiked with lyalosidic acid. The observed differences in chemical shift may be accounted for by intermolecular H-bonding between molecules which is likely with the presence of several electron rich centers in the molecule. Finally, Circular Dichroism spectra for both compounds showed identical absorptions thus establishing unambiguously that Oa-4A-1 is lyalosidic acid.

The ^{13}C NMR data for Oa-4A-1 were assigned using DEPT 135 and by comparison with the chemical shift values established for Oa-3A (Harman) and those recently acquired data provided by Prof. Aimi These ^{13}C NMR data acquired by Prof. Aimi of which some of the chemical shift values were assigned using ^{1}H-^{13}C correlation NMR technique showed slight

differences in chemical shift values to his previous assignments. These differences which Prof. Aimi thinks could be due to temperature-dependency are, on the basis of my results, more likely to be due to intermolecular H-bonding. It is important to point out that our assignments at the four quaternary centers at C-2, C-7, C-8, and C-13 are not in agreement with those reported for lyalosidic acid **45**. These were based on the revised assignments established by Welti using 2-D INADEQUATE NMR technique on harman **10**. Table 8 showed the comparison of the quaternary carbons at positions 2, 7, 8 and 13 to those reported by Aimi. A long range ^{1}H-^{13}C heteronuclear multiple bond correlation (HMBC) will be performed later on Oa-4A-1 to confirm our assignments.

Table 8. ^{13}C NMR Data for Oa-4A-1 and Lyalosidic Acid on Selected Carbons [CD_3OD, Varian 400 MHz, referenced relative to residual CH_3OH at δ3.35].

Carbon	Oa-4A-1	Lyalosidic Acid
2	δ136.8	δ143.5
7	δ131.2	δ122.0
8	δ123.1	δ131.9
13	δ143.6	δ135.8

With the structure of Oa-4A-1 found to be lyalosidic acid, the mechanism of the enzyme hydrolysis with β-glucosidase was investigated. Initially, Aimi and his group isolated harman as the major product of enzyme hydrolysis of lyalosidic acid or lyaloside. Similarly, 10-hydroxylyalosidic acid **46** produced the corresponding β-carboline derivative 10-hydroxyharman **49**.

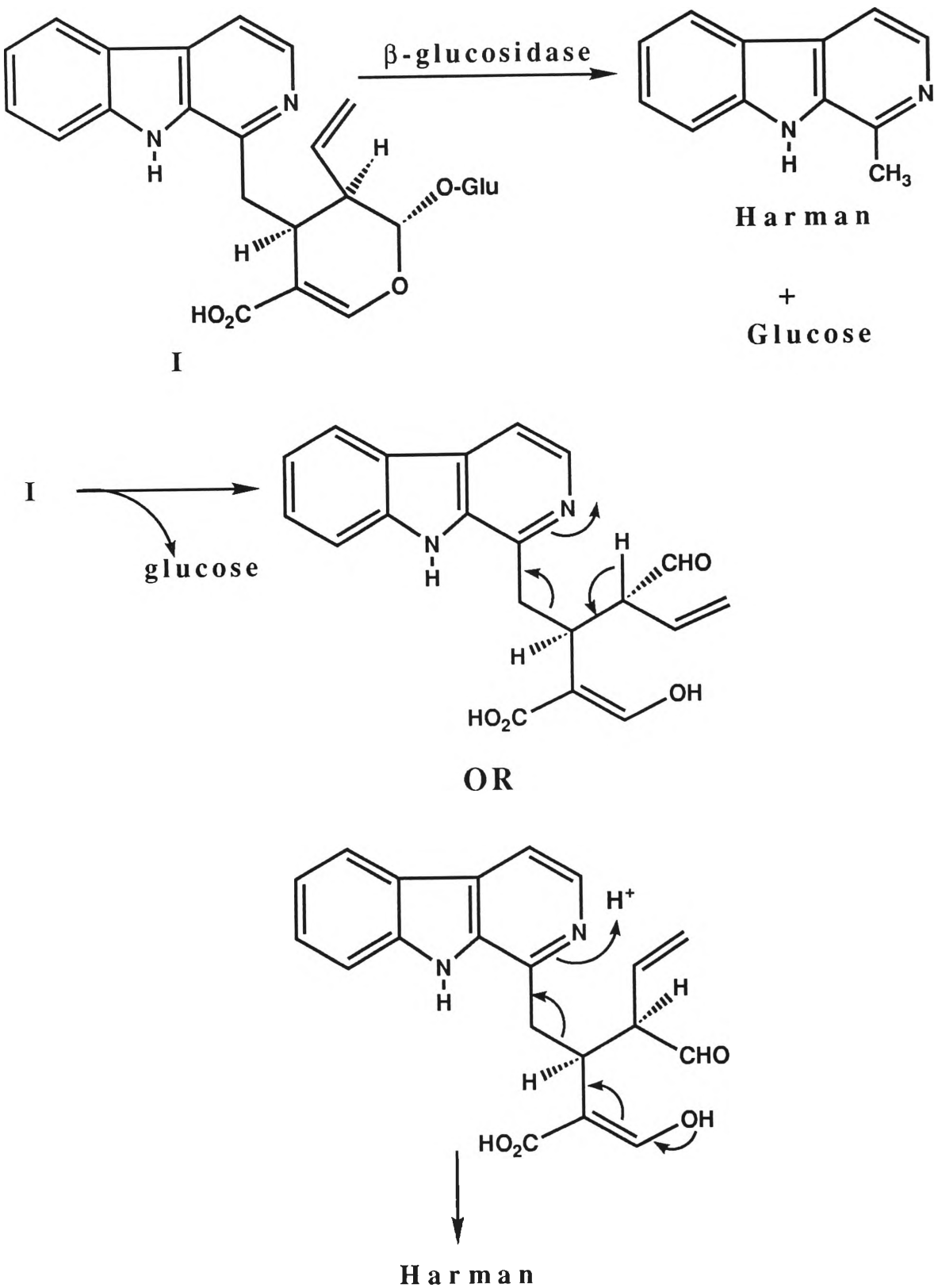

Figure 11. Mechanism for the Formation of Harman from Lyalosidic acid by Enzyme Hydrolysis Proposed by N. Aimi.

Both observations suggested the co-existence of simple β-carbolines alkaloids and their corresponding glucoindole alkaloids. A possible mechanism for the formation of harman was proposed by Aimi (Figure 11).

During discussions with Prof. A. R. Battersby, another possible mechanism for the harman formation was considered and is presented in Figure 12. This involves the formation of a 6-membered ring intermediate which has precedent in these glucoindole alkaloids (cf, Strictosamide lactam). Breakdown is then triggered through the positive nitrogen. With these observations, it is possible that in the Rubiaceae family more particularly in the genus *Ophiorrhiza*, harman **10** may occur in the plant as a degradation product which arises by the action of endogenous glucosidase enzymes on the monoterpenoid indole alkaloids. This would possibly explain the low rates of incorporation of acetate into harman **10** observed by O'Donovan and Kenneally.[51]

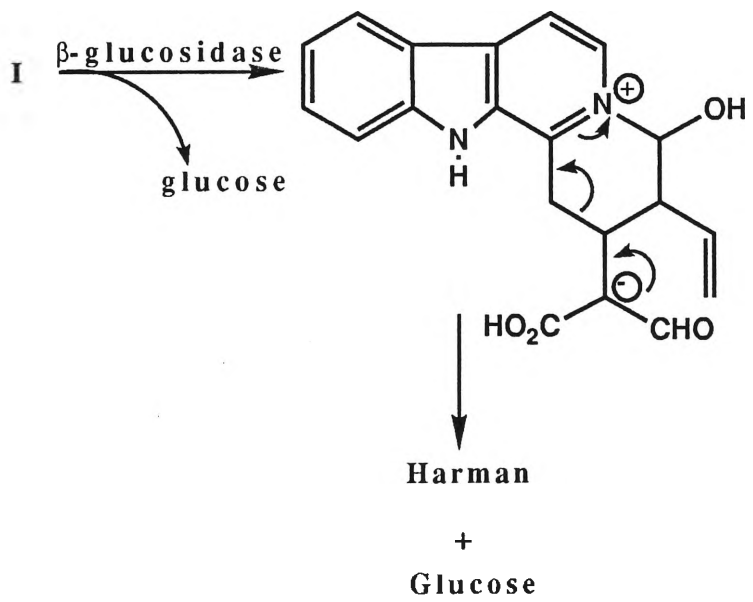

Figure 12. Another Possible Mechanism for the Formation of Harman from Oa-4A-1 by Enzyme Hydrolysis.

2.2.2.2 Structure Elucidation of Oa-4A-2

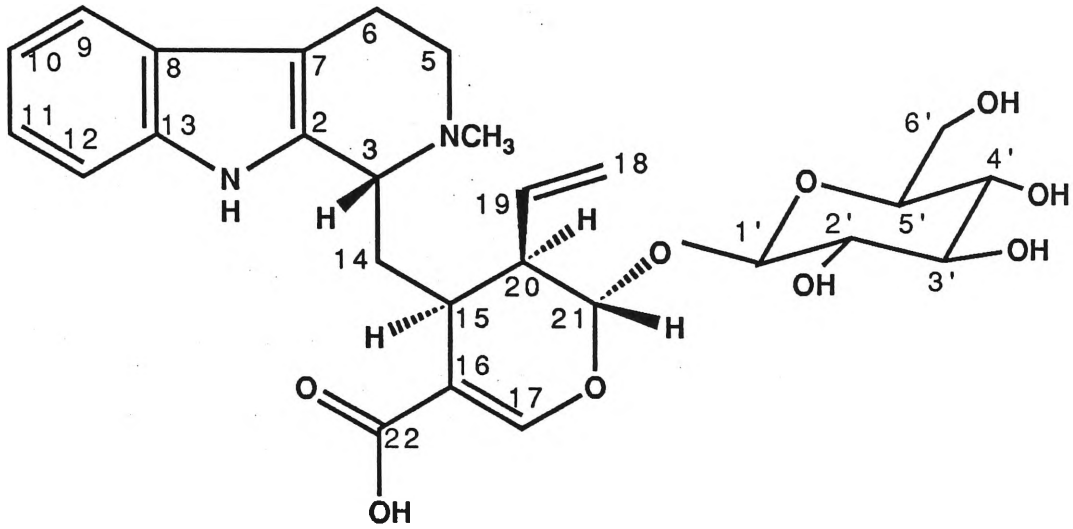

The minor glucoindole alkaloid, labelled as Oa-4A-2 and obtained as a white amorphous solid, gave a m. pt. of 220-223° with decomposition. The UV absorbances at λ289.2, 272.4, 226.6 and 218 nm were consistent for a tetrahydro-β-carboline ring nucleus.[110]

A molecular weight of 513.2318 (M^+ + H) was obtained by HRDCIMS and was in accordance for $C_{27}H_{35}N_2O_9$. These gave 11 double bond equivalents, which is two less than for Oa-4A-1. Fragments ions were measured by scanning HRDCI as described previously for the Oa-4A-1 MS analysis. Table 9 presents the possible elemental compositions of the generated ions using the proposed molecular ion composition.

The strong tendency to lose CO_2 from its mass spectrum indicated a carboxylic acid which was confirmed when Oa-4A-2 was reacted with CH_3OH/CD_3OD in $(CH_3CO)_2O$. The mass spectrum of the reaction product gave two signals 3 mass units apart at 546 and 549 for the methyl ester and deuteromethyl ester derivatives of Oa-4A-2.

Table 10. ^1H NMR Assignments for Oa-4A-2 (CD_3OD, Varian 400 MHz, referenced relative to CD_3OD at δ3.35).

H on Carbon	^1H, δ (multiplicity, integration, J in Hz)
3	4.65 (m, 1H)
5	3.06-3.11 (m, 1H) and 2.98-2.00 (m, 1H)
6	2.26 (m, 1H)
9	7.48 (d, 1H, 8.0Hz)
10	7.06 (t, 1H, 7.0Hz)
11	7.15 (t, 1H, 7.0Hz)
12	7.37 (d, 1H, 8.0Hz)
14	3.50 (m, 1H) and 3.69 (m, 1H)
15	3.58 (m, 1H)
17	7.51 (s,1H)
18_{trans}	5.34 (d,1H, 17.0Hz)
18cis	5.27 (d, 1H, 10.0Hz)
19	5.93 (m,1H)
21	5.70 (bd d, 1H)
20	2.75 (m, 1H)
1'	4.79 (d, 1H, 7.0Hz)
2'	3.25 (t, 1H, 7.0Hz)
3	3.20-3.55 (m, 1H)
4'	3.20-3.55 (m, 1H)
5'	3.40 (m, 1H)
6'	3.72 (d, 1H, 12.0Hz) and 4.05 (d, 12.0Hz)
N-CH_3	2.80 (s, 3H)

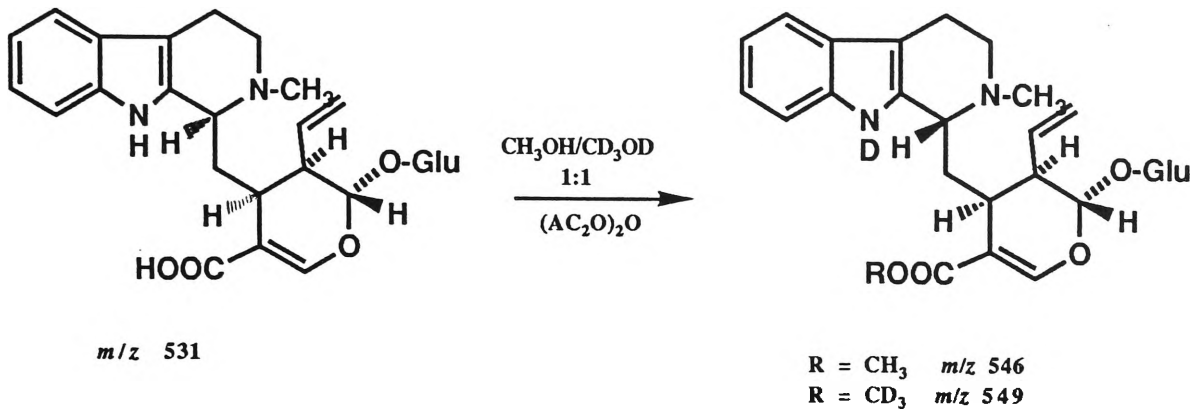

m/z 531

R = CH_3 *m/z* 546
R = CD_3 *m/z* 549

Spectroscopic analysis of Oa-4A-2 was done by comparison of the data with those obtained for Oa-4A-1. A combination of 1D and 2D NMR experiments were also utilised to elucidate the structure of Oa-4A-2. The ^1H NMR assignments for Oa-4A-2 were presented in Table 10.

The ^1H NMR spectrum of Oa-4A-2 obtained in CD_3O D showed 5 aromatic protons, four of which were assigned for the 4 spin-system at H-9, -10, -11,-12 and the fifth aromatic proton was assigned for the isolated proton at position 17 (Figure 13). H-9 and H-17 occured on the same chemical shift, δ7.51, however, a spectrum acquired at 50°C resolved the two signals to a doublet at δ7.49 (H-9) and a singlet at δ7.48 (H-17). Again the indole proton was not observed due to deuterium exchange.

The COSY spectrum (Figure 14) showed coupling between the overlapping doublets at δ7.51 (H-9 and H-17) and the signal at δ7.08 (t, 1H, 7.0Hz, H-10) which showed a crosspeak to the triplet at δ7.21 (H-11). The doublet at δ7.37 (8.0Hz, 1H) was assigned to H-12. Well-resolved signals for δ7.40 (H-17) and δ7.36 (H-12) were observed from the ^1H NMR spectrum obtained in DMSO-d_6 (Figure 15).

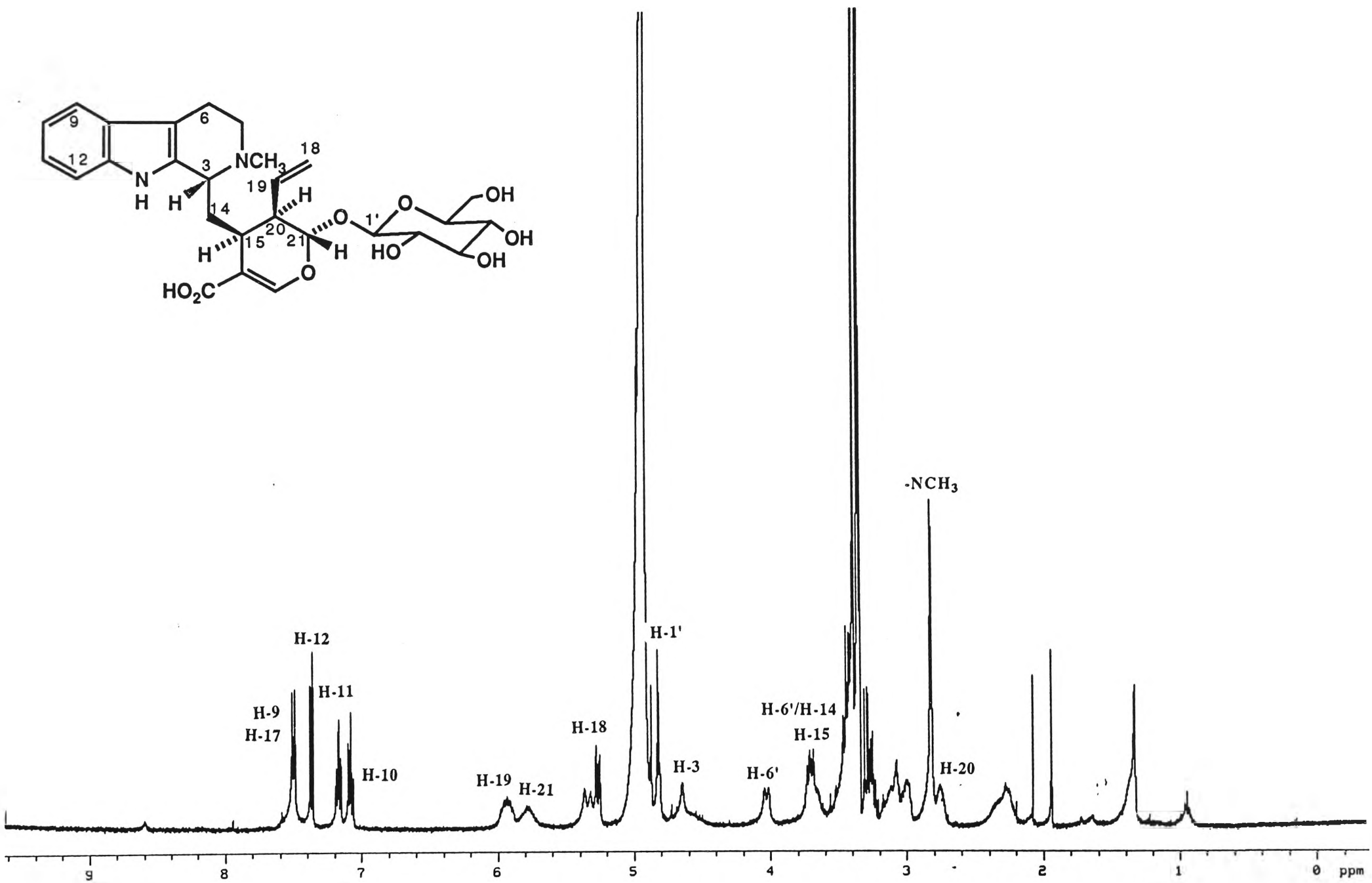

Figure 13. ^{1}H NMR Spectrum of Oa-4A-2 [400 MHz, CD_3OD, referenced at δ3.35].

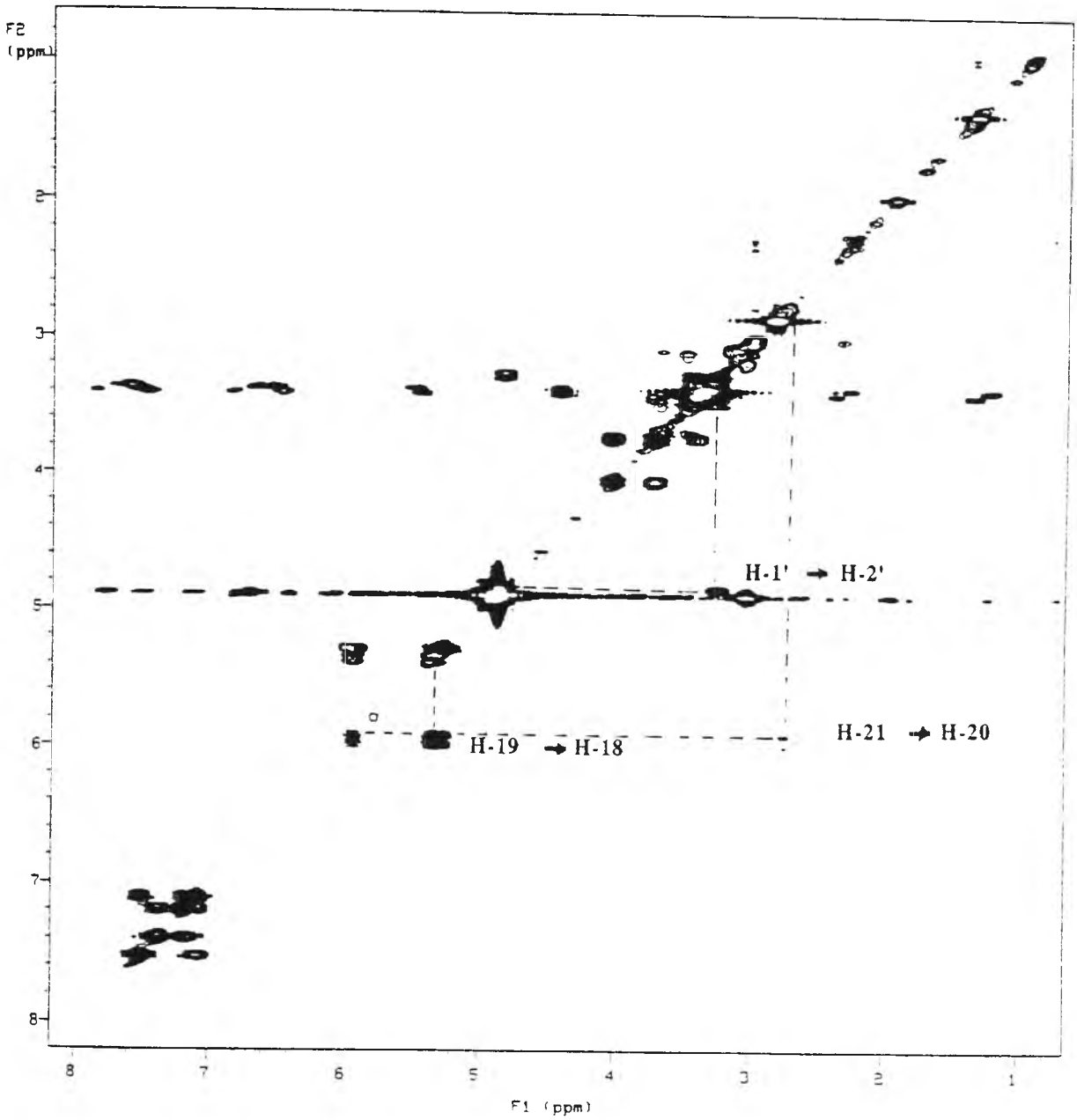

Figure 14. ^{1}H-^{1}H COSY NMR Spectrum of Oa-4A-2 [400 MHz, CD_3OD, referenced at δ3.35].

The signal centred at δ5.93 (H-19) occurred as a broad signal on the ^1H NMR spectrum obtained in CD_3OD. However, in DMSO-d_6 spectrum it appeared as a 7 line spin-spin splitting, ddd (J17.6, 10.2, 7.4 Hz). Irradiation of the H-19 signal at δ5.93 caused the ddd signal for H-20 to change to a doublet of doublets. The H-19 signal showed strong COSY crosspeaks to the signals at δ5.34 (d, 17.0Hz, H-18_{trans}), δ5.27 (d, 10.0Hz, H-18_{cis}), and a weak COSY crosspeak to δ2.77 (J7.4Hz).

Another broad signal was observed at δ5.77 and was assigned to H-21. Broad signals in NMR are caused by rapid FID (Free Induction Decay) decay due to short T_2 (dipole-dipole or transverse relaxation time). These phenomenon are associated with exchange processes or some experimental factor such as poor shimming of the magnetic field. In the case of Oa-4A-2, the occurrences of broad signals at δ5.93 (H-19) and δ5.77 (H-21) may be attributed to steric crowding. The presence of the methyl group which is attached to $N_{(4)}$ causes restricted rotation for protons at C-19 and C-21. Increasing probe temperature to 50°C gave sharp signals for H-19 and H-21 with defined multiplicity indicating that the signal appearance is temperature dependence. An increase in temperature increases the rate of rotation causing all the spins to exchange rapidly thus giving a single average signal.

The ^1H NMR spectrum obtained in DMSO-d_6 (Figure 15) showed a well resolved sharp signals for H-21 and H-19 which may indicate that solvent effect may be another reason for the broadening of the NMR signals at δ5.77 and δ5.93

The signal at δ5.93 (H-21) was not observed from the COSY spectrum thus selective decoupling experiment was used to

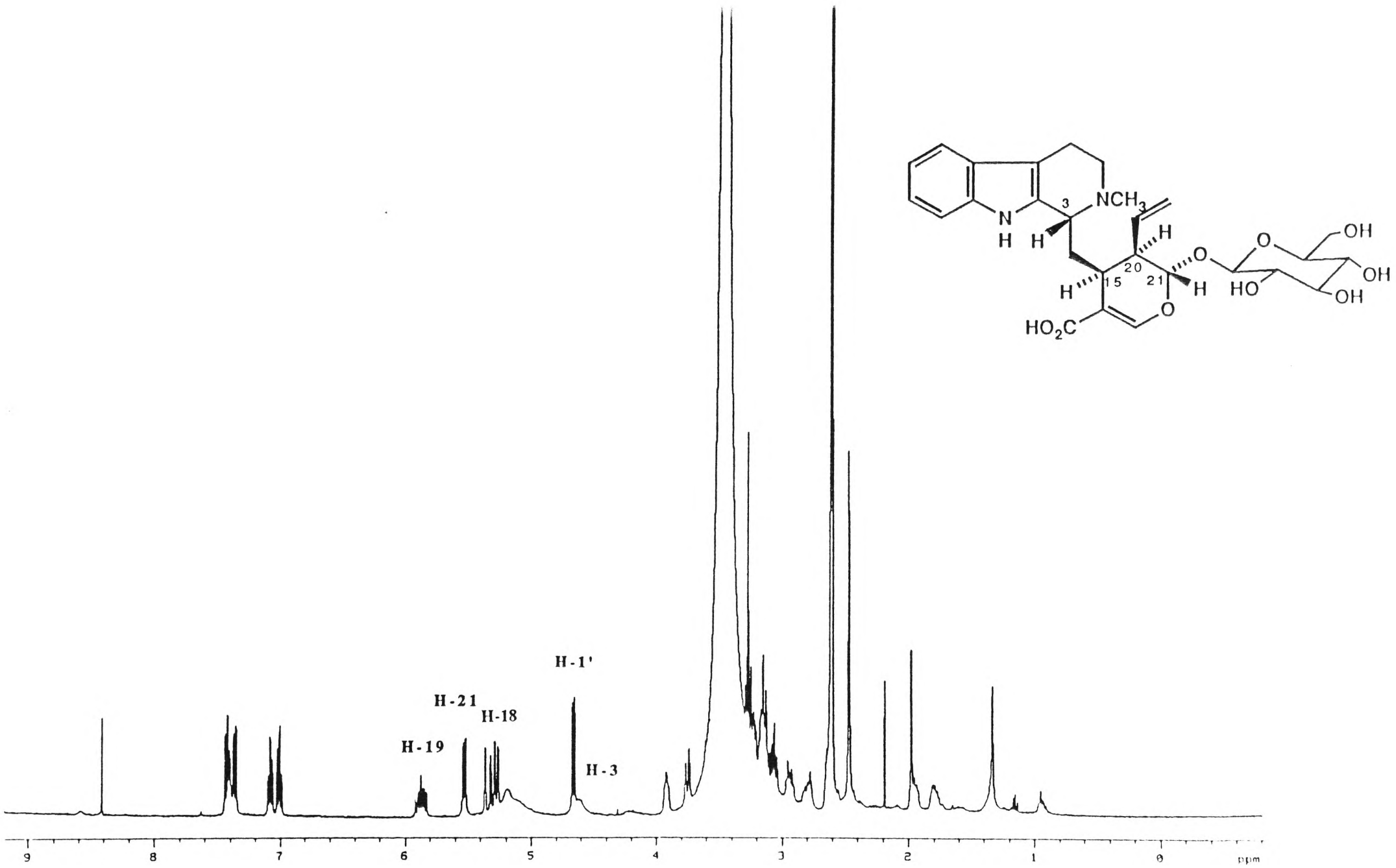

Figure 15. ^{1}H NMR Spectrum in DMSO-d_6 for Oa-4A-2 [400MHz, referenced at δ2.00].

establish the proton-proton connectivity between H-21 and H-20 (δ2.77). H-20, on the other hand, showed COSY crosspeaks to H-21 (δ5.77), H-19 (δ5.93) and H-15 (δ3.58). The olefinic protons at C-18 appeared more downfield, δ5.34 ($H\text{-}18_{trans}$) and δ5.27 ($H\text{-}18_{cis}$) in comparison with those for Oa-4A-1.

The anomeric proton at δ4.79 (d, J6.8Hz), showed a crosspeak to δ3.25 for H-2' which occured with the overlapping signals between δ3.20 - 3.55. H-6' protons were assigned to the signals at δ4.05 (d, J12Hz) and the doublet at δ3.72. These protons correlated with the signal at δ3.40 for H-5'. The overlapping signals between δ3.20 - 3.55 were assigned to H-3', H-4'. The H-14 protons overlapped with H-6' signal at δ3.69.and at δ3.50.

H-5 and H-6 of the tetrahydro-β-carboline unit was compared with a piperidine ring in which the protons were expected to resonate at δ2.74 and δ1.50, respectively. The broad signals centred at δ2.26 were assigned to the H-6 protons while the H-5 protons to the multiplets at δ 3.06-3.11 and δ2.98-3.00.

A 3H singlet observed at δ2.82 is characteristic of a methyl group attached to a heteroatom. On comparison of this observed methyl signal to some of the model compounds such as 1,4-dimethyl-β-carboline, it was established that it was attached to $N_{(4)}$. Methyl groups attached to the indolic nitrogen resonate farther downfield at δ4.08.

A reaction of Oa-4A-2 with CH_3OH/CD_3OD in $(Ac_2O)_2O$ yielded only the methyl ester derivative rather than the N-acetyl derivative as observed from its mass spectrum. This result supported the assignment for the $N\text{-}CH_3$ group in the molecule.

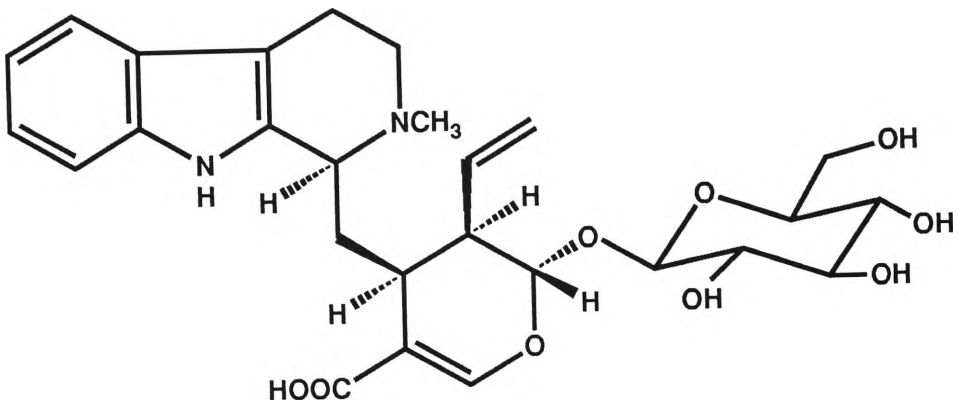

Palicoside **58**

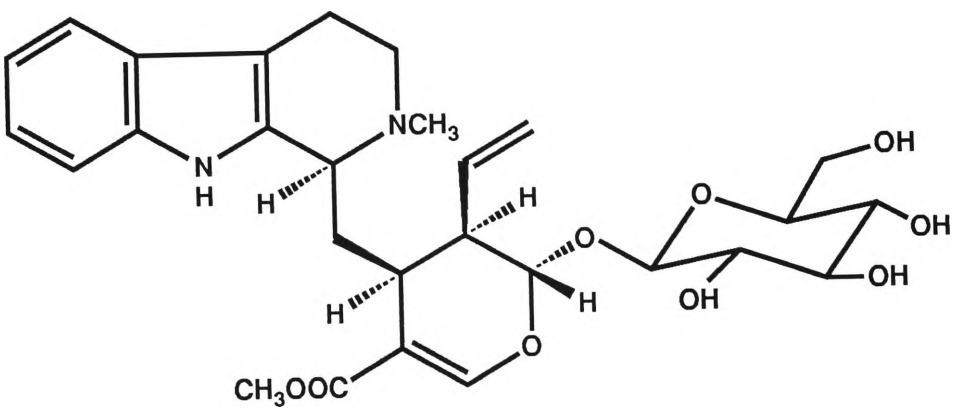

Dolichantoside **55**

Oa-4A-2 was proposed to have the same stereochemistry at H-15, H-20 and H-21 to that of Oa-4A-1 as observed from the similarity in their proton NMR data and their circular dichroism absorption.

From the literature, the structure of Oa-4A-2 was found to be related to palicoside **54**, recently isolated from the species *Palicourea marcgravii* of the Family Rubiaceae by Morita et al.[111]

Palicoside was proposed by Morita to have a stereochemistry of 3S (α), 15S (α), 20S (α), and 21S(β). The stereochemistry was established by conversion of palicoside to strictosamide. Methylation of palicoside with CH_2N_2 yielded a methyl ester derivative, which is structurally identical to the known compound dolichantoside **55**.

Dolichantoside **55** was isolated from *Strychnos gossiweleri* by Coune and Angenot[112] and from *Strychnos tricalysoides* by Leclerq and Angenot[113]. This compound was proposed to have a relative configuration of 3S(α), 15S(α), 20S(α), 21S(β), identical to strictosidine and has a positive CD in the region 270-290 nm (indolic chromophore region). Both dolichantoside **55** and palicoside methyl ester were reported to have identical stereochemistry at C-3 (3α).[114] However, a significant difference in their observed ^1H NMR chemical shift values for H-3 was apparent. The H-3 chemical shift for dolichantoside was observed at δ4.57 (90MHz, $CDCl_3$) while for palicoside methyl ester it was reported at δ3.77 (400MHz, DMSO-d_6). No CD measurement in the region 270-290 nm was reported for palicoside instead a negative CD measurement at 230 nm was reported which was not in any way useful in establishing the stereochemistry at H-3. De Bruyn[115] disclosed that an 'α' proton resonates more upfield

δ3.30 (500MHz, $CDCl_3$) than a 'β' proton (δ4.62). Based on the observed proton chemical shifts of other tetrahydro-β-carboline alkaloids, a generalisation was made by Crabb[116] that most 3α configuration tetrahydroderivatives resonates at proton chemical shift < 3.8 ppm and those with 3β configuration occurred farther downfield (>3.8 ppm). In terms of CD measurements, it had been established that 3α configuration gave a negative CD maxima in the region 270-290 while a positive CD in the same region was observed for 3β configuration.[117,118] Clearly, the H-3 stereochemistry of one of these compounds must be incorrect. If the NMR trends are correct then this will suggest that dolichantoside has 3R(β) stereochemistry and palicoside have the correct assignment (3S) as reported.

Oa-4A-2 gave a proton chemical shift of δ4.65 for H-3 which conformed for a 'β' configuration. This was substantiated by the observed cotton effect on the CD spectrum where a negative CD maxima were observed in the region 270-290 nm supporting a 'β'-orientation for H-3. Leclerq and Angenot[113] found that isodolichantoside, a C-3 epimer of dolichantoside (N_4-methyl vincoside) gave a negative CD at 270-290nm. However, no proton chemical shift value for H-3 of isodolichantoside was reported for comparison. Our observed proton chemical shifts and CD measurements were more consistent with those established in the literature. Also, the positive CD measurements obtained for an authentic sample of dolichantoside provided by Leclerq indicated that Oa-4A-2 was its C-3 epimer. Therefore we believed that the stereochemistry of Oa-4a-2 would be 3β(R), 15α(S), 20α(S), 21β(S) although clarification by X-ray would be desirable.

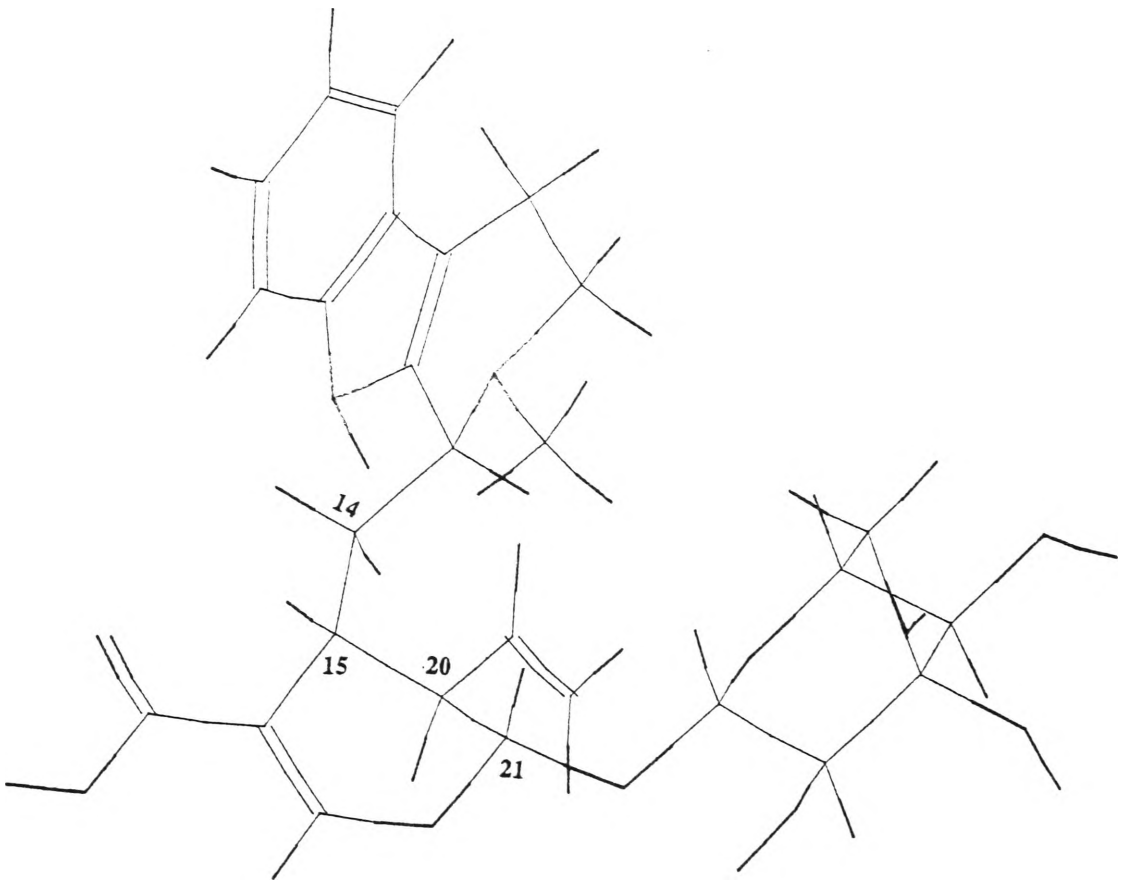

Figure 16. Possible Conformation of Oa-4A-2 Based on Molecular Modelling Using ALCHEMY Program with Energy Minimisation.

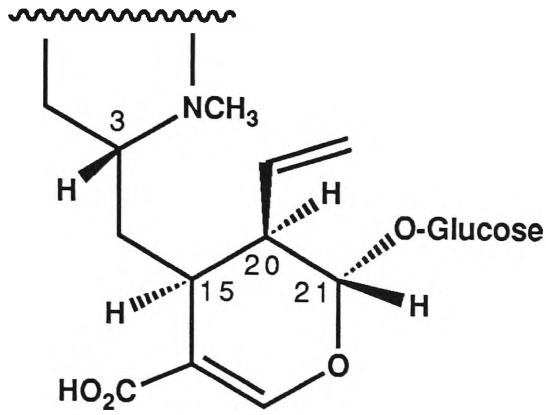

The above structure maybe derived from vincoside **23** with N-methylation at $N_{(4)}$. The observed chemical shift for H-3 at δ4.65, are analogous to that reported for vincoside (δ4.44, β configuration).[116]

Molecular modelling using the ALCHEMY program with minimisation provided a stable conformation of Oa-4A-2 as shown in Figure 16. The molecular model clearly showed the proximity of the N-CH_3 group to the vinylic protons of the monoterpenoid unit.

The fragment ions obtained from HRFABMS spectrum correlate well with those for dolichantoside as shown in Figure 17. Both gave the *m/z* at 185 and 199. The pyrilium ion commonly obtained for methyl ester derivatives of glucoindole alkaloids with *m/z* of 165 was not observed for Oa-4A-2. Both strictosidine and dolichantoside exhibited *m/z* at 165 while a *m/z* 151 was observed for Oa-4A-2, the difference of 14 amu suggesting for a carboxylic acid.

Oa-4A-2 established as a tetrahydro-β-carboline and methylated at the N-4 position has not been isolated from any other species of genus *Ophiorrhiza*. This is the first reported isolation of a C-3 epimer of palicoside.

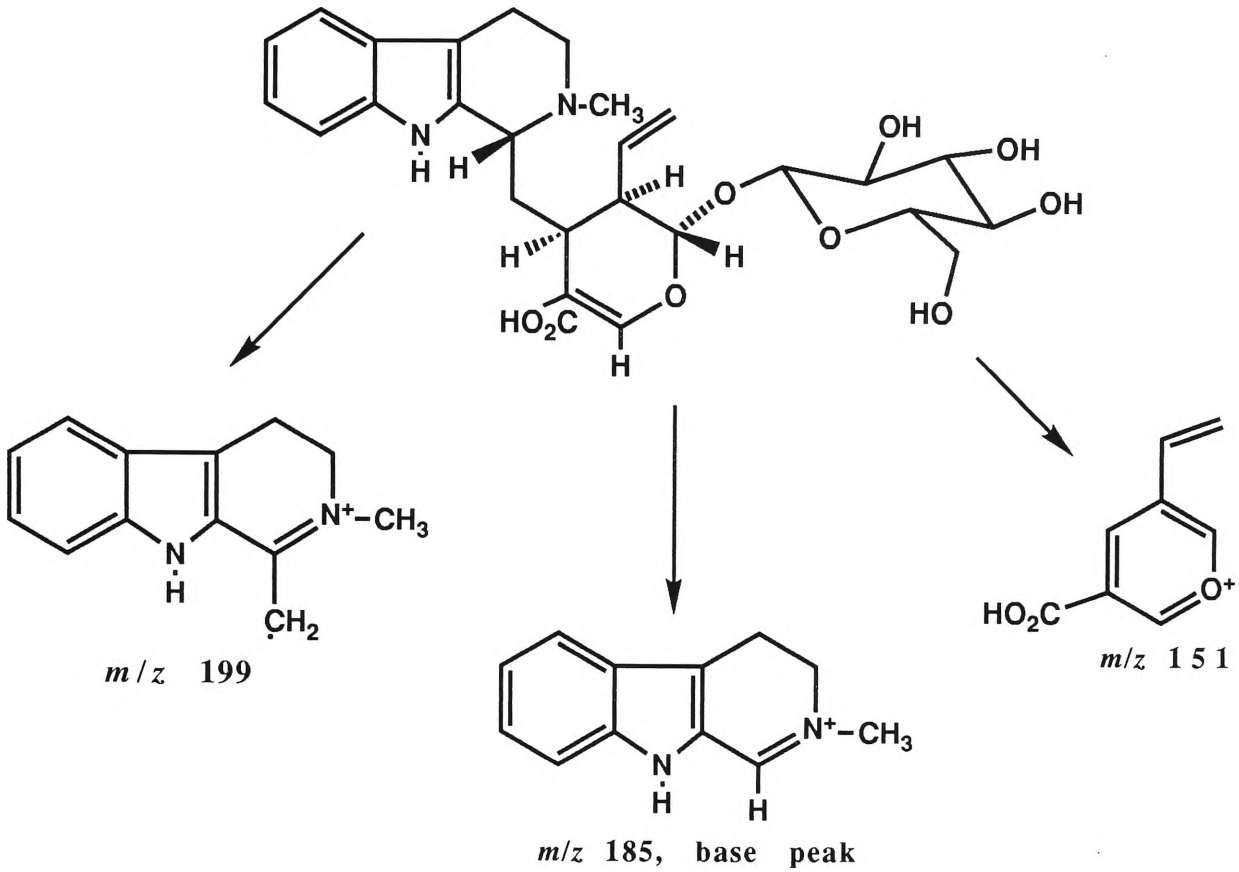

m/z 143,144, indole ions
m/z 156,169,171, -4H-β-carboline ions

Figure 17. MS Fragmentation Pattern of Oa-4A-2.

2.2.3 Isolation of the Glucoindole Alkaloids as Methyl Ester Derivatives

Most of the glucoindole alkaloids reported in the literature were either isolated or characterised as their methyl esters. The glucoindole alkaloids Oa-4A-1 and Oa-4A-2 were isolated and elucidated as their carboxylic acids. To confirm the structures of these two glucoindole alkaloids, we attempted to prepare their methyl esters derivatives in the expectation of isolating their methyl esters derivatives which might be compared with palicoside methyl ester and dolichantoside **55**. However, it was

later found that two different compounds were isolated which prompted us to investigate their structures.

Methyl ester derivatives were prepared from the crude water-soluble extract (Oa-WS) to facilitate and provide ease of isolation and purification. The vermiculite-like semi-purified water soluble alkaloid, Oa-WS, was methylated with CH_2N_2. The methylated alkaloids were isolated by PTLC on silica developed in CH_3OH. The major alkaloid which appeared under UV_{254} as a bright blue band and the dark blue minor alkaloidal band were labelled as Oa-WS-Me-I and Oa-WS-Me-II, respectively. Other minor alkaloids were detected although their amounts were minute. A methyl ester derivative of Oa-4A-1, labelled as Oa-4A-1-Me was also prepared by methylation with CH_2N_2.

Oa-WS-Me-I was purified twice by HPLC on a C18 column eluting initially with isocratic 60%CH_3OH/H_2O; then 80%CH_3OH/H_2O in the second step. After concentration, Oa-WS-Me-I which eluted after 10.2 mins., was obtained as a white solid. Oa-WS-Me-II, obtained as a light brown resin after PTLC, was purified by HPLC in 80%CH_3OH/H_2O at 1.5 ml/min eluting after 28.0 mins.

Table 11. Comparison of Percentage Intensity of Observed Fragment Ions for Oa-WS-Me-I and Oa-4A-1-Me.

Observed Ion	Oa-WS-Me-I	Oa-4A-1-Me
527.0 (M+H)	90%	40%
365.0	80%	30%
304.2*	15%	10%
182.0	15%	50%
177.0	10%	100%

* Odd e^- fragment ions are very unusual in protonating ionisation techniques even though odd-electron molecular ions are sometimes observed.

2.2.3.1 Structure Elucidation of Oa-WS-Me-I

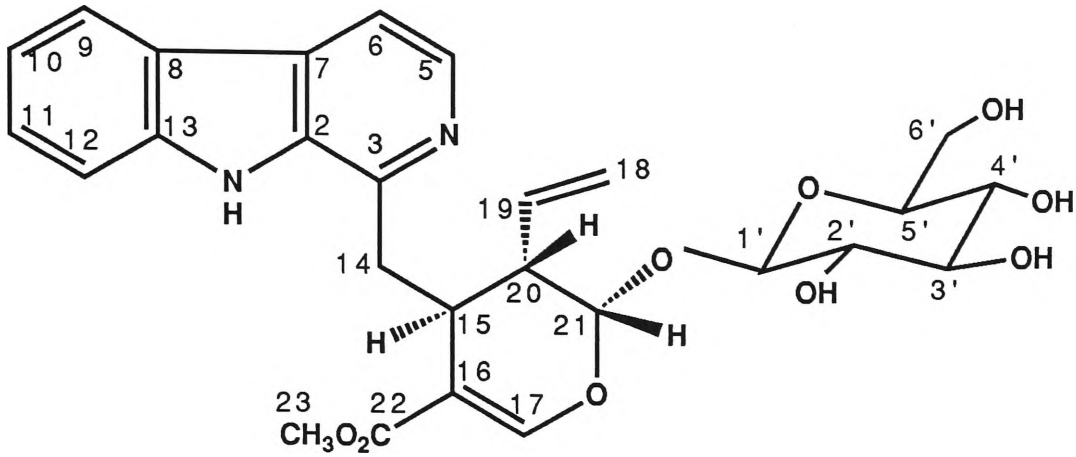

Oa-WS-Me-I co-chromatographed on tlc with the methyl ester derivative of Oa-4A-1 labelled as Oa-4A-1-Me. A *m/z* of 526 was obtained by LRFABMS with its fragment ions identical to those for Oa-4A-1-Me, although differences in the intensity of some of the ions were observed, as shown in Table 11. These suggest the possibility that Oa-WS-Me-I and Oa-4A-1-Me are isomers. Figure 18 presents the fragmentation of Oa-WS-Me-1 corresponding to the observed ions as shown in Table 11.

The ^{1}H NMR spectrum of Oa-WS-Me-I (Figure 19) showed differences in some proton chemical shifts to those for Oa-4A-1-Me, even at equal concentration. Thus a closer look at the structure of Oa-WS-Me-1 was carried out utilising 2-D NMR techniques such as COSY, TOCSY and ROESY supported by 1D selective decoupling experiments.

Analysis of the structure of Oa-WS-Me-I was carried out in comparison with the established structure of Oa-4A-1. The two and four spin systems of the β-carboline unit were established from the COSY spectrum (Figure 20). All the ^{1}H and ^{13}C NMR assignments were summarised in Table 12.

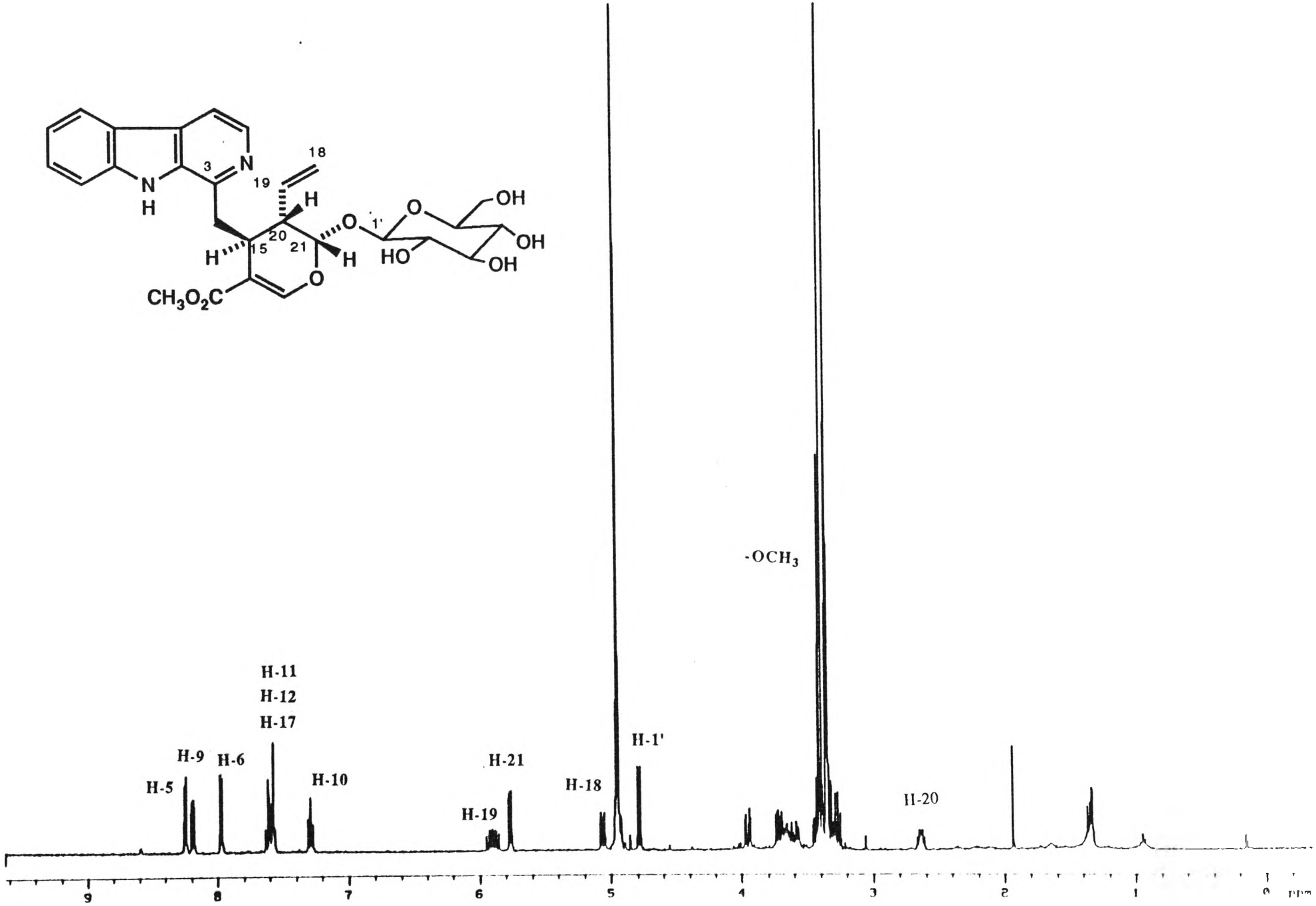

Figure 19. ^{1}H NMR Spectrum of Oa-WS-Me-I [400 MHz, CD_3OD, referenced at δ3.35].

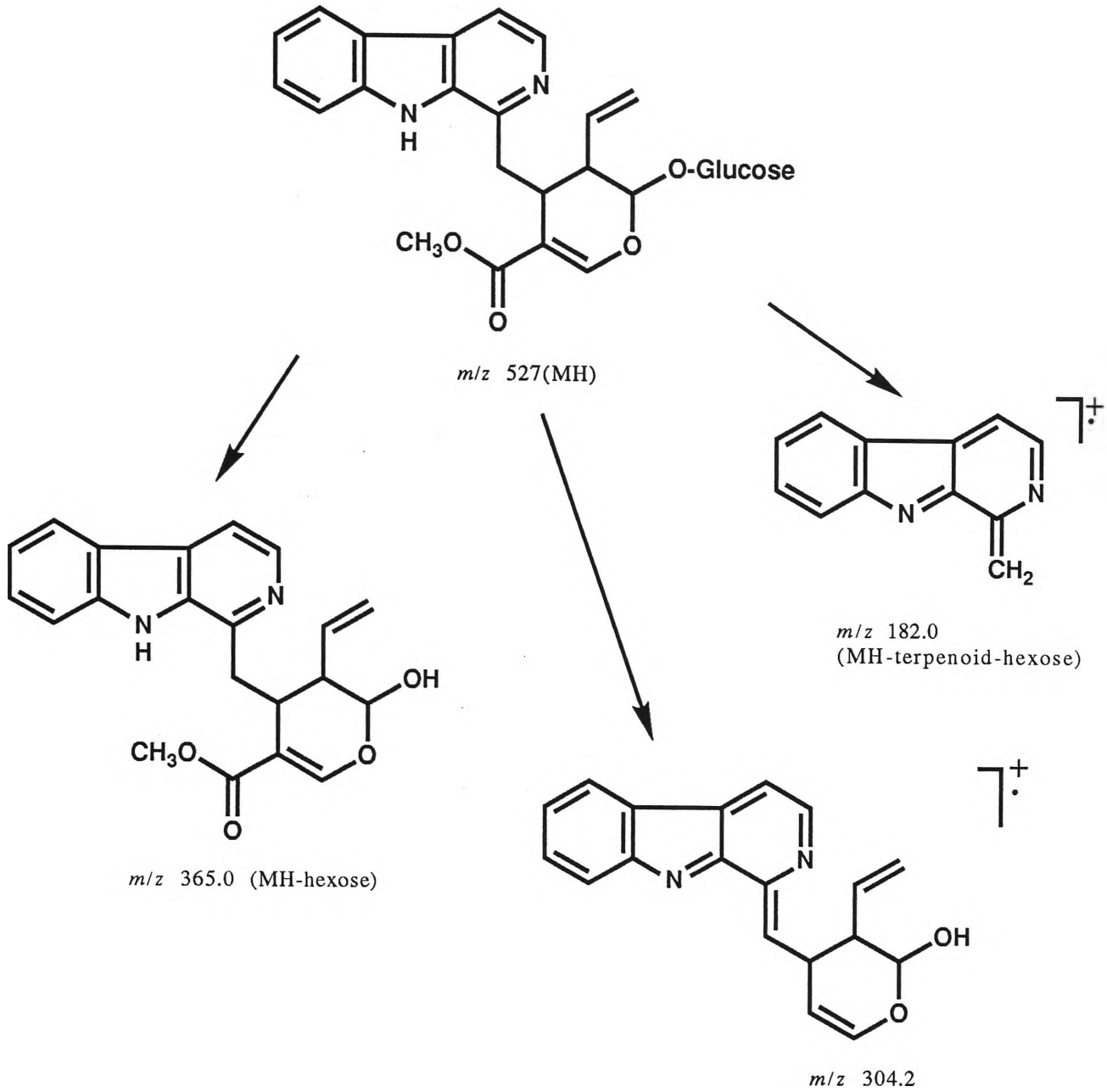

Figure 18. MS Fragmentation of Oa-WS-Me-I.

A methyl signal resonating at δ3.40 assigned for the CH_3O- group was observed in both spectra although its chemical shift is somewhat downfield for the usual δ3.70-3.80 signal characteristic of a conjugated methoxy group. The signals for the β-carboline unit of the molecule were assigned based from the COSY crosspeaks and the 1D selective decoupling experiment which are presented in Table 12.

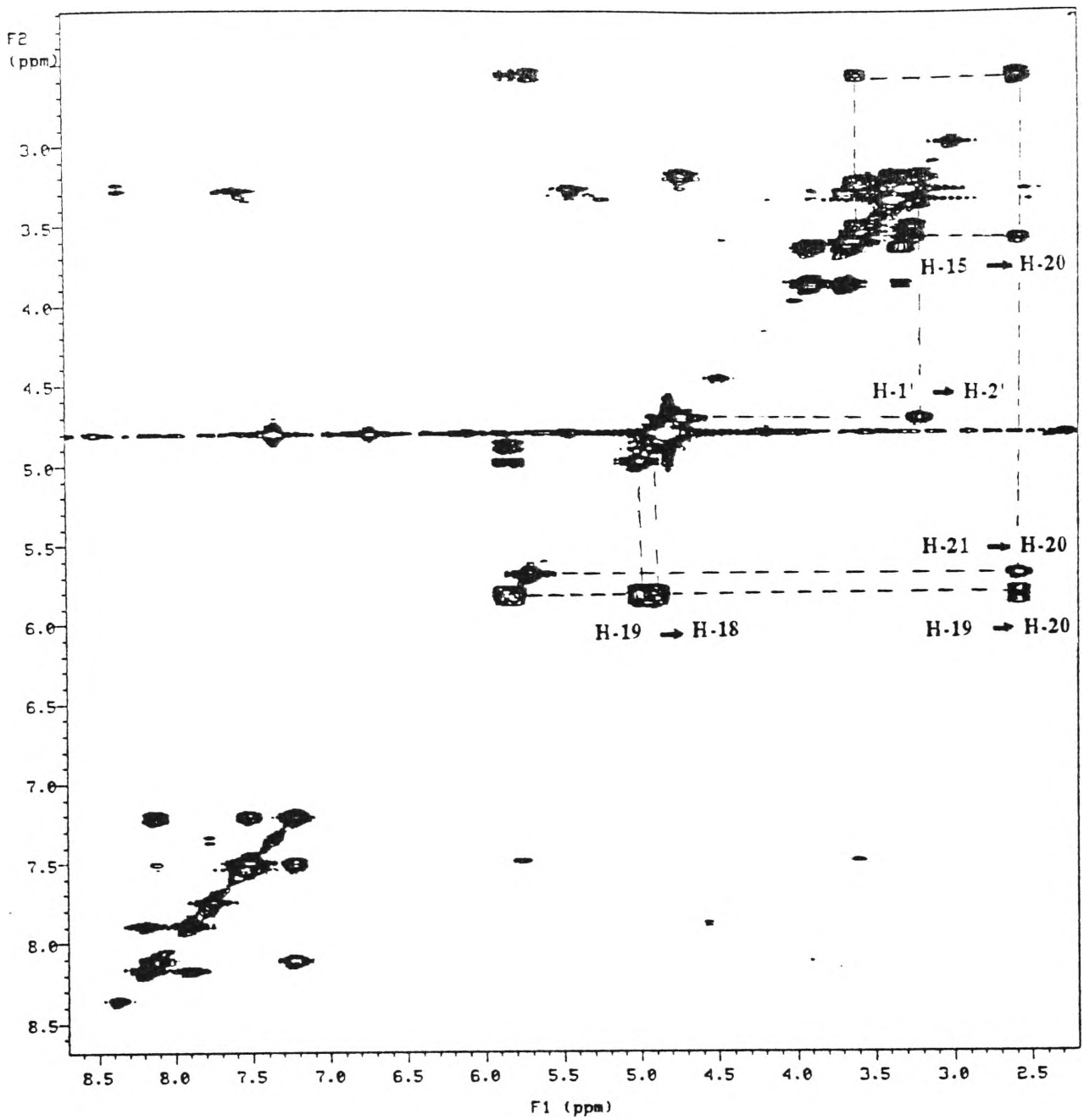

Figure 20. ^{1}H-^{1}H COSY NMR Spectrum of Oa-WS-Me-1 [400 MHz, CD_3OD, referenced at δ3.35].

Table 12. ^{1}H NMR Assignments for Oa-WS-Me-1 [CD_3OD, 400 MHz, referenced relative to residual CH_3OH at δ3.35 (^{1}H) and δ49.0(^{13}C)].

Carbon #	^{1}H, δ, (multiplicity, integration, J in Hz)	^{13}C, δ
2		136.8
3		145.2
5	δ8.24 (d, 1H, 5.2Hz)	138.0
6	7.97 (d, 1H, 5.6Hz)	114.2
7		130.0
8		122.0
9	8.19 (dd, 1H, 8.0)	122.6
10	7.29 (td, 1H7.4, 1.2Hz)	122.5
11	7.61 (td, 1H, J8.8, 1.0Hz)	129.4
12	7.59 (dd, 1H, 6.8Hz, 1.2Hz)	112.8
13		142.4
14	3.58 (m, 1H) and 3.29 (m,1H)	35.3
15	3.65 (m, 1H)	45.5
16		117.4
17	7.57 (s, 1H)	154.1
18	5.06 (dd, 1H, 10.4, 1.6Hz, H-18_{cis}) and 4.93 (d, 1H, 17.2 Hz, H-18_{trans})	119.4
19	5.91 (ddd, 1H,17.2, 10.4, 8.8Hz)	135.4
20	2.64 (m, 1H)	48.0
21	5.77 (d, 1H, 6.8Hz)	97.4
22		181.0
23	3.39 (s, 3H)	51.7
1'	4.78 (d, 1H, 8.0Hz)	100.2
2'	3.26 (t, 1H)	74.6
3'	3.43 (t, 1H)	77.9
4'	3.32 (t, 1H)	71.6
5'	3.39 (m, 1H)	78.6
6'	3.95 (dd, 1H, 12, 2Hz)/3.73 (d, 1H, 12.0Hz)	62.8

Table 13. Chemical Shift Differences of Selected Protons Between Oa-WS-Me-I and Oa-4A-Me-I [CD_3OD, 400 MHz, referenced relative to residual CH_3OH at δ3.35].

H on Carbon	Oa-WS-Me-I	Oa-4A-1-Me
5	δ8.23	δ8.19
12	δ7.58	δ7.74
14	δ3.29/d3.58	δ3.18/d3.71
15	δ3.66	δ3.51
17	δ7.56	δ7.38
18_{cis}	δ5.04	δ4.83
19	δ5.88	δ5.92
21	δ5.76	δ5.65

H-19 resonates at δ5.88 as ddd (J17.0,10.2, 8.8Hz) while H-21 was observed to occur as a doublet at δ5.76 with a J value of 6.4 Hz. The H-18_{cis} olefinic proton was observed at δ5.04 (J10.8Hz) and the H-18_{trans} resonated at δ4.88 (J17.0Hz). Both H-19 and H-21 are coupled to H-20 which resonates as an 8 line spin system and occurred as a ddd (J8.8, 6.8, 6.0 Hz) at δ2.62. A 6.0Hz coupling was observed between H-20 and H-15 which resonates at δ3.65. H-15 show COSY crosspeaks to the signal at δ3.29 for one of the H-14 protons. Selective decoupling assigned the other H-14 proton to the signal at δ3.58.

The anomeric proton (H-1') occurred at δ4.79 with an 8.0Hz coupling constant which was still consistent for a β-configuration of the sugar ring This resonance from the COSY spectrum correlates with the overlapping signals between δ3.25-3.45 for H-2' which was established to be δ3.26 by decoupling experiment. Correlations observed from the COSY and TOCSY spectra supported by decoupling experiments established the other sugar protons as follows: δ3.43 (H-3'), δ3.32 (H-4'), δ3.39 (H-5') and δ3.73 and 3.95 (H-6').

Table 13 presents the differences in the chemical shift of selected protons for Oa-WS-Me-1 and Oa-4A-1-Me. The Oa-WS-Me-1 signals for H-5, H-15, H-17, H-18_{cis}, H-21 and one of the H-14 protons were observed further downfield while H-12, H-19 and one of the H-14 methylene protons were shifted upfield.

Most of these protons are those around the 3 chiral centres at H-15, H-20 and H-21. These differences suggested possible differences in stereochemistry at one of these chiral centres. The comparison of the J values between H-15, H-20 and H-21 are shown below.

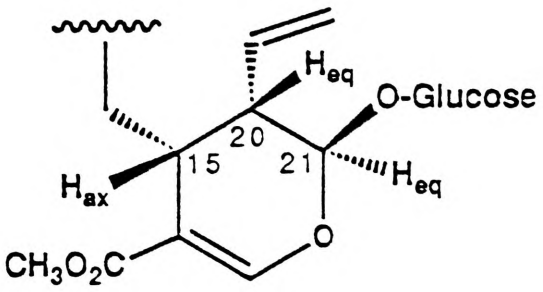

I

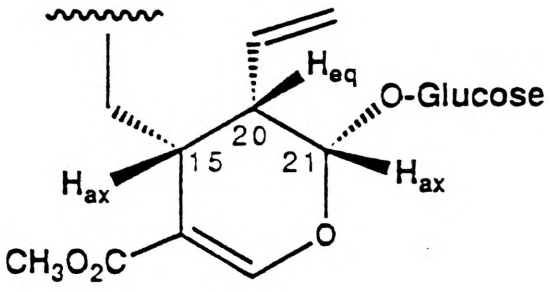

II

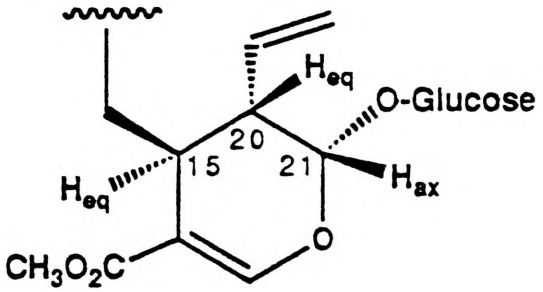

III

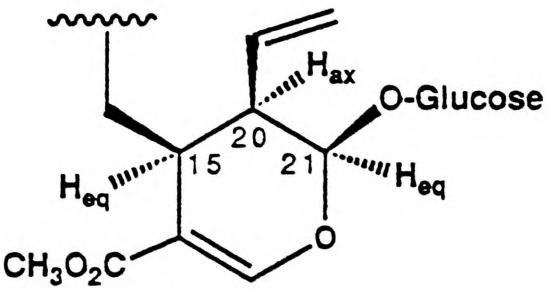

IV

Figure 21. Four Possible Structures of the Monoterpernoid Unit of Oa-WS-Me-I Based on the Observed Coupling Constants.

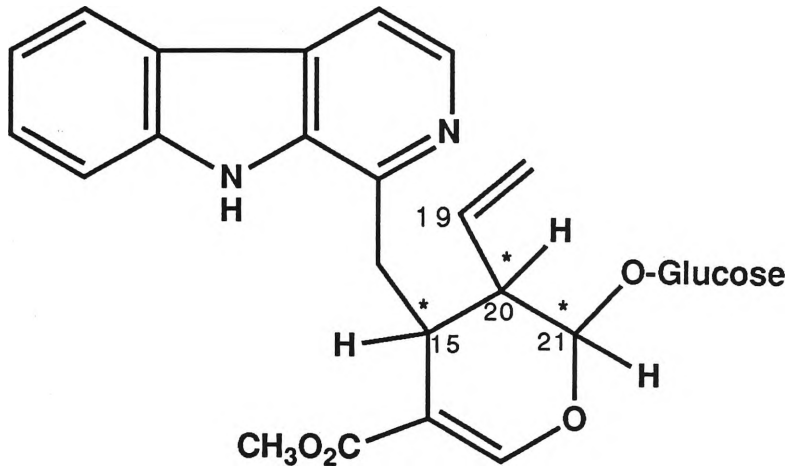

	Oa-WS-Me-I	Oa-4A-1-Me
J_{15-20}	6.0 Hz	5.0 Hz
J_{20-21}	6.4 Hz	6.8 Hz
J_{20-19}	8.8 Hz	10.0 Hz

A 6.0Hz coupling observed between H-15 and H-20 is still characteristic for an axial-equatorial or equatorial-equatorial dispositions. The J value difference between H-20 and H-21 was insignificant while the coupling constant differences between H-19 and H-20 was pronounced. Based on the observed coupling constants, four stereoisomers for H-15, H-20 and H-21 are shown in Figure 21.

Structures II and IV would show W-coupling between H-15 and H-21, however no coupling were observed from the COSY spectrum, making structures II and IV less likely. The NOESY spectrum showed an nOe between one of the protons of H-14 and H-21. This observation ruled out structure I leaving behind structure III. Strong NOESY crosspeaks were observed between H-15 and H-20 and H-20 and H-21. The signal for H-21 showed NOESY crosspeaks for H-1' and one of the protons of H-14. No

crosspeaks were observed between δ3.51 (H-15) and H-21. Based on all the observed data, Oa-WS-Me-I was assigned to have the stereochemistry as shown in structure III which is 15α, 20β, 21β.

A conformation obtained by molecular modelling with energy minimisation using ALCHEMY software is shown in Figure 22. Bond distances between the 3 chiral centres, H-15, H-20 and H-21, were measured and correlated with the observed nOe responses which were presented in Table 14.

Table 14. Correlation of Observed nOe Responses with the Measured Bond Distances from the Energy Minimised Structure (ALCHEMY) of Oa-WS-Me-I.

	Bond Distance, A°	ROESY responses
H_{20} - H_{21}	2.561	nOe (+++)
H_{20} - H_{15}	2.536	nOe (+++)
H_{20} - H_{14}	2.2376/3.617	nOe (+++)
H_{21} - $H_{1'}$	2.539	nOe (+++)
H_{21} - H_{14}	2.927/3.864	nOe (+)
H_{15} - H_{21}	3.707	no nOe (n.o.)
H_{21} - H_{18}	3.867(t)/5.080(c)	no nOe (n.o.)

(+++) Large nOe (+) Small nOe (n.o.) Not Observed

This unusual C-20 stereochemistry of Oa-WS-Me-1 is more likely to represent an epimerisation via ring opening at the later stage in the biosynthesis prior to the sugar being attached.

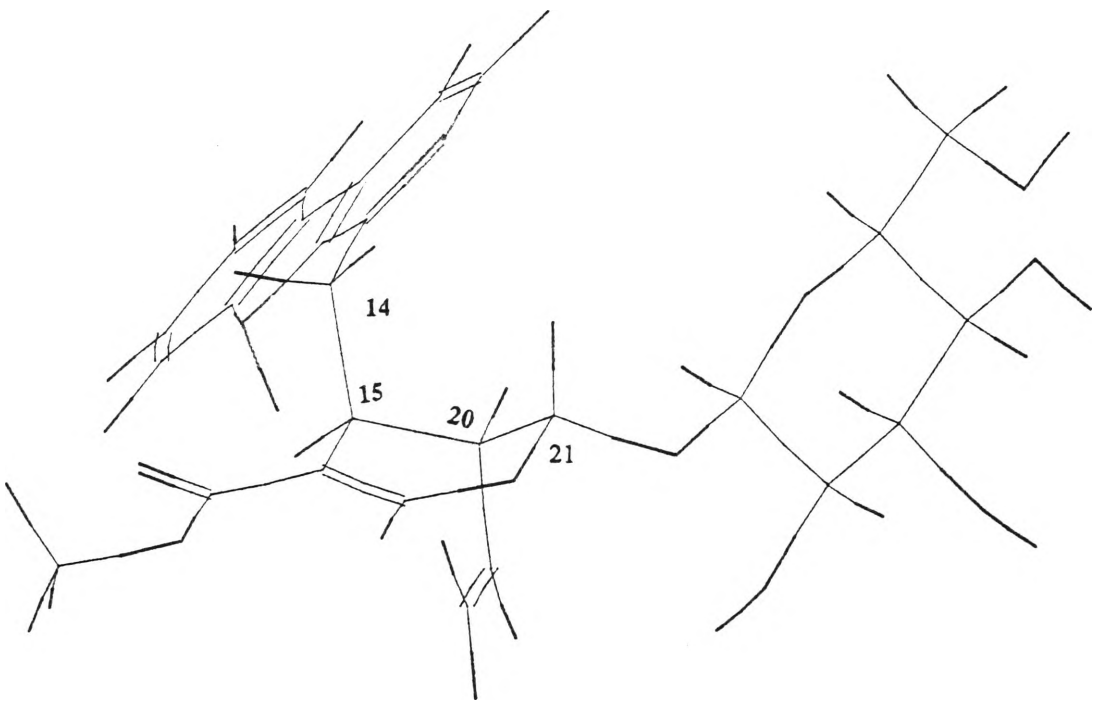

Figure 22. Possible Conformation of Oa-WS-Me-1 Based on Molecular Modelling Using ALCHEMY Program with Energy Minimisation.

2.2.3.2 Structure Elucidation of Oa-WS-Me-II

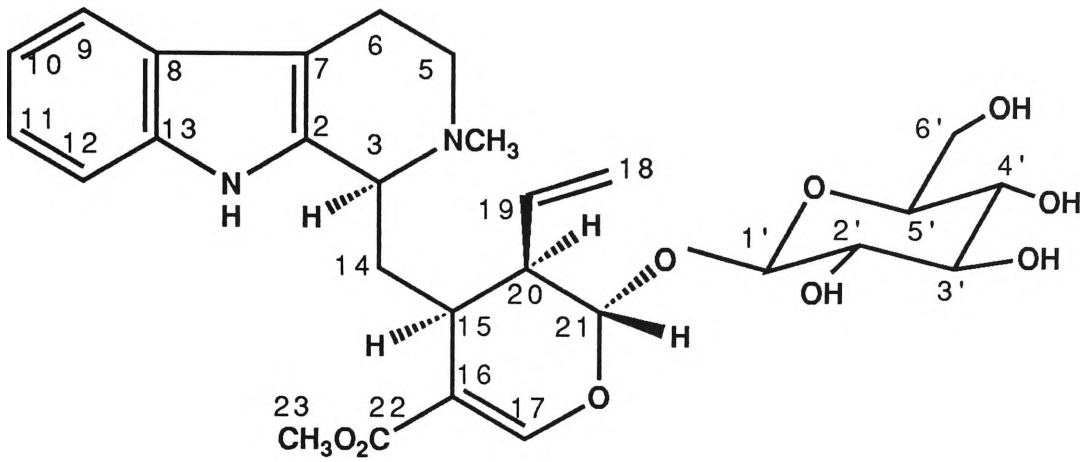

The UV absorption of this minor methyl ester alkaloid, labelled as Oa-WS-Me-II were identical to those for Oa-4A-2 which conformed for a tetrahydro-β-carboline ring system.

The structure analysis of Oa-WS-Me-II was based on the established data for the other glucoindole alkaloid (Oa-4A-2) previously discussed. It was unfortunate though that insufficient Oa-4A-2 was available for methylation as this would have facilitated spectral comparison.

2-D Homonuclear (^{1}H-^{1}H) COSY, TOCSY and ROESY (Appendix 2) NMR experiments together with 1-D selective decoupling experiments provided the ^{1}H assignments shown in Table 15 and substantiated the proposed structure for Oa-WS-Me-II.

The ^{1}H NMR spectrum of Oa-WS-Me-II (Figure 23) showed two 3H singlets at δ3.74 and δ2.53 which were assigned to the methyl ester and the N-methyl resonances, respectively.

The aromatic proton assignment were achieved in the same manner of analysis as for those in the other 3 glucoindole alkaloids. The signals at δ7.41 (d, J8.0Hz), δ7.31 (d, J8.0Hz), δ7.07

Table 15. ^{1}H NMR Assignments for Oa-WS-Me-II.[CD_3OD, 400 MHz, referenced relative to the residual CH_3OH at δ3.35].

H on Carbon	δ, multiplicity, integration, J in Hz
3	3.86 (br t, 1H)
5	2.87-2.94 (m,1H) & 3.32 (m, 1H)
6	2.60-2.67 (m,1H) & 2.87-2.94 (m,1H)
9	7.41 (d, 1H, 8.0Hz)
10	6.99 (td, 1H, 7.2Hz, 1.2Hz)
11	7.07 (td, 1H, 7.8Hz, 1.2Hz)
12	7.31 (d, 1H, 8.0Hz)
14	1.99 - 2.04 (m, 2H)
15	3.27 (m, 1H)
17	
18_{cis}	5.30 (d, 1H, 10.0Hz)
18_{trans}	5.36 (d, 1H, 17.0Hz)
19	5.86 (ddd, 1H,
20	2.74 (m, 1H)
21	5.62 (d, 1H,
22	3.74 (s, 3H)
N-CH_3	2.54 (s, 3H)
1'	4.78 (d, 1H, 8.0Hz)
2'	3.25 (t,1H, Hz)
3'	3.41 (m, 1H)
4'	3.34 (m, 1H)
5'	3.66 (m, 1H)
6'	3.94 (d, 1H, 12.0Hz) & 3.64 (d, 1H, 12.0Hz)

(td, J7.8,1.2Hz) and δ6.99 (td, J7.2, 1.2Hz) were all assigned to H-9, H-12, H-11 and H-10, accordingly. The monoterpenoid unit and the sugar moiety were established from the combined informations derived from the COSY, TOCSY and 1D decoupling experiments.

The ddd signal at δ5.86 (H-19) is coupled to δ5.30 ($H18_{cis}$), δ5.36 ($H18_{trans}$) and δ2.74 (H-20) for the AA'BX system. H-20 is coupled to δ5.62 for H-21 and the multiplet at δ3.27 for H-15. From the TOCSY spectrum, H-15 showed a crosspeak with the 2H multiplet at δ2.04-1.99, which in turn was coupled to the broad triplet at δ3.86 for H-3.

The multiplet at δ2.60-2.67 integrating for 1H and with an undefined multiplicity, was assigned to one of the H-6 non-equivalent methylene protons. This, in turn showed COSY crosspeak to another multiplet at δ2.87-2.94, integrating for 2 protons, which were assigned to the other H-6 protons and to one of the H-5 protons. The other non-equivalent H-5 proton resonates on top of the multitude of signals at δ3.23-3.41 which through selective decoupling experiment was found to be centred on δ3.32. This is characteristic of a β, γ-unsaturated piperidine ring, where H-3, H-5 and H-6 resonates at δ3.33, δ2.95 and δ2.07, respectively.

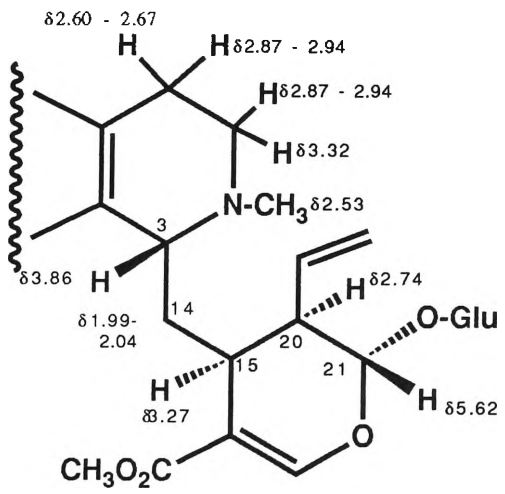

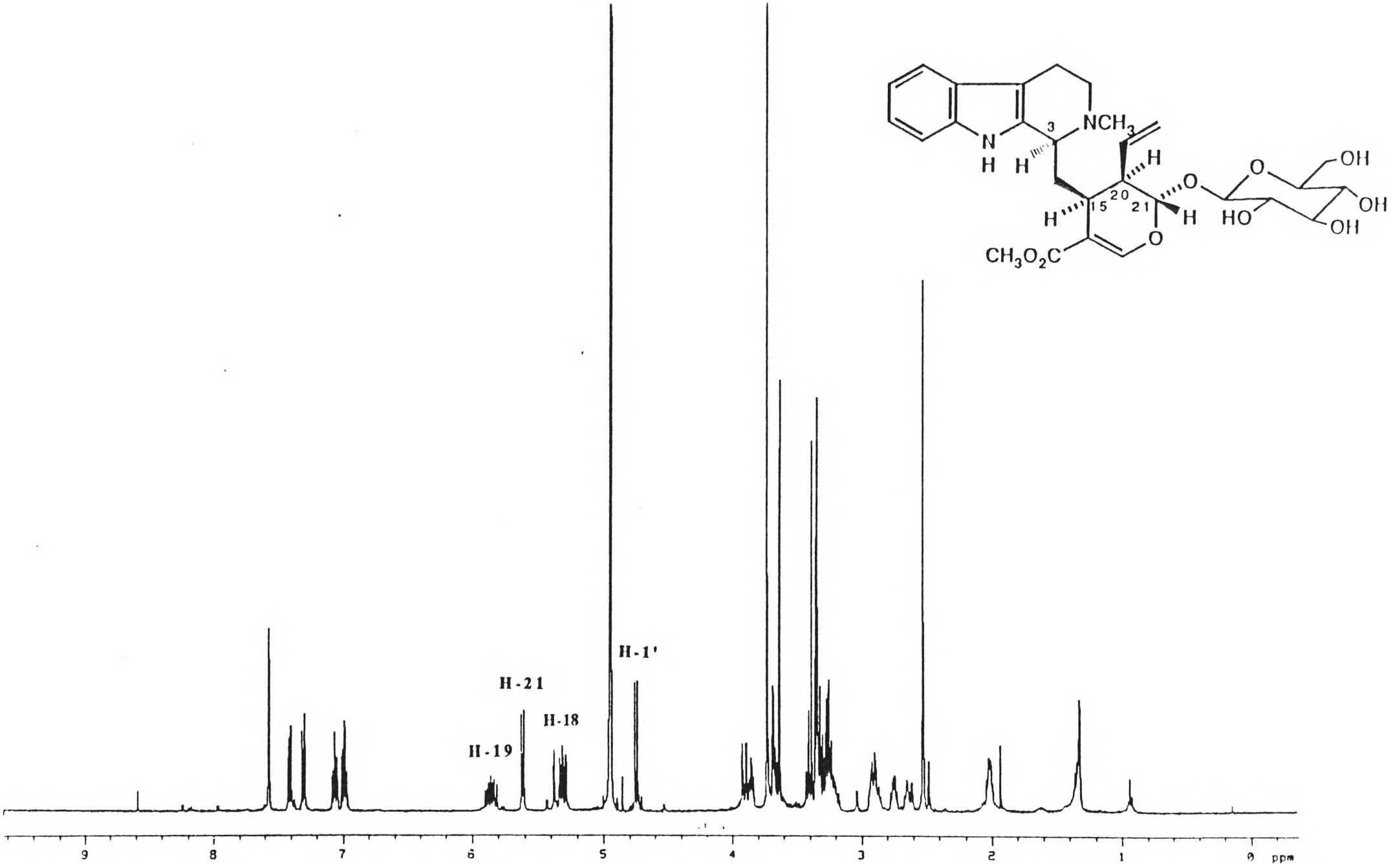

Figure 23. ^{1}H NMR Spectrum of Oa-WS-Me-II [400 MHz, CD_3OD, referenced at δ3.35].

The chemical shift values of the sugar protons were assigned as follows: δ4.78 (H-1'), δ3.25 (H-2'), δ3.41 (H-3'), δ3.34 (H-4'), δ3.66 (H-5'), and δ3.94 and δ3.64 (H-6').

The stereochemistry of H-15, H-20 and H-21 were determined on the basis of their observed coupling constants. The 6.4 Hz coupling between H-20 and H-21 was assigned for a pseudo axial-axial disposition with the monoterpenoid ring assuming a half-chair conformation. The J-value for H-20 and H-15 were not clearly defined from the ^1H NMR spectrum. However, with 1D selective decoupling experiment, H-20 was found to be an 8 line spin-spin splitting. Lines 2-4 and 5-7 were so close to each other such that they appeared as a broad line which made the signal for H-20 to appeared as a broad quartet.

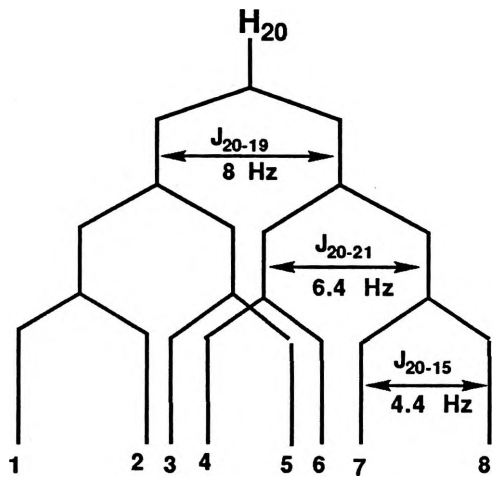

On irradiation of δ1.99-2.00 (H-14), H-15 became a doublet with J value of 4.4 Hz for an axial-equatorial or equatorial-equatorial disposition. However, with the established axial-axial relationship between H-20 and H-21, H-15 is then equatorially disposed. These observations gave rise to the relative configuration of 15S (α), 20S(α) and 21R (β), which are identical to Oa-4A-1 and Oa-4A-2.

Oa-WS-Me-II has the same overall structure as glucoindole alkaloid, dolichantoside **55**, previously isolated by Coune and Angenot.[112] However, the stereochemistry at C-3 seems to be different based on the proton NMR chemical shift value for H-3. The proton chemical shift value reported for Dolichantoside[112] occurred at δ4.57 while Oa-WS-Me-II was observed at δ3.86. According to the established NMR trends[115,116] for H-3 chemical shift value, dolichantoside would have a 3β configuration while Oa-WS-Me-II will have a 3α configuration. As earlier pointed out, there was an ambiguity in the stereochemical assignments of H-3 for dolichantoside where its observed proton NMR value fits a β configuration while its observed positive CD maxima in the region 270-290 conformed for an α configuration. Oa-WS-Me-II gave a positive CD absorbances in the region 270-290 nm which was characteristic for an 'α'-oriented H-3. The observed H-3 chemical shift value and CD measurements for Oa-WS-Me-II were more in agreement with an 'α'-oriented protons described in the literature.[116-118] Thus we believed that Oa-WS-Me-II have the same stereochemistry at C-3 as strictosidine (3α).

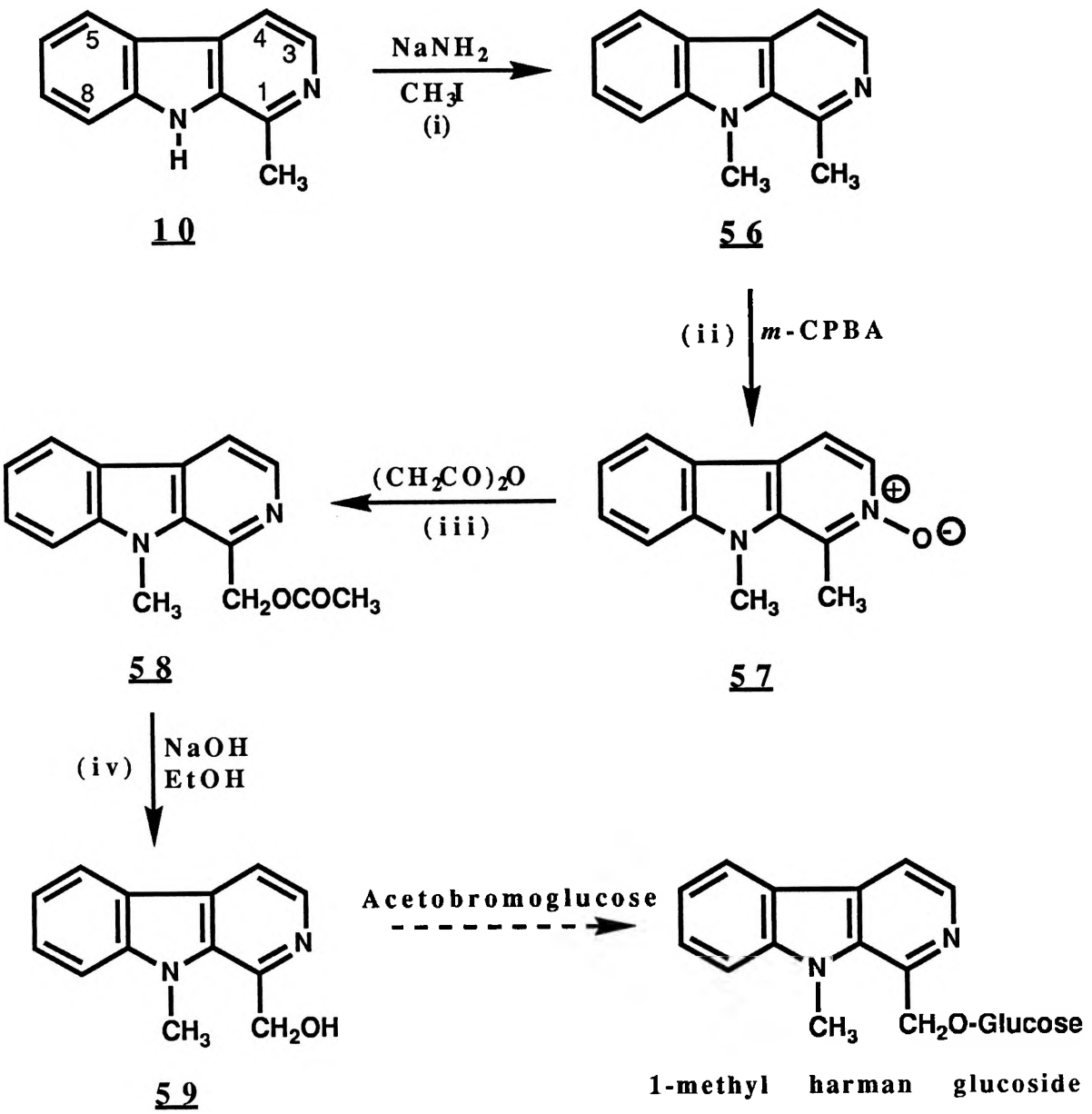

Scheme 7. Proposed Synthesis of 1-Methylharman Glucoside.

2.2.4 Synthesis of β-Carboline Derivatives

During the early stage in the structure elucidation of Oa-4A-1, we had the notion that the sugar unit may be directly linked to the β-carboline ring nucleus. Thus, attempts were made to synthesised two glucoside derivatives of harman **10** as model compounds for the structure elucidation of the *O. acuminata* glucoindole alkaloids. However, the synthesis of the target molecules were not completed since the NMR data acquired suggested that the Oa-4A-1 was not a glycoside of harman. Thus the synthesis was not pursued to completion. Commercial harman was used as the starting materials in the synthesis of these β-carboline derivatives. Schemes 7 and 8 present the proposed syntheses for 1-methylharman glucoside and harman glucoside.

2.2.4.1 1,9-Dimethyl-β-carboline 56

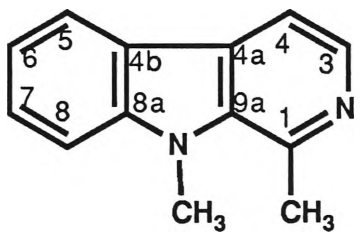

Preparation of 1,9-dimethyl-β-carboline was first attempted by the reaction of harman **10** with CH_3I/K_2CO_3. The reaction did not work with the isolation of the starting material. With $KHCO_3$ a low yield of **56** was produced. However, a reaction of **10** with CH_3I and $NaNH_2$[120] gave a pale yellow solid of **56** which was purified by column chromatography on silica.

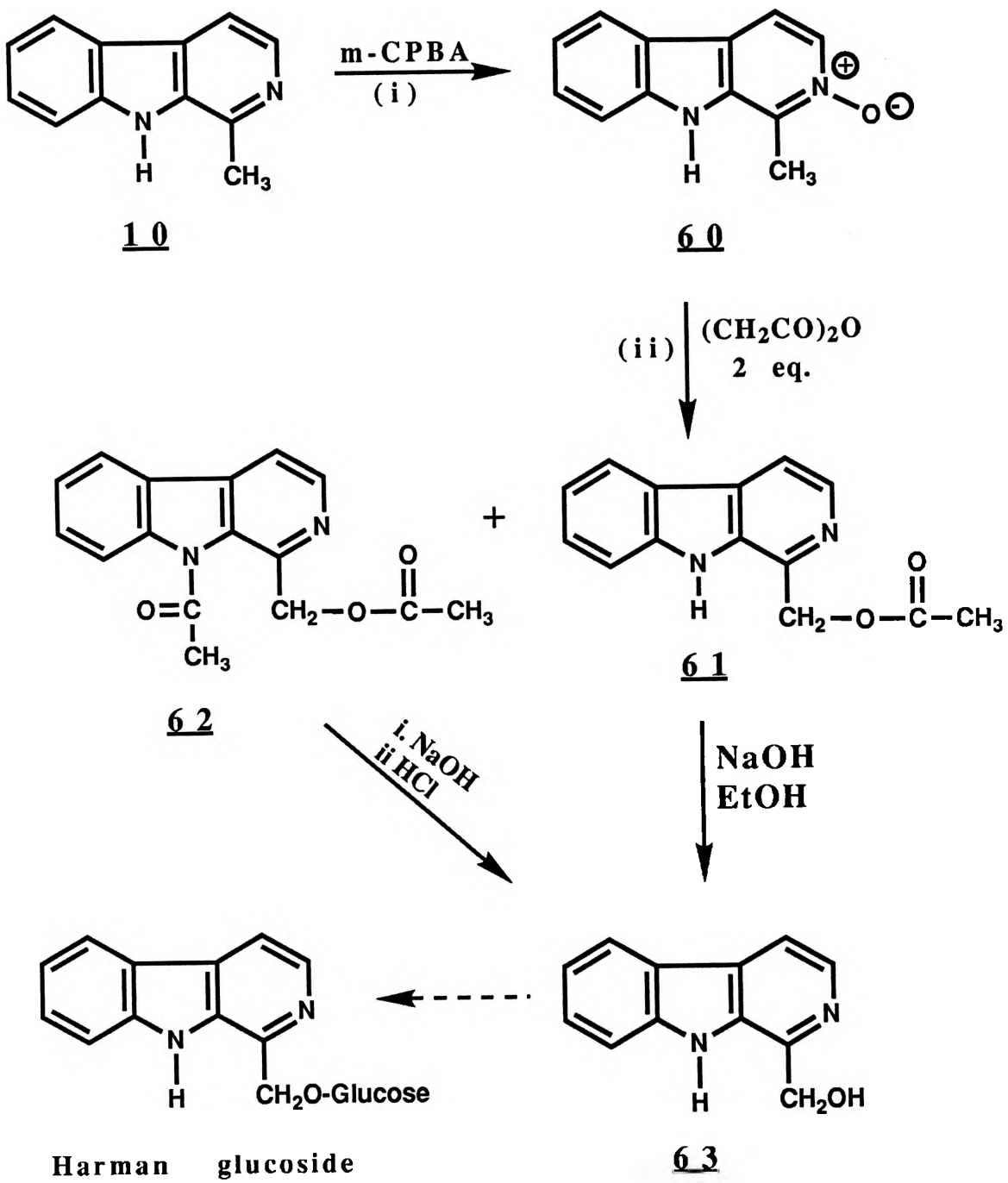

Scheme 8. Proposed Synthesis for Harman Glucoside.

The UV absorptions was typical of a β-carboline unit, λ 358.2, 342.8, 289.6, 279.2, 245.4, 233.2 and 215.6. The ^{1}H NMR and ^{13}C NMR assignments for **56** is shown in Table 16.

Table 16. ^{1}H and ^{13}C NMR Assignments for Harman **10** and 1,9-Dimethyl-β-carboline **56** [CD_3OD, 400 MHz, referenced relative to residual CH_3OH at δ3.35 (^{1}H) and δ49.0 (^{13}C)].

Carbon	^{1}H, δ		^{13}C, δ	
1	**10**	**56**	**10**	**56**
2			δ136.2	
3			δ143.0	δ137.9
5	δ8.12	δ8.09	δ137.8	δ138.0
6	δ7.84	δ7.85	δ114.0	δ112.8
7			δ122.6	
8			δ129.7	
9	δ8.09	δ8.09	δ122.6	δ121.4
10	δ7.23	δ7.27	δ120.7	δ119.5
11	δ7.53	δ7.50	δ129.3	δ128.1
12	δ7.57	δ7.60	δ112.8	δ109.3
13			δ142.5	
14 CH_3	δ2.78	δ2.98	δ20.0	δ23.5
15 NCH_3		δ4.04		δ32.1

2.2.4.2 1,9-Dimethyl-β-carboline N-oxide 57

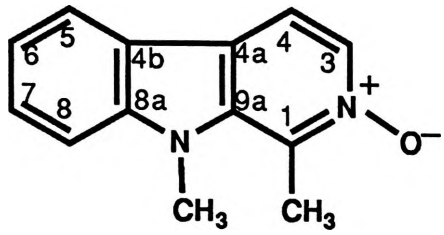

Reaction of **56** with *m*-chloroperoxybenzoic acid[121] afforded a white solid, m. pt. 46-50°C in 75% yield. The UV spectrum was different from that of the starting material, showing absorptions at λ317.2, 261.4 and 219.4 nm. The mass spectrum gave a *m/z* at 213 (MH) exemplified a typical N-oxide fragmentation with a strong tendency to lose oxygen giving rise to an ion at *m/z* 196. The ^{1}H NMR spectrum showed H-5, H-6 and the methyl group at C-1 to shift farther downfield due to the deshielding effect of the electronegative oxygen substituent.

2.2.4.3 1-Acetoxymethyl-9-methyl-β-carboline 58

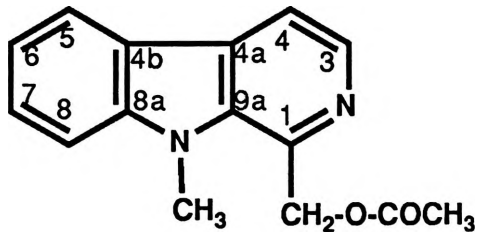

Preparation of **58** was carried out by the reaction of **57** with acetic anhydride.[122,123] Purification by column chromatography provided a yellow amorphous solid in 90% yield. The structure was supported by the absorptions shown in its UV spectrum and was characteristic of a β-carboline. The ^{1}H NMR spectrum showed the signals arising from the β-carboline

protons and three singlets at δ5.76, 4.17 and 2.18 for H-14, N-CH_3 and the acetyl methyl group.

2.2.4.4 1-Hydroxymethyl-9-methyl-β-carboline 59

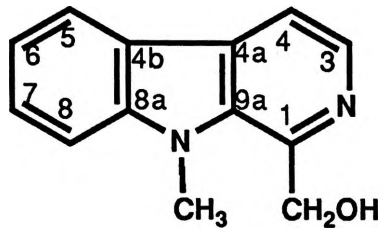

Reaction of **57** with acetobromoglucose in ethanol and NaOH afforded 1-hydroxymethyl-9-methyl-β-carboline instead of the desired glucoside as evident from its ^1H NMR spectrum. The hydroxymethyl derivative was obtained as a yellow amorphous solid, m. pt. 178-179°C.

2.2.4.5 1-Methyl-β-carboline N-oxide 60

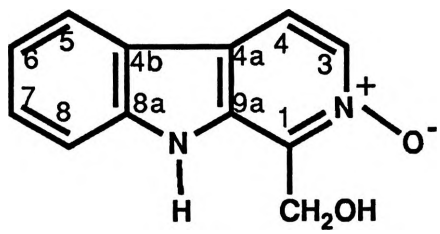

Reaction of **10** with *m*-chloroperoxybenzoic acid[121] afforded its N-oxide derivative as a pale yellow solid. Its mass spectrum showed the facile loss of oxygen.

2.2.4.6 1-Acetoxymethyl-β-carboline 61

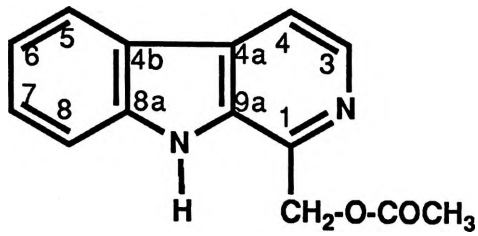

Reaction of **60** with acetic anhydride[122,123] afforded two products, the yellow solid acetoxymethyl derivative (33% yield) and a diacetoester derivative, 1-acetoxymethyl-9-acetyl-β-carboline **62**. The product **61** was obtained from a 1 equivalent reaction of **10** with acetic anhydride and **62** was obtained with 2 equivalents of acetic anhydride.

The ^1H NMR spectrum of **62** showed the presence of rotational isomerism due to the restricted rotation of the amide group. Similar exchange process in the NMR spectrum was observed with 1-methyl-9-acetyl-β-carboline **64**.

2.2.4.7 1-Hydroxymethyl-β-carboline 63

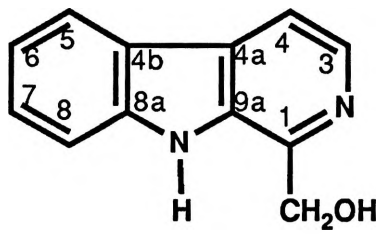

1-methyl-9-acetyl-β-carboline upon reaction with ethanol in NaOH produces the alcohol derivative of harman as a yellow amorphous solid.

2.2.4.8 1-Methyl-9-acetyl-β-carboline 64

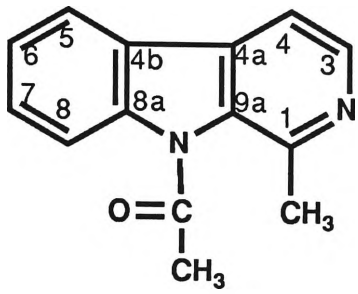

Reaction of **10** with acetic anhydride[122,123] gave the amide derivative of β-carboline **64.** The ^{1}H NMR and ^{13}C NMR spectra showed the occurence of two signals with a 2:1 ratio for the rotational isomers.

2.3 SUMMARY AND CONCLUSION

Numerous alkaloids have been isolated from members of the Rubiaceae family. Two genera in particular, *Cinchona* and *Cephaelis*, are renowned sources of the medicinally important quinine, quinidine and emetine.

The three major types of alkaloid from this family are all derived from the iridoid precursor, loganin, and contain either indole, tetrahydroisoquinoline or quinoline moieties.

The majority of the alkaloids which have been characterised from the Family Rubiaceae are derived via secologanin which when condensed with tryptamine produce strictosidine, the known precursor of numerous indole-iridoid alkaloids.

Ophiorrhizeae is one of ten, out of a total of 35 genera belonging to the family Rubiaceae, to contain iridoid-derived alkaloids. The leaves of *Ophiorrhiza acuminata* afforded five alkaloids, four of which were glycosides. The alkaloids labelled as Oa-3A and Oa-4A-1 were elucidated to be identical to the simple-β-carboline alkaloid, harman **10** and the glucoindole alkaloid, lyalosidic acid **45**, respectively. These two alkaloids have previously been isolated from two other species of *Ophiorrhiza* with harman postulated by Aimi to occur in the genus *Ophiorrhiza* as a breakdown product of the parent glucoindole alkaloids. The same relationship between **10** and Oa-4A-1 was observed in this study

Oa-WS-Me-1, though related in structure to lyalosidic acid, was proposed to have a different stereochemistry at C-20 based on all the observed physical data. This is the first report of the isolation of a lyalosidic acid C-20 epimer. This inversion at C-20 may have occurred during the later stage of biosynthesis by epimerisation via ring opening.

It is uncertain whether Oa-WS-Me-1 is a natural product. It does not seem probable that methylation with CH_2N_2 in CH_3OH caused the inversion at C-20. It is therefore possible that both epimers were present in the water soluble extract however, during the isolation procedure, these alkaloids may have been selectively purified yielding Oa-4A-1 from the unmethylated water soluble extract and the C-20 epimer from the methylated water soluble extract.

Oa-4A-2 and Oa-WS-Me-II, both tetrahydro-β-carbolines and methylated at the N-4 position have not previously been isolated from any other species of *Ophiorrhiza*. Only 2 compounds related in structure to the isolated alkaloids have so far been reported in the literature, palicoside **54** and dolichantoside **55**. Palicoside was isolated from the genus *Palicourea* of the same family Rubiaceae while dolichantoside was obtained from the plant family, Loganiaceae.

The isolated alkaloid labelled Oa-4A-2 was related in structure to palicoside but found to differ in stereochemistry at H-3 which was assigned to be 'β'-oriented with the three chiral centres at C-15, C-20 and C-21 to be α, α, β, respectively. Morita *et al.* had established palicoside to be 3α, 15α, 20α, and 21β while dolichantoside was also reported to have the same stereochemistry (3α,15α, 20α, 21β). However the reported proton chemical shift value for H-3 for the two compounds were not identical. The observed data for Oa-4A-1 were more consistent to those in literature thus we believed that it has a 3β configuration. This work was the first reported isolation of a palicoside epimer at C-3 in nature.

Oa-WS-Me-II is related in structure to dolichantoside and palicoside methyl ester. The proton at C-3 position was established to have an 'α' configuration based on the observed NMR chemical shift value and the CD measurement in the region 270-290 nm. Oa-WS-Me-II was proposed to have a stereochemistry of 3α,15α, 20α, and 21β, similar to those for strictosidine.

This work presents the first full spectroscopic characterisation of lyalosidic acid using state of the art NMR methods. As incomplete characterisation of literature compounds are available, this work could serve as a basis for the structure elucidation of other similar type of 'alkaloid-monoterpenoid-sugar' acid indole alkaloids. Isolation of a novel alkaloid as its methyl derivative, Oa-WS-Me-1, is reported together with the occurrence of two novel tetrahydroderivatives, Oa-4A-2 and Oa-WS-Me-II, isolated for the first time, from the genus *Ophiorrhiza*.

CHAPTER 3

ISOLATION AND STRUCTURE ELUCIDATION OF *TALAUMA GITINGENSIS* ALKALOIDS

3.1 INTRODUCTION

The aporphines represent a large and expanding group of isoquinoline alkaloids. These alkaloids are based on the 4H-dibenzo[de,g]quinoline structure (I) or its N-methylderivative (II), commonly known as the aporphine nucleus (Figure 24).[123]

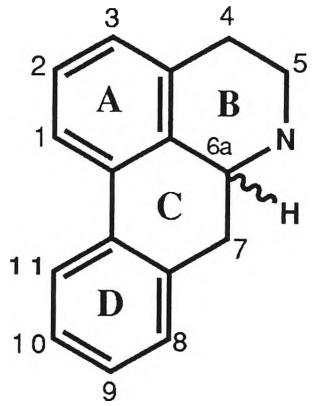

Figure 24. Aporphine Nucleus.

The aporphine alkaloids can be divided into three groups depending upon the degree of methylation of the N-atom. These groups are: (a) the aporphines as such, which contain an N-methyl function, (b) the noraporphines which possess a secondary nitrogen atom, and (c) the quaternary aporphine salts.

The aporphines are distributed in at least 18 plant families, of which the most important are the Papaveraceae, where the N is methylated; the Annonaceae, Lauraceae, and the Monimeaceae, where the aporphines occur as secondary amines. Other species belonging to the families such as Berberidaceae, Magnoliaceae, Menispermaceae, Ranunculaceae, and Rhamnaceae have been found to contain aporphine alkaloids.[124]

The most diverse structural feature of the aporphines is the oxygenation pattern. Positions 1 and 2 are always oxygenated, either by hydroxy, methoxy or methylenedioxy groups. It is

common to find further oxygen substituents at C-9, C-10 and C-11, and occasionally at C-8. It is rare to find oxygenation at C-7 except in the oxoaporphines and even rarer to find any oxygenation in ring B.[30]

Aporphines, as pointed out by Shamma,[123] are not planar and exist in either of two stereochemical arrangements as shown in Figure 25. Naturally occurring aporphines are usually dextrorotatory and belong to the L configuration.

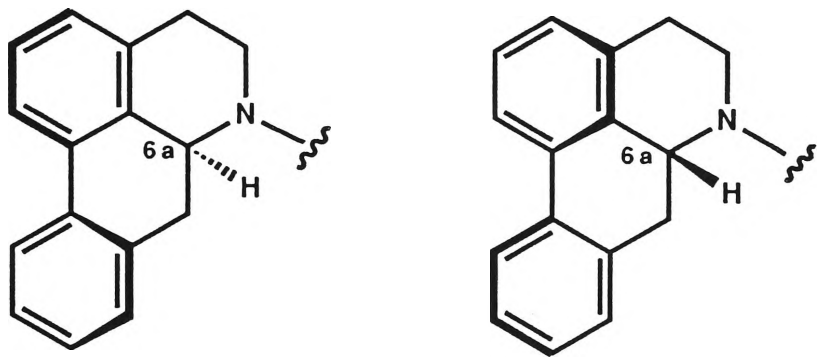

L - *S* Configuration **D - *R*** Configuration

Figure 25. Stereochemical Arrangements of Aporphine Alkaloid.

The first aporphine alkaloid was obtained not by isolation but as the result of chemical modification. Thus, in 1869 it was found that hot conc. HCl caused rearrangement of morphine **65** to apomorphine **66**, which is not a natural product.[30]

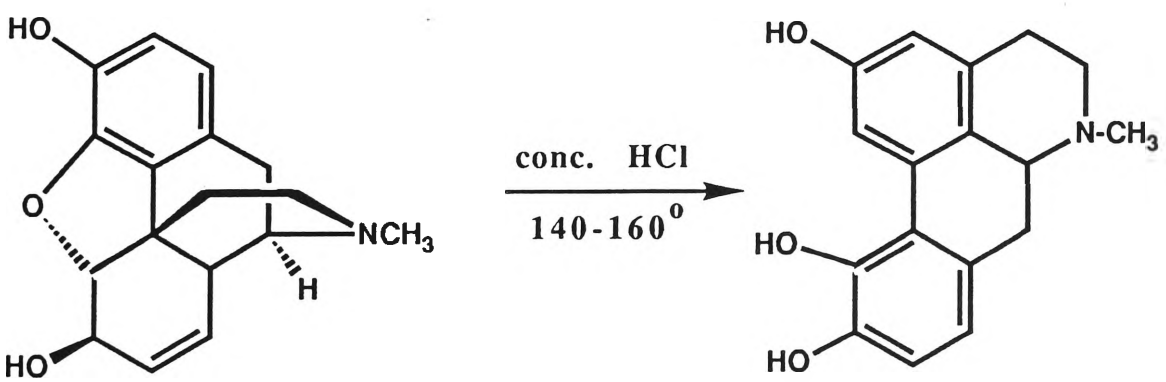

Morphine 65 **Apomorphine 66**

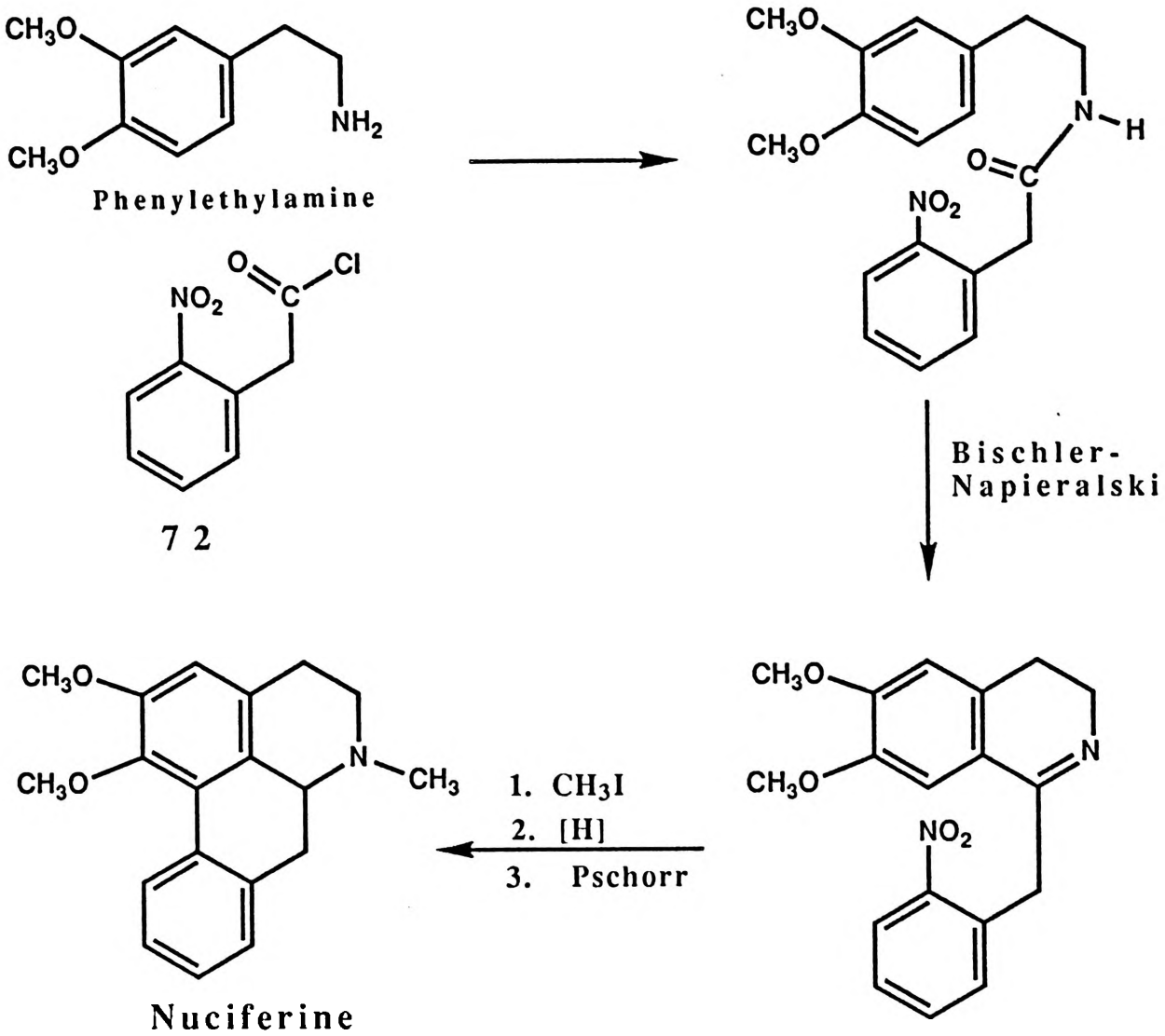

Scheme 9. Aporphine Synthesis via Condensation of *o*-Nitrophenylacetylchloride **72** with Phenylethylamine.

Glaucine **67**, corytuberine **68**, corydine **69**, isocorydine **70**, and bulbocapnine **71** were among the first aporphines from natural sources to have their structures elucidated.[125]

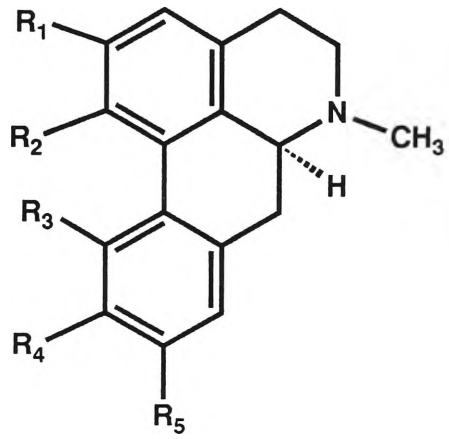

R_1	R_2	R_3	R_4	R_5	
OCH_3	OCH_3	H	OCH_3	OCH_3	**Glaucine 67**
OCH_3	OH	OH	OCH_3	H	**Corytuberine 68**
OCH_3	OH	OCH_3	OCH_3	H	**Corydine 69**
OCH_3	OCH_3	OH	OCH_3	H	**Isocorydine 70**
$-O-CH_2-O$		OH	OCH_3	H	**Bulbocapnine 71**

3.1.1 Synthesis of Aporphine Alkaloids

Three classical methods of aporphine syntheses have been demonstrated in the literature.[126] The first approach involves condensation of an *o*-nitrophenylacetylchloride **72** with an appropriately substituted phenylethylamine, Bischler-Napieralski cyclisation, methylation, reduction, and finally by a Pschorr cyclisation (Scheme 9).

Nitration of a benzyl tetrahydroisoquinoline followed by reduction, diazotization, and cyclization is the second known approach for aporphine synthesis This procedure led to the first synthesis of the aporphine alkaloid, glaucine **67** (Scheme 10).

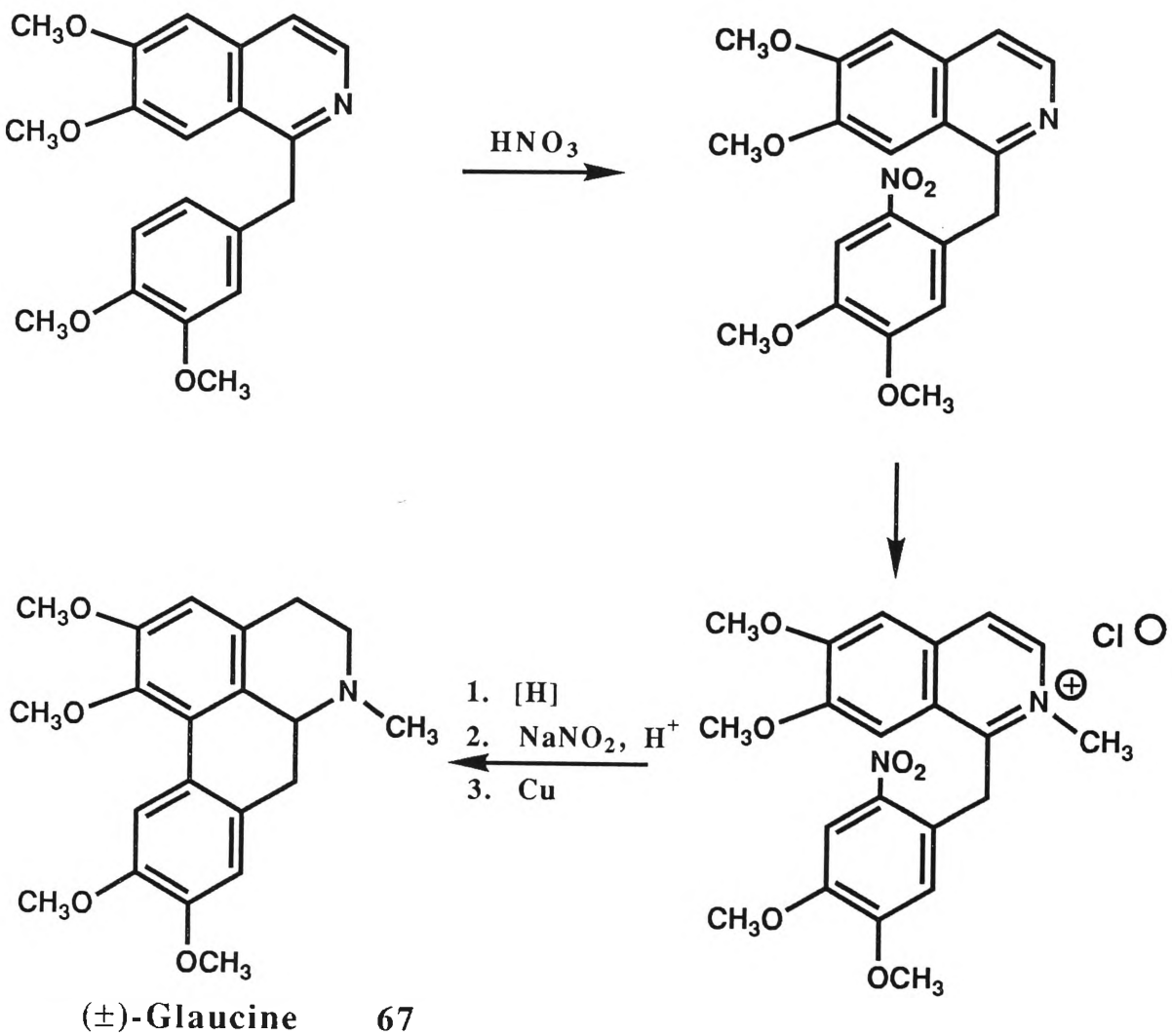

Scheme 10. Synthesis of Glaucine.

The third classical approach to the synthesis of aporphines is the base-catalysed condensation of *o*-nitrotoluene **73** with isoquinolinium salt **74** (Scheme 11).

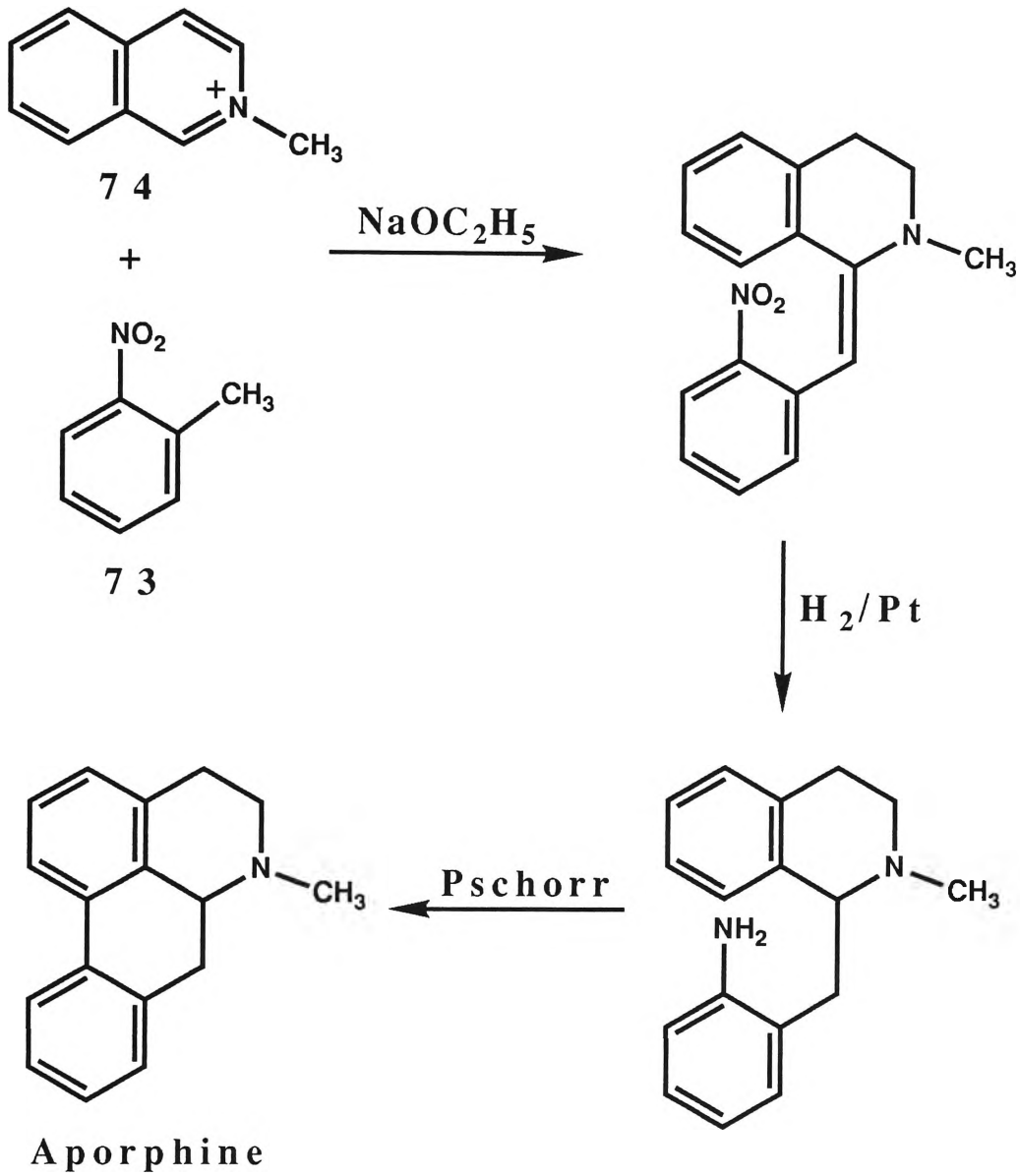

Scheme 11. Aporphine Synthesis by Based-Catalysed Condensation of *o*-Nitrotoluene with Isoquinolinium Salt.

Several modifications and new approaches have so far been cited in the literature. These, however, are beyond the scope of this survey.

3.1.2 Biosynthesis of Aporphine Alkaloids

Biogenetically, aporphine alkaloids are known to be derived from the corresponding phenolic tetrahydrobenzylisoquinoline. Three possible routes, supported by labelling experiments, have been considered for the biosynthesis of aporphine alkaloids in plants. These proceed from tetrahydroisoquinoline either by (a) direct phenolic oxidative coupling, (b) intermediacy of neoaporphine, and (c) neoproaporphines.

Robinson and Sugasawa[127] proposed the first plausible biosynthetic pathway based on *in vitro* reactions. Several feeding experiments then substantiated this route. Incorporation experiments of labelled reticuline **75** in *Papaver somniferum* have shown that isoboldine **76** was derived by direct *ortho-para* oxidative coupling (Scheme 12).[128]

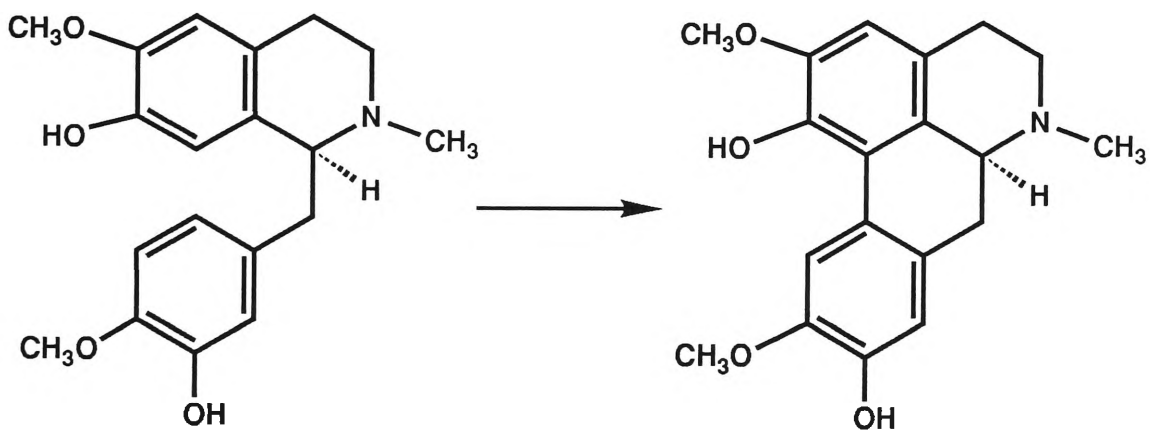

Reticuline 75 **Isoboldine 76**

Scheme 12. Biosynthetic Conversion of Reticuline to Isoboldine.

Barton *et al*[129], proposed a second route which involves the formation of dienone derivatives (proaporphines or proerythrinadienone), which then rearrange into aporphine through dienones-phenol or dienol-benzene rearrangements as represented in Scheme 13.

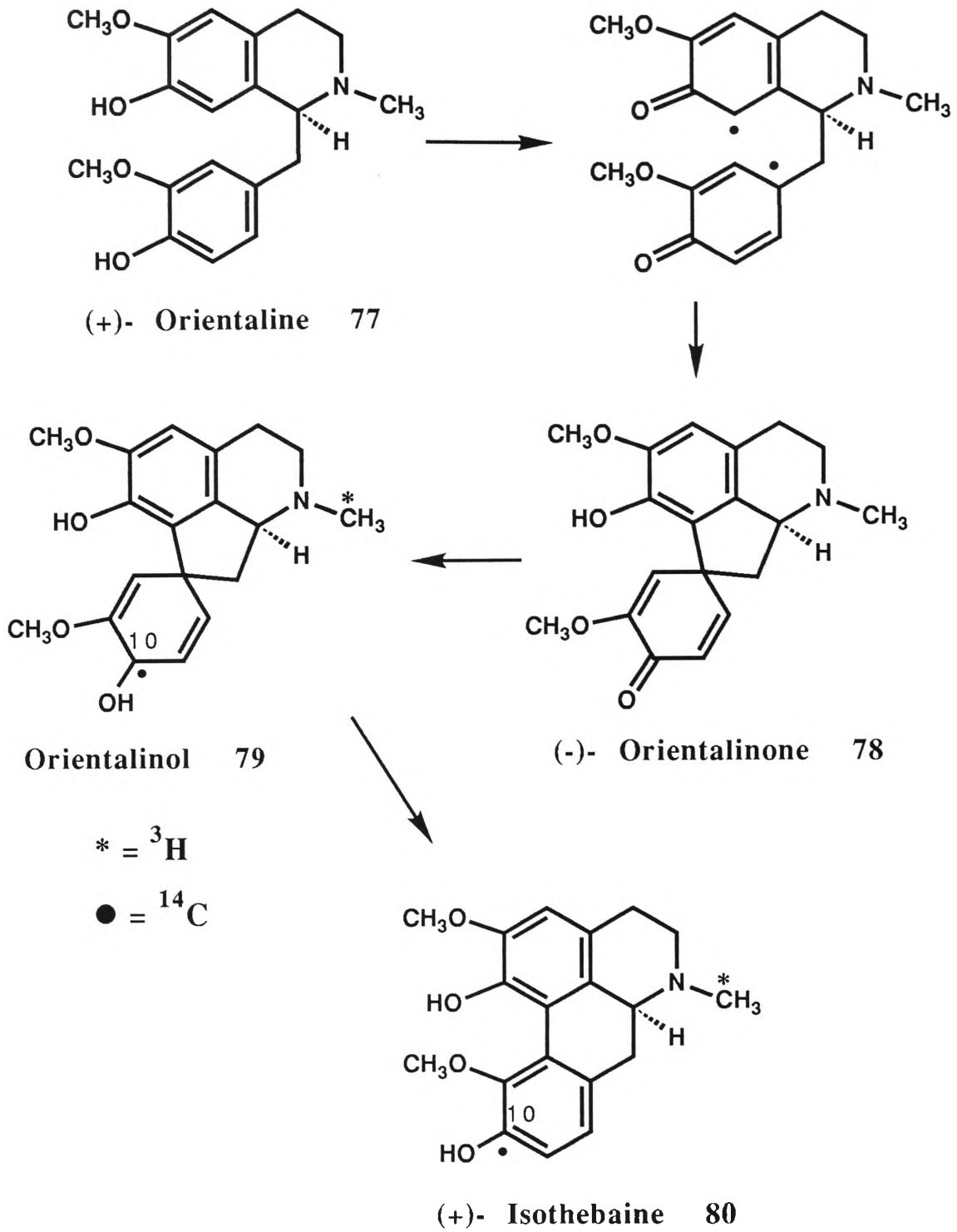

Scheme 13. Biosynthesis via Formation of Dienone

(+)-Orientaline **77** is derived from tyrosine presumably via decarboxylation of 3,4-dihydroxyphenylalanine, before or after condensation with 3,4-dihydroxyphenylpyruvic acid or 3,4-dihydroxyphenylacetaldehyde. Cyclization, reduction to norlaudanosine, and finally, methylation by S-adenosylmethionine yield (+)-orientaline. Alternatively, methylation at the 3,4-dihydroxyphenylalanine, dihydroxyphenethylamine and/or pyruvic acid might occur before condensation and cyclisation to (+)-orientaline.

According to Scheme 13, (+)-orientaline is converted to (-)-orientalinone **78** via intramolecular radical coupling. Reduction of (-)-orientalinone to orientalinol **79** and the dienol-benzene rearrangement, with loss of water afforded (+)-isothebaine **80**. This was supported by feeding experiments to *Papaver orientale* using tritium-labelled (at the N-Me and at C-10) of orientalinol epimers. Only one of the two orientalinols was incorporated well into (+)-isothebaine.

The biosynthetic pathway by coupling to neoproaporphines[130] shown in Scheme 14 is the third possible route. This, however, raises some challenging questions as to its mechanism. So far, no neoproaporphines have been isolated from natural sources. Assuming that neoproaporphines do exist, it would be likely that they could be reduced in plants and undergo a dienol-benzene rearrangements to furnish aporphine unsubstituted at C-2.

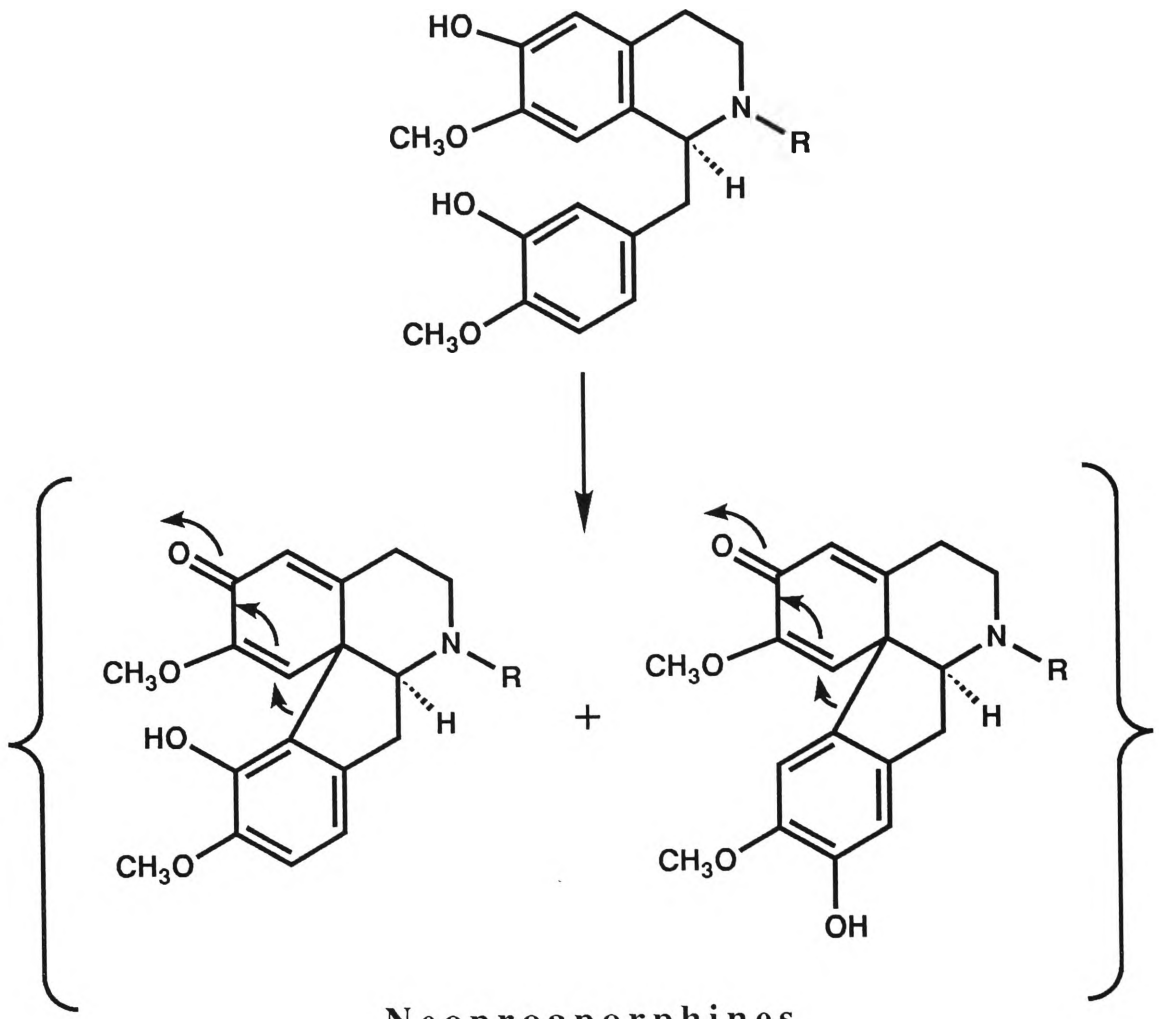

Scheme 14. Biosynthesis of Aporphine Alkaloid by Coupling to Neoproaporphines.

3.1.3 Pharmacology

Interest in evaluating the biological activities of aporphines stems from their structural relationship to apomorphine **66**, which has been demonstrated to produce a dopamine-like renal vasodilation in dogs[131] and to have a hypertensive effect on cats.[132] Apomorphine hydrochloride was found to be hypotensive; in larger doses though it can have a hypnotic effect. It also exerted a direct stimulating action on the vomiting centre in the brain and thus initiated emesis.[130] The biochemical mechanism of action is still obscure.

The aporphine alkaloids display a wide range of pharmacologic activities, although none have been produced commercially. 1,2-Methylenedioxyaporphine **81** increased arterial blood pressure, but higher doses caused strychnine-like convulsions. The methoxyhydroxide salt had a curare-like action.

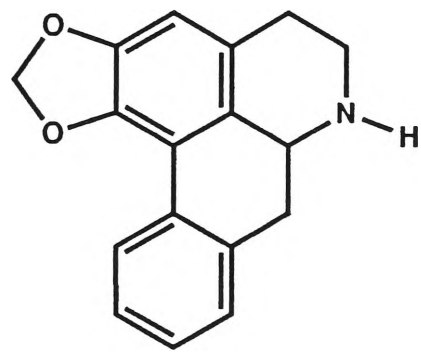

1,2-Methylenedioxyaporphine 81

Isothebaine **80** increased intestinal muscle tone in rabbit and also amplified contractions in the rat. Other activities observed include decreased motor activity and analgesia (mice) and an anti-inflammatory effect (rats).

Glaucine **67** reduced blood pressure and inhibited respiration in cats and had antitussive effects resembling codeine, but of longer

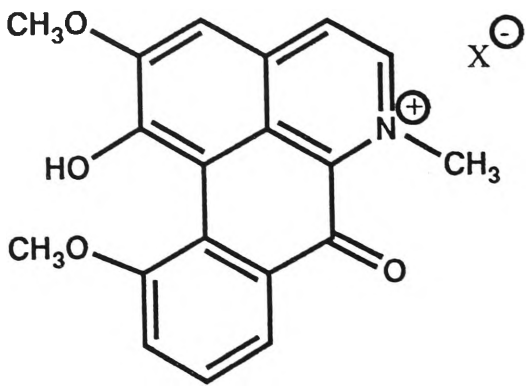

Alkaloid PO-3 **83**

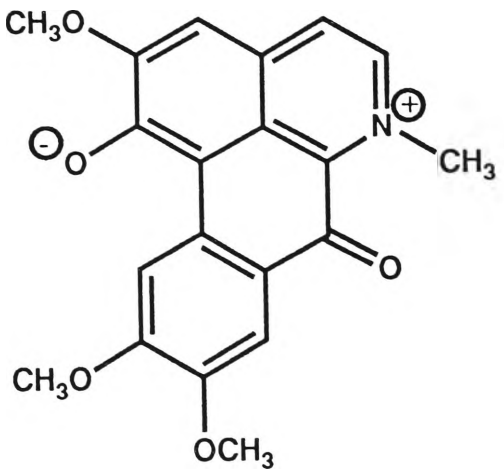

Corunnine **84**

duration. In rats and cats a potentially useful hypoglycemic effect was observed at 12mg/kg doses.

Bulbocapnine **71** affected the central nervous system and caused catatonia. Boldine **82** had a mild sedative, diuretic, and antiparasitic action, and also increased the secretions of the liver and salivary glands.

3.1.4 Oxoaporphine Alkaloids

The oxoaporphine alkaloids are most probably derived in plants by oxidation of the corresponding aporphines. Several naturally occurring oxoaporphines with the 7-keto-4H-dibenzo[de,g]quinoline skeleton are presently known. They are found in members of the Annonaceae. Araceae, Hernandiaceae, Lauraceae, Magnoliaceae, Menispermaceae, Monimeaceae, Papaveraceae and Ranunculaceae.[133]

The oxoaporphines can be divided into two distinct subgroups. The larger one is made of weakly basic, nonphenolic compounds which are bright yellow or orange yellow in colour. These are without exception high melting and usually show a decomposition point rather than an actual melting point. Since they possess conjugated carbonyl functions they show IR absorption bands near 1650 cm^{-1}. Additionally, this subgroup of oxoaporphines turn red upon addition of acid, and their $CHCl_3$ solutions show a greenish fluorescence.

The smaller subgroup of oxoaporphines, which presently includes only the alkaloids PO-3 **83** and corunnine **84**, consists of high-melting, monophenolic quaternary N-metho-salts which are green in neutral to basic solutions and red in acid.

Liriodenine **85** was the first oxoaporphine alkaloid to be isolated from natural sources and to be fully characterised.[133]

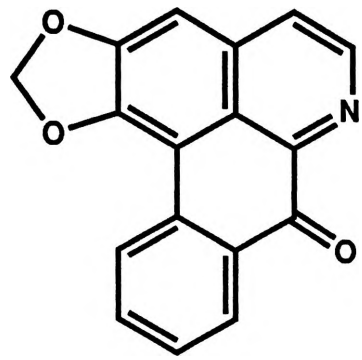

Liriodenine 85

The presumed oxidation of an aporphine into an oxoaporphine in nature can be duplicated in the laboratory, usually using either chromium trioxide in pyridine complex or manganese dioxide as oxidizing agents. Thus, liriodenine was obtained by oxidation of either ushinsunine **86** or roemerine **87**, while, 1,2,9,10-tetramethoxyoxoaporphine was produced from glaucine **67** Oxoaporphine can therefore be prepared *in vitro* either by synthesis via Pschorr cyclisation or by oxidation of the corresponding aporphine base. The oxidation of aporphines to oxoaporphines in nature is substantiated from the fact that in several instances, the corresponding aporphine or noraporphine bases are found in the same plant.

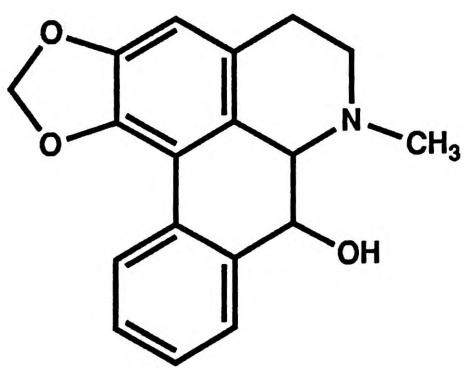

Ushinsunine 86

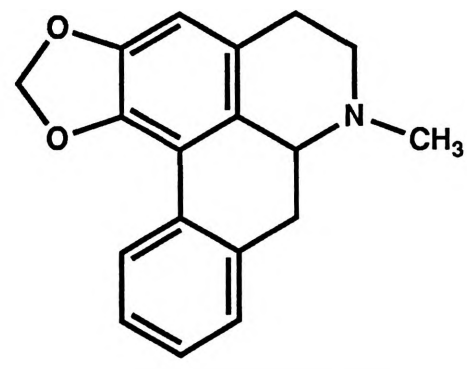

Roemerine 87

Oxoaporphine can be reduced with zinc in HCl or under Clemmensen conditions to noraporphines; thus, lanuginosine **88** was reduced to xylopine **89** and liriodenine **85** to anonaine **90**.

Liriodenine has shown significant cytotoxic inhibitory activity *in vitro* against cells derived from human carcinoma of the nasopharynx.

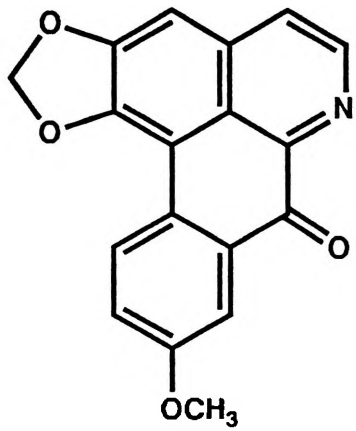

Lanuginosine 88

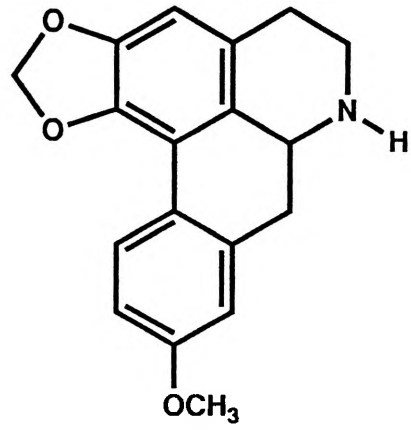

Xylopine 89

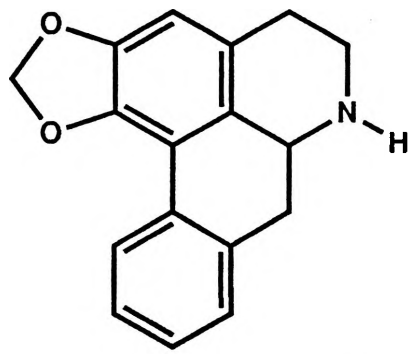

Anonaine 90

3.1.5 Genus *Talauma*

The genus *Talauma* comprises about 15 species of trees or shrubs from East Asia, South America and Japan[135], of which four species have been investigated chemically.

3.1.5.1 *Talauma mexicana*

Talauma mexicana was the first species to be reported in the literature. In 1948, Pallares and Garza[136] isolated a new benzylisoquinoline alkaloid named aztequine **91** from the leaves of this plant.

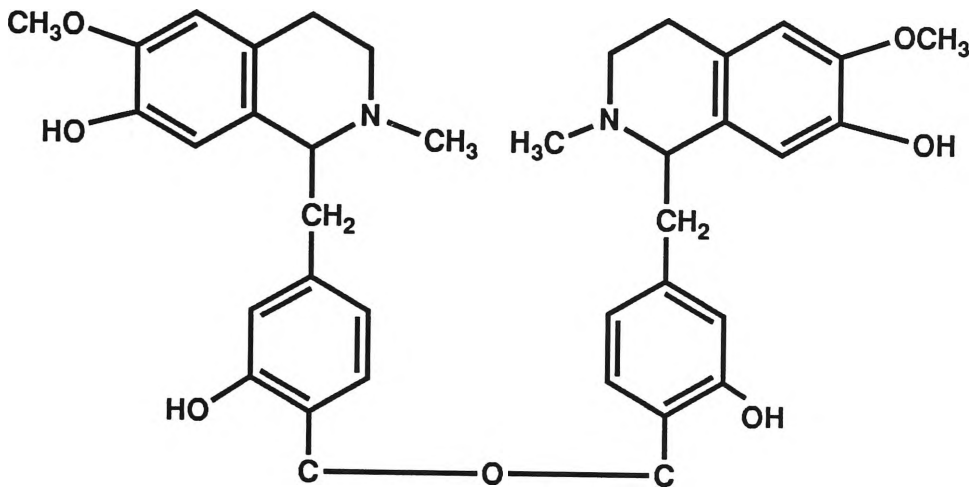

Aztequine 91

Kametani[137], in an attempt to reisolate the alkaloid aztequine from*Talauma* mexicana isolated the oxoaporphine alkaloid, liriodenine **85** instead of the previously described alkaloid.

The leaves of *T. mexicana* are used as a cardioactive drug.[136]

3.1.5.2 *Talauma hodgsoni*

Chemical investigation of *T. hodgsoni* revealed the presence of the oxoaporphine alkaloids, liriodenine **85** and lanuginosine **88**.[138]

3.3.3 *Talauma obovata*

In 1985, Plantinet and his group[139] reported the first isolation of noraporphine alkaloids in the genus *Talauma*. Together with these alkaloids, lanuginosine **88** was also isolated, this being the

first report of the co-occurrence of noraporphines and oxoaporphines in the genus *Talauma*.

The noraporphine alkaloids, anolobine **92**, asimilobine **93** and xylopine **89** together with lanuginosine **88** were isolated from the bark of *T. obovata*. No detailed spectral data were reported.

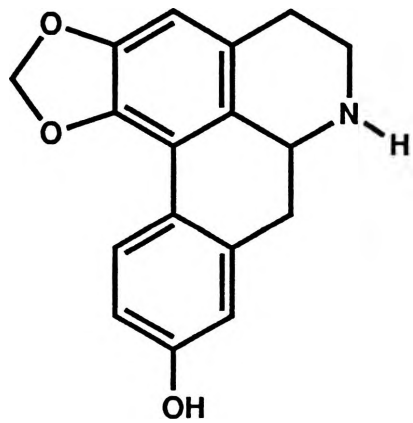

Anolobine 92

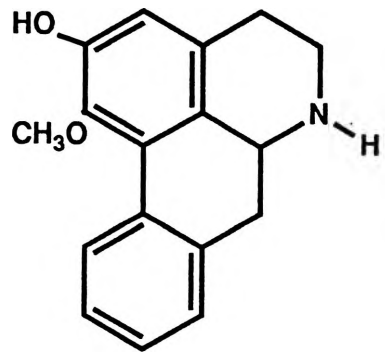

Asimilobine 93

3.1.5.4 *Talauma ovata*

This species is the only one reported of the genus *Talauma* that does not contain alkaloids. Hoffmann *et al*[140] reported that the petroleum ether extract of the roots showed activity towards the human epidermoid carcinoma of the nasopharynx test system. On chemical examination, the cytotoxic activity was identified with the compound costunolide **94**.

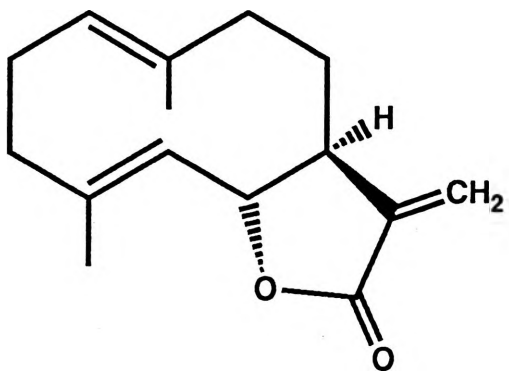

Costunolide 94

Another species, *Talauma singapurensis* was reported to contain alkaloids although no chemical work had been published so far.[141]

No chemical examination of *Talauma gitingensis* has been found in the literature.

3.1.5.5 *Talauma gitingensis*

In a study of the distribution of alkaloid-containing plants on Palawan Island, Philippines, one plant that gave a positive test for alkaloids in the field was identified as *Talauma gitingensis* Elm. of the family Magnoliaceae, an endemic plant locally known as "anobling" or "batangis". This plant is found from northern Luzon to Mindanao, and is common in hills and forests at low and medium altitudes.[142]

Preliminary antimicrobial studies on this plant revealed that the alcoholic extract exhibits antibacterial activity against gram positive and gram negative bacteria.

3.2 RESULTS AND DISCUSSION

The alcoholic extract of the dried ground leaves of *Talauma gitingensis* on fractionation yielded a green resinous $CHCl_3$ extract which contained the crude tertiary alkaloids. This extract showed strong antibacterial activity against *Bacillus subtilis* (ATCC 6633) at 8.5×10^4 mg/ml.

3.2.1 Isolation and Structure Elucidation of Tg-3A-1

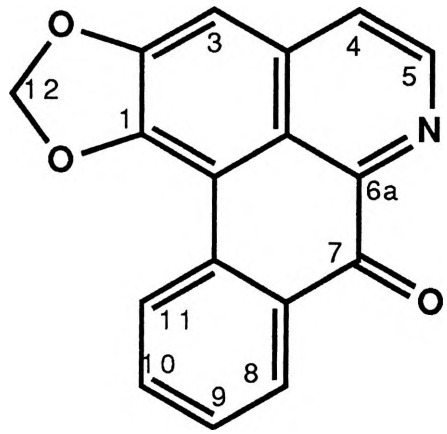

The alkaloid extract on fractionation by flash column chromatography using $CHCl_3$ yielded a lemon yellow solid upon concentration *in vacuo*. On purification by prep TLC and recrystallisation from $CHCl_3$, fine yellow needle-like crystals, mp 268-270° (dec.) were obtained. The UV spectrum of the crystal in $CHCl_3$ showed maximum absorbance at λ_{max} 268nm and 309 nm suggesting a 1,2 dioxygenated aromatic system.[143] A further absorption at 415 nm implied that the yellow colour was due to a highly conjugated system. The mass spectrum gave a *m/z* of 275 corresponding to a molecular formula of $C_{17}H_9NO_3$. The 14 double bond equivalents are accounted for by 5 rings and a double bond. This, together with the low hydrogen integration observed from its ^1H NMR spectrum (Figure 26) suggested the benzylisoquinoline

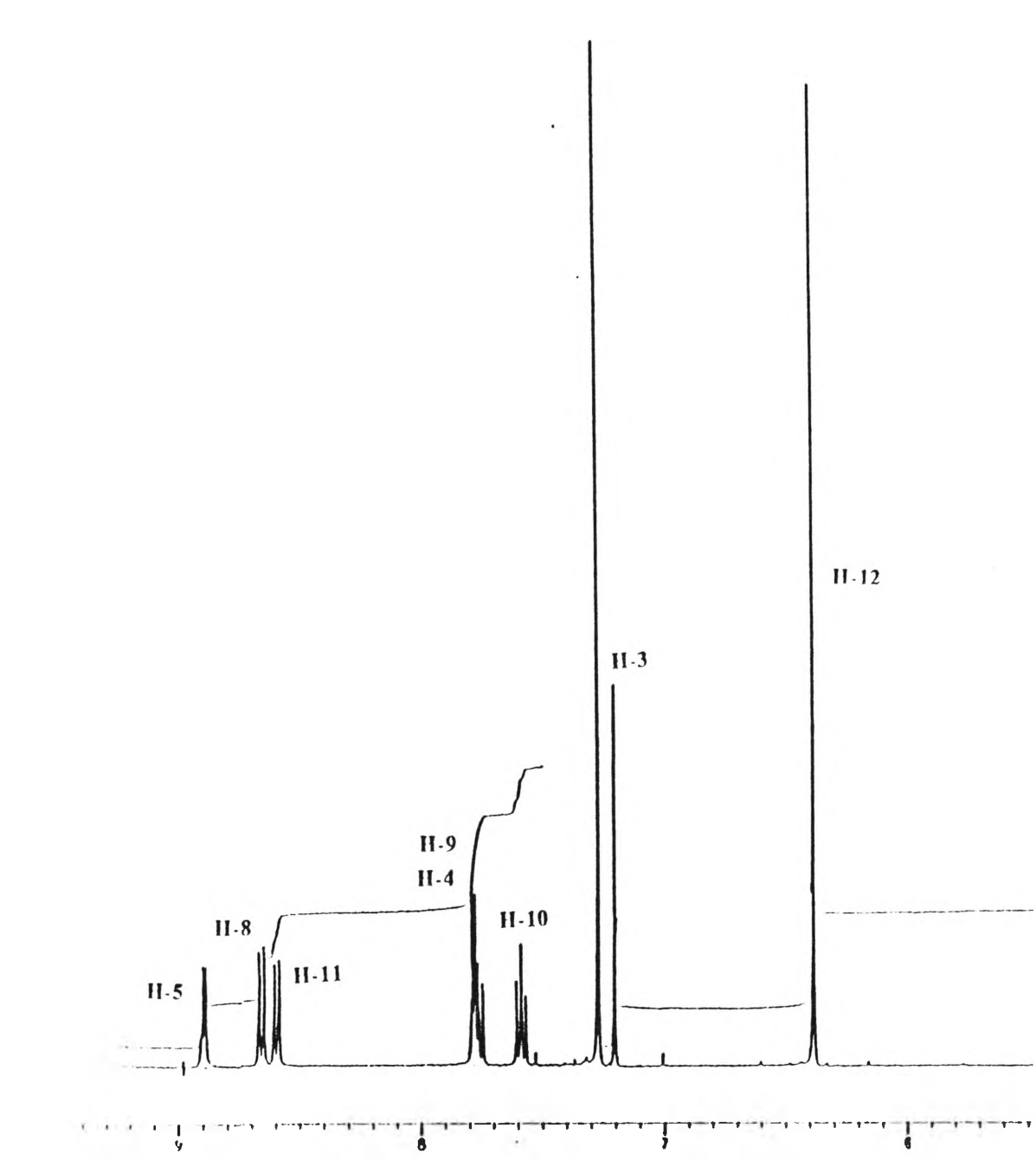

Figure 26. ^{1}H NMR Spectrum of Tg-3A

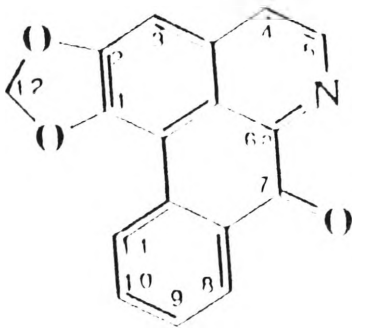

1 [400 MHz, $CDCl_3$, referenced at δ7.25].

structure of the aporphine alkaloids. The IR spectrum showed an absorption at 1664 cm^{-1} which was assigned to the carbonyl group of a ketone while absorptions at 2960, 1490, 1425, 1367, 1265, 1125 and 1045 cm^{-1} were diagnostic peaks for the presence of methylenedioxy groups.[144]

The ^1H NMR integrated for only 9 protons, seven of which were observed to resonate in the aromatic region. A singlet at δ6.39 (H-12) integrating for two protons was assigned to the equivalent protons of the methylenedioxy group. On comparison with the resonances of the isoquinoline protons, the doublet observed at δ8.92 was assigned to H-5 of the pyridine ring resonating more downfield (lit. δ8.50) due to the presence of the C=O group in conjugation with the pyridine ring. Another doublet at δ7.90 was assigned to H-4 being coupled to H-5 by 5.0 Hz as an AB system. The singlet at δ7.23 was assigned to H-3 and was shifted upfield by 0.5 ppm due to the effect of the substitution at C-1 and C-2 with the methylenedioxy group. The above assignments led to the structure of fragment A.

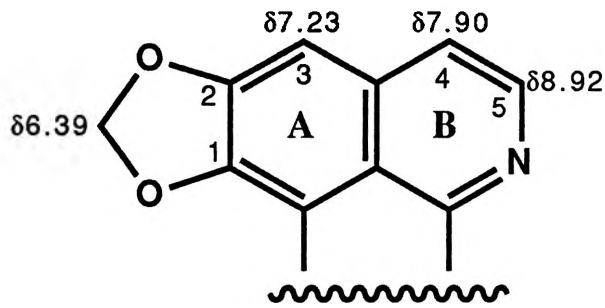

Fragment A

The remaining four aromatic signals at δ8.67, δ7.78, δ7.61 and δ8.59 were assigned to the protons of ring D. The doublet doublet

resonating at δ8.67 was assigned to H-8 which on comparison with the resonances of benzene protons (δ7.27) differed by 1.4 ppm. The downfield shift was attributed to the presence of the electron-withdrawing C=O group at ring C which caused deshielding effect on H-8. Irradiation of H-8 caused the signal at δ7.78 to simplify to a doublet of doublets hence was assigned to H-9. Another signal, δ7.68, split to a ddd was assigned to H-10. This assignment was confirmed with the collapse of the triplet doublet signal at δ7.78 to a doublet doublet on irradiation of H-10. The remaining aromatic signal at δ8.59 was assigned to H-11 as the X part of an AMX system with H-9 and H-10. All these aromatic signals formed ring D and labelled fragment B of the aporphine alkaloid.

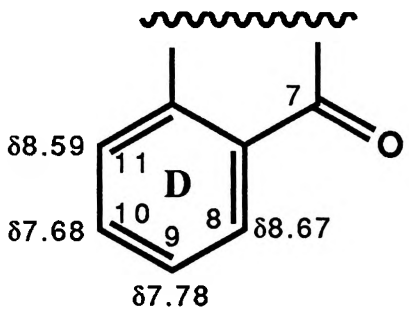

Fragment B

Preparation of the oxime derivative of Tg-3A-1 confirmed the presence of a carbonyl group in ring C. The Tg-3A-1 was found identical with the oxoaporphine, liriodenine. Liriodenine was the first oxoaporphine isolated in nature from *Liriodendron tulipifera* (Magnoliaceae) by Buchanan and Dickey.[144] Direct comparison (mp, mmp, TLC , UV and ^{1}H NMR) with an authentic sample of liriodenine obtained from Prof. I. R. C. Bick (University of Tasmania) confirmed the structure of Tg-3A-1.

3.2.2 Isolation of the N-acetyl derivatives of the Noraporphine Alkaloids

By reference to the literature, it was anticipated that noraporphine alkaloids might co-occur with the oxoaporphine Tg-3A-1 and that they might prove difficult to isolate. N-acetyl derivatives were therefore prepared to stabilised these alkaloids and at the same time to improve separation. The crude alkaloid fraction was acetylated with acetic anhydride in pyridine. The acetylated product was purified by HPLC yielding Tg-3A-1 and the N-acetyl derivatives of Tg-3A-2 and Tg-3A-3. A strong N-acetyl signal at δ2.20 ppm confirmed the presence of an acetyl group in the noraporphine alkaloids.

3.2.2.1 Structure Elucidation of N-Acetyl-Tg-3A-2

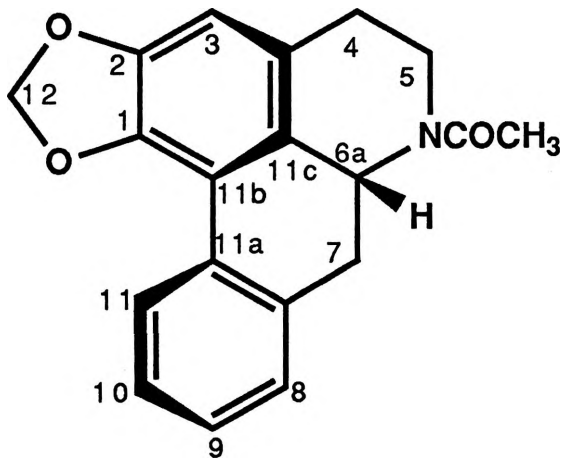

The N-acetyl derivative of Tg-3A-2 was obtained as a white amorphous solid with a mp of 227-229°. The UV bands at λ_{max} 330 and 272 nm in chloroform solution indicated a 1,2 dioxygenated aromatic system[145] while the IR spectrum on comparison with the spectrum of Tg-3A-1 showed the same absorptions for the diagnostic peaks of methylenedioxy group[143] and the absorption

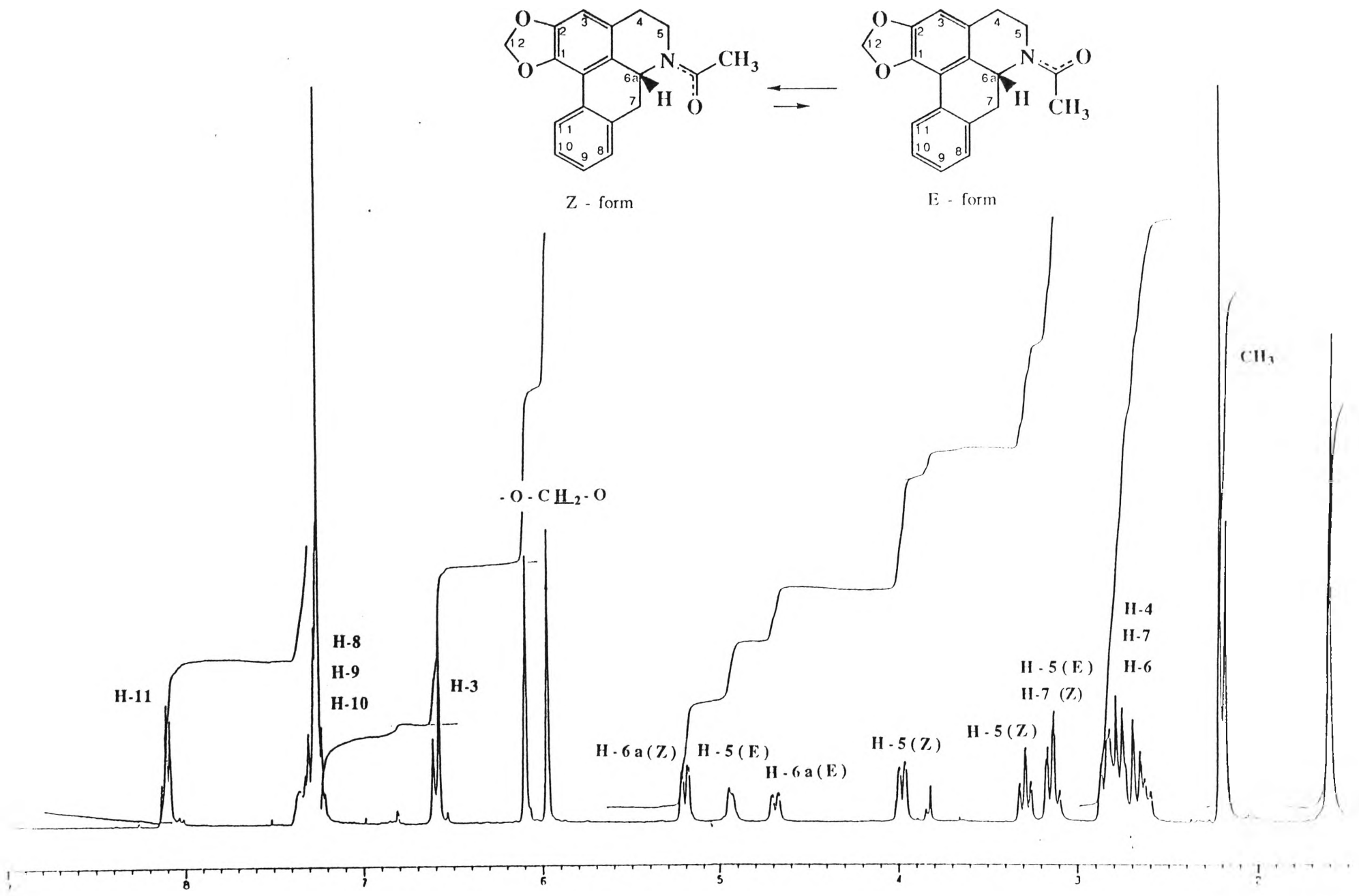

Figure 27. ^{1}H NMR Spectrum of N-Acetyl-Tg-3A-2 [400 MHz, $CDCl_3$, referenced at δ7.25].

bands of the carbonyl group of a tertiary amide at 1649 cm^{-1}. The compound gave a *m/z* of 307.1210 by HREIMS for the formula $C_{19}H_{17}NO_3$ giving 12 double bond equivalents, two double bonds less than the isolated oxoaporphine, indicative of a noraporphine structure.

The ^1H NMR spectrum of N-acetyl Tg-3A-2 (Figure 27) was complex, arising from the resonances of the two rotational isomers which occur due to the restricted rotation about the N-$COCH_3$ group.[146] Two separate signals in the ratio of 2:1 for each contributing isomer were observed accounting for the slow exchange on the chemical shift time scale of the rotational isomers in solution. Previous workers have not reported the existence of these two isomers.

The absence of the absorbance at 415 nm in UV spectrum of Tg-3A-2 was consistent with tetrahydroisoquinoline structure. Comparison of the ^1H NMR spectrum of N-acetyl-Tg-3A-2 with Tg-3A-1 showed differences in the upfield region suggesting an aporphine nucleus with a 4H dibenzo[*de,g*]quinoline structure Two doublets centred at δ6.09 and δ5.97 instead of the singlet at δ6.39 were observed and were assigned to the two protons of the methylenedioxy group (H-12) which are non-equivalent due to a twisted biphenyl system. The isolated H-3 (δ7.23, s) at ring A observed in the spectrum of Tg-3A-1 was replaced with two singlets at δ6.58 and δ6.61 for the two isomers of N-acetyl-Tg-3A-2. The occurrence of the signal at the upfield region was caused by the loss of conjugation with ring B being non-aromatic. The other aromatic protons at ring D were assigned based on the decoupling experiments; H-11 resonating at δ8.11 as a doublet of doublets. Overlapping resonances for H-8, 9, 10 are observed at δ7.24 -7.32

and differ from the resonances of these protons in the oxoaporphine Tg-3A-1 as a result of the loss of conjugation due to the absence of the C=O group in ring C.

Two-dimensional Homonuclear (^1H-^1H) Correlation spectroscopy (COSY)[98,99], Nuclear Overhauser Effect (nOe) Difference spectra and 1- D selective decoupling experiments were used to fully characterise N-acetyl-Tg-3A-2 particularly with respect to the methylene protons of rings B and C.

The configuration at C-6a followed the established rule for the aporphines whereby a negative rotation indicates the R configuration and a positive rotation the S arrangement.[123] The H-6a at the junction of rings B and C was proposed to be in the axial position with N-acetyl-Tg-3A-2 being levorotatory in chloroform. This methine proton (H-6a) was assigned to the signal at δ5.20 (dd, J10.0, 4.0Hz) for the major isomer and at δ4.69 ppm (dd, J14.0, 5.0Hz) for the minor isomer. Figure 28 showed the partial ^1H NMR assignments of the protons at rings A and D for N-acetyl-Tg-3A-2.

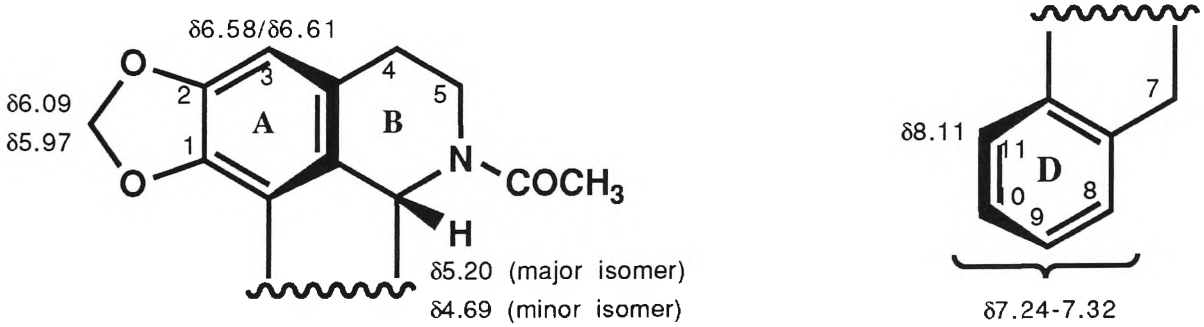

Figure 28. Partial ^1H NMR Assignments for N-Acetyl-Tg-3A-2.

Assignment of the resonances for the protons at C-4, -5 and -7 were difficult due to overlapping resonances for these protons. Decoupling experiments alone proved inadequate in resolving the

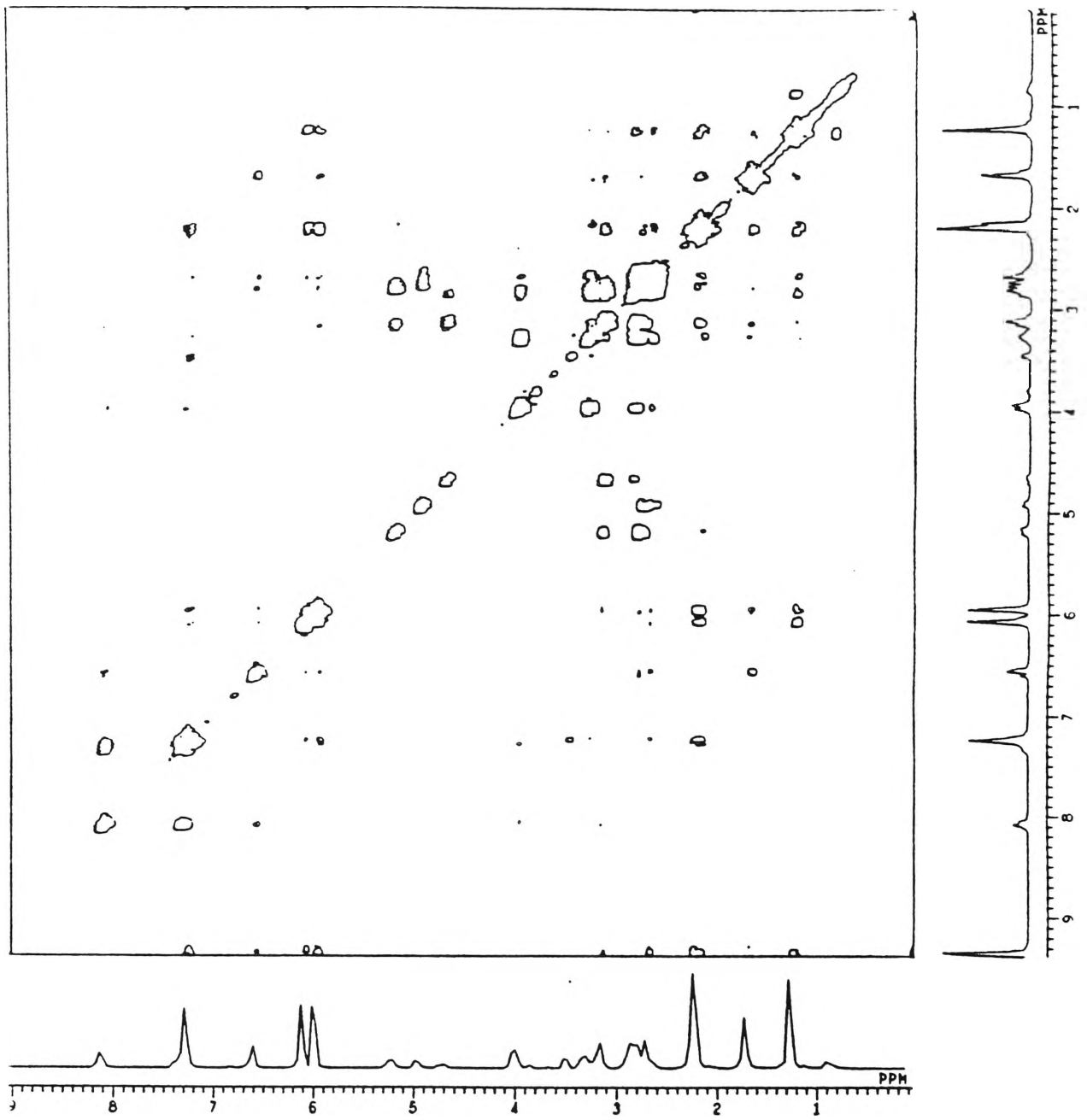

Figure 29. ^{1}H-^{1}H COSY NMR Spectrum of N-Acetyl-Tg-3A-2 [400 MHz, $CDCl_3$, referenced at δ7.25].

signals of the methylene protons. However, by interpretation of a 2-D COSY spectrum (Figure 29), the chemical shift assignments for the C-7 methylene protons as well as their orientations were attained.

The axial H-6a was used as a marker to enable easy analysis of the spectrum for N-acetyl-Tg-3A-2. The methine signal at δ5.20 for H-6a of the major isomer was found to be coupled by 5.0 Hz to the resonance at δ3.16 (dd, 1H) assigned to H-7_{eq}. Decoupling the signal at δ3.16 (H-7_{eq}) loses the 5.0 Hz coupling, with the signal at δ5.20 (H-6a) collapsing to a doublet (J14.0Hz) hence an axial-equatorial relationship for the two protons. An 11.6% enhancement of the δ3.16 signal was observed from the nOe difference spectrum when H-6a at δ5.20 was irradiated suggesting the proximity of the two protons (H-7_{eq} and H-6a). Cross peaks from the 2-D

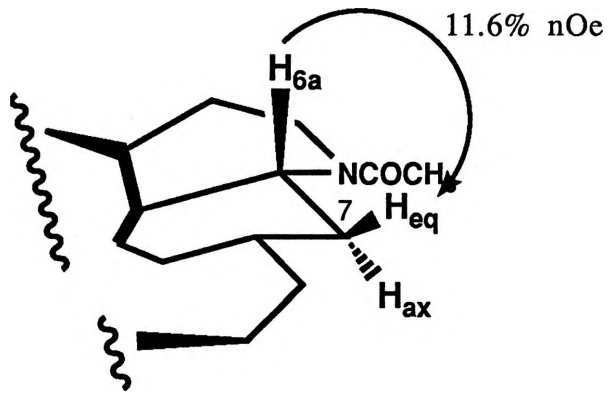

COSY spectrum showed H-6a signal at δ5.20, to be coupled also to the complex signals at δ2.78-2.86 assigned to the proton at C-7. Decoupling δ2.78-2.86 (H-7_{ax}) simplified the signal at δ5.20 (H-6a) to a doublet (J5.0Hz) losing its 14.0Hz coupling. Thus H-7_{ax} and H-6a shared an axial-axial-relationship.

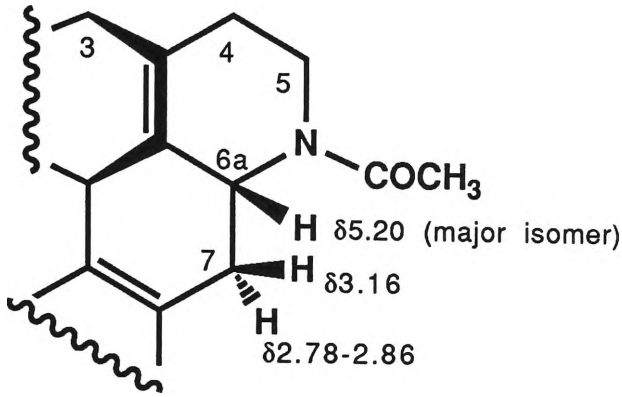

The COSY spectrum showed the methine proton at δ4.69 (H-6a, minor isomer) to correlate with the signals at δ3.16 and δ2.78-2.86 assigned to the C-7 protons. On irradiation at δ3.16, the signal at δ4.69 (H-6a) became a sharp singlet eliminating the 14.0Hz coupling between these protons for an axial-axial relationship. Based on these results, the complex signals at δ2.78-2.86 arises for the H-7 at equatorial proton to that of H-6a. These suggested assignments were confirmed when the signal at δ2.70-2.86 was irradiated resulting in a doublet with a J14.0Hz for δ4.69 (H-6a). Irradiation at δ3.16 ($H\text{-}7_{ax}$) showed an nOe enhancement of 13.8% onto δ4.69 (H-6a).

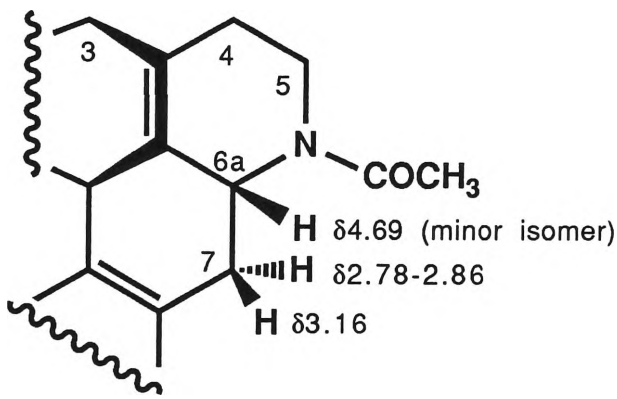

The doublet of doublets at δ3.98 was found to correlate with δ3.28 as shown from their crosspeaks observed in the COSY spectrum. A 15.4% nOe enhancement onto δ3.28 was obtained after δ3.98 was irradiated. These two signals were assigned for the

methylene protons at C-5 of the major isomer, which was expected to resonate downfield due to its proximity to the amide group. Two other signals, δ4.95 and the complex signals at δ2.60-2.77, coupled to each other by 2.0Hz were assigned for the two protons at C-5 of the minor isomer.

Among the three sets of methylene protons of rings B and C, the protons at C-4 were expected to resonate at the upfield region. The overlapping signals at δ2.60-2.77, integrating for 2H and 0.33H suggest that the methylene protons at C-4 lies underneath these complex signals together with the resonances for one of the proton of C-5 of the minor isomer. Irradiation of this complex signal causes the δ4.95 resonance to collapse to a singlet supporting the above deduction. The complexity of the signals prevented assignments for the orientation of the C-4 protons.

Decoupling experiments showed the phenomenon of negative nOe caused by the slow exchange process in the NMR time scale.[109] Irradiation at δ4.95 (H-5, minor isomer) gave rise to a negative nOe onto δ3.98 (H-5, major isomer) alongside with a positive enhancements for both signals at δ3.28 (H-5, major isomer) and δ2.60-2.77 (H-5, minor isomer). This behaviour clearly showed that slow exchange magnetisation was occuring during the irradiation time hence the observed effect. This also suggests that δ4.95 signal would have the same orientation (axial or equatorial) as the δ3.98 signal for the most stable conformation. The same follows for the signals at δ3.28 and δ2.60-2.77.

To assign the orientation for C-5 protons and at the same time determine the conformation of the major isomer, Nuclear overhauser effect (nOe) difference experiments were used. Irradiation at the signal at δ3.98 (H-5, major isomer) resulted in

2.6% enhancement onto δ2.22 (CH_3, amide, major isomer) as compared to a 7.0% increase in intensity of δ2.22 when the signal at δ3.28 (H-5, major isomer) was irradiated. This suggested that the δ3.28 signal was closer in space to the methyl group of the amide functionality, in agreement for an equatorial orientation of H-5 relative to the methyl group. Thus, the multiplet at δ2.60-2.77 (H-5, minor isomer) could be assumed to have an equatorial position since it was established (nOe difference spectrum) that these signals were the counterpart of $H\text{-}5_{eq}$ (δ3.28) for the minor isomer. All of these data pointed to the signals at δ3.98 (H-5, major isomer) and δ4.95 (H-5, minor isomer) to have an axial orientation.

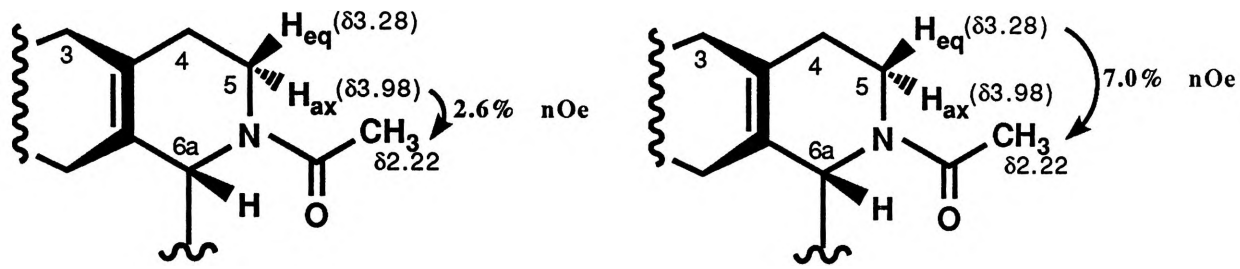

Major Isomer

To assign the conformation of the most stable structure, an nOe, irradiating at δ3.16 ($H\text{-}7_{eq}$) was carried out. No enhancement was observed onto the δ2.22 signal suggesting the possibility that the isomers existed in a 2:1 ratio favouring the Z-form (Figure 30). Interpretation of an absence of a particular enhancement at one proton may be risky at some point for the absence may be due to causes other than a long distance between the spins involved.[109] This observed result from the nOe difference spectrum conformed with the assignment of the axial proton at C-5 to the signal at δ4.98 due to the deshielding effect of the carbonyl functionality of the amide group. The Z-form was preferred over the E-form, in which

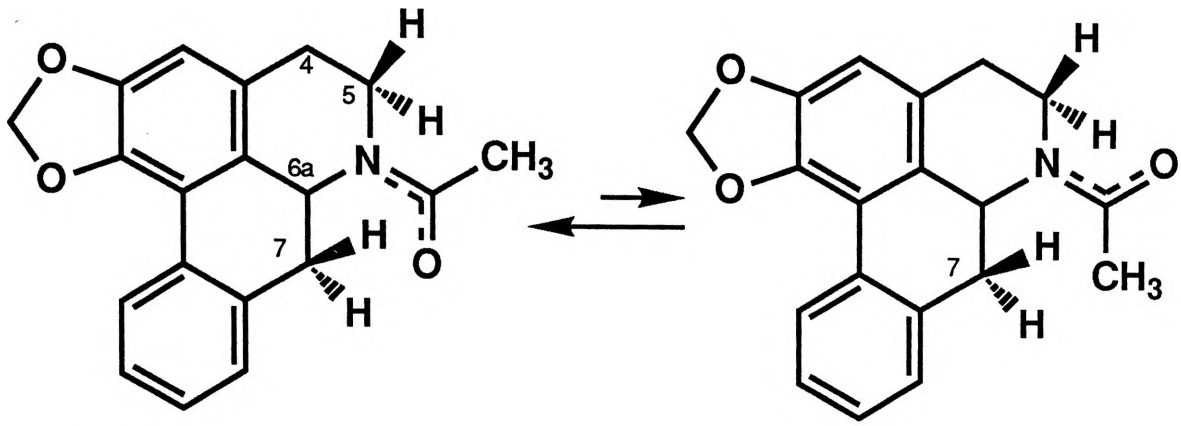

Figure 30. The Two Rotational Isomers of N-Acetyl-Tg-3A-2.

the C-7 protons experienced a crowding effect due to the proximity of the methyl group of the amide functionality. The ^{1}H NMR assigments of the Z and E isomers were summarised in Table 17.

Resonances for both the Z and the E isomers were also obtained from the ^{13}C NMR spectrum of N-acetyl-Tg-3A-2 with a total of 38 signals observed from the spectrum. Assignments were done by comparison to those reported by Achenbach[147] for Anonaine and were presented in Table 18.

The structure for N-acetyl-Tg-3A-2 is identical to the noraporphine alkaloid, anonaine, first isolated from *Anona reticulata* (Annonaceae) by Santos.[148] Since then it has been isolated from species of the Annonaceae and Magnoliaceae families. Confirmation of the structure was established by direct comparison (^{1}H NMR) with an authentic sample of anonaine provided by Prof. Andre Cave.

Table 17. ^{1}H NMR Assignments for the Z and E Isomers of N-Acetyl-Tg-3A-2.[a]

	Z	E
-O-C<u>H</u>$_2$-O-	6.09/5.97 (2H)	6.09/5.97 (2H)
H - 3	6.58 (1H, s)	6.61 (1H, s)
H - 4_{ax}	2.58-2.77 (1H, m)	2.58-2.77 (1H, m)
H - 4_{eq}	2.58-2.77 (1H, m)	2.58-2.77 (1H, m)
H - 5_{ax}	3.98 (1H, dd, J12,1 Hz)	4.95 (1H, dd, J12,1 Hz)
H - 5_{eq}	3.28 (1H, td, J12,1 Hz)	2.58-2.77 (1H, m)
H - 6a	5.20[b] (1H, dd, J10,4 Hz)	4.69 (1H, dd, J14,5 Hz)
H - 7_{ax}	2.78-2.86 (1H, m)	3.16 (1H, dd, J14,4 Hz)
H - 7_{eq}	3.16 (1H, dd, J14,4 Hz)	2.78-2.86 (1H, m)
H - 8	7.24-7.32	7.24-7.32
H - 9	7.24-7.32 (3H, m)	7.24-7.32 (3H, m)
H - 10	7.24-7.32	7.24-7.32
H - 11	8.11 (1H, dd, J8,1 Hz)	8.11 (1H, dd, J8,1 Hz)
C<u>H</u>$_3$ amide	2.22 (3H, s)	2.19 (3H, s)

[a]$CDCl_3$ relative to TMS, Z:E ratio (2:1).

[b]literature value for an axial H is δ5.18 .[149]

Table 18. ^{13}C NMR Assignments for the Z and E Isomers of N-Acetyl-Tg-3A-2.[a]

Carbon	Z-isomer	E-isomer
C-1	143.2 (142.5, s)	143.0
C-2	147.0 (146.8, s)	147.5
C-3	107.5 (108.0, d)	108.0
C-3a[b]	128.8 (1287, s)	
C-4	29.5 (29.6, t)	30.0
C-5	42.0 (43.6, t)	36.5
C-6a	50.5 (53.6, d)	54.0
C-7	33.5 (37.4, t)	36.0
C-7a	136.0 (135.4, s)	135.5
C-8	128.5 (128.1)	128.5 (128.1)
C-9	128.0 (127.5)	128.0 (127.5)
C-10	127.5 (127.1)	127.5 (127.1)
C-11-c[b]	127.0 (127.0)	127.0 (127.0)
C-11-a	130.5 (131.4, s)	131.0
C-11[b]	118.0 (116.3, s)	117.0
C-11-b	126.0	125.0
-O-CH_2-	101.0 (100.6, t)	100.0
C=O, amide	167.0	167.5
CH_3	22.5	21.5

[a]referenced relative to $CDCl_3$, δ77.0; values in parentheses are for anonaine [$CDCl_3$, 250 MHz][147]

[b]may be interchanged

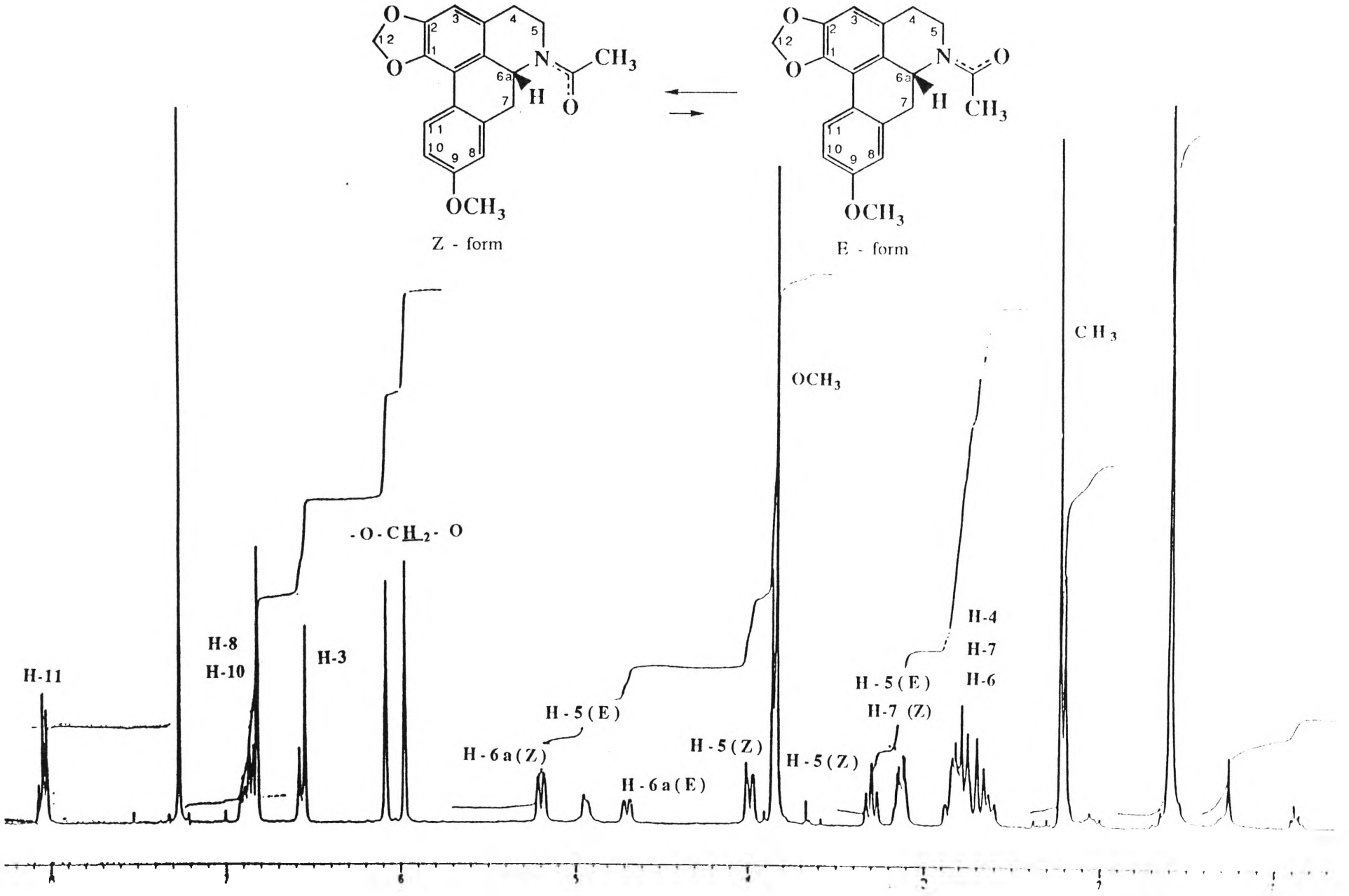

Figure 31. ^{1}H NMR Spectrum of N-Acetyl-Tg-3A-3 [400 MHz, $CDCl_3$, referenced at δ7.25].

3.2.2.3 Structure Elucidation of N-acetyl-Tg-3A-3

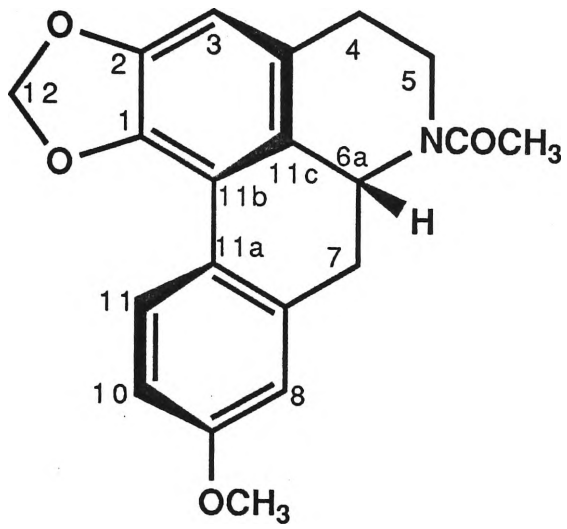

The minor N-acetyl noraporphine alkaloid, Tg-3A-3, was obtained as a white amorphous solid, mp 210-211°C. The the HREIMS gave a molecular ion of *m/z* 337.1312 which corresponds to $C_{20}H_{19}NO_4$ giving the same double bond equivalent as N-acetyl-Tg-3A-2 suggesting similarity in their parent structure. The 31 mass unit difference evident from its mass spectrum suggested for the presence of a methoxy substituent. Its optical rotation $[\alpha]_D$= -417° suggested an axial orientation of H-6a, identical to the major noraporphine alkaloid isolated, Tg-3A-2. The position of the methoxy substituent was established by comparison of its ^1H NMR spectrum (Figure 31) with that of N-acetyl Tg-3A-2.

The ^1H NMR spectrum showed the presence of a three proton singlet at δ3.85 characteristic for a methoxy signal. All the signals for the protons at rings A, B and C were identical to those in Tg-3A-2 suggesting methoxy substitution of ring D. The aromatic protons for ring D were observed to resonate upfield due probably to the presence of the methoxy group. The presence of three aromatic signals at δ8.04 (d, J8.0Hz), δ6.90 (d, J1.0Hz) and δ6.82 (dd,

J8.0,1.0Hz) supported either C-9 or C-10 substitution. However, between H-11 and H-8, the former was expected to resonate further downfield due to the deshielding effect of the adjacent aromatic ring A. Thus, the doublet at δ8.04 was assigned to H-11 establishing C-9 substitution. This signal was coupled as an AX system to δ6.82 (assigned to H-10) while the doublet with meta-coupling at δ6.90 is H-8.

Two sets of resonances were also observed from the ^{1}H NMR spectrum. Parallel analyses with Tg-3A-2 showed the Z-isomer to exist preferentially. All the data pointed to N-acetyl-Tg-3A-3 as identical to the noraporphine alkaloid xylopine. Schmultz[150] has previously isolated xylopine from *Xylopia discreta*. Only one occurrence of this noraporphine alkaloid in the genus *Talauma* has been cited.[139] A direct comparison (^{1}H NMR) with an authentic sample of xylopine provided by Dr. Richard I. Willing (CSIRO, Melbourne) established the identity of Tg-3A-3.

3.3 SUMMARY AND CONCLUSION

In a study of alkaloid-containing plants on Palawan Island, Philippines, one plant that gave a positive test for alkaloids in the field was identified as *Talauma gitingensis* Elm. (Magnoliaceae), an endemic plant locally known as "anobling" or "batangis".

Three of the four species of the genus Talauma which have been investigated chemically contain alkaloids. The oxoaporphines liriodenine and lanuginosine have been isolated from *T. mexicana*, *T. hogsoni* or *T. obovata*, while the noraporphine xylopine has been isolated from *T. obovata* .

Preliminary work on *T. gitingensis* suggested the presence of an oxoaporphine alkaloid together with noraporphine alkaloids. Since a literature survey revealed that noraporphines might prove difficult to isolate, N-acetyl derivatives were prepared to stabilise the alkaloids and to facilitate separation. This chapter described the isolation and characterisation of the noraporphines xylopine and anonaine as their N-acetyl derivatives from the leaves of *T. gitingensis*, together with liriodenine. The existence of conformational isomerism for the N-acetyl derivatives is described for the first time together with a complete ^{1}H NMR characterisation of the compounds by 1-D decoupling experiments, nOe enhancement and 2-D COSY spectroscopy. Previous ^{1}H NMR characterisation of these compounds was poor by today's standards considering the spectroscopic advances particularly in NMR techniques.

CHAPTER 4

FALSE-POSITIVE ALKALOID FROM *GRAPTOPHYLLUM PICTUM*

4.1 INTRODUCTION

In the search for novel alkaloids from Philippine flowering plants, a commonly cultivated ornamental foliage shrub gave a heavy precipitate with Mayer's reagent in the alkaloid field test. This plant was identified to be *Graptophyllum pictum* of the family Acanthaceae.

The family Acanthaceae is known to be a source of quinazoline alkaloids (Figure 32). The quinazoline nucleus occurs in relatively few alkaloids and has an interesting taxonomic distribution. These types of alkaloids have been found to occur together with harman alkaloids in the family Zygophyllaceae, specifically in the species *Peganum harmala* L.

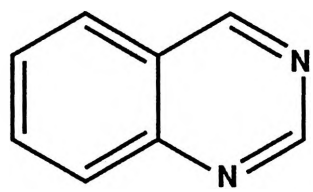

Figure 32. Quinazoline Nucleus

To date, there is no reported literature on the chemical constituents of this plant nor on any other species of the genus *Graptophyllum*.

4.1.1 *Graptophyllum pictum* (L.) Griff.

Graptophyllum pictum (L.) Griff. (Acanthaceae) is locally known in names such as kalpueng, sarasa, and balabas. The plant, probably a native of Polynesia is now cultivated in most tropical countries.[151]

Two types of *G. pictum* are known in the Philippines. The form called "morado" with dull, brownish-purple leaves is the most

common; the other form has green leaves, blotched along the midrib with white patches.

Locally, an infusion of the leaves is used as a diuretic and can cure constipation. The leaves are used as an emollient poultice on skin ulcers and swellings. The juice is used as a treatment for ear ache.

Ozaki *et al*[152] reported the alcoholic extract of this plant to exhibit antiinflammatory as well as analgesic activity in the carageenin-induced hind-paw edema test and acetic acid-induced vascular permeability as well as the writhing system in mice. The activity was localised in the methanol-soluble fractions with the active compound characterised as a flavonoid.

Preliminary antimicrobial studies on the crude alcoholic extract of this plant conducted at the Research Centre for the Natural Science, Philippines revealed that it inhibited both gram positive (*Bacillus subtilis*) and gram negative (*Escherichia coli* and *Pseudomonas aeruginosa*) bacteria.

Although many pharmacological studies on the crude extract of this plant have been reported, little is known about its chemical constituents. Thus, work was carried out in order to isolate the alkaloids that were supposedly present based on the results of the alkaloid field test. Instead, a false-positive alkaloid identified to be a hydroxy terpene was isolated.

4.2 RESULTS AND DISCUSSION

Dried leaves of *Graptophyllum pictum* on extraction with 95% EtOH yielded a dark green resinous material (174 g, 21.8%) which on partitioning between Et_2O and 1% H_2SO_4, followed by alkalinisation and extraction with $CHCl_3$ gave a green resinous material (2.38 g). The $CHCl_3$ fraction, after column chromatography, PTLC and HPLC afforded a white amorphous solid false-positive alkaloid labelled as Gp-78 (5.08 mg) (Figure 33).

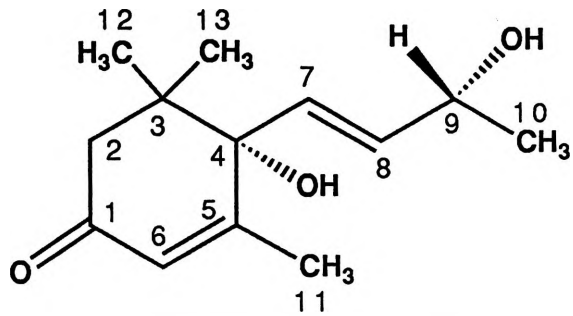

Figure 33. Structure of Gp-78.

Gp-78 gave a *m/z* of 224.1307 (HREIMS) corresponding to a molecular formula $C_{13}H_{20}O_3$ indicating 4 double bond equivalents. The UV spectrum showed an absorbance at λ_{max} 252 (Σ3148) suggesting a C=O group in conjugation with a double bond.[142] The IR spectrum showed a signal at 1650 cm^{-1} assigned to an α,β-unsaturated ketone, a signal at 1380 cm^{-1} for a geminal methyl group and at 975 cm^{-1} for a trans-substituted double bond of an enone.[145] A strong absorption at 3400 cm^{-1} was assigned to a hydroxyl group whose presence was also confirmed by a D_2O exchangeable signal in the ^1H NMR at δ1.55 (br s).

The ^1H NMR of Gp-78 (Figure 34) showed the occurrence of three olefinic protons, four 3H singlets (methyl groups), two non-

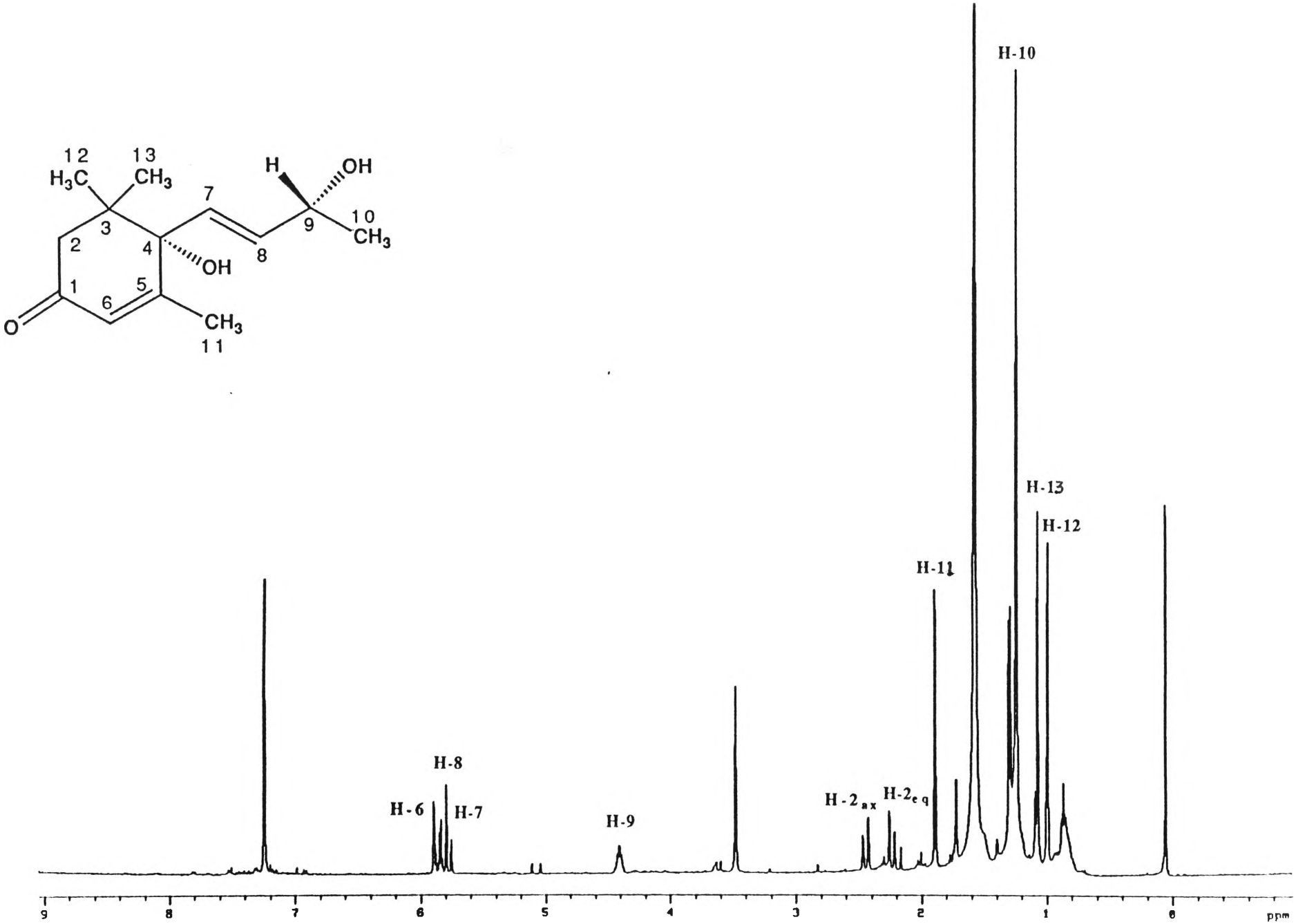

Figure 34. ^{1}H NMR Spectrum of Gp-78 [400MHz, $CDCl_3$, referenced at δ7.25].

equivalent methylene protons and a methine proton occurring as a multiplet.

Signals at δ0.99 and δ1.08, integrating for 3 protons each, are consistent with a geminal dimethyl group (H-12 and H-13). The methyl group resonating further downfield at δ1.89 (H-11) was assigned to a methyl group attached to an olefinic group while the signal at δ1.30 (H-10) is in agreement with a methyl group β to an oxygen.

The olefinic proton at δ5.89 (H-6) was found to be allylically coupled to the methyl signal at δ1.89. The two mutually coupled olefinic protons at δ5.79 (H-7) and δ5.84 (H-8) indicated a trans-substituted double bond.

A quintet at δ4.40 (H-9) integrating for 1 H is coupled to the methyl group at δ1.30 (H-10) and to the olefinic proton at δ5.84 (H-8), and was assigned to the secondary hydroxyl centre. Resonances for an AB (2H) system centred at δ2.24 and δ2.44 were also found and assigned to the non-equivalent H-2 protons.

The ^{13}C NMR spectrum of Gp-78 assigned by comparison with literature data[153,154], showed a C=O signal (δ186.0), four olefinic signals (δ135.9, δ129.1, δ127.0 and δ97.9 ppm), three of which were protonated, and four methyl signals at δ24.1, δ23.8, δ22.9 and δ18.8 ppm. A low intensity signal at δ79.1 was assigned to the tertiary hydroxyl centre, C-4, while a more intense signal at δ68.0 ppm was assigned to the secondary hydroxyl, C-9. These data are consistent with the proposed structure of Gp-78 (Figure 33).

An identical compound, vomifoliol[155] **95**, (4-hydroxy-4-(3-hydroxy-1-butenyl)-3, 5, 5,-trimethyl-cyclohexe-1-one), has been previously isolated from the flowers of *Rauwolfia vomitoria* Afz (Apocynaceae). Subsequently the same compound was isolated,

using the name Blumenol A,[156] from *Podocarpus blumei* Endl. Horn *et. al.*[157] suggested that Blumenol A should be compared to theaspirone **96** based on their close biogenetic relationship and therefore the stereochemistry of Blumenol A should be (4S,9S). No proof however was presented. In the same year, Nakanishi *et. al.*[158]

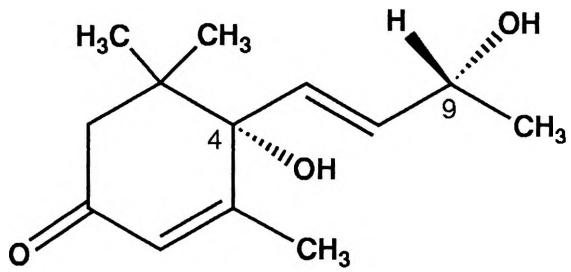

Vomifoliol (Blumenol A) 95

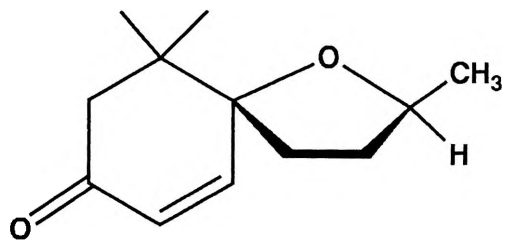

Theaspirone 96

defined the stereochemistry of Blumenol A as (4S,9R) by comparison of its circular dichroism spectrum with that of a semi-synthetic compound.

In our compound, the stereochemistry at C-4 was established by a nuclear overhauser effect (nOe) difference experiments. Irradiation of the signal at δ1.89 (H-13) showed enhancement of the signal at δ1.56 assigned to the tertiary hydroxyl group, and of the olefinic signal at δ5.84 (H-8). No enhancement on the hydroxyl signal at C-4 was observed upon irradiation of the signal at δ5.79 (H-7). These observations were consistent for an α-oriented -OH group assigning the stereochemistry to be 4S

Gp-78 has $[\alpha]_D$ +40.0 (c = 0.22, $CHCl_3$) compared with a value of $[\alpha]_D$ +233 (c=1, $CHCl_3$) for Blumenol A. Circular dichroism determination (MeOH) for Gp-78 gave $\Delta\Sigma_{235}$ +36.4 and $\Delta\Sigma_{317}$ - 3.0 compared with the CD (MeOH) value for Blumenol A of $\Delta\Sigma_{242}$ +96 and $\Delta\Sigma_{317}$ -4.4. Lack of an authentic sample of Blumenol A prevented direct comparison although all of the spectroscopic data

obtained conformed to that of Blumenol A with the exception of the CD data which is qualitatively but not quantitatively the same.

Recently, a related compound inamoside **97** has been isolated from *Ophiorrhiza pumila*, showing co-existence of this type of compound with harman alkaloids.[159]

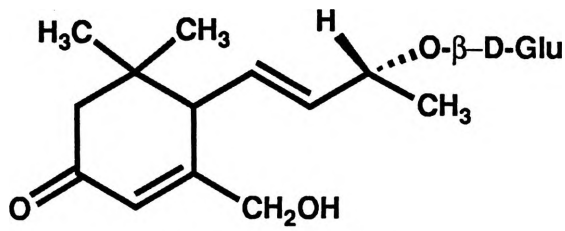

Inamoside 97

4.3. SUMMARY AND CONCLUSION

This investigation presents the first reported chemical examination of the species *Graptophyllum pictum* and the isolation of the terpene alcohol, Blumenol A, from the family Acanthaceae and the genus *Graptophyllum*.

This study also serves as a good example of the isolation of a false-positive alkaloid and supports the findings of Farnsworth[160] that non-nitrogenous compounds are capable of responding positively with alkaloid precipitating agents. In his study, he found that the minimum structural feature necessary in certain non-alkaloid compounds for a positive reaction is a conjugated carbonyl (ketone or aldehyde) or lactone function.

Gp-78, identical to Blumenol A, and which contains this structural feature thus appears to behave as an alkaloid. Similar behaviour was observed for the related compound ionone **98**.

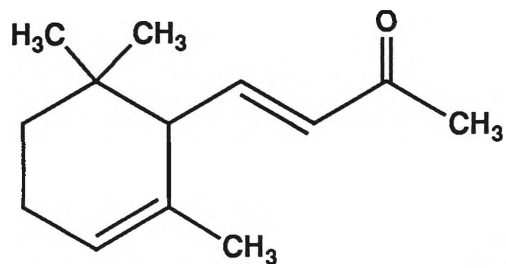

Ionone 98

Pousset and Poisson[155] reported that vomifoliol (Blumenol A) was also isolated during their attempt to isolate bases from the flowers of *Rauwolfia vomitoria*.

CHAPTER 5

ISOLATION AND STRUCTURE ELUCIDATION OF ALKALOIDS FROM *PANDANUS AMARYLLIFOLIUS*

5.1 INTRODUCTION

The genus *Pandanus* of the family Pandanaceae is found throughout the tropics.[161] This genus of woody plants comprises some 600 species of which 52 have been reported to occur in the Philippines.[162] The leaves of genus *Pandanus* grow up to 15 feet and being tough are generally used for weaving although some species are recognised as medicinal plants.[163] These leaves are often armed with strong prickles, hooked forwards in one line and backwards in another, in a way which protects them from grazing animals.

The genus *Pandanus* is not well studied chemically with only 4 species reported in the literature. *Pandanus tectorius*[164] and *Pandanus latifolius*[165] were found to contain sterols and the terpene, linalool, respectively. Alkaloids were found in two other species, *P. veitchii* and *P. amaryllifolius*. The diastereoisomers, (2S,4R)-4-hydroxy-4-methylglutamic acid **99** and (2S,4S)-4-hydroxy-4-methylglutamic acid **100** were isolated from *P. veitchii* separately by two groups.[163,164] Recently, 2-acetyl-1-pyrroline **101**, the same compound responsible for the odour of scented rice, has been isolated from the leaves of *Pandanus amaryllifolius*.[168] Alkaloids have been detected in an unidentified species of *Pandanus* [169] and in *Pandanus odoratissimus* [170] (synonymous with *P. amaryllifolius*) but these have not been isolated and identified.

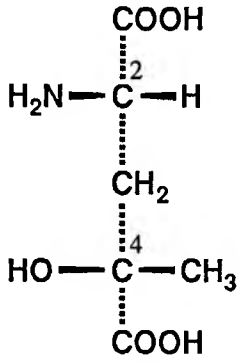

(2S,4R)-4-Hydroxy
-4-methylglutamic acid
99

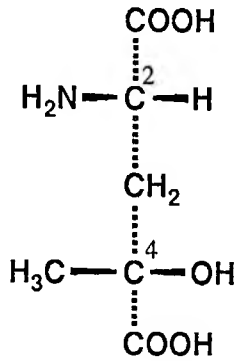

(2S,4S)-4-Hydroxy
-4-methylglutamic acid
100

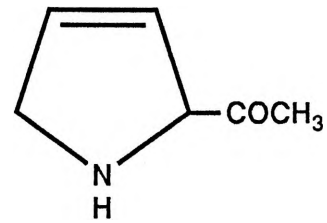

2-Acetyl-1-pyrroline
101

4-Hydroxyglutamic acid **102** has been found previously in species such as *Phlox decussata*[171], *Hemerocallis fulva*[172] and *Linaria vulgaris*[173] while 4-hydroxy-4-methylglutamic acid is a well known plant constituent.[174-177] Glutamic acid **103**, a known precursor of many amino acids, is widely distributed in higher plants and plays a key role in metabolic reactions.

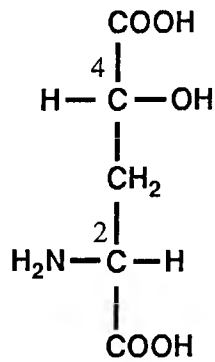

4-Hydroxyglutamic Acid
102

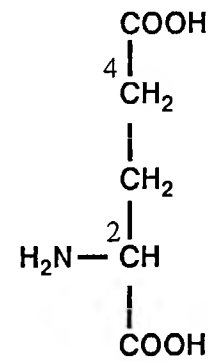

Glutamic Acid
103

Recently, a novel alkaloid Pandamarine **104** was isolated and identified by X-Ray crystallography from the leaves of *Pandanus amaryllifolius*.[178] From the X-ray structure it was shown that the piperidine ring is in the chair conformation and is perpendicular to the lactam ring.

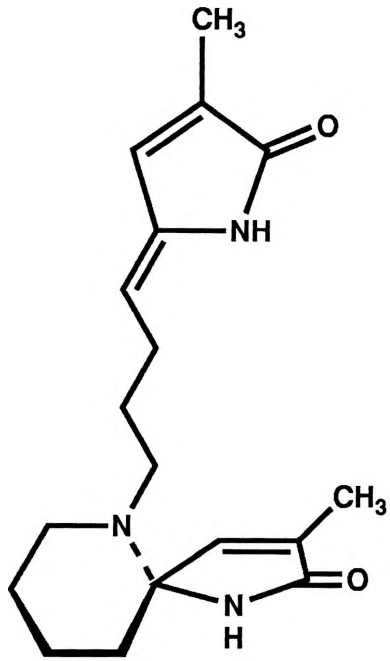

Pandamarine 104

5.1.1 *Pandanus amaryllifolius* Roxb.

This species which is also known as *Pandanus odoratissimus* has been introduced in the Philippines and is now cultivated as an ornamental plant. This plant, which forms groves in valleys and hillsides, was originally from Southern Asia but also occurs in India, Iran and Malaysia. Locally, the plant is known as "pandan-mabango" or in English, fragrant screwpine.

The plant is an erect and branched shrub with a height of 2-3 m and a trunk bearing few to many proroots. The 1.5 m long, 3.5 cm wide, smooth, slenderly lanceolate and fragrant leaves are spirally crowded toward the ends of the branches. The numerous

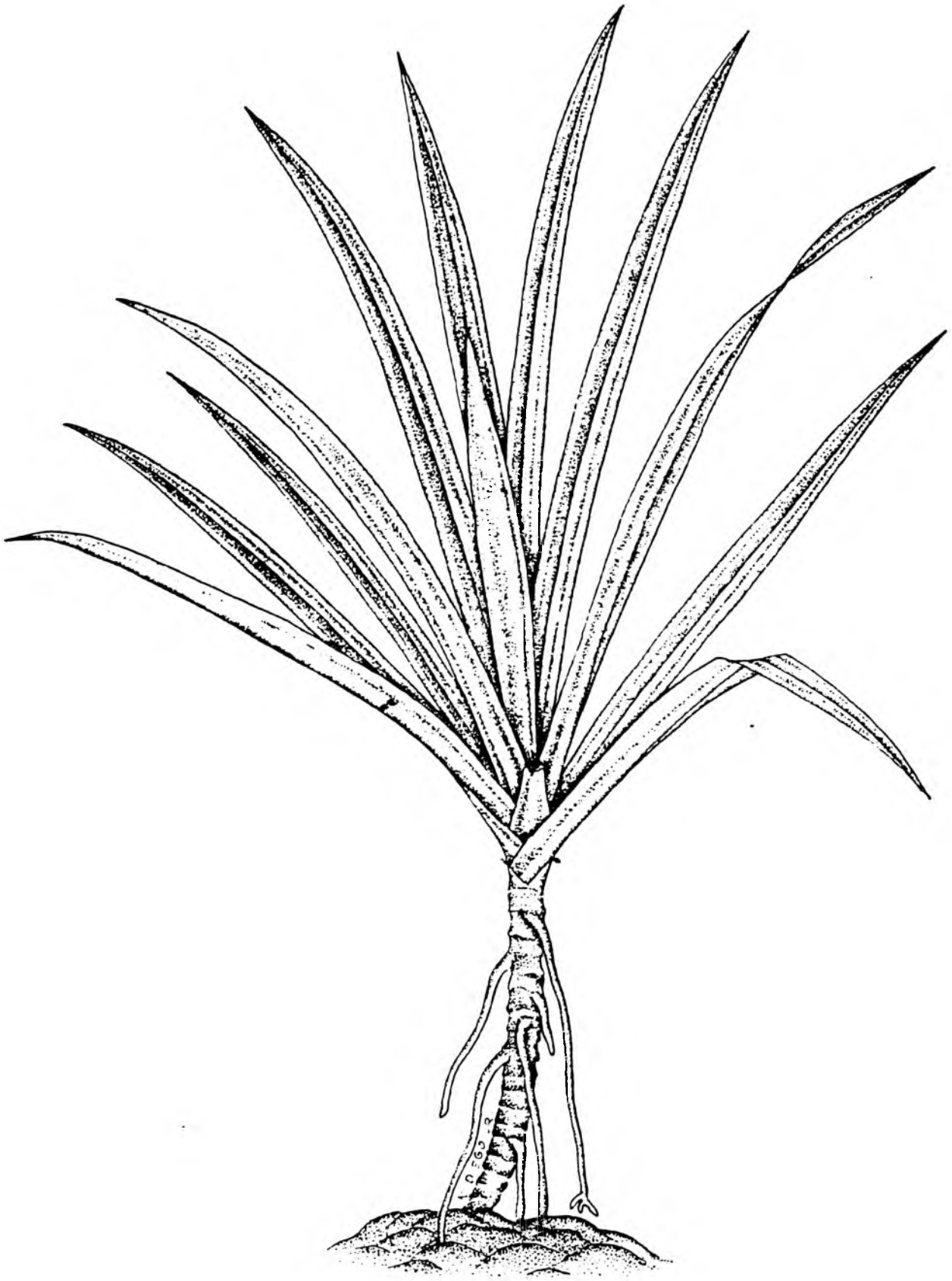

Figure 35. *Pandanus amaryllifolius (Pandanaceae)* Plant.

white flowers are fragrant, pendulous and densely disposed. They mature into 4-6 cm. long, broadly egg-shaped, fibrous and fleshly fruits (Figure 35).[161]

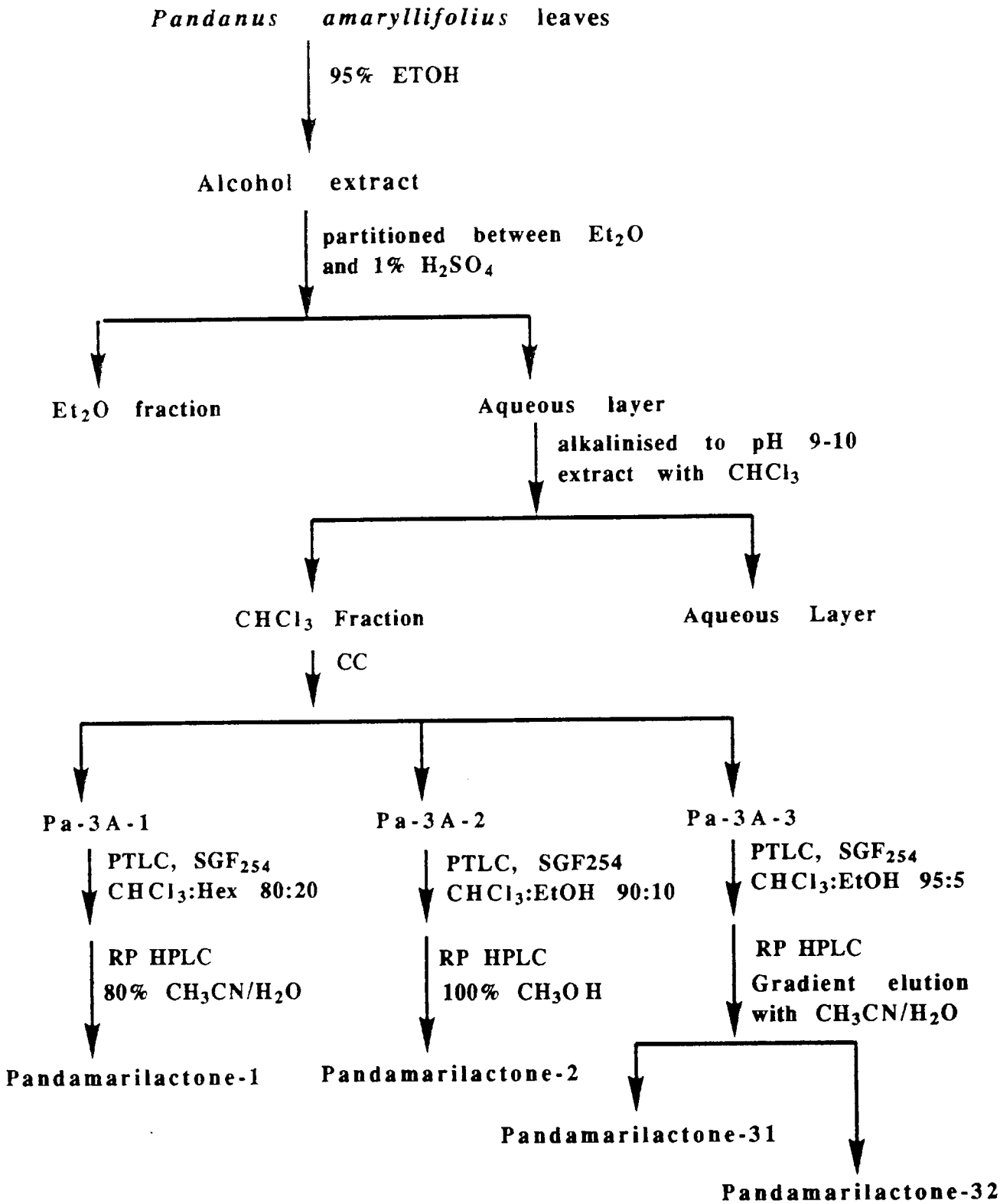

Scheme 18. Schematic Diagram for the Isolation and Purification of the *Pandanus amaryllifolius* Alkaloids.

5.2 RESULTS AND DISCUSSION

Four novel alkaloids were isolated from the $CHCl_3$ fraction of the *P. amaryllifolius* leaves, three of which were fully characterised while the fourth alkaloid was partially elucidated. Each of the alkaloids were purified using different chromatographic methods as shown in Scheme 18. These alkaloids were found to oxidise easily and changed from pale yellow to brown colour on standing thus posing difficulty in their purification.

5.2.1 Pandamarilactone-1 (Pa-3A-1)

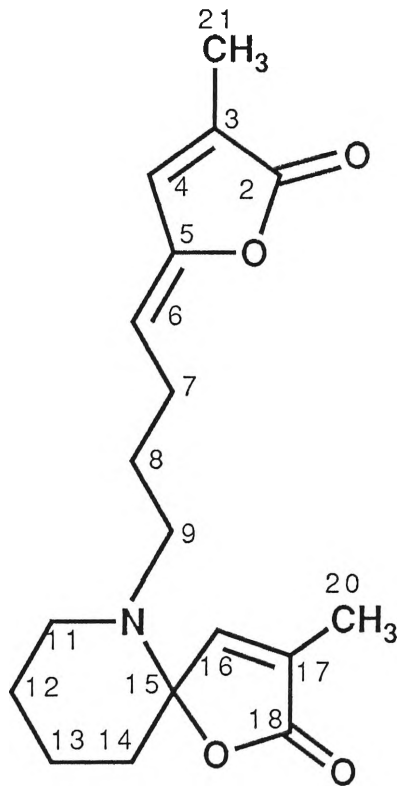

Pandamarilactone-1, labelled as Pa-3A-1, absorbed at λ_{max} 275.0 and 203.8 nm consistent with an α,β-unsaturated carbonyl group.[145] Its IR spectrum showed absorption bands at 1764 cm^{-1} agreeing with a α, β -unsaturated five-membered ring lactone and at 1695 cm^{-1} for an enol ether.[145] A molecular ion at *m/z* 317.1635 was obtained by HREIMS which conformed for $C_{18}H_{23}NO_4$ and gave

Table 19. ^{1}H and ^{13}C NMR Assignments for Pandamarilactone-1 [500 MHz, $CDCl_3$, referenced relative to residual $CHCl_3$ at δ7.25 (^{1}H) and δ77.0 (^{13}C)].

Carbon	^{1}H, δ (multiplicity, integration, J in Hz)	^{13}C, δ
2		171.0
3		129.2
4	6.98 (d, 1H, 1.2Hz)	137.6
5		148.6
6	5.04 (t, 1H, 8.0Hz)	113.7
7	2.31 (qt, 2H, 7.2Hz)	24.0
8	1.54 (quintet., 2H, 7.2Hz)	27.2
9	2.45 (t, 2H, 7.0Hz)	50.7
11	2.79 (t, 2H, 7.0Hz)	47.2
12	1.72 (m, 6H)	20.8
13	1.72 (m, 6H)	25.1
14	1.72 (m, 6H)	36.2
15		101.7
16	6.68 (d, 1H, 1Hz)	149.7
17		131.5
18		173.0
20	1.86 (s, 3H)	10.6
21	2.00 (s, 3H)	10.4

8 double bond equivalents. The ^{1}H NMR spectrum showed two methyl signals and three olefinic protons. The ^{13}C NMR spectrum showed two carbonyls and six olefinic carbons thus indicating three rings in the molecule.

Structure elucidation of Pandamarilactone-1 was carried out using combined 2-D NMR techniques such COSY, HMQC (Heteronuclear Multiple Quantum Coherence)[179] and HMBC (Heteronuclear Multiple Bond Correlation).[179] Table 19 presents the summary of ^{1}H and ^{13}C NMR assignments for Pandamarilactone-1 (Pa-3A-1) obtained from the HMQC and HMBC spectra.

From the COSY spectrum (Figure 36), the olefinic protons at δ6.98 (q, J1.2Hz, H-4) and δ6.68 (q, J1.2Hz, H-16) were allylically coupled to the methyl singlets at δ2.00 (H-21) and δ1.86 (H-20) respectively. The triplet at δ5.04 (1H, J8.0Hz, H-6) was coupled to δ2.31 (2H, H-7) which in turn correlates with δ1.54 (2H, H-8). This methylene group at δ1.54 (H-8) showed a COSY crosspeak to the triplet at δ2.45 (H-9).

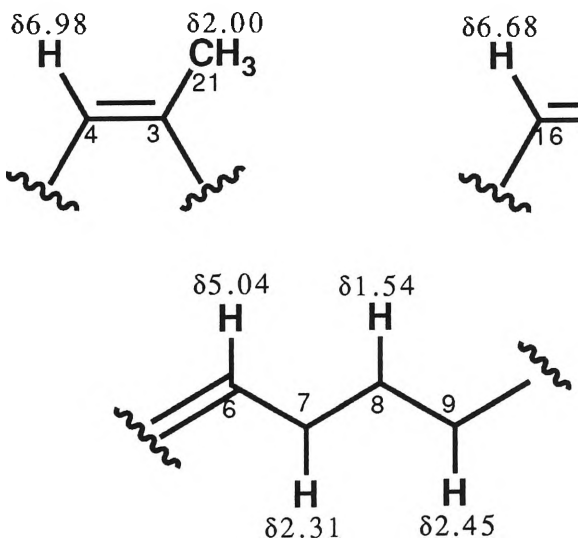

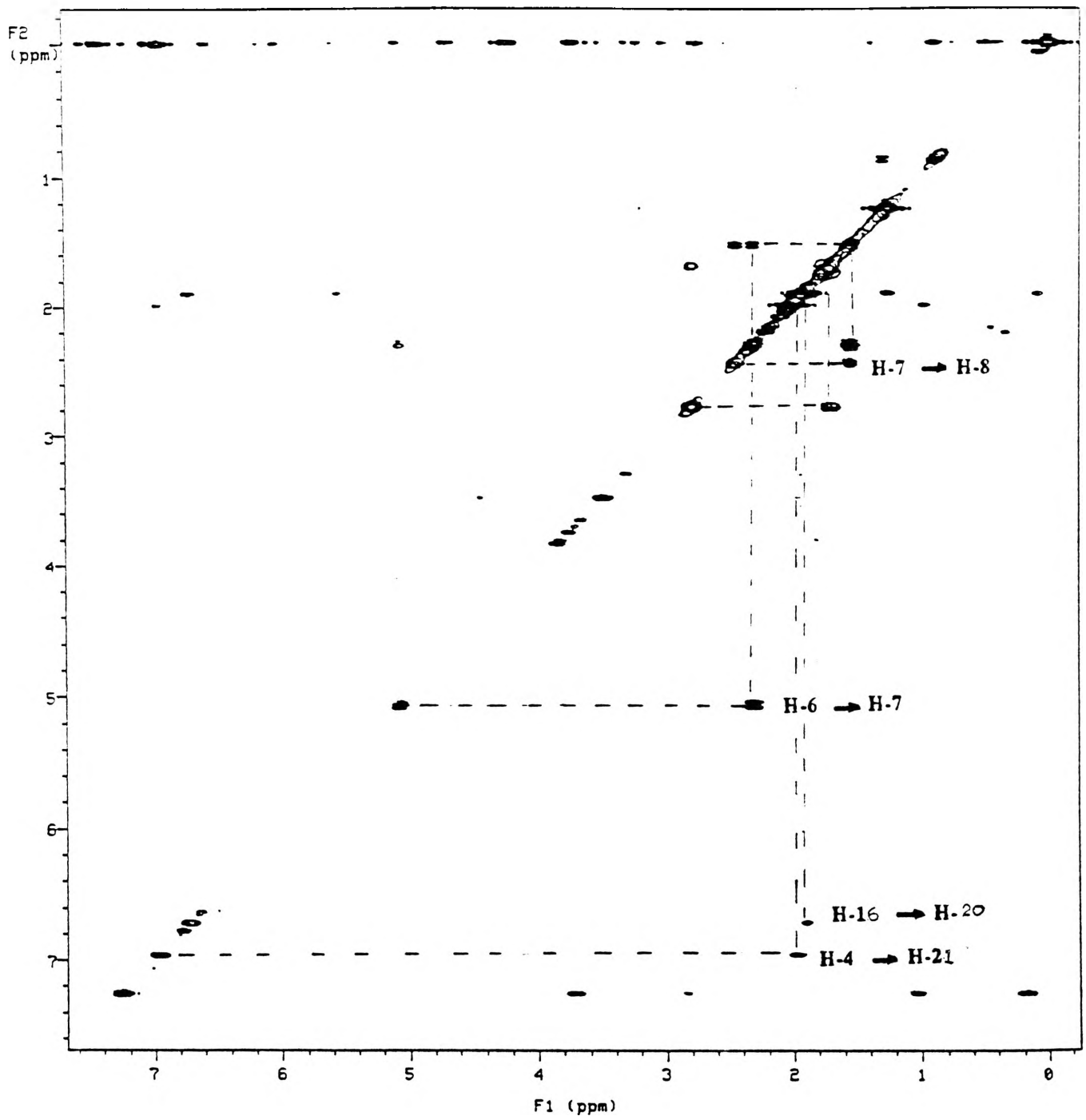

Figure 36. ^{1}H-^{1}H COSY NMR Spectrum of Pandamarilactone-1 [400 MHz, $CDCl_3$, referenced at δ7.25].

The triplet at δ2.79 (2H, H-11) showed a COSY crosspeak to a multiplet centred at δ1.72 (H-12,-13, and -14) which integrated for 6 protons.

The one-bond ^{1}H-^{13}C correlation was acquired by the inverse-detection HMQC. This NMR technique was considered more sensitive than other heteronuclear NMR experiments for detection of the ^{13}C signals through the protons attached to it. From the TOCSY (Appendix 2) and HMQC (Figure 37) crosspeaks, fragments A, B, and C were formed and are shown below.

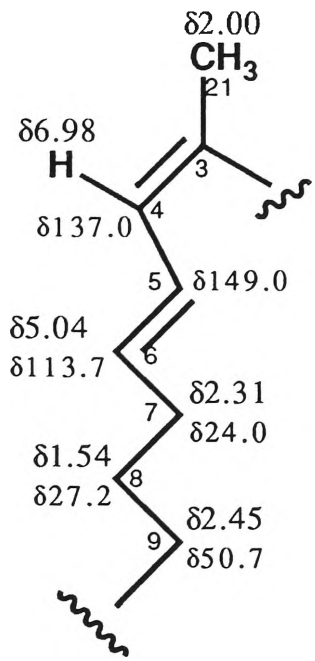

Fragment A

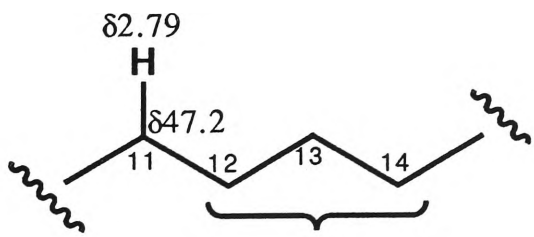

multiplet
centred at δ1.72
(δ20.8, δ25.1, δ36.2)

Fragment B

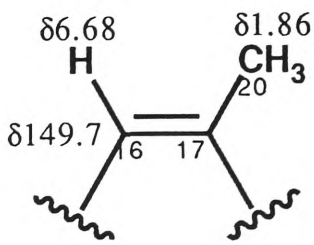

Fragment C

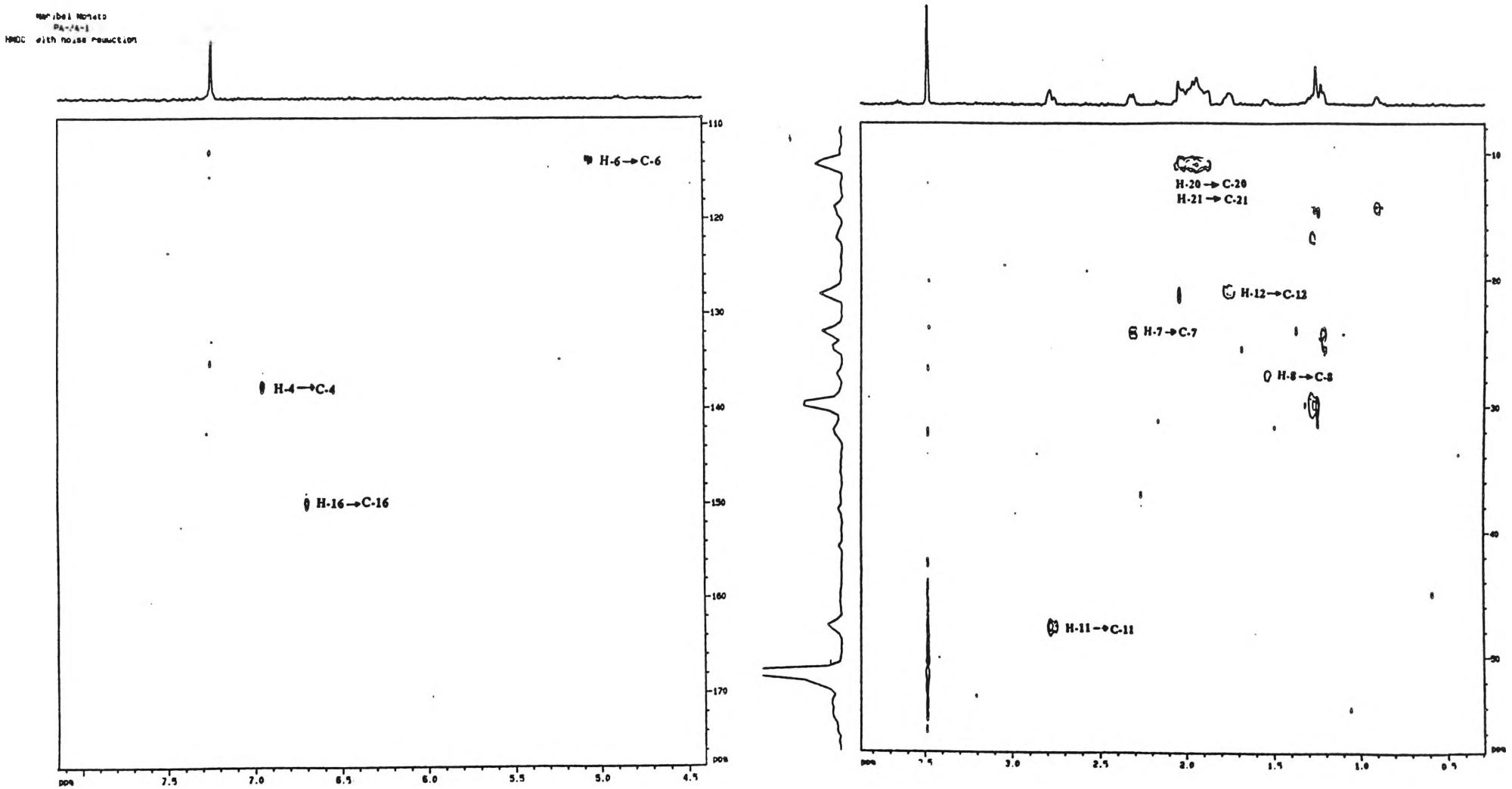

Figure 37. Expanded Regions of Inverse-Detection (^{1}H-^{13}C) Heteronuclear Multiple Quantum Coherence (HMQC) NMR Spectra of Pandamarilactone-1 [500 MHz, $CDCl_3$, referenced at δ7.25 (^{1}H) and δ77.0 (^{13}C)].

The 2-D homonuclear (COSY and TOCSY) and the one-bond heteronuclear (HMQC) NMR experiments could not provide the information necessary to form the connectivity between the three fragments. Thus, another 2-D Heteronuclear NMR technique was utilised. Long range ^{1}H-^{13}C Heteronuclear Multiple Bond Correlation (HMBC) by inverse detection was then used for establishing the connectivities between the observed fragments. This NMR technique conveniently provides the means of assigning quaternary carbons thereby assembling the carbon skeleton and it also allows establishment of connectivities across heteroatoms thus giving the chemist extremely powerful structural information. HMBC experiment were considered more sensitive compared to other ^{1}H-^{13}C NMR correlation experiments. The 2-D COLOC (COrrelation by LOng range Coupling) suffers low sensitivity and yields spectral intensities that are modulated by the size of both the one-bond $J_{C\,H}$ coupling and the homonuclear proton coupling while the 1-D selective INEPT experiment has the disadvantage of requiring exact adjustment of pulse width and are time consuming if a large number of connectivities are to be considered.

The long range HMBC NMR experiment was optimised to observe an 8.0Hz coupling between ^{1}H and ^{13}C which may arise from two to three bond couplings.

From the HMBC spectrum (Figure 38), the olefinic proton at δ6.98 (H-4) showed crosspeaks at δ171.0 (C=O, C-2) and a quaternary carbon at δ148.6 (C-5). On the other hand, the methyl group at δ2.00 (H-21) showed correlations with δ171.0 (C-2), δ137.6 (C-4) and δ129.2 (C-3) carbons. The quaternary carbon at δ148.6 (C-5) showed connectivity with H-6 at δ5.04.

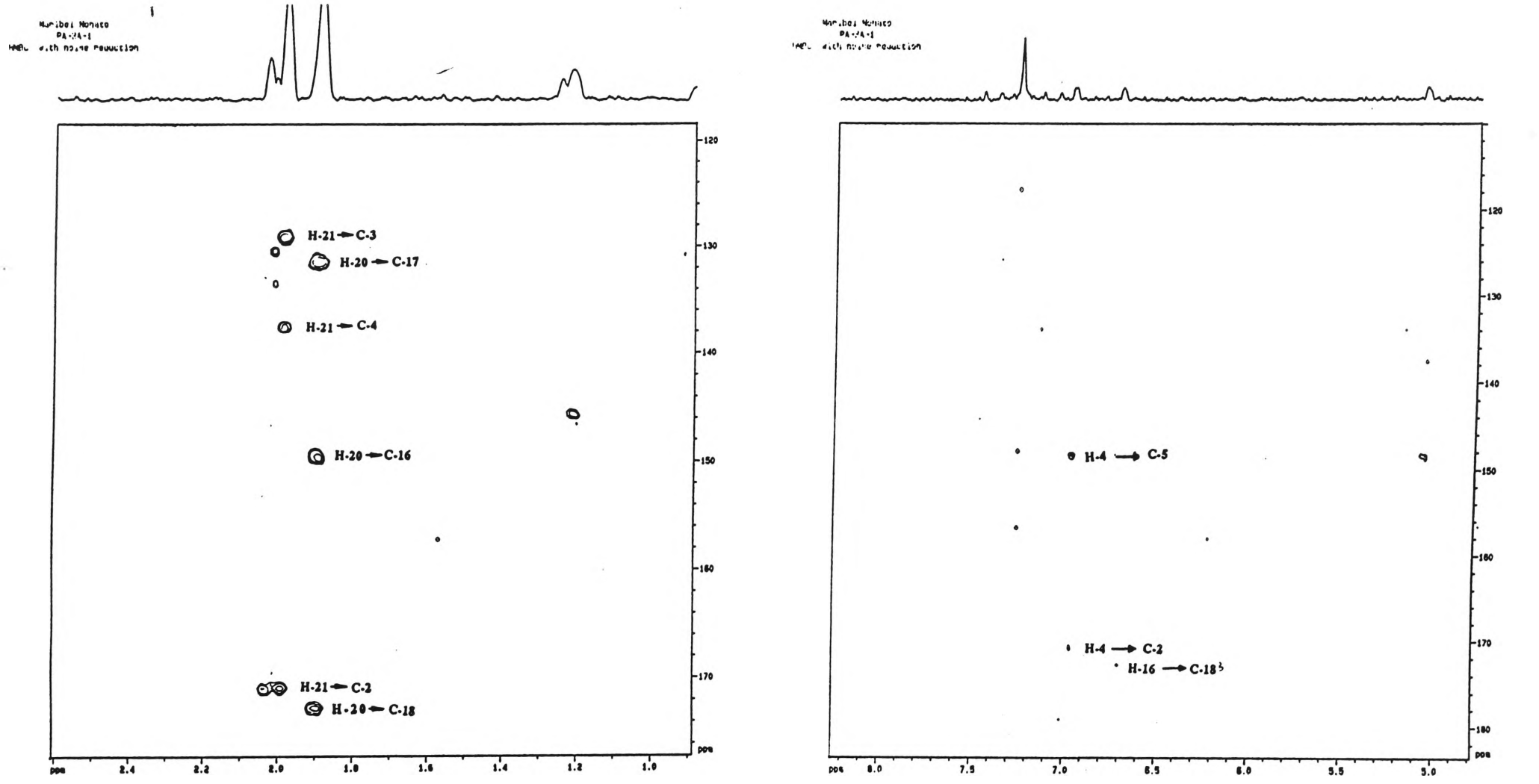

Figure 38. Expanded Regions of Inverse-Detection (^{1}H-^{13}C) Heteronuclear Multiple Bond Correlation (HMBC) NMR Spectra of Pandamarilactone-1 [500 MHz, $CDCl_3$, referenced at δ7.25 (^{1}H) and δ77.0 (^{13}C)].

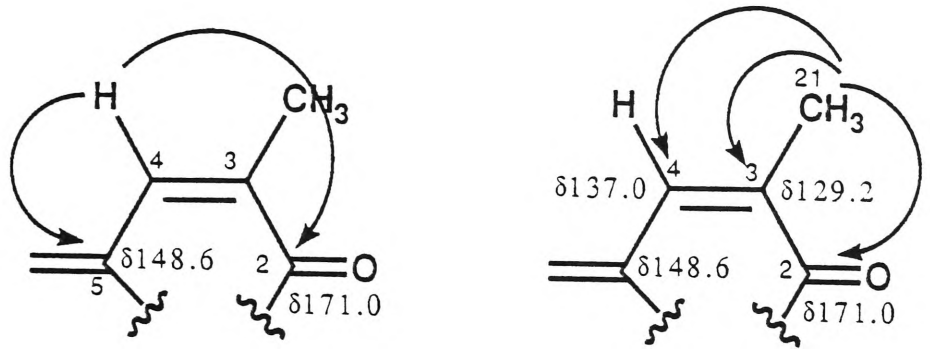

The allylically coupled proton at δ6.68 (H-16) showed carbon correlations with the resonances at δ173.0 (C=O, C-20) and to a quaternary carbon at δ101.7 (C-15). The methyl group was established to be coupled to δ149.7 (C-16) and δ131.5 (C-17). All these data formed the fragments below.

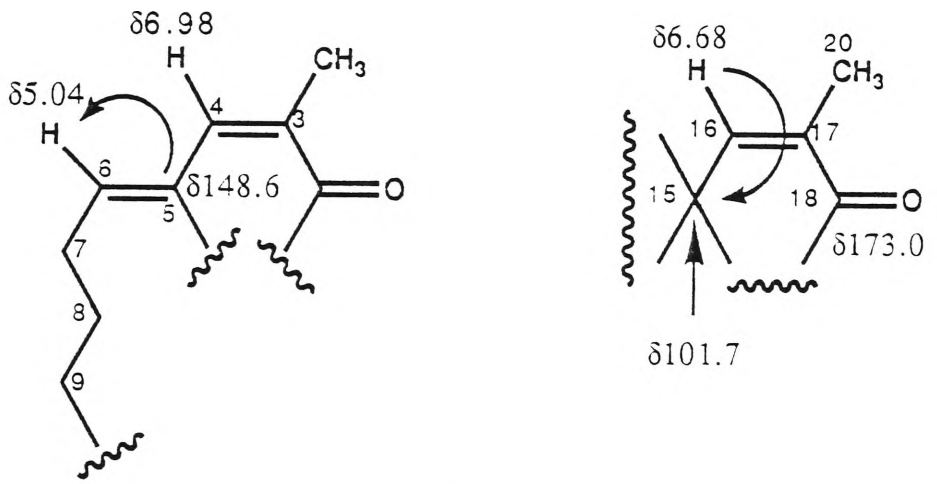

At this stage, 18 carbons, 23 hydrogens and two oxygens had been assigned. Two more oxygens and 1 nitrogen remained to be incorporated into the structure. A total of five double bond equivalents were already found hence leaving three DBE more to consider and these were assigned for 3 rings in the molecule.

The resonance at δ2.45 integrating for 2H and a ^{13}C chemical shift at δ50.7 was consistent for a methylene group attached to a nitrogen and these were assigned to H-9 (δ2.45). The signal at δ148.6 was in agreement for an olefinic carbon attached to a heteroatom such as oxygen. This formed the lactone part of the

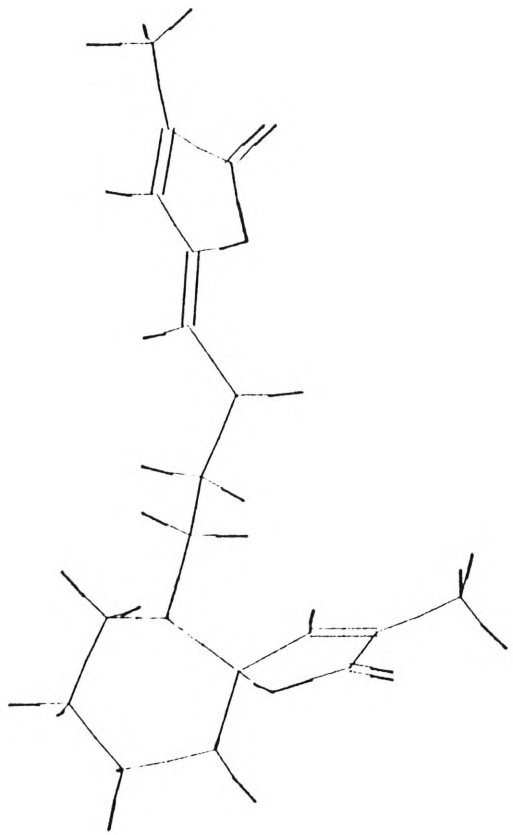

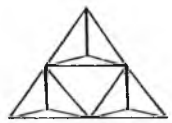

Alchemy II
TRIPOS Associates
St. Louis. Mo.

PANDAMARILACTONE-1

molecule which was in accord with the IR absorption at 1764 cm^{-1}. The other oxygen atom was assigned to the other lactone ring. The remaining one DBE was assigned to form the 6-membered piperidine ring structure. All these data best fit the proposed structure for Pandamarilactone-1 (Pa-3A-1). NOe crosspeaks were observed from the ROESY spectrum between δ6.98 (H-4) and δ2.00 (H-21) and δ6.98 (H-4) and δ5.04 (H-6).

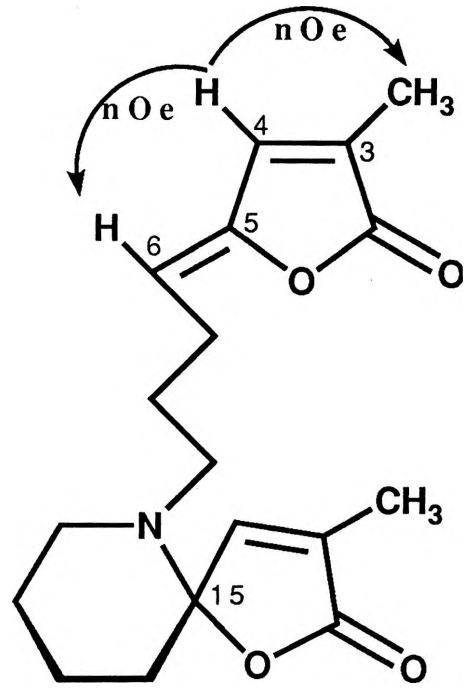

The absolute stereochemistry at C-15 cannot be assigned from the NMR data alone. X-ray crystallography was not possible since insufficient material was available to allow recrystallisation. Pandamarilactone-1 gave a specific rotation of $[\alpha]_D^{25}$ -33.0 which arose due to the chirality observed at C-15. By comparison with Pandamarine **104**, it may be possible that the piperidine ring is perpendicular to the five-membered lactone ring. Molecular modelling using the Alchemy program with energy minimisation showed the most likely conformation of Pandamarilactone-1 with

the six-membered ring in a perpendicular position to the lactone ring.

It was surprising to note that the previous novel alkaloid, pandamarine[175] isolated from this same plant has two lactam rings. Pandamarilactone-1 has the same C_9-N-C_9 skeleton as that for Pandamarine however on the basis of all the observed spectroscopic data, it was clear that our compound has a lactone functionality.

5.2.2 Pandamarilactone-32 (Pa-3A-32)

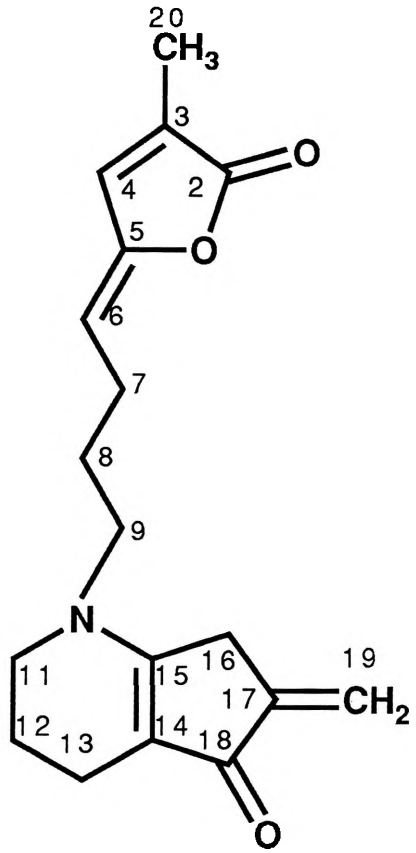

Pandamarilactone-32, labelled as Pa-3A-32, was obtained as a colourless solid and showed a UV absorption at λ_{max} 325.4 consistent with an α,β-unsaturated five membered ring ketone with a nitrogen auxochrome attached to the β position, and at 278.6 nm which are in accord for a five-membered lactone.[145] The IR spectrum showed a carbonyl signal at 1764 cm^{-1} for a vinyl ester; a

Table 20. ^{1}H and ^{13}C NMR Assignments for Pandamarilactone-32 (Pa-3A-32) [$CDCl_3$, referenced relative to the residual signals for $CHCl_3$ at δ7.25 (^{1}H) and δ77.0 (^{13}C)].

Carbon	^{1}H (δ, multiplicity, integration, J Hz)	^{13}C, δ
2		171.0
3		129.0
4	6.98 (q, 1H, 2.0Hz)	137.0
5		149.0
6	5.09 (t, 1H, 8.0Hz)	111.6
7	2.39 (q, 2H, 8.0Hz)	23.6
8	1.77 (quintet, 2H, 8.0Hz)	27.8
9	3.30 (m, 2H)	50.9
11	3.27 (m, 2H)	48.0
12	1.85 (quintet, 2H, 6.0Hz)	21.1
13	2.33 (t, 2H, 6.0Hz)	18.0
14		113.0
15		168.0
16	3.16 (2H, br s)	30.9
17		141.0
18		188.0
19	5.89 (t, 1H, 1.0Hz)	110.8
19	5.14 (t, 1H, 1.0Hz)	110.8
20	2.00 (d, 3H, 2.0Hz)	10.6

five carbon ring ketone carbonyl signal at 1710 cm^{-1}; and an enol ether at 1667 cm^{-1}.[145] An *m/z* of 299.1521 (HREIMS) was obtained for the molecular formula $C_{18}H_{21}NO_3$ and 9 double bond equivalents. The ^1H NMR spectrum showed the presence of 1 methyl signal and four olefinic protons. The ^{13}C spectrum showed 18 C and the APT (Attached Proton Test) spectrum showed 1 CH_3, 8 CH_2, 2 CH, and 7 quaternary carbons. Initially, it was thought that the compound had three carbonyl signals based on the observed molecular formula and the observed ^{13}C signals at δ188.0, δ171.0 and δ168.0. Difficulty in coming up with a logical structure that fitted all the NMR, UV and IR data made us question the MS value. However, the observed *m/z* of 299 was further corroborated by LRFAB and electrospray MS[180] techniques. Since the *m/z* s obtained from the three MS techniques were in agreement with each other, it was then suggested that the signal at δ168.0 was not due to a carbonyl group but instead to an olefinic carbon. Thus, Pandamarilactone-32 has only two carbonyl signals which was also in accordance with the IR data.

Structural elucidation of this alkaloid was carried out utilising the combined spectroscopic data obtained from 2-D COSY, TOCSY, ROESY, HMQC (Heteronuclear Multiple Quantum Coherence) and HMBC (Heteronuclear Multiple Bond Correlation) NMR techniques. Table 20 presents the summary of ^1H and ^{13}C NMR assignments for Pandamarilactone-32 obtained from the HMQC and HMBC spectra.

The ^1H NMR spectrum (Figure 39) showed 4 olefinic protons at δ6.98 (q, J 2.0Hz, H-4), δ5.89 (t, J 1.0Hz, H-19), δ5.14 (t, J 1.0Hz, H-19), and the triplet at δ5.09 (J 8.0Hz, H-6). From the COSY spectrum (Figure 40), the correlations between each of these protons were established. The signal at δ6.98 (H-4) showed an

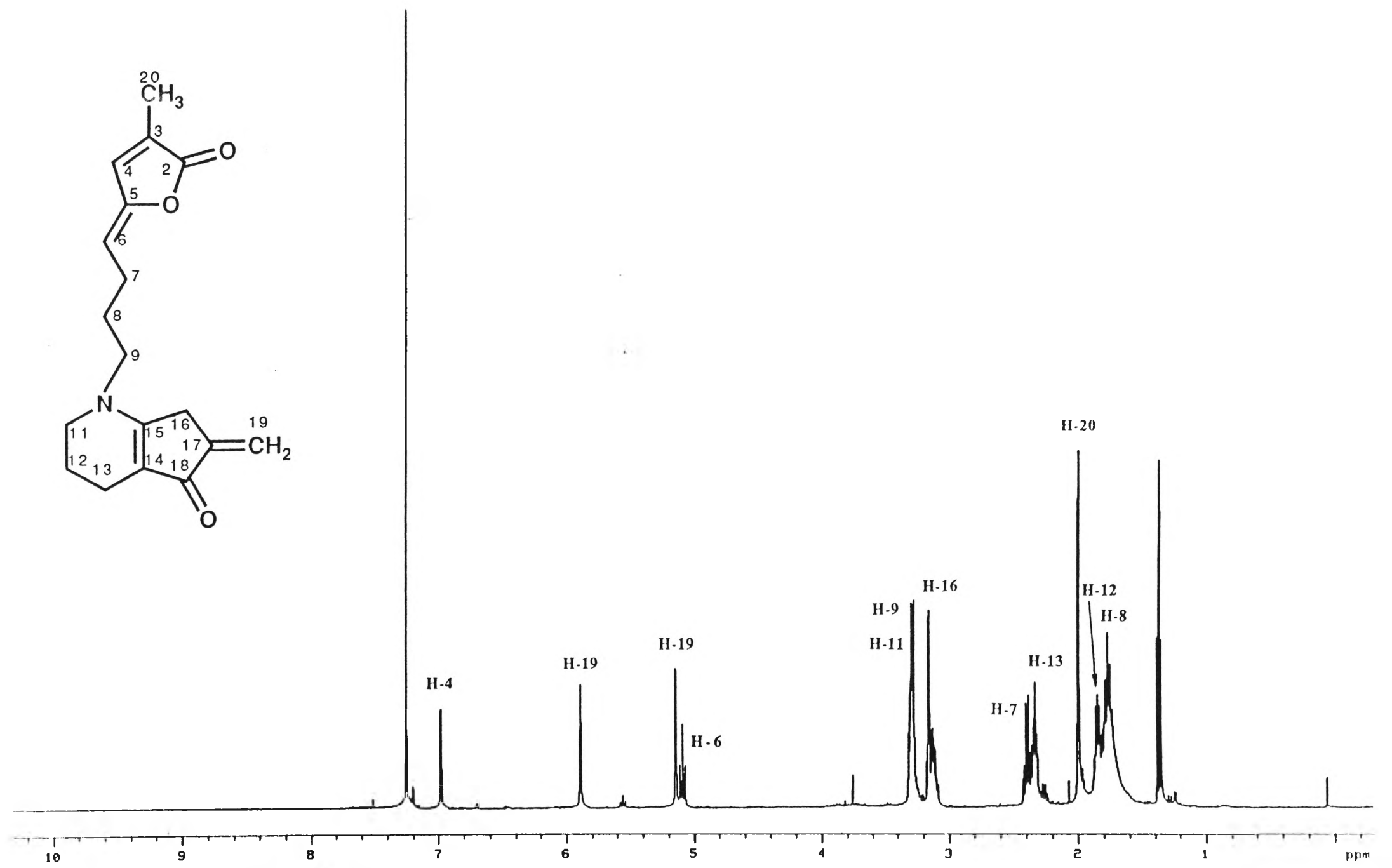

Figure 39. ^{1}H NMR Spectrum of Pandamarilactone-32 [400MHz, $CDCl_3$, referenced at δ7.25].

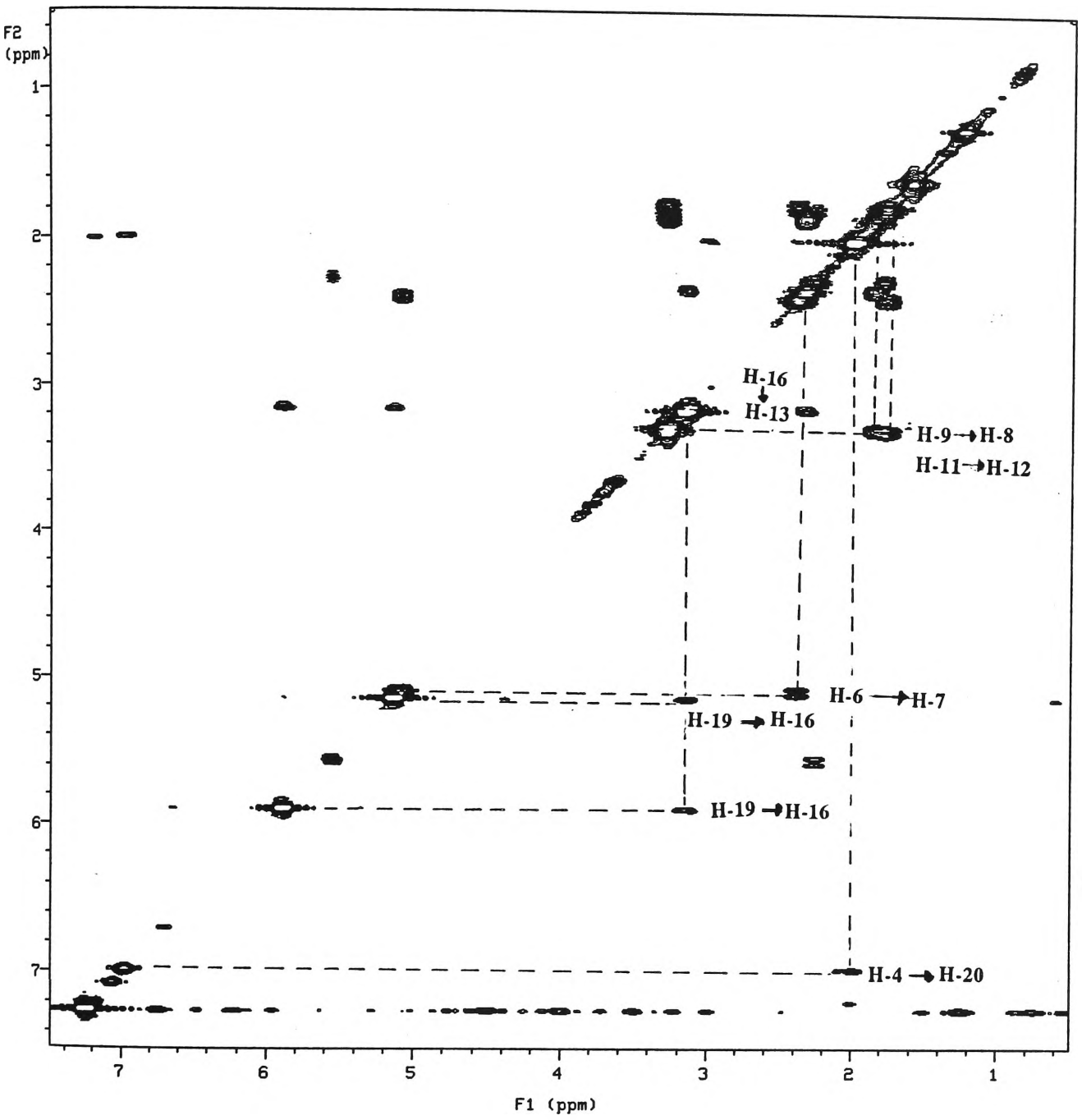

Figure 40. ^{1}H - ^{1}H COSY NMR Spectrum of Pandamarilactone-32 [400 MHz, $CDCl_3$, referenced at δ7.25].

allylic coupling to the methyl signal at δ2.00 (H-20). The triplet at δ5.09 (H-6) was coupled to the quartet at δ2.39 (H-7) which showed a crosspeak to the signal at δ1.77 (quintet, 2H, H-8). A multiplet centred at δ3.30 (H-9) integrating for 2H correlated with the signal at δ1.77.

Another multiplet centred at δ3.27 (H-11) showed a COSY crosspeak with the quintet at δ1.85 (H-12). This signal at δ1.85 showed a correlation with the triplet at δ2.33 (H-13) which showed a long range coupling with the signal at 3.16 (br s, 2H, H-16). This broad singlet at δ3.16 showed COSY crosspeaks to the signals at δ5.89 (H-19) and δ5.14 (H-19) due to allylic coupling.

To establish further the proton connectivities in the molecule, a TOCSY experiment was carried out. From the TOCSY spectrum (Appendix 2), the signal at δ5.09 (H-6) showed a relayed crosspeak to the signal at δ6.98 (H-20). The signals at δ5.89 (H-19) and δ5.14 (H-19) showed relayed crosspeaks to each other. Also, the δ2.33 (H-13) signal showed weak relayed crosspeaks with the olefinic protons at δ5.89 and δ5.14. The quintet at δ1.85 (H-12) showed relayed crosspeak with the signal at δ3.16 (H-16).

^{1}H-^{13}C correlation was elucidated by 2-D Heteronuclear Multiple Quantum Coherence (HMQC) in the indirect mode (Figure 41). All these data gave rise to fragments A and B

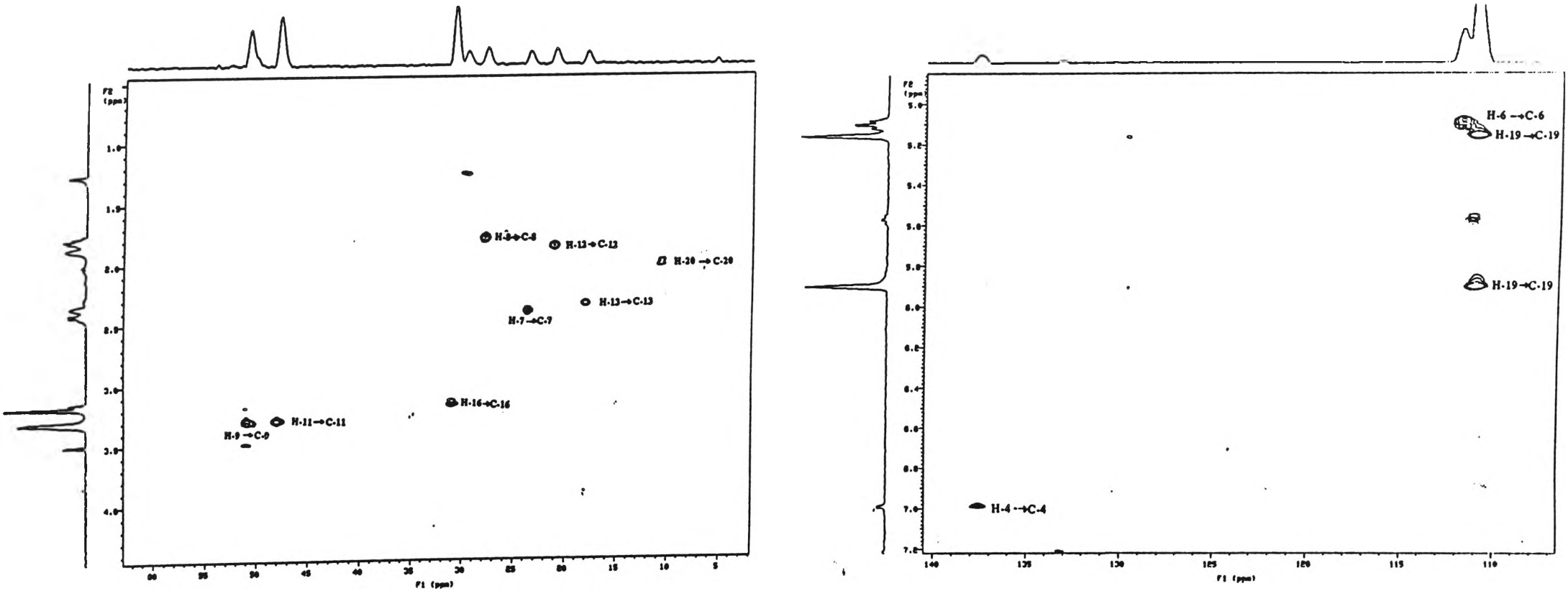

Figure 41. Expanded Regions of Inverse-Detection (^{1}H-^{13}C) Heteronuclear Multiple Quantum Coherence (HMQC) NMR Spectra of Pandamarilactone-32 [500 MHz, $CDCl_3$, referenced at δ7.25 (^{1}H) and δ77.0 (^{13}C)].

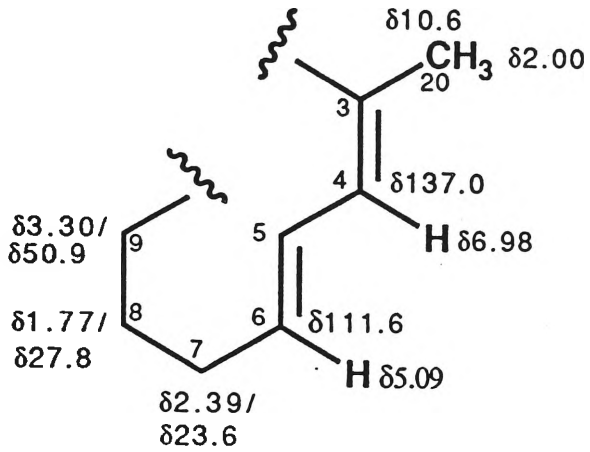

Fragment A

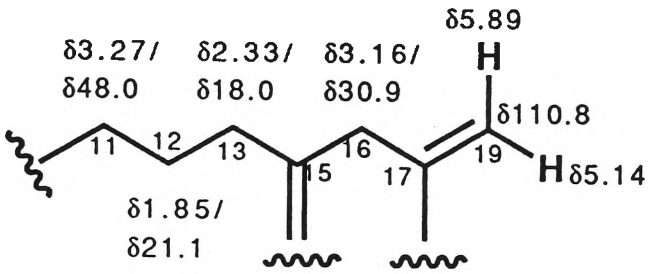

Fragment B

Fragments A and B were joined together using the ^{1}H-^{13}C long range 2-D Heteronuclear Multiple Bond Correlation (HMBC) experiment optimised for 9.0Hz coupling between ^{1}H and ^{13}C (Figure 42). The proton at δ6.98 (H-4) correlated with the carbon signal at δ149.0 (C-5) which showed crosspeaks with the protons at δ5.09 (H-6) and at δ2.39 (H-7). The proton signal at δ5.09 (H-6) attached to the carbon signal at δ111.6 (C-6), showed a long range coupling to a quaternary carbon at δ129.0 (C-3). A weak crosspeak was observed between the olefinic proton at δ6.98 (H-4) and the quaternary carbon at δ129.0 (C-3). These connectivities observed from the HMBC spectrum led to the assignment of the olefinic carbon adjacent to the methyl group to have a carbon chemical shift of δ129.0. The quaternary carbon at δ171.0 (C-2) showed HMBC correlations with both proton signals at δ2.00 (H-20) and δ6.98 (H-4). These correlations established fragment C.

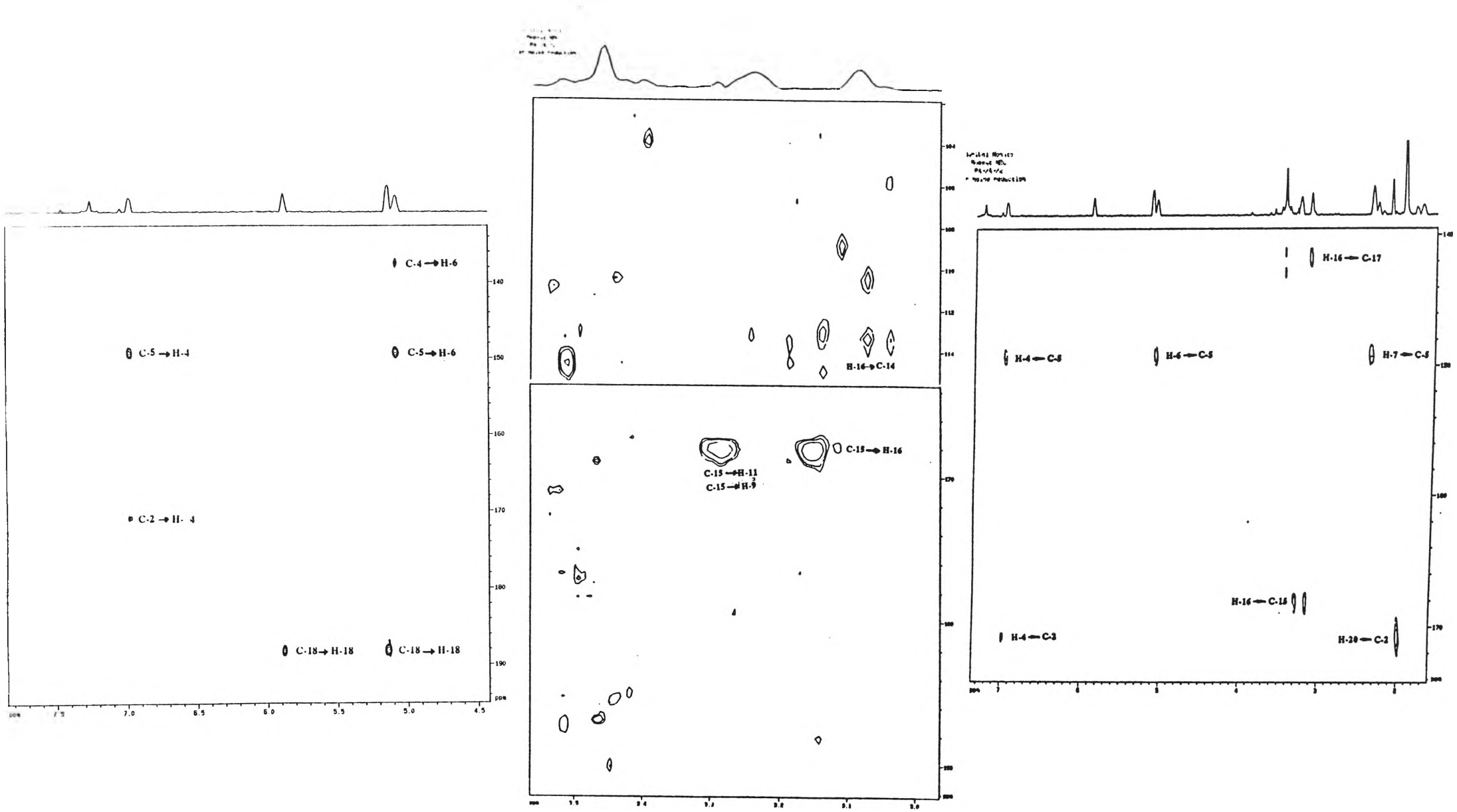

Figure 42. Expanded Regions of Inverse-Detection (^{1}H-^{13}C) Heteronuclear Multiple Bond Correlation (HMBC) NMR Spectra of Pandamarilactone-32 [500 MHz, $CDCl_3$, referenced at δ7.25 (^{1}H) and δ77.0 (^{13}C)].

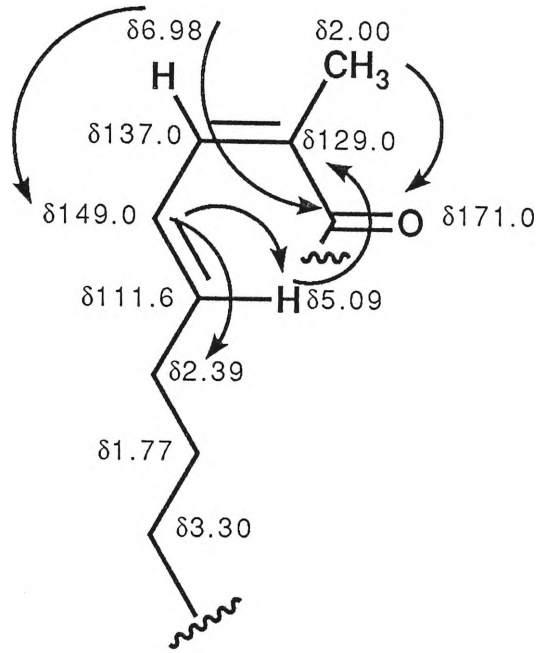

Fragment C

Information about the remaining portion of the molecule was achieved as follows. A second carbonyl signal at δ188.0 (C-18) showed HMBC correlations with the vinylic protons at δ5.89 (H-18) and δ5.14 (H-18). The proton signal at 3.16 (H-16) showed crosspeaks with the three quaternary carbons at δ168.0 (C-15), δ141.0 (C-17), and δ113.0 (C-14). The signal at δ168.0 (C-15) showed connectivities with the protons at δ2.33 (H-13), δ3.16 (H-16), δ3.27 (H-11) and δ3.30 (H-9) while the signal at δ113.0 (C-14) showed HMBC crosspeaks with δ3.16 (H-16), δ2.33 (H-13) and δ1.85 (H-12). This information afforded the other half of the molecule of Pandamarilactone-32 shown below as fragment D.

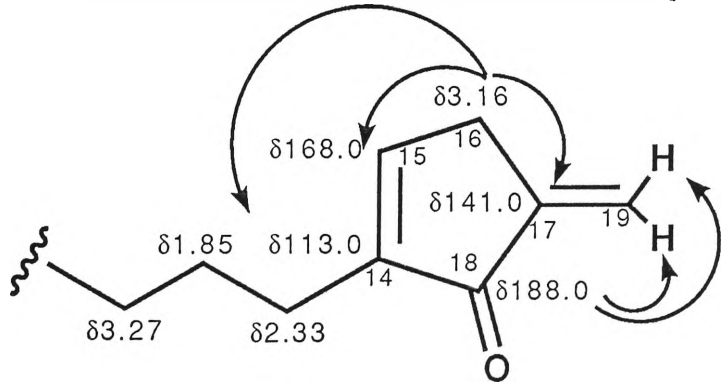

Fragment D

The ^{13}C chemical shifts at δ50.9 (C-9) and δ48.0 (C-11) with proton signals at δ3.30 and δ3.27 were consistent for methylene group attached to a nitrogen. The quaternary carbon at 168.0 (C-15) was assigned for an olefinic carbon attached to a nitrogen.[178] The remaining oxygen was attached to Fragment C forming the five-membered ring lactone. Incorporating the nitrogen into the structure created a six-membered ring in fragment D and formed the linkage with fragment C thus the proposed structure for Pandamarilactone-32.

From the ROESY spectrum (Appendix 2), nOe crosspeaks were observed between H-4 and H-6 and H-4 and H-20, establishing the stereochemistry at those positions.

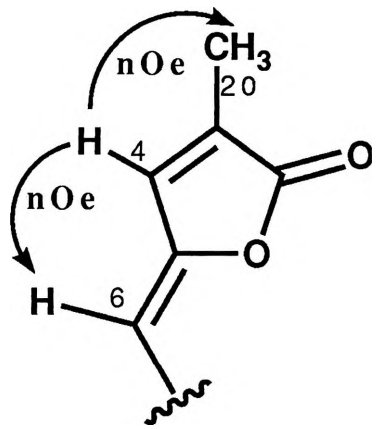

This compound was found to be optically inactive which was expected from the established structure. Pandamarilactone-32 has the C_9-N-C_9 skeleton with a modification at the piperidine-lactone ring. The vinyl group adjacent to the carbonyl group would be expected to be chemically labile and may explain why the compound is unstable.

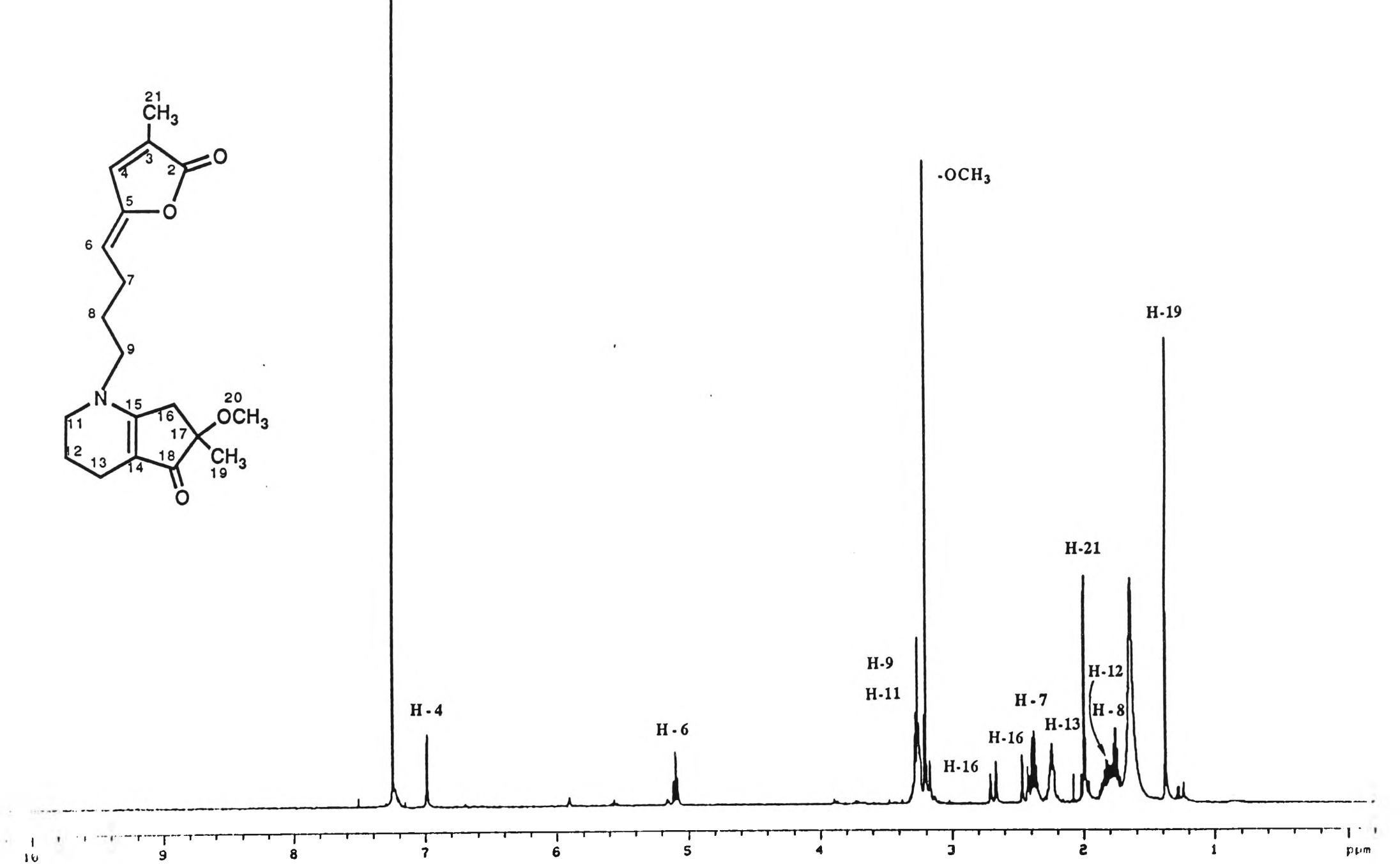

Figure 43. ^1H NMR Spectrum of Pandamarilactone-31 [400 MHz, $CDCl_3$, referenced at δ7.25].

5.2.3 Pandamarilactone-31 (Pa-3A-31)

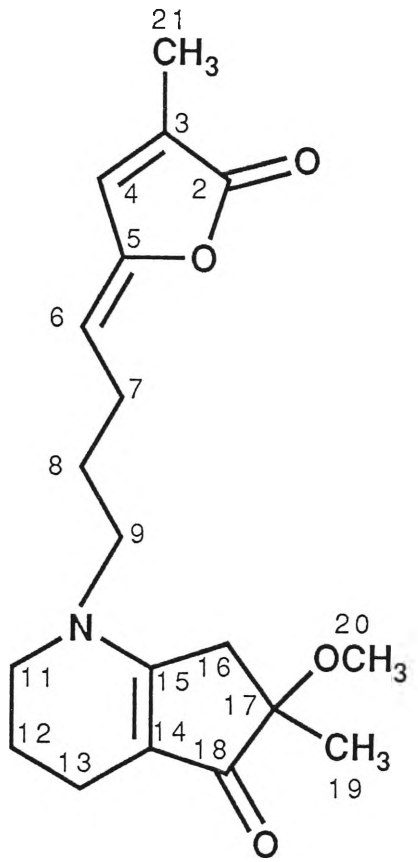

Pandamarilactone-31, labelled as Pa-3A-31, absorbed at a shorter wavelength, λ295.0 nm, compared with Pa-3A-32. This was consistent with a vinyl lactone. The HREIMS gave a *m/z* of 331.1940 which best fits $C_{19}H_{25}NO_4$, corresponding to 8 double bond equivalents. The ^1H NMR spectrum (Figure 43) of Pandamarilactone-31 showed similar signals to those for Pandamarilactone-32 except that the signals for the methylene protons at δ5.89 and δ5.14 were missing. Four other proton resonances however were observed, the signals at δ2.69 (d, 17.0Hz) and δ2.45 (d, 17.0Hz) for a non-equivalent geminal protons, a methoxy signal at δ3.20 (s, 3H) and a methyl singlet at δ1.37. Again structure elucidation of this compound was carried out by comparison to Pandamarilactone-32 and by use of the 2-D NMR

Table 21. ^{1}H and ^{13}C NMR Assignments for Pandamarilactone-31 (Pa-3A-31) [$CDCl_3$, referenced relative to the residual signals for $CHCl_3$ at δ7.25 (^{1}H) and δ77.0 (^{13}C)].

Carbon	^{1}H (δ, multiplicity, integration, J in Hz)	^{13}C, δ
2		171.0
3		130.0
4	6.99 (q, 1H, J1.2 Hz)	137.0
5		149.0
6	5.10 (t, 1H, J8.0 Hz)	112.0
7	2.39 (q, 2H, J7.6Hz)	23.0
8	1.76 (quintet, 2H, J7.6Hz)	28.0
9	3.27 (t, 2H, J5.6 Hz)	51.0
11	3.25 (m, 2H)	48.0
12	1.80-1.90 (m, 2H)	21.0
13	2.25 (br td, 2H, J4.8, 1.2 Hz)	18.0
14		108.0
15		168.0
16	2.69 (d, 1H, J17.0 Hz)	37.0
	2.45 (d, 1H, J17.0 Hz)	37.0
17		80.0
18		188.0
19	1.37 (s, 3H)	23.0
20	3.20 (s, 3H)	52.0
21	2.00 (d, 3H, J1.2Hz)	10.4

experiments previously mentioned in the discussion of Pandamarilactone-32.

Table 21 presents the ^{1}H and ^{13}C NMR assignments for Pandamarilactone-31 acquired from the HMQC (Figure 44) and HMBC spectra (Figure 45). A long range coupling were observed in the HMBC spectrum between the protons at δ2.69 (H-16) and δ2.45 (H-16) and the methoxy signal at δ52.0 (C-20), and the methyl signal at δ23.0 (C-19) and the quaternary carbon at δ188.0 (C-18) for the fragment below.

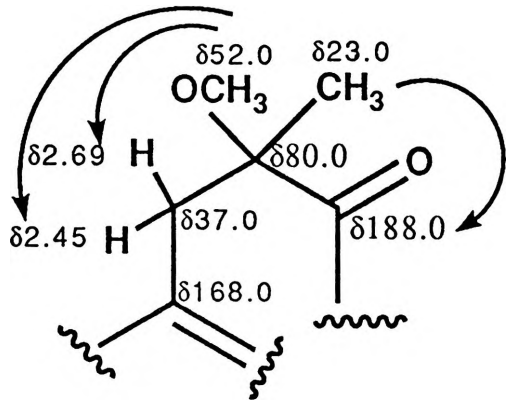

Both the methoxy signal and the methyl signal showed an HMBC crosspeak with the quaternary carbon at δ80.0. The assignments and ^{1}H-^{13}C correlations for the rest of the molecule were established via arguments analogous to Pandamarilactone-32 analysis.

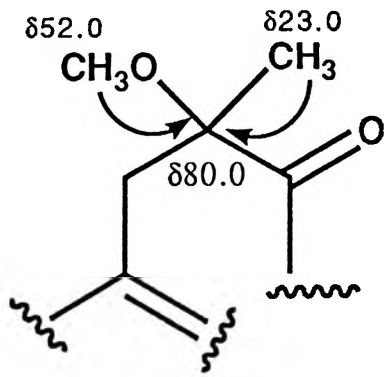

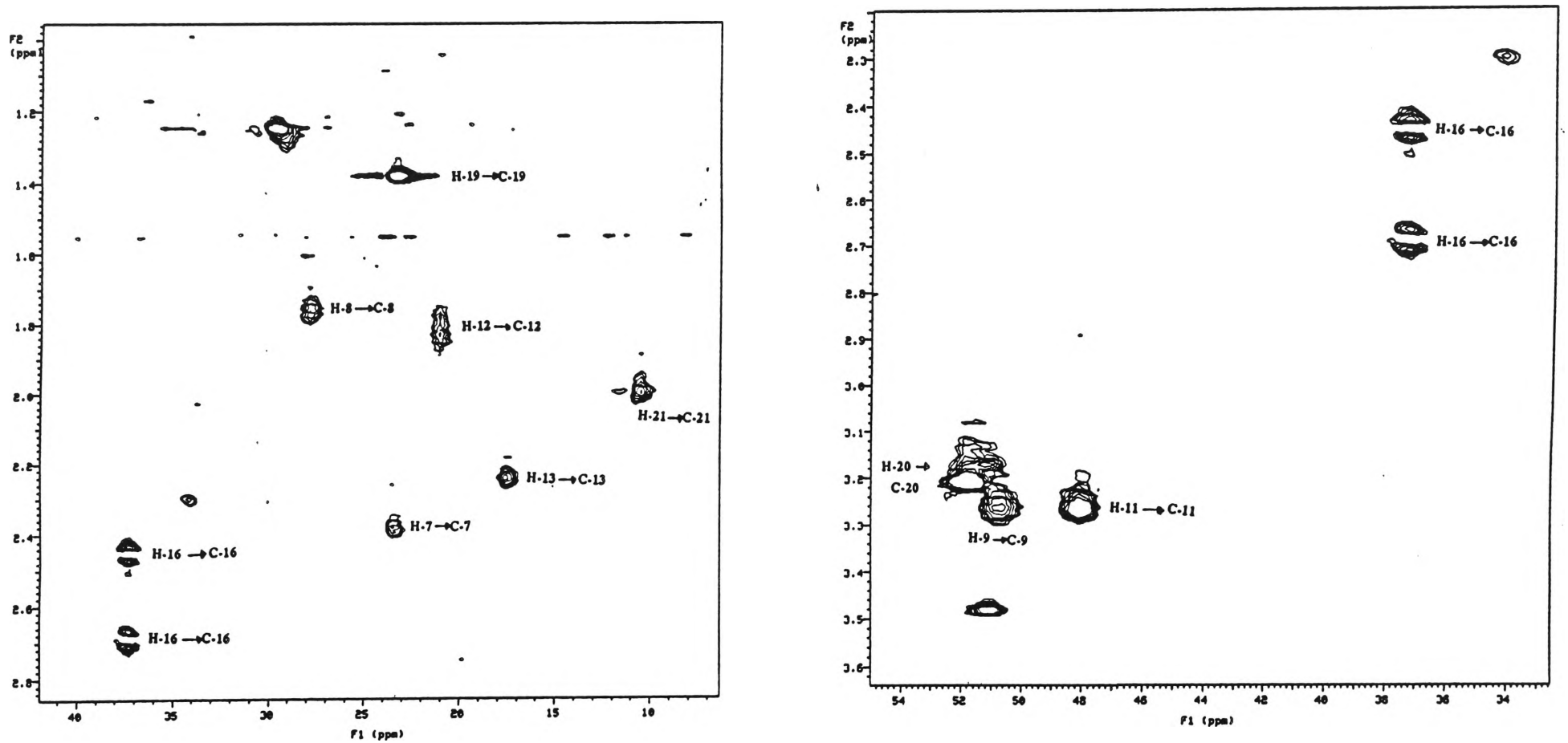

Figure 44. Expanded Regions of Inverse-Detection (^{1}H-^{13}C) Heteronuclear Multiple Quantum Coherence (HMQC) NMR Spectra of Pandamarilactone-31 [500 MHz, $CDCl_3$, referenced at δ7.25 (^{1}H) and δ77.0 (^{13}C)].

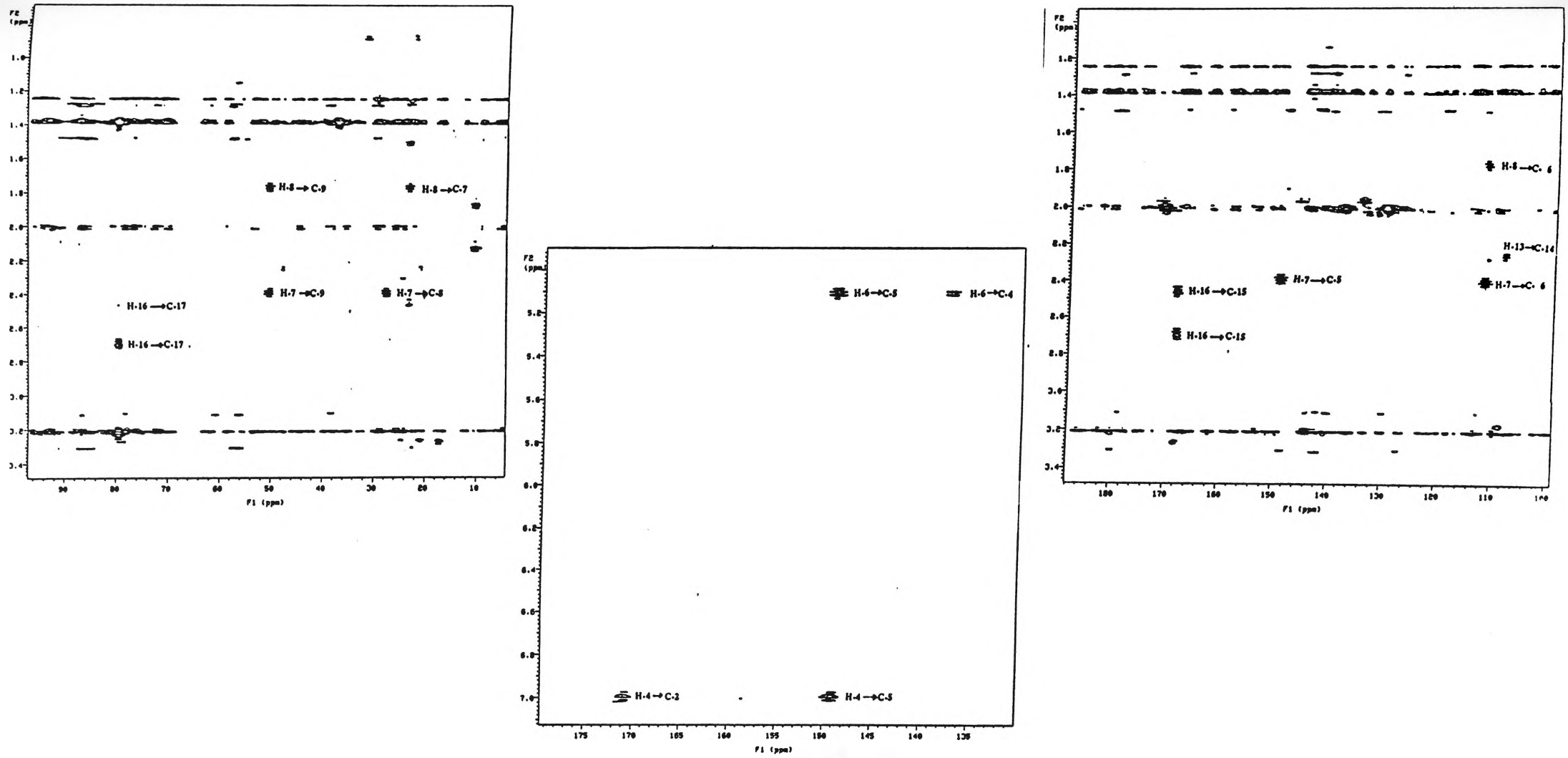

Figure 45. Expanded Regions of Inverse-Detection (^{1}H-^{13}C) Heteronuclear Multiple Bond Correlation (HMBC) NMR Spectra of Pandamarilactone-31 [500 MHz, $CDCl_3$, referenced at δ7.25 (^{1}H) and δ77.0 (^{13}C)].

The stereochemistry at C-4 and C-6 were identical to Pandamarilactone 32. The stereochemistry at C-17 was not defined as not enough sample was available to recrystallise the sample for X-ray analysis. Initially it was thought that Pandamarilactone-31 could possibly be an artifact. However this compound had not been in contact with methanol during the isolation process thus it is believed that it is a genuine natural product.

5.2.4 Pandamarilactone-2 (Pa-3A-2)

Pandamarilactone-2, labelled as Pa-3A-2, was initially purified by column chromatography but this was unsuccessful as no separation was obtained. Preparative TLC on silica developed in 10% EtOH in $CHCl_3$ provided the alkaloid although the appearance of another band at a lower Rf than Pa-3A-2 was always observed during the purification of this alkaloid particularly in silica. This band, which responded positively with Dragendorff reagent, was possibly a decomposition product of Pandamarilactone-2. A 2-D thin layer chromatography on silica showed that Pandamarilactone-2 was sensitive to acid and brokedown to a more polar structure. This was further substantiated by the addition of a dilute acid to Pandamarilactone-2 which completely converted Pa-3A-2 to the more polar decomposition product observed earlier in its tlc chromatogram.

Purification by column chromatography on alumina using hexane and $CHCl_3$ was attempted however, this also afforded Pandamarilactone-2 together with the decomposition product. Efforts to isolate pure Pandamarilactone-2 failed, hence the

structure elucidation of this alkaloid was carried out on an impure sample containing the more polar decomposition product.

The UV spectrum of the mixture showed absorption at 274 nm which was consistent with an α, β-unsaturated five-membered ring lactone with extended exocyclic double bond.[142] An absorption at 1764 cm^{-1} in the IR region conformed for an unsaturated five-ring system lactone.[145] LRFABMS gave a *m/z* of 315. However, the same compound after repurification by HPLC on a reversed phase system with elution in CH_3OH showed molecular ions at 317 and 345 by HREIMS. This clearly suggested that the compound was very unstable.

The ^1H NMR spectrum still showed the presence of olefinic protons at δ6.98 and δ5.10 while the ^{13}C spectrum showed the signals for the two carbonyl protons at δ171.0 and δ174.0. Working through the COSY, TOCSY, HMQC and HMBC NMR spectra provided fragment A as shown below.

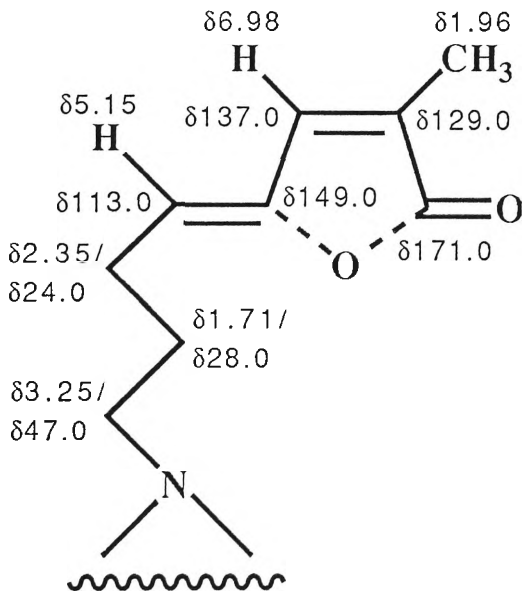

Fragment A

The second half of the molecule was found difficult to establish with some signals being inconsistent in both the HMQC and the HMBC spectra. This observation indicated that the sample may be decomposing during the acquisition of the two heteronuclear spectra. Because of this uncertainty, the structural elucidation of this compound was not continued however this preliminary investigation shows that it is related in structure to the other three alkaloids. Future work will be carried out to find a way to prevent the decomposition of the compound.

5.3. SUMMARY AND CONCLUSION

The leaves of *Pandanus amaryllifolius* which showed slight antibacterial activity against *Staphylococcus aureus* and *Bacillus subtilis* , afforded four alkaloids, three of which were established to have novel structures. Structural elucidation of the fourth alkaloid was not completed due to the instability of the alkaloid which made it difficult to characterise. The novel alkaloids, Pandamarilactone-1, Pandamarilactone-32 and Pandamarilactone-31, all contain a C_9-N-C_9 skeleton with at least a five-membered lactone ring in the molecule. Pandamarilactone-31 and -32 are closely related to each other with the only difference being at C-17 where Pandamarilactone-31 has a methoxy group and methyl group attached at C-17.

It is most likely that the five-membered lactone was derived from 4-hydroxy-4-methylglutamic acid which has been identified in some higher plants.[182-184] Other 4-substituted derivatives of glutamic acid such as 4-hydroxyglutamic, 4-methylglutamic, 4-methyleneglutamic, 4-ethylideneglutamic, 3-hydroxy-4-methylglutamic, and 3,4-dihydroxyglutamic acid have also been

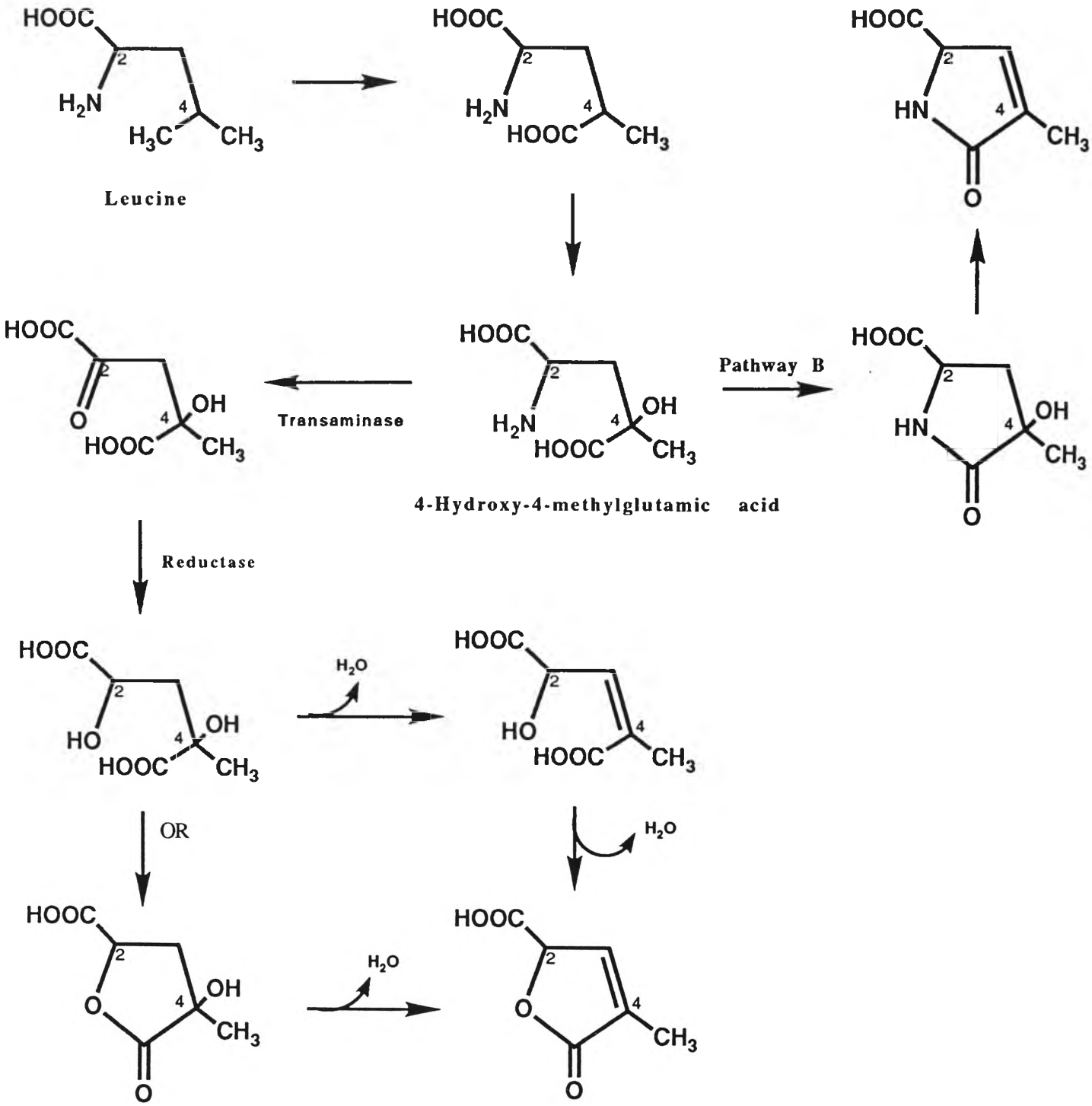

Scheme 19. Proposed Biosynthetic Pathway for the Conversion of Leucine to 2-Carboxylic acid-4-methyl-oxacyclopent-3-ene-5-one or 2-Carboxylic acid-4-methyl-azacyclopent-3-ene-5-one.

reported in higher plants.[185-190] A biosynthetic study conducted by Peterson and Fowden[191] revealed that leucine was the biogenetic origin of 4-methylglutamic acid which was then converted to 4-hydroxy-4-methylglutamic acid. This chemical could cyclise to the five-membered lactam (Pathway B) or via transamination which lead to the formation of a lactone (Scheme 19).

The carbon chain from C-6 to C-9 may possibly be derived from a unit of glutamic acid. Looking closely to the structures of the three novel *Pandanus* alkaloids, it is tempting to say that they are formed from two molecules of a condensation product of glutamic acid with 4-hydroxy-4-methylglutamic acid. It would be interesting to do the biosynthetic studies of these alkaloids to unambiguously established their biogenetic origin.

Future work to establish the absolute stereochemistry of Pandamarilactone-1 and Pandamarilactone-31 will be carried out by preparing synthetic compounds of these alkaloids and possible chemical interconversions between these novel *Pandanus* alkaloids.

It is intriguing to observed that Pandamarine, whose structure was elucidated using X-ray techniques, and Pandamarilactone-1 differ in structure only by the replacement of an NH by an O in the two heterocyclic rings. This is especially interesting since the extract from which Pandamarilactone-1 was isolated, was supposedly obtained from the same plant species collected at a different time and place. No pandamarine was observed in our experiments.

At present we are unable to rationalise these findings however, the pathways shown in Scheme 19 may provide a possible explanation. If indeed the same *Pandanus* species from which Pandamarine was isolated has been studied here then

environmentally-induced variability in transaminase activity could explain the difference in alkaloid profile (Scheme 19 Pathway B). Alternatively, a different species or subspecies may have been studied in the investigations reported here.

CHAPTER 6

BIOSYNTHESIS OF *IPOMOEA MURICATA* INDOLIZIDINE ALKALOIDS

6.1 INTRODUCTION

Indolizidine alkaloids comprise about 500 alkaloids and have as the characteristic feature a nitrogen atom which forms part of 2 or 3 different rings (Figure 46).[192] The indolizidines are distributed among the *Elaeocarpaceae*, *Orchidaceae*, *Lycopodiaceae*, and *Convolvulaceae* families.

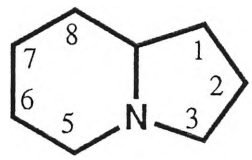

Figure 46. Indolizidine nucleus

Biosynthetic studies on indolizidine alkaloids have been carried out on the alkaloid tylophorine **105**.[193,194] Feeding experiments have established the possible origin of the phenanthroindolizidine alkaloids, with the amino acids, phenylalanine[195], tyrosine[196] and ornithine[195] found to be precursors (Scheme 20).

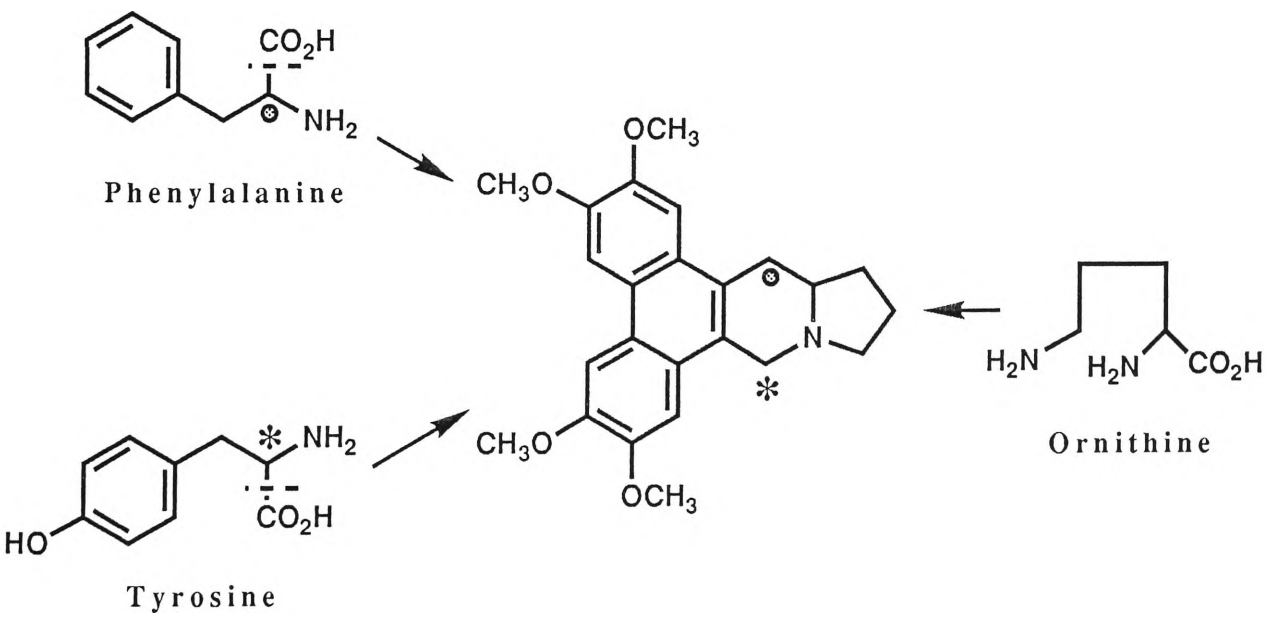

Tylophorine 105

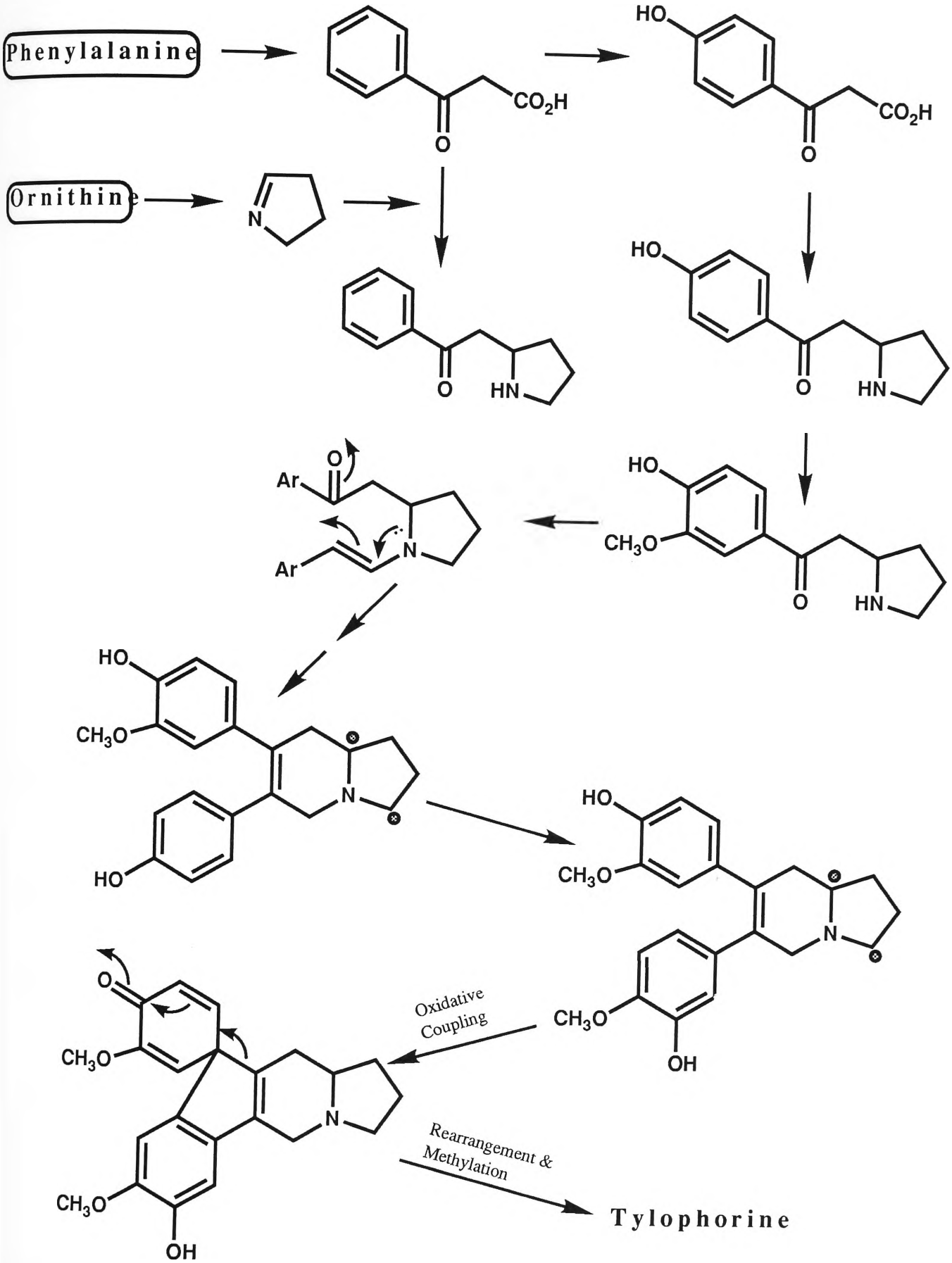

Scheme 20. Biosynthesis of Tylophorine **105.**

Toxic indolizidine alkaloids, swainsonine **106** and slafranine **107** isolated from *Rhizoctorius leguminicola* were found to be derived from L-lysine via L-pipecolinic acid (Scheme 21) with 1-oxoindolizidine as the branch point in the biosynthetic pathway to indolizidines.[197]

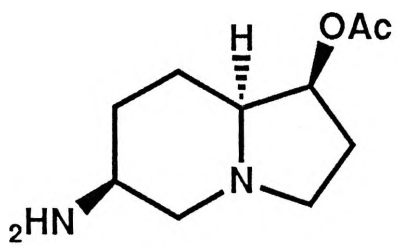

Slafranine 107

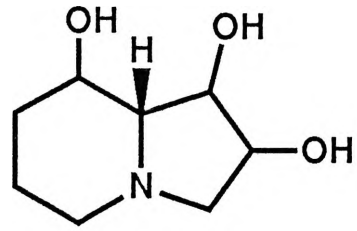

Swainsonine 106

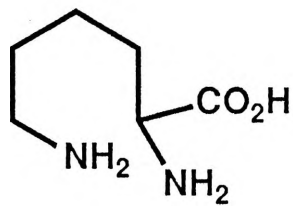

Lysine

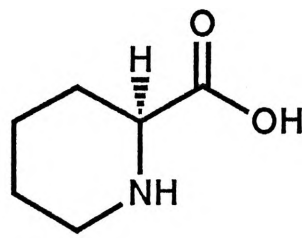

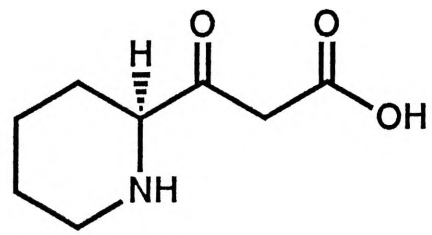

L-pipecolinic acid

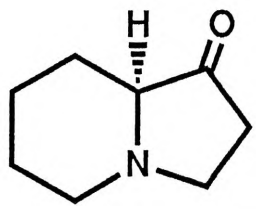

1-oxoindolizidine

Scheme 21. Biosynthesis of Indolizidine Alkaloids via Pipecolinic Acid.[197]

The genus *Ipomoea* of the family Convolvulaceae comprises 17 species. However, only three species, *Ipomoea alba*, *I. muricata* and *I. hardwickii*, have been reported to contain alkaloids. In 1969,

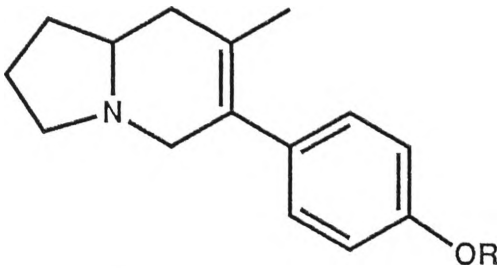

R	
H	Ipalbidine 108
β-D-Glucosyl	Ipalbine 109

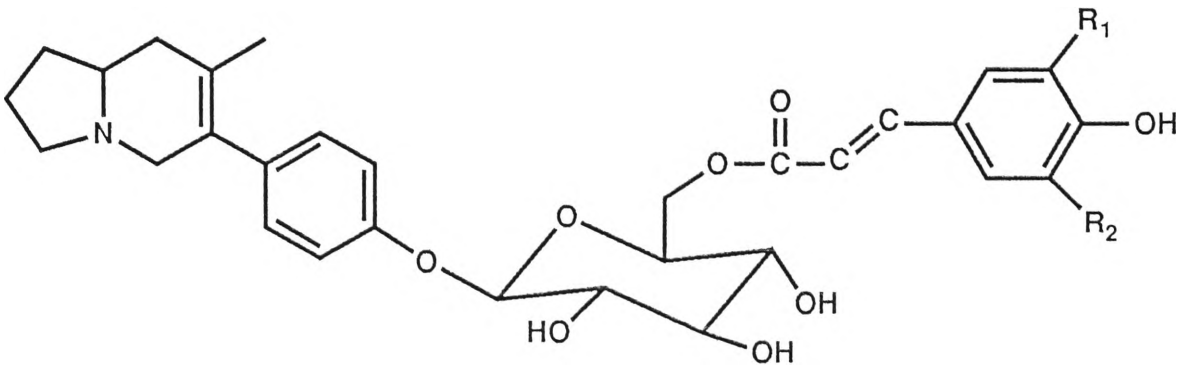

R_1	R_2	
H	H	Ipomine (E) 110
H	H	Isoipomine (Z) 111
H	OCH_3	Methoxyipomine 112
OCH_3	OCH_3	Dimethoxyipomine 113

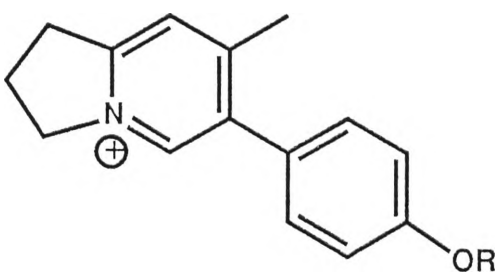

R	
H	Ipohardine (Ipalbinium) 114
β-D-glucosyl	Ipoharine 115

Gourley[198] isolated ipalbidine **108** from *I. alba*. This was the first reported instance of indolizidine alkaloids being present in the *Ipomoea* species. Other indolizidine alkaloids that were later isolated from other genera of *Ipomoea* include ipalbine[199] **109**, ipomine[199,200] **110**, isoipomine[199] **111**, methoxyipomine[199] **112** and dimethoxyipomine[199] **113**. From *I. hardwickii* the quaternary indolizidine alkaloids, ipohardine **114** and ipoharine **115** weres isolated by Liu *et al.*[201] Another water-soluble indolizidine alkaloid named ipalbinium[199,202] was recently isolated from *I. muricata*. Ipalbinium was later found to be identical to ipoharine.

The ipalbidine skeleton and other related *Ipomoea* alkaloids are novel since these are the only indolizidine alkaloids that occur in Nature which contain a methyl substituent on the indolizidine nucleus. This intriguing feature became a focal point of a number of biomimetic syntheses. Several synthetic approaches for the total synthesis of ipalbidine were carried out independently by different groups. [203-206]

Being structurally related to tylophorine, it was hypothesised that its biosynthetic pathway may take a similar course; that is, via the analogous pyrrolidine norhygrine (Scheme 22).

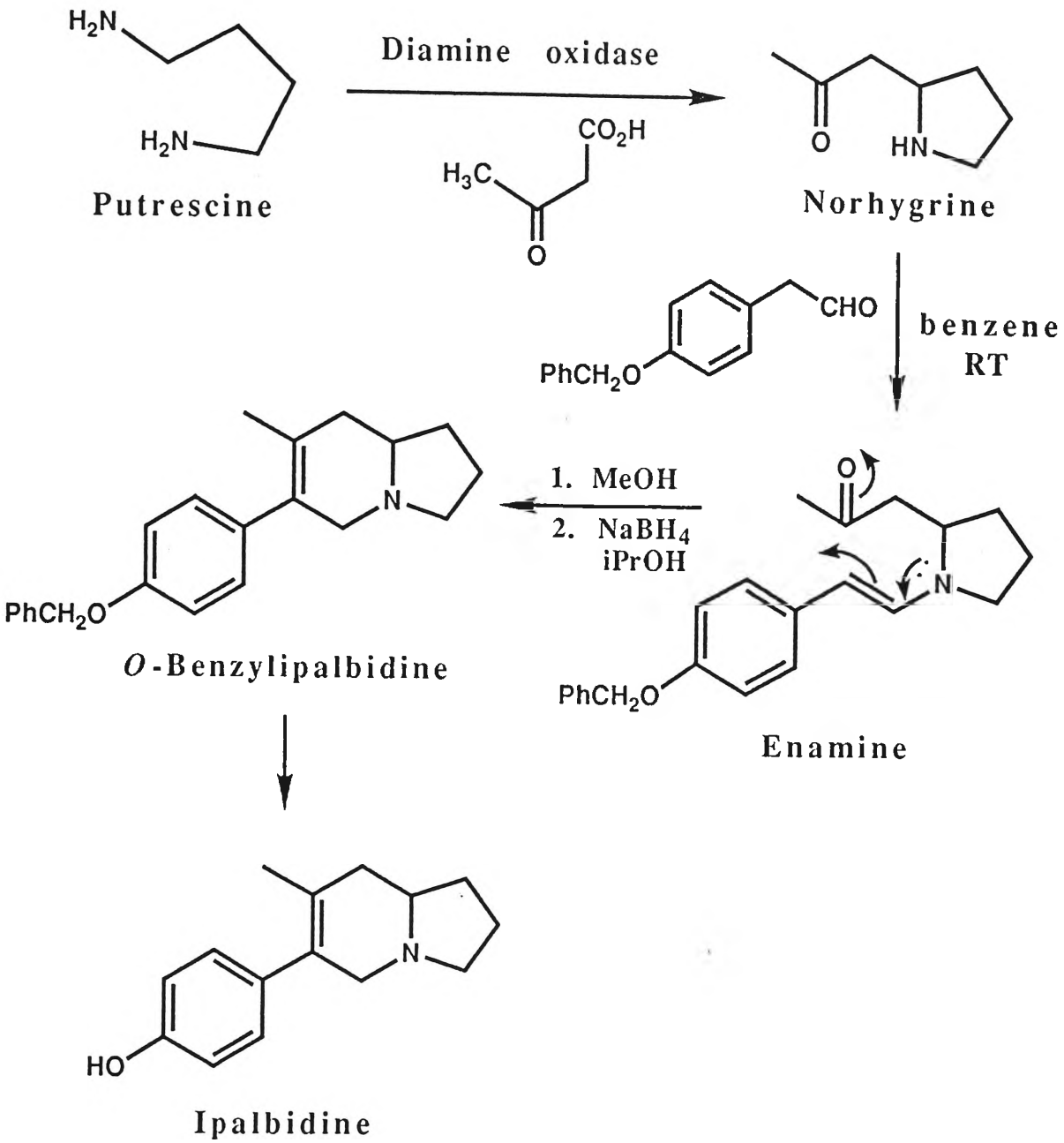

Scheme 22. Biogenetically Based Synthesis of Ipalbidine.[205]

In 1979, Hedges and Herbert[207] reported a biogenetically based synthesis of ipalbidine. In their work norhygrine was obtained by enzymic oxidation of putrescine in the presence of acetoacetic acid. Condensation of norhygrine with *p*-benzyloxyphenylacetaldehyde proceeded rapidly in benzene without a catalyst to give an enamine which underwent cyclisation and dehydration in methanol, most efficiently at reflux in dilute

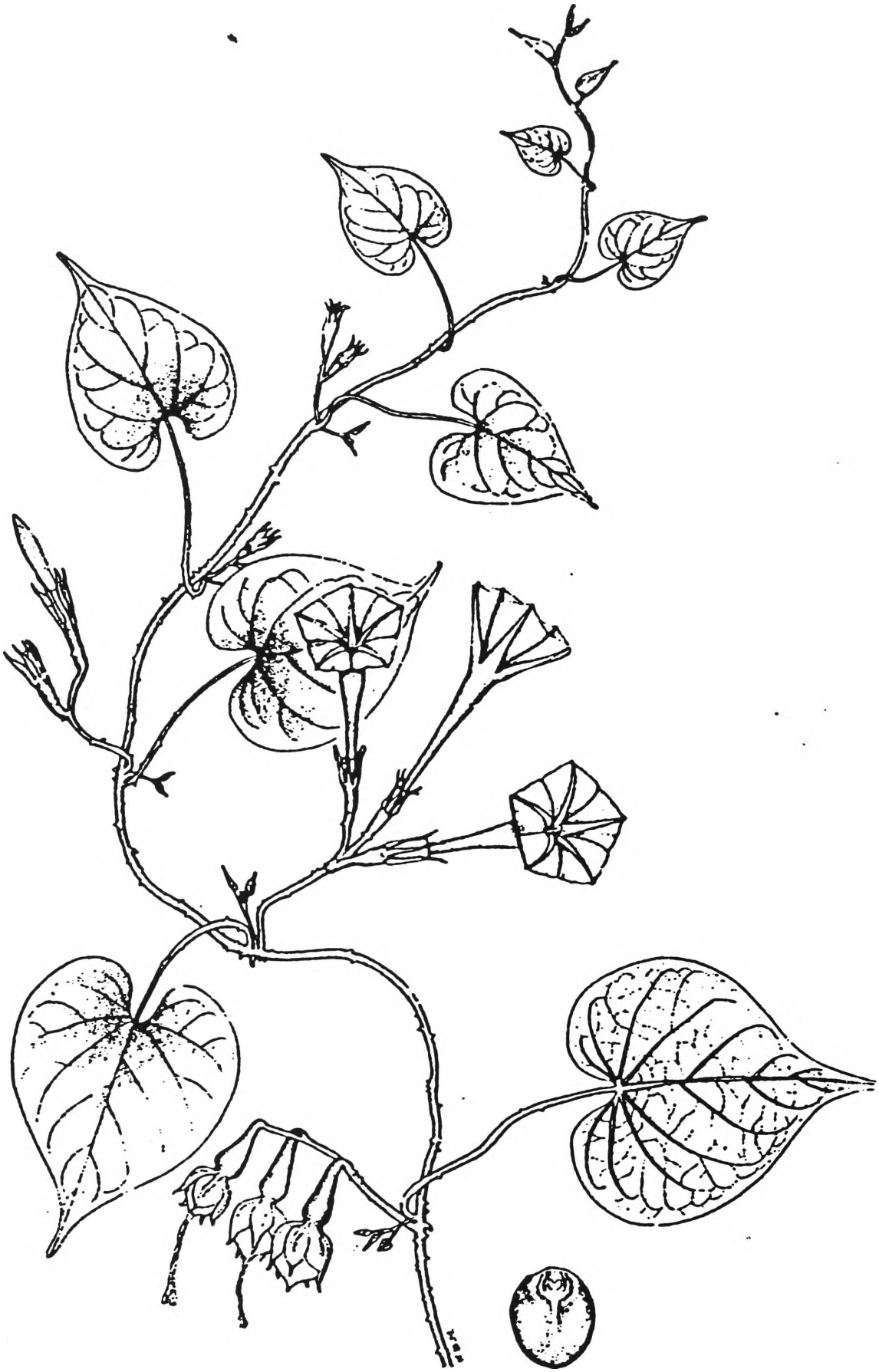

Figure 47. *Ipomoea muricata* (Convolvulaceae) Plant.

solution. Reduction gave *o*-benzylipalbidine and afforded ipalbidine after debenzylation.

So far, no feeding experiments of any labelled precursors on the intact plant of *I. muricata* have been reported in literature thus the work was carried out.

6.1.1 *Ipomoea muricata Jacq. (Linn.)*

Ipomoea muricata, locally known as tonkin, has been grown at the UST Botanic Garden since the late Fr. Lorenzo Rodriguez, became interested in the reputed medicinal properties of the seed and the leaves.

The plant was identified as *Calonyction muricatum*, Linn by Hermes Gutierrez, then curator of the Philippine National Museum, Botany Division. Its identity was verified at the Rijksherbarium in Leiden, Netherlands.

The tonkin plant grown in the UST Botanic Garden is an herbaceous, twining vine which can grow several meters high when trellises are used for support. The stems with small prickles are rough. The leaves are smooth, soft, entire, cordate-ovate with the apex tapering into a short candex. The bright green palmately net-veined blades are 4-9 cm wide and 6-10 long while the petioles reach up to 10 cm in length. The pink-purple tubular flowers are axilliary and are borne singly or in small clusters held by short peduncles. The fruits with brown papery pericarps are rounded and 0.8-1.5 cm diameter. The capsules contain 2-4 whitish-beige glabrous seeds (Figure 47).[208]

6.2 RESULTS AND DISCUSSION

Biosynthestic studies on intact plants are often difficult to perform. Researchers are usually faced with several problems such as a) cultivation and maintenance of the experimental plant, b) determination of the appropriate time of precursor feeding, c) the most efficient method of incorporation, d) the choice of isotopic labelling, and e) tracking the likely precursors through to the metabolites of interest.

One of the first problems encountered in this work was the cultivation of a tropical species for use in the biosynthetic work. Attempts to grow *I. muricata* for example in a completely different environment from its natural habitat was quite a challenge. Being a tropical plant, cultivation caused many difficulties. Eventually, conditions that simulated the natural growing environment were found. *I. muricata* was found to grow best in a temperature-controlled environment. The glasshouse was set at a temperature of 25°C with a continuous watering system during the early stage up to about one month old. A slow release fertiliser was utilised to provide sufficient nutrients for the plants which were grown in pots.

Previous studies had shown that the seeds of *I. muricata* plant had the highest percentage of alkaloid, hence work on incorporation of precursors was confined to the seeds. An appropriate time of feeding of precursors into the seed capsule of the plant was one factor that was considered to ensure efficient uptake of labelled compounds by the plant. A simple experiment based on that employed by Clarke and Hawkins[209], with a little modification was used to determine the approximate time of formation of the alkaloids in the seeds. Flowering of the plant was observed after 3

Table 22. Level of ^{14}C Radioactivity in Different Solvent Extracts of *I.muricata* seeds ([2-^{14}C]acetate).

Extract/Isolate	weight, mg	μCi/mg[1]	% Incorporation
EtOH extract	2050	3.55×10^{-3}	18.31
EtOEt extract	901	2.26×10^{-3}	5.13
EtOAc extract	59	5.39×10^{-3}	0.80

[1]Background corrected. Average of three readings.

Table 23. Radioactivity Counting of the [2-^{14}C]Acetate Labelled Alkaloids.

Alkaloid	DPM/mg[a]	Specific Activity (μCi/mmole)	% Incorporation	Dilution Factor μCi/mmol
Ipalbidine[b]	1453.1	0.15	9.0×10^{-3}	710.1
Ipalbidine[c]	1525.7	0.16	3.3×10^{-3}	675.0
Ipomine[d]	1239.0	0.30	8.6×10^{-3}	360.0
Ipomine[e]	1982.0	0.46	6.5×10^{-3}	234.8

[a]Average of three readings with background correction.

[b]5.4 mg obtained after PTLC, SGF_{254}, $CHCl_3$:CH_3OH 70:30

[c]1.9 mg obtained after purification by CC, Silica, $CHCl_3$:CH_3OH:NH_3 36:6:0.5.

[d]6.2 mg obtained after PTLC, SGF_{254}, $CHCl_3$:CH_3OH 70:30.

[e]3.0 mg obtained after purification by CC, Silica, $CHCl_3$:CH_3OH:NH_3 36:6:0.5.

months, after which the seed capsules started to form. One week and two week-old seed capsules were collected and extracted through an alumina column with a mixture of EtOH:H_2O:HOAc (90:9:1). TLC and visualisation with Dragendorff reagent revealed that a one week-old seed capsule contained trace levels of the alkaloids. A darker orange colour with Dragendorff reagent was observed for the two week old seed capsules.

The appropriate method of incorporation was another factor that was considered in this biosynthetic studies. Herbert[210] has described a variety of methods appropriate for feeding precursors to intact plants. Among them are: (a) the wick method whereby a wick is threaded through the lower part of the plant stem and dipped into an aqueous solution of the precursor, (b) assimilation through the roots by standing the plant in an aqueous solution of the precursor, (c) injection into a hollow stem or seed capsule, and (d) standing excised parts of the plant in an aqueous solution of the precursor. The third method (injection into the seed capsule) was preferred over the others mainly because it seemed more appropriate in our studies since it allowed incorporation experiment to be performed over a long time period and was easier to carry out.

6.2.1 Incorporation of [2-^{14}C]Acetate

In the biomimetic studies conducted by Herbert and Hedges, acetoacetic acid was utilised as the source of the methyl substituent of the indolizidine nucleus. Based on this *in vitro* results, it is most likely that the methyl substituent of the *Ipomoea* indolizidine alkaloids was derived from an acetate unit. The [2-^{14}C]acetate

precursor was expected to be incorporated on the sites marked on the structures below.

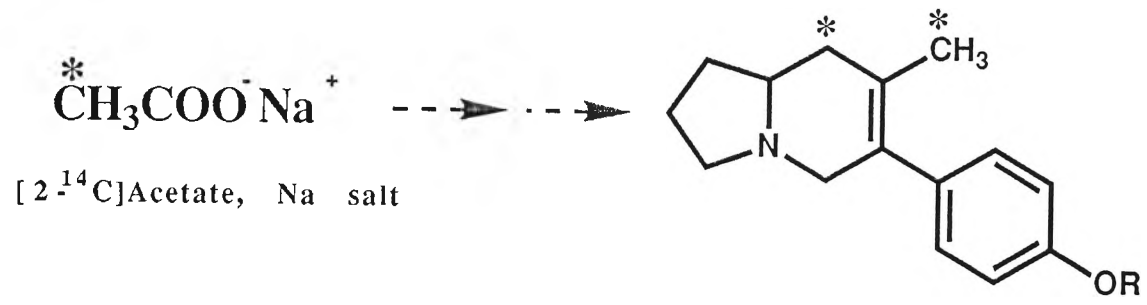

4.0 μCi per seed capsule of [2-^{14}C]acetate was injected into one to two-week old seed capsule and the plants grown for a further 3-4 weeks. The acetate labelled seeds (16.0 g) were subjected to the sequential solvent fractionation methods for the isolation of alkaloids. The alcohol extract (2.05 g), the yellow oily diethyl ether fraction (0.90 g) and the ethyl acetate fraction (0.06 g) were all assessed for their ^{14}C radioactivity. The results as shown in Table 22 revealed that radioactivity was distributed among the different extracts. The observed distribution of ^{14}C radioactivity was not unexpected since acetate is a known precursor of many secondary metabolites other than alkaloids. A relatively high level of incorporation was observed for the diethyl ether fraction implying efficient utilisation of the acetate precursor for the formation of other secondary metabolites and lipids in the plant.

Ipalbidine and ipomine were isolated from the EtOAc fraction. Attempts were made to purify the alkaloids by column chromatography until they appeared radiochemically pure however, insufficient amounts of the isolated alkaloids were available for recrystallisation to constant specific activity. Table 23 presents the level of ^{14}C incorporation of the acetate labelled precursor into the isolated alkaloids.

The results show a low level of incorporation of the ^{14}C acetate into the alkaloid. It was initially planned to do degradation of these isolated labelled alkaloids to established the position of the labelled sites. Kuhn-Roth degradation[199] will give the labelled acetic acid which will be characterised and counted as its *p*-bromophenacylester (Scheme 23). However due to unavailability of enough material, degradation of the labelled alkaloids were not carried out.

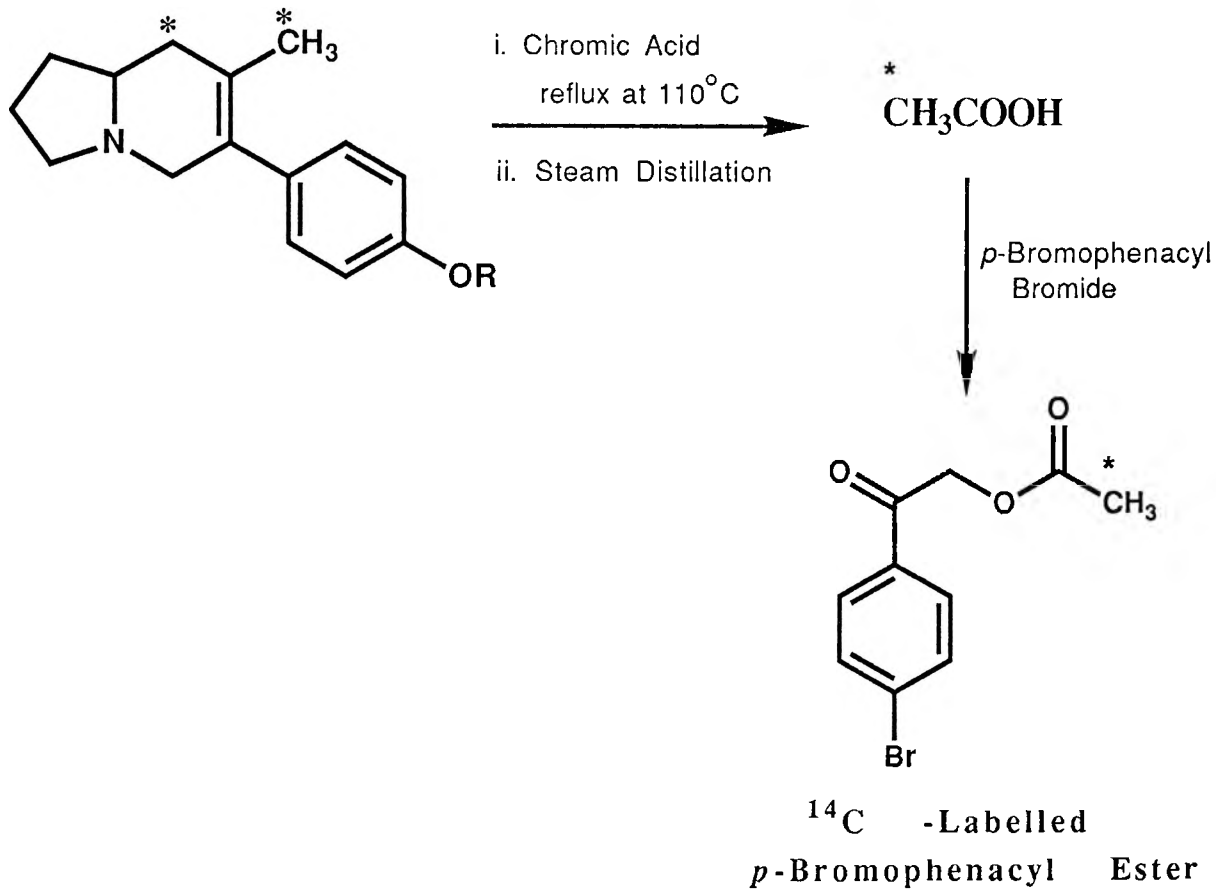

Scheme 23. Proposed Kuhn-Roth Degradation of Labelled Alkaloids.

Based on the biomimetic synthesis of ipalbidine by Hedges and Herbert[195], the precursor may be incorporated into the alkaloids by the route shown in Scheme 24.

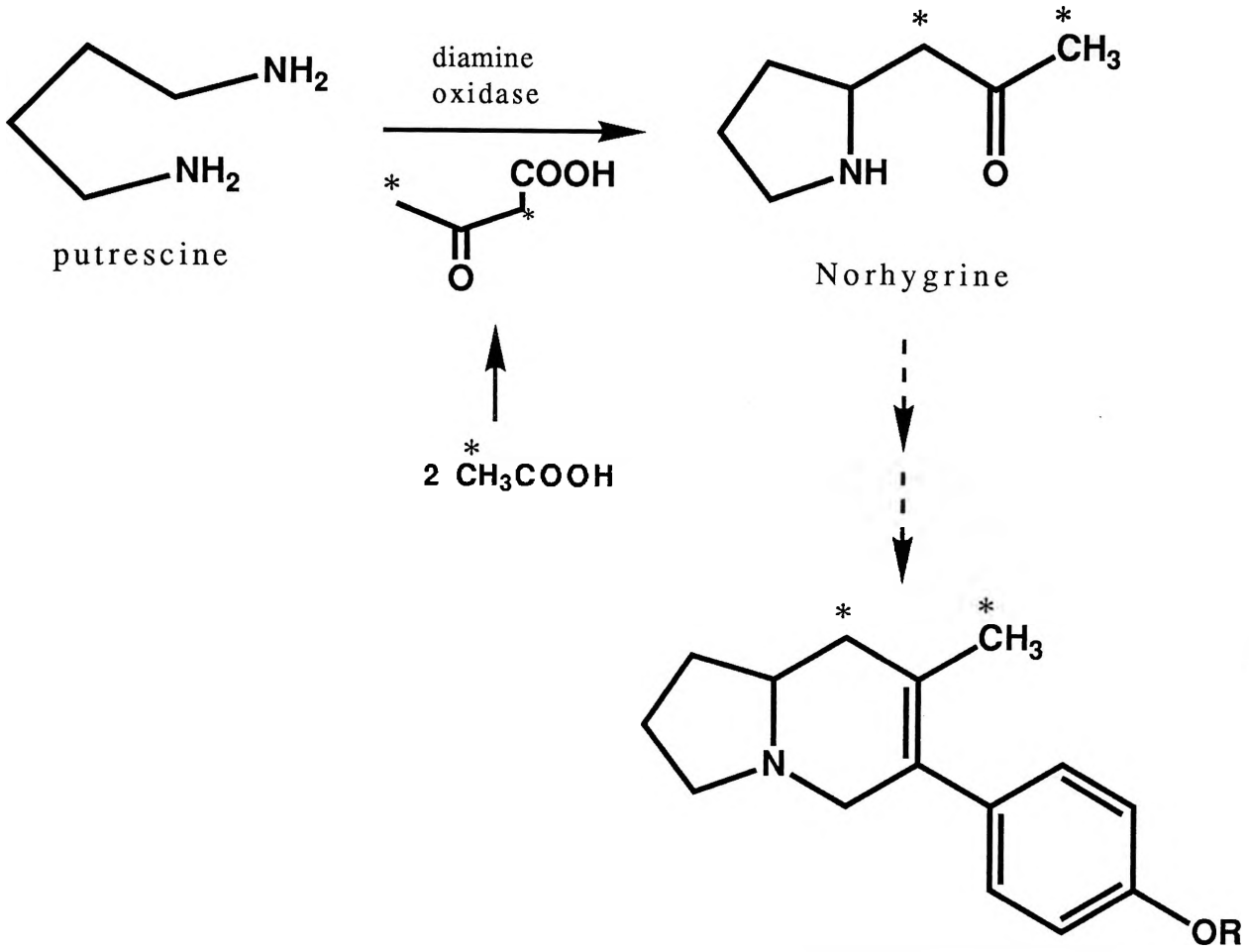

Scheme 24. Possible Biosynthetic Fate of Acetate in the Indolizidine alkaloid.

6.2.2 Incorporation of [U-^{14}C]Tyrosine

Seeds were labelled as described in the previous section except that 2.2 μCi was administered to each of 67 seed capsules and plants grown for a further 3-4 weeks. The tyrosine labelled seeds (20.36 gms) yielded 1.64 g of crude alcoholic extract. Upon fractionation, the alcohol extract gave a yellow oily EtOEt fraction (1.12 g.) and the $CHCl_3$ soluble fraction (46.6 mg). The different fractions were assessed for their content of ^{14}C radioactivity. Table 24 shows the radioactivity present in the different extracts.

A higher % incorporation level was observed for the diethyl ether fraction compared with the $CHCl_3$ fraction indicating efficient incorporation of tyrosine into other compounds. The alkaloids,

Table 24. Level of ^{14}C Radioactivity in the Different Solvent Extracts of *I. muricata* seeds Labelled with [U-^{14}C]Tyrosine.

Extract/Isolate	Weight, mg	μCi/mg[a]	% Incorporation
Alcohol extract	1640	3.60 x 10-4	0.38
EtOEt extract	1120	2.53 x 10-4	0.19
$CHCl_3$ extract	46.6	1.24 x 10^{-3}	0.04

[a]Average of three readings with background correction.

Table 25. Incorporation of the [U-^{14}C]Tyrosine into Ipalbidine and Ipomine.

Alkaloid	wt, mg	DPM/mg[a]	Specific Activity (μCi/mmole)	% Incorporation	Dilution Factor μCi/mmol
Ipalbidine					
1st[b]	3.45	7369.0	0.77	7.8 x 10^{-3}	631.2
2nd[b]	1.36	13750.5	1.42	5.7 x 10^{-3}	342.2
3rd[b]	1.16	13407.7	1.38	4.7 x 10^{-3}	352.2
Ipomine					
1st[b]	2.02	6484.5	1.56	4.0 x 10^{-3}	311.5
2nd[b]	1.41	11264.1	2.72	4.8 x 10^{-3}	178.7
3rd[b]	0.40	7133.6	2.57	1.3 x 10^{-3}	189.1

[a]Average of three readings with background correction.

[b]Purified by CC, Silica, $CHCl_3$:CH_3OH (36:6:0.5).

ipalbidine and ipomine were purified by column chromatography to constant specific activity. Table 25 presents the incorporation of the tyrosine labelled precursor into the alkaloids.

The results show that incorporation of the tyrosine precursor was observed but that the % incorporation was low. Interestingly, ipalbidine was found to have a three fold higher incorporation of label than ipomine.

Values between successive recrystallisation differ by less than 4% and 7% respectively, indicating that constant specific activity had not quite been achieved. Had sufficient material been available for recrystallisation, then most likely constant specific activity could have been demonstrated. It was clear by TLC that the isolated compounds were chemically pure.

Thus, both acetate and tyrosine appear to be incorporated into the alkaloids ipalbidine and ipomine. The low incorporation may result from several possibilities. One is that neither acetate nor tyrosine are precursors for indolizidine alkaloid biosynthesis. A more likely reason is that the rate of uptake of the precursors may be slow and that there may be too much dilution and removal of the label which was applied initially to the seed capsule. Other competing metabolic pathways e.g. for lipid biosynthesis ([2-^{14}C]acetate) and protein biosynthesis ([U-^{14}C]tyrosine) may also act to diminish the amount of radiolabel available for incorporation into the alkaloids.

These results are preliminary and indicate that further studies on the biosynthesis of *Ipomoea* indolizidine alkaloids are required. It is recommended that in future, studies be performed on the mode and rate of incorporation, and that the collection of sufficient seed materials be undertaken to allow for chemical

degradation of the labelled metabolites. Other worthwhile experiments would involve synthesis of labelled precursors which are thought to be intermediates in the indolizidine biosynthetic pathway. Labelled norhygrine could be easily synthesised by the reaction of putrescine and labelled acetoacetic acid (C-2 and C-4) with diamine oxidase. This labelled precursor could then be incorporated into the plant. The biosynthesis of secondary metabolites is increasingly being followed by use of stable isotopes such as ^{13}C and ^{2}H as precursors. Analysis can then be done either by the use of sophisticated NMR techniques or mass spectrometry. Although these methods of analysis are much less sensitive than those of radioactive isotopic labels like ^{14}C and ^{3}H, they have the advantage of yielding structural information much more rapidly than radioactive ones. However, a high enrichment is necessary and more precursors need to be fed to the plant.

CHAPTER 7

EXPERIMENTAL

7.1 General Procedures

7.1.1 Solvents

All solvents used were either Analytical Grade or HPLC Grade unless otherwise stated.

7.1.2 Chromatography

a) Column Chromatography

Flash chromatography and gravity column chromatography were carried out using silica gel 60 (Merck 7730 or 773) or 60 G (Merck 7734, 0.063-0.200 mm particle size). Elution was done by step gradient elution using solvent mixtures of increasing polarity. All eluates were monitored by thin layer chromatography (TLC).

b) Thin Layer Chromatography/Preparative TLC

Thin layer chromatography was carried out using aluminium-backed silica gel plates with indicator at 254 nm (Merck 5554) Plates were visualised initially under ultraviolet light (λ 254 nm) and then sprayed with Dragendorff spray reagent.

Preparative thin layer chromatography (PTLC) was done on 2 mm thickness silica gel F_{254} glass plates (Merck 7731). Similar methods of visualisation as for TLC was performed.

c) High Pressure Liquid Chromatography

High Pressure Liquid Chromatography was performed using Waters Associates Model M-45 solvent delivery system connected to U6K injector. Waters Model 450 Variable Wavelength detector set at 254 nm or Waters R403 Refractive Index detector were utilised. Normal phase separation was done on silica semipreparative column while reversed phase was done on either C18 semipreparative column or Radial-Pak column (8 x 100 mm).

7.1.3. Melting Points

Melting points were measured using a Koffler Hotstage apparatus and are uncorrected.

7.1.4 Optical Rotations

Optical Rotations were measured on either Bendix NPL-Automatic Polarimeter for solution in $CHCl_3$ (Chapter 2), Perkin Elmer 141 Polarimeter for solutions in $CHCl_3$ (Chapter 4), or Jasco DIP 370 for solutions in CH_3OH (Chapters 2 and 5).

7.1.5 Ultraviolet (UV) Spectra

UV spectra were recorded on Shimadzu UV-265 Recording Spectrophotometer for solutions in CH_3OH or EtOH.

7.1.6 Circular Dichroism

Circular dichroism measurements were performed on a Jasco Model 500-C Polarimeter for solutions in CH_3OH carried out either at Macquarie University or at Sydney University.

7.1.7 Infrared (IR) Spectra

IR spectra were recorded on Perkin Elmer 783 Infrared Spectrophotometer for $CHCl_3$ film on KBr discs.

7.1.8 Mass Spectra (MS)

Low resolution electron impact, chemical ionisation and FAB (Fast Atom Bombardment) mass spectrometry were carried out on a VG Micromass 12-12 at 70eV. (University of Wollongong)

High Resolution Electron Impact mass spectrometry was carried out on a V.G. Micromass 7070F at 70eV at the Australian National University Research School of Chemistry.

7.1.9 ^{1}H and ^{13}C Nuclear Magnetic Resonance (NMR) Spectra

^{1}H or ^{13}C NMR spectra were either recorded using Varian Unity 400 and 500 MHz spectrometers, Bruker AMX 500 MHz spectrometer or Jeol JNM GX-400 MHz spectrometer. These spectra were acquired in one of the following solvents: deuteriochloroform ($CDCl_3$, δ7.25 (^{1}H) and δ77.0 (^{13}C), deuterated methanol (CD_3OD, δ3.35 (^{1}H) and δ49.0 (^{13}C), Deuterated dimethylsulfoxide (DMSO-d_6, with TMS as internal standard, δ0.0) and Deuterium Oxide (D_2O with TSP as internal standard, δ0.0). Signals multiplicity were assigned as **s** (singlet), **d** (doublet), **t** (triplet), **q** (quartet), **m** (multiplet), **d d d** (doublet of doublet of doublet), **td** (triplet of doublet) and **b** (broad) with their coupling constants (J) measured in Hertz.

7.2 Experimental Section for Chapter 2

7.2.1 NMR Spectroscopy

NMR spectra were acquired on Jeol JNM GX-400 or a Varian Unity 400 spectrometers operating at 400 MHz for protons. For the Varian spectrometer, a dedicated $^{1}H/^{19}F$ Varian probe fitted with a deuterium lock and Varian temperature control was used. Acquisition and processing were under the control of Varian's VNMR software, version 3.2. All spectra were recorded in CD_3OD at 25°C. Chemical shifts are reported in ppm with reference relative to the residual methyl signal as internal standard at 3.35 ppm.

7.2.1.1 2D NMR Experiments

Absolute Value COSY. The COSY spectrum was performed using the pulse sequence described by Bax *et al.*[98] A total of 512 blocks of 2048 data points were collected with 16 scans per block. The data matrix was 'zero-filled' once in t_1 to obtain a 1024 x 2048 matrix prior to Fourier transformation.

Relay and Double Relay COSY. The Relay and Double Relay COSY experiments were carried out using the pulse sequence described by Wagner.[102] The fixed duration delay between the 90° pulses in the mixing step of the pulse sequence (τ_m) was set at 30 ms. Other acquisition parameters were as for the COSY spectra.

Phase Sensitive Double- and Triple-Quantum Filtered COSY. The phase sensitive double- and triple-quantum filtered COSY spectra were performed using the pulse sequence described by Piatini *et al*[100] and Rance *et al.*[101] A total of 512 blocks containing 2048 data points were collected. The data were zero-filled to 1024

points in t_1 dimension and Gaussian window functions were applied to both dimensions prior to Fourier transformation.

Total Correlation Spectroscopy. The TOCSY experiment, also known as the Homonuclear Hartmann-Hahn (HOHAHA) experiment was performed using the pulse sequence described by Bax[104] and was acquired in the phase sensitive mode. A total of 64 scans were collected for each of 512 FIDs. The mixing time was set at 80ms. The data were zero filled as above and multiplied in both dimensions by Gaussian window functions prior to Fourier transformation.

2-D Nuclear Overhauser Effect (NOESY) and Rotating-Frame NOE (ROESY) Spectroscopy. The NOESY experiment was carried out in the phase sensitive manner as described by States et al[105] while the ROESY experiment was performed following the pulse sequence described by Kessler.[212] Both experiments were performed with a mixing time of 250 ms and the relaxation delay was set at 1.5 s. A total of 512 x 2048 blocks with 32 scan per block were collected. The data were zero filled and processed as described above

7.2.2 MS analysis by Smith-Kline Beecham Pharmaceutical groups for Oa-4A-1, Oa-4A-2, Oa-4A-1-Me and Oa-WS-Me-1.

A mass spectrometer study performed on Oa-4A-1 and Oa-4A-2 was carried out using MS/MS technique using a mixture of thioglycerol and MNBA (3-nitroglycerol). Accurate mass measurements were done by HRFABMS using peak matching and voltage scanning. Average results were obtained to get the *m/z* for each compounds. The fragment ions were measured by

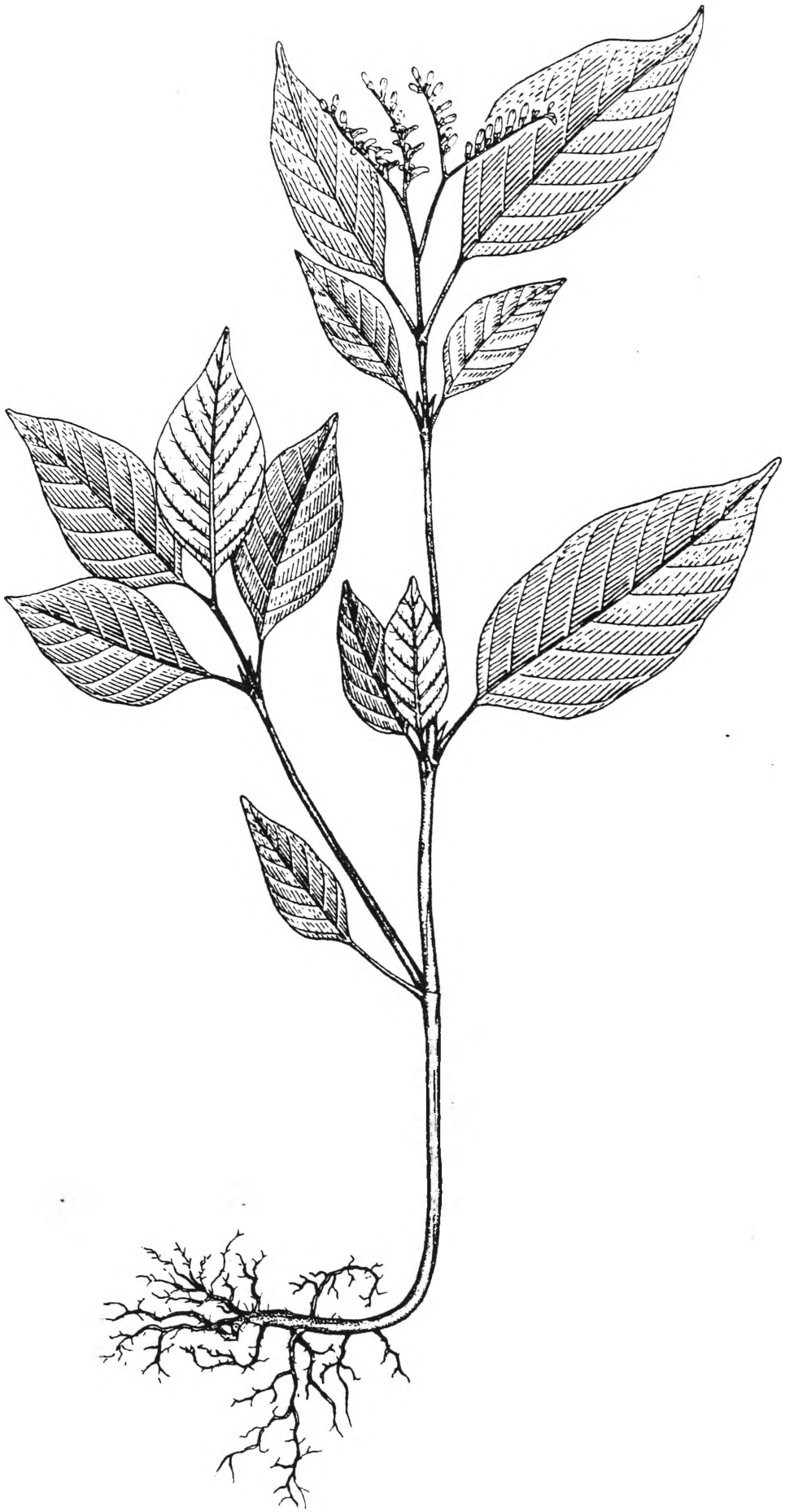

Figure 48. *Ophiorrhiza acuminata (Rubiaceae)* Plant.

scanning HRDCIMS using a novel method of mixed reagent gases (NH_3/CH_4).

MS/MS and HRFABMS (M/ΔM 10,000) data were obtained on a VG ZAB-SE4F tandem double focusing mass spectrometer equipped with a standard FAB source and Cs Ion gun. Scanning HRDCIMS (M/ΔM 5,000) and LR NH_3-DCIMS spectra were obtained on a VG 70-VSE mass spectrometer equipped with a standard EI/CI source modified for introduction of a second reagent gas. LRFAB spectra were acquired on a VG ZAB-HF mass spectrometer equipped with either a standard FAB source or a standard continuous flow FAB source operated in the normal FAB mode; the FAB beam was produced with a standard Ion Tech gun using xenon as the gas.

LRFAB mass spectra were acquired on a VG ZAB-HF mass spectrometer equipped with either a standard FAB source or a standard continuous flow FAB source operated in the normal FAB mode; the FAB beam was produced with a standard Ion Tech gun using xenon as the gas.

7.2.3 Plant Description

O. acuminata, locally known as Payang-payang-gubat (Tagalog) or mongoose plant (English) is found from the Bataan and Babuyan Islands and northern Luzon to Palawan and Mindanao, in thickets and forests at low altitudes. It also occurs in India and Malaysia.

The plant (Figure 48) is described as a a half-wooden, erect, smooth plant up to 30 centimeters in height. The leaves are very thin, elliptic or elliptic-lanceolate, 4 to 12 centimeters long, 2 to 6 centimeters wide, and pointed at both ends. The cymes are flat-topped, 2 to 7.5 centimeters in diameter, and smooth or hairy; their

branches are subumbellate and very spreading. The calyx-teeth are very short. The corolla is white and smooth, with very short, obtuse lobes which are keeled at the back. The pedicelled capsules are 2 to 5 millimeters in diameter. The seeds are many, minute and angled.

7.2.4 Extraction of the Alkaloids from *Ophiorrhiza acuminata*

Ground leaves of *Ophiorrhiza acuminata* (149.9 g) were extracted exhaustively with 95% EtOH (1.8 l). The alcoholic extract on concentration in vacuo yielded a greenish resinous material, 11.9 g (8.0%). Preliminary group separation was done by sequential extraction of the alcoholic extract with hexane and chloroform. On concentration the hexane soluble fraction gave an oily layer, 0.23 g (1.9%), and a green resinous chloroform layer, 3.2 g (26.9%). The remaining alcohol soluble fraction (63.4%) was further subjected to group separation. Partition between diethyl ether and 1% sulfuric acid separated the nitrogenous compounds from the other secondary metabolites such as the steroids, terpenoids, etc. The acid layer was basified to pH 9-10 to convert the nitrogenous compounds into free amines and was subsequently extracted with chloroform. The aqueous basic layer was brought back to neutral pH by slowly pumping off excess ammonia under vacuum

7.2.4.1 Purification of Oa-3A

Fractionation of the $CHCl_3$ layer, 0.6100 g. was carried out by column chromatography eluting the major alkaloid in chloroform with increasing methanol concentration. A yellow powder, 74.27 mg, was obtained which on purification twice by PTLC on silica in 10% CH_3OH in $CHCl_3$ (R_f = 0.34) afforded a pale yellow

amorphous solid, 17.96 mg. Final purification was achieved by HPLC on a normal phase μ-porasil column eluting with 10% EtOAc in $CHCl_3$ at 1.0 ml/min. with refractive index detection. The tertiary alkaloid, labelled Oa-3A, was obtained with retention time of 6.8 min.

The ^1H NMR spectrum showed traces of impurities, hence it was further purified by reversed-phase HPLC. The alkaloid was eluted isocratically with CH_3OH at 1.0 ml/min, yielding a light yellow amorphous solid, 5.42 mg. Oa-3A showed a single spot on tlc on silica SGF_{254} developed in 10% MeOH/$CHCl_3$ (Rf = 0.34) and fluoresced (blue) under both short (254 nm) and long (365 nm) wave UV light.

7.2.4.2 Spectroscopic Data of Oa-3A

UV(CH_3OH): λ_{max}348.4 (Σ84.94), 335.2 (Σ84.27), 287.6 (Σ285.39), 235.6 (Σ529.44), 217 0(Σ354.61), 208.2 (Σ349.89) nm.

HREIMS: 182.08290, $C_{12}H_{10}N_2$

^1H NMR (Bruker 400 MHz, $CDCl_3$): δ 8.65 (br s, 1H, NH, D_2O exchangeable), 8.36 (d, J 5.3Hz, 1H, H-5), 8.12 (d, J 8.0Hz, 1H, H-9), 7.76 (d, J 5.3Hz, 1 H H-6), 7.56-7.54 (d on top of another d (m), 2H, H-11, -12), 7.31 (ddd, J 8.0, 5.6, 2.3Hz, 1H, H-10), 2.83 (s, 3 H, CH_3).

^{13}C NMR (Bruker 100.6 MHz, $CDCl_3$): δ141.7 (C-3), 140.0 (C-13), 138.8 (C-5), 134.5 (C-2), 128.3 (C-11), 128.2 (C-7), 122.1 (C-9), 121.8 (C-8), 120.2 (C-10), 112.9 (C-6), 111.5 (C-12) and 21.2 (CH_3) ppm.

7.2.5 Isolation and Purification of the Water-Soluble Alkaloids

Preliminary purification of the aqueous fraction was done by ion exchange chromatography using DOWEX 50, a strongly acidic cation exchange resin in order to remove salts and other water soluble compounds that were not of interest.

The ion exchange resin was prepared by washing sequentially with 1N NaOH; water; 1N HCl; and again with water until the pH was neutral. The dark brown viscous aqueous layer was dissolved in a minimum amount of water and filtered to a brown solution. The water soluble alkaloids were eluted from the resin with 1N NH_4OH monitoring with Mayers reagent. Similar eluates by tlc were combined together and the pH brought down to about pH7.0. The water soluble eluates were freeze dried yielding a brown, vermiculite-look solid, 540.3 g and labelled as Oa-WS. On tlc (C_{18} TLC plate, n-Butanol:Acetic Acid:H_2O 4:2:1), a spot at Rf=0.68 gave a positive response with Dragendorff reagent. A violet colouration was observed with α-naphthol-sulfuric acid reagent indicating the presence of sugar in the molecule.

7.2.5.1 Purification by High Pressure Liquid Chromatography

Isolation of the glycoalkaloids was attempted on a reversed phase HPLC system using several solvent systems.

To start with, the freeze dried crude water soluble alkaloids (Oa-WS) were separated by elution of the C-18 column with 100% CH_3OH and UV detection at 254 nm. Two major peaks eluting at 5.6 and 4.1 min. were obtained. The peaks were quite

close to each other. To improve separation, the solvent system was made more polar by the addition of water. Different ratios of CH_3OH and H_2O were tried. Gradient elution was found to give better separation than isocratic elution. Isocratic elution with 70% CH_3OH/H_2O gave poor resolution while a gradient system from a 65% CH_3OH/H_2O to 70% CH_3OH/H_2O over 30 mins at 1.0 ml/min provided good resolution. One major alkaloid eluted after 8.2 mins and the other at 12.3 min.

Acetonitrile was also considered although 100% CH_3CN was not used as the sample was not soluble in it. Hence, different ratios of CH_3CN/H_2O were tested on. Elution with 70% CH_3CN/H_2O proved to be better than CH_3OH/H_2O. The two major components eluted as sharp peaks after 8.3 and 10.0 mins. Gradient elution from 100% H_2O to 70% CH_3CN/H_2O in 10 mins. and isocratic elution at that concentration for 40 mins provided well resolved peaks. Starting with 65% CH_3CN/H_2O and eluting to 70% CH_3CN/H_2O proved better than CH_3OH/H_2O. One alkaloid eluting as a sharp peak at 16.0 mins and the other at 17.5 min.

7.2.5.2 Purification by Gel Chromatography on Sephadex LH-20

The Oa-WS was subjected to gel filtration chromatography using Sephadex LH-20. Gel filtration or gel permeation chromatography works on the principle of molecular sieving. It has the potential to remove high molecular weight compounds from the glycoalkaloids. Sephadex LH-20 was chosen for its stability to organic solvents.

Method A.

Sephadex LH-20 was prepared by allowing the resin to swell in water for several hours prior to its use. The freeze dried water soluble extract (121.9 mg.) suspended in 1 ml of water was added into the column. Three bands were obtained after elution with water. The yellow coloured fraction had a UV absorptions consistent with a β-carboline ring system, were combined together. A light yellow solid, m. pt. 214-219° (dec.) was obtained after concentration by freeze drying.

Method B.

Another purification method was attempted whereby elution of the water soluble alkaloids from Sephadex LH-20 was tried using CH_3OH. Three bands were again observed although in a different order of elution. The yellow band eluted first from the column followed by a brown coloured band. The eluate showing UV absorption consistent for a β-carboline ring system was the yellow coloured band. Freeze drying of the combined eluate afforded 16.91 mg of a pale yellow solid.

Eventually a method utilising both Gel Permeation or Gel Filtration chromatography and HPLC was developed to isolate and purify the water soluble alkaloid. The Oa-WS was chromatographed twice on Sephadex LH-20 using CH_3OH. Two separate bands were obtained, one a yellow and the other a pale brown coloured band. Both gave UV spectra conforming for a β-carboline ring system.

The two fractions were chromatographed by tlc on SGF_{254} developed in CH_3OH/H_2O (6:4) and visualised by UV_{254} and the Dragendorff spray reagent. A common component in both fractions was a bright blue band at Rf 0.78 (UV_{254} and

Dragendorff) with the yellow fraction containing it as the major component. A minor spot that gave an orange colour with Dragendorff was observed at Rf 0.71. Both alkaloids stained positive with the α-naphthol-sulfuric acid reagent for sugars.

Isolation of the two glycoalkaloids from both the yellow and brown fractions was carried out by PTLC on SGF_{254} developed in 75% CH_3OH/H_2O. The major alkaloid labelled as Oa-4A-1 appeared as a bright blue spot under both short and long wavelength UV light, and on concentration, yielded a 39.1 mg. A total of 20.8 mg of the minor alkaloid labelled as Oa-4A-2 and which was present as a dark blue band under UV_{254} was obtained.

7.2.5.3 Enzyme Hydrolysis of Oa-4A-1

To a solution of Oa-4A-1 (3.3 mg) in either water or buffer solution was added β-glucosidase (3.2 mg). The reaction mixture at pH5.0 was stirred for one hour on a water bath at 37°C A dark pink coloured solution was obtained and was freeze dried. The light pink powder was extracted with CH_3OH which yielded a light pink solid (2.7 mg) upon concentration in vacuo. The pink solid was purified by PTLC on SGF_{254} (Merck 5554) developed in 100% CH_3OH and visualised under shortwave (254 nm) UV light. The major hydrolysis product which appeared as dark blue band under UV light gave a positive responsed with Dragendorff. The ^1H NMR data were in agreement for harman.

The aqueous layer after extraction with $CHCl_3$ was freeze dried and compared to standard sugars by TLC on SGF_{254} developed in EtOAc:Pyridine:H_2O (60:21:15) and sprayed with α-naphthol-sulfuric acid for sugar.

7.2.5.4 Spectroscopic Data for Oa-4A-1

m. pt. (uncorrected): 215-220°C

UV (CH_3OH): λ_{max}351.4, 337.6, 304.0, 289.4, 282.2 and 253.0 nm.

IR (KBr disc, cm^{-1}): υ_{max}3883, 3823, 2932, 2860, 2425, 2372, 2360, 2346, 2250, 2193, 2127, 2042,1986,1879,1733 (C=O) ,1639, 1457, 758, 665, 639 and 614 cm^{-1}.

$[\alpha]_D$= -89.0° (1.03 x 10^{-3} g/ml, CH_3OH)

CD (CH_3OH, 5.0 x 10^{-5} M): $\Delta\Sigma_{339}$ = -8.5 ; $\Delta\Sigma_{289}$ = -9.7, $\Delta\Sigma_{255}$ = +32.0

[Lyalosidic Acid: CD (CH_3OH, 9.5 x 10^{-5} M): $\Delta\Sigma_{304}$ = -15.0 ; $\Delta\Sigma_{289}$ = -5.7; $\Delta\Sigma_{255}$ = +9.6]

^{1}H NMR (CD_3OD, Varian 400 MHz): δ 8.19/8.18 (d, 2H, H-5, H-9), 8.01 (d, J 5.0Hz, 1H, H-6), 7.74 (d, J 8.0Hz, 1H, H-12), 7.59 (t, J 7.0Hz,1H, H-11), 7.41 (s, 1H, H-17), 7.29 (t, J 8.0Hz, 1H, H-10), 5.92 (ddd, J 17.0, 10.0, 9.0Hz, 1H, H-19), 5.65 (d, J 7.0Hz, 1H, H-21), 4.91 (d, J 17.0Hz, 1H, H-18_{trans}), 4.83 (d, J 10.0Hz, H-18_{cis}), 4.77 (d, J 8.0Hz, H-1'), 3.95 (dd, J 12.0,1.0Hz, 1H, H-6'), 3.74/3.71 (m or dd, J 12.0Hz, 2H, H-6'; H-14), 3.57 (m, 1H, H-15), 3.41 (q, J 9.0Hz, 1H, H-5'), 3.39 (t, J 8.0Hz, 1H, H-14), 3.30 (t, J 9.0Hz, 1H, H-3'), 3.23 (t, J 9.0Hz, 1H, H-4'), 3.20 (t, J 8.0Hz, 1H, H-2') and 2.64 (m, 1H, H-20) ppm.

^{13}C NMR (CD_3OD, Bruker 100.6 MHz): δ 170.0 (C-22, C=O), 151.4 (C-17), 146.6 (C-3), 143.6 (C-13), 137.1 (C-5), 137.2 (C-19), 136.8 (C-2), 131.2 (C-7), 130.6 (C-11), 123.5 (C-9), 123.1 (C-8), 121.6 (C-10), 119.4 (C-18), 115.4 (C-16), 114.1 (C-6, C-12), 101.1 (C-1'), 97.9 (C-21), 79.2 (C-5'), 78.7 (C-3'), 75.4 (C-2'), 72.4 (C-4'), 63.7 (C-6'), 47.2 (C-20), 37.8 (C-15), and 36.6 (C-14) ppm.

^{1}H NMR (D_2O, Varian Unity 400 MHz): δ 8.05 (d, J 6.6Hz, 1H, H-9), 7.99 (br d, J 4.6Hz, 1H, H-5), 7.86 (br d, 1H, H-6), 7.63 (t, J 6.8Hz, 1H, H-11), 7.55 (d, J 8.8Hz, 1H, H-12), 7.31 (t, J 7.1Hz, 1H, H-10), 7.13 (s,

1H, H-17), 5.69 (ddd, J 17.0, 9.6, 8.3Hz, 1H, H-19), 5.41 (d, J 5.6Hz, 1H, H-21), 4.93 (d, J 9.6Hz, 1H, H-18_{cis}), 4.81 (d, J 7.2Hz, 1H, H-1'), 4.71 (d, J 17.0Hz, 1H, H-18_{trans}), 3.90 (dd, J 11.6, 1.7Hz, 1H, H-6'), 3.70 - 3.64 (m, 2H, H-6', H-5'), 3.58 - 3.48 (m, 2H, H-4', H-3'), 3.36 (br t, 1H, H-15), 3.27 (t, J 8.0Hz, 1H, H-2'), 3.15 (br m, 1H, H-14), 2.82 (br m, 1H, H-14), and 2.39 (m, 1H, H-20) ppm.

^{1}H NMR (DMSO-d_6, Varian Unity 400 MHz): δ 8.61 (s, 1H, NH), 8.26 (d, J 7.6Hz, 1H, H-9), 8.22 (d, J 5.6Hz, 1H, H-5), 7.97 (d, J 5.2Hz, 1H, H-6), 7.71 (d, J 8.0Hz, 1H, H-12), 7.60 (t, J 7.6Hz, 1H, H-11), 7.28 (t, J 7.6Hz, 1H, H-10), 7.24 (s, 1H, H-17), 6.05 (ddd, J 18.0, 12.0, 10.0Hz, 1H, H-19), 5.58 (d, J 7.6Hz, 1H, H-21), 5.53 (br s, 4H, OH for sugar), 4.87 (d, J 18.0Hz, 1H, H-18_{trans}), 4.71 (d, J 12.8Hz, 1H, H-18_{cis}), 4.69 (d, J 8.0Hz, 1H, H-1'), 3.83 (d, J 10.6Hz, 1H, H-6') 3.60 (t, J 12.0Hz, 1H, H-6'), 3.27 (t, J 8.4Hz, 1H, H- 4'), 3.16 (t, J 6.0Hz, 1H, H-14), 3.14 (t, J 8.8Hz, 1H, H-3'), 3.01 (t, J 8.0Hz, 1H, H-2') and 2.53 (m, H-20) ppm.

7.2.5.5 Spectroscopic Data for Oa-4A-2.

white amorphous solid

m.p. 220-223°C (uncorrected)

$[\alpha]_D$-211.5° (8.69 x 10^{-2}, CH_3OH)

UV (CH_3OH): λ_{max} 289.2, 272.4, 226.6 and 218.0 nm.

CD (CH_3OH, 5.0 x 10^{-5} M): $\Delta\Sigma_{289}$ -9.8; $\Delta\Sigma_{267}$ -3.6; $\Delta\Sigma_{223}$ -30.4.

^{1}H NMR (CD_3OD, Varian Unity 400 MHz): δ 7.51 (s, H-17), 7.48 (d, J 8.0Hz, 1H, H-9), 7.37 (d, J 8.0Hz, 1H, H-12), 7.15 (t, J 7.0Hz, 1H, H-11), 7.06 (t, J 7.0Hz, 1H, H-10), 5.93 (br m, 1H, H-19), 5.70 (br d, 1H, H-20), 5.34 (d, J 17.0Hz, d, H-18_{trans}), 5.27 (d, J 10.0Hz, 1H, H-18_{cis}), 4.79 (d, J 7.0Hz, 1H, H-1'), 4.65 (m, 1H, H-3), 3.58 (m, 1H,

^{13}C NMR (CD_3OD, Varian Unity 100.6 MHz): δ 137.3 (C-13), 128.3 (C-8), 124.1 (C-11), 121.4 (C-10), 120.1 (C-9) 113.1 (C-16), 101.2 (C-1'), 97.6 (C-21), 79.4 (C-3'), 78.8 (C-5'), 75.2 (C-2'), 73.4 (C-4'), 62.9 (C-6'), and 46.2 (N-$\underline{C}H_3$) ppm.

7.2.6 Isolation of Oa-WS-Me-I and Oa-Ws-Me-II

To the semipurified water soluble alkaloid (Oa-WS), 66.5 mg, in CH_3OH was added CH_2N_2 (excess). The reaction mixture was left overnight. After solvent evaporation under vacuum, the methylated alkaloids were isolated by PTLC on SGF_{254} developed in CH_3OH. A major band appeared as bright blue under UV_{254} and a minor dark blue band were obtained, and labelled as Oa-WS-Me-I and Oa-WS-Me-II respectively.

Oa-WS-Me-I obtained as a dark brown resin, 53.2 mg, was purified by HPLC on a C_{18} column (Radial-Pak), using isocratic elution with 60% CH_3OH/H_2O at 1.0 ml/min with the UV detector set at 254 nm. The major component eluting after 16.3 mins was once again rechromatographed by HPLC on a semi-preparative C_{18} column the component eluted at 10.5 min. with 80% CH_3OH/H_2O at 1.5 ml/min using UV detection at 254 nm. Oa-WS-Me-I was obtained as white solid in 14.7 % yield, 9.8 mg.

Oa-WS-Me-II, a light brown resin, 18.2 mg, was purified by HPLC on semi-preparative C_{18} column eluting out with 80% CH_3OH/H_2O at 1.5 ml/min with UV detection at 254 nm. The alkaloid eluted after 28 min.

7.2.6.1 Spectroscopic Data for Oa-WS-Me-I

MS(LRFAB) : 527.O (M + H)

$[\alpha]_D^{30}$ -136.9° (2.26 x 10^{-4} g/ml, CH_3OH)

CD (CH_3OH, 1.5 x 10^{-4} M): $\Delta\Sigma_{339}$ = +7.1 ; $\Delta\Sigma_{304}$ = -0.6

^{1}H NMR (DMSO-d_6, Varian Unity 400 MHz): δ 8.36 (d, J 5.2Hz, 1H, H-5), 8.28 (d, J 8.0Hz, 1H, H-9), 8.07 (d, J 5.6Hz, 1H, H-6), 7.64 (d, J 8.0Hz, 1H, H-12), 7.60 (t, J 8.0Hz, 1H, H-11), 7.57 (s, H-17), 7.31 (t, J 7.6Hz, 1H, H-10), 5.75 (ddd, J 17.4, 10.2, 9.2 Hz, 1H, H-19), 5.61 (d, J 5.2Hz, 1H, H-21), 5.04 (dd, J10.8, 2Hz, 1H, H-18_{cis}), 4.84 (d, J 17.2Hz, 1.0Hz, 1H, H-18_{trans}), 4.66 (d, J 8.0Hz, 1H, H-1'), 3.81-3.77 (m, H-15), 3.68 (d, J 6.0 Hz, 1H, H-6'), 3.64 (q, J 6.0Hz, H-14), 3.61 (s, OCH_3), 3.57 - 3.51 (m, H-6', and H-5'), 3.30-3.09 (m, H-14, H-2', and H-3'), and 2.82, (quintet, J.3.5.,2.5.Hz, 1H, H-20) ppm.

7.2.6.2 Spectroscopic Data for Oa-WS-Me-II

CD (CH_3OH, 9.5 x 10^{-5} M): $\Delta\Sigma_{290}$ = +6.4 ; $\Delta\Sigma_{280}$ = +3.5; $\Delta\Sigma_{273}$ = +2.6

^{1}H NMR (CD_3OD, Varian Unity 400 MHz): δ 7.58 (s, 1H, H-17), 7.41 (d, J 8.0Hz, 1H, H-9), 7.31 (d, J 8.1Hz, 1H, H-12), 7.07 (td, J 7.8, 1.2Hz, 1H, H-11), 6.99 (td, J 7.6, 1.2Hz, 1H, H-10), 5.86 (ddd, J 17.4, 10.8, 8.0Hz, 1H, H-19), 5.62 (d, J 6.6Hz, 1H, H-21), 5.36 (d, J 17.3Hz, 1H, H-18_{trans}), 5.30 (d, J 10.5Hz, 1H, H-18_{cis}), 4.75 (d, J 7.8HZ, 1H, H-1'), 3.94 (dd, J 12.0, 1.0Hz, 1H, H-6'), 3.87 (t, J 6.6Hz, 1H, H-3), 3.74 (s, 3H, C$\underline{H}_3$OCO-), 3.64-3.66 (m, 2H, H-6', H-5'), 3.41 (qt, J 8.7Hz, 1H, H-3'), 3.34 (qt., J 8.8 Hz, 1H, H-4'), 3.32 (m, 1H, H-5), 3.25 (t, J 9.0Hz, 1H, H-2'), 2.94-2.87 (m, 2H, H-5 and H-6), 2.76 (br q, J 6.1Hz, 1H, H-20), 2.66-2.60 (m, 1H, H-6), 2.53 (s, 3H, N-C$\underline{H}_3$), and 1.99-2.00 (m, 2H, H-14).

7.2.7 Synthesis of β-Carboline Derivatives

7.2.7.1. 1,9-Dimethyl-β-carboline 56

Method 1:

To a stirred solution of harman **10** (1-methyl-β-carboline, 55.92 mg, 3.07 x 10^{-4} mole) in CH_3OH (5 ml) was added CH_3I (43.60 mg, 19 ul, 3.07 x 10^{-4} mole) and K_2CO_3 (67.27 mg). After 15 mins, the colourless solution turned yellow. On concentration under vacuum, a yellow solid was obtained which was extracted with benzene, dried and petroleum ether (30-60°) added. The solid did not dissolve in petroleum ether but turned brown when $CHCl_3$ was added. The ^1H NMR spectrum (90 MHz, $CDCl_3$) showed the presence of the indolic proton indicating the the indole nitrogen had not been methylated

Method 2:

To a stirred solution of harman **10** (50.28 mg, 2.76 x 10^{-4} mole) in CH_3OH (5 ml) was added K_2CO_3 (49.90 mg). The mixture was refluxed for 30 mins. and cooled to RT then CH_3I (39.16 mg, 17 μl) was added. The solution was stirred at room temperature overnight. The yellow solution upon evaporation of the solvent gave a yellow solid. The solid was washed with H_2O and the residue dissolved in CH_3OH. The alcohol soluble solid gave a dirty white solid upon concentration under vacuum. The tlc and NMR spectrum again indicated that harman was still present.

Method 3:

To a stirred solution of harman **10** in CH_3OH was added CH_3I(40 μl). The solution was stirred at room temperature for about 5 min. then $KHCO_3$ (40 mg) was added. The solution was stirred overnight. The green solution was concentrated under vacuum to

green material. The ^1H NMR spectrum showed the absence of the indolic proton and the appearance of the signal at δ4.08 (s,1H), 3.34 (s,1H) and 3.09(s,1H). Poor yield of the desired product was obtained.

Method 4: Sodamide Reaction

Preparation of sodamide:

Liquid ammonia was prepared by passing ammonia gas through a cold finger. Ammonia gas was added until about 10 ml of NH_3 liquid had condensed into the flask. Dry ice was continuously added to keep the whole system at approximately -77°C. To the stirred solution of liquid NH_3, small pieces of Na metal (0.040 gm.) were added slowly until it completely dissolved giving a blue solution of sodamide.

1,9-Dimethyl-β-carboline 56

Metallic Na (0.928 g, 2.942 x 10-3 mole) in small pieces was added with stirring to liquid NH_3 (30 ml) containing $Fe(NO_3)_3 \cdot 9H_2O$ as a catalyst. When the solution turned dark blue, harman **10** (1-methyl-β-carboline, 0.53542 g, 2.942 x 10^{-3} mole) was added to the stirred mixture. After 15 mins., CH_3I (250 μl) in dry Et_2O (20 ml) was slowly added into the solution. The solution was continuously stirred under N_2 atmosphere until the solution dried. The pale yellow solid with dark brown residue was stirred in benzene. The benzene soluble (colourless) material was concentrated under vacuum yielding a pale yellow solid. The product was purified by column chromatography on silica (Merck 7734) eluting with $CHCl_3$ containing increasing CH_3OH. 1-9-dimethyl-β-carboline **56** was obtained as beige crystals, m. pt. 99-100°C and obtained in 37% yield.

UV (CH_3OH, 7.36 x 10^{-3} mg/ml):λ_{max}359.4 (Σ4613.3), 343.6 (Σ4186.7), 288.0 (Σ27,786.7), 261.4 (Σ38,720.0), 254.2 (Σ38,133.3), 243.6 (Σ36.160.0) and 209 (Σ23,920.0) nm.

^{1}H NMR (CD_3OD, Varian Unity 400 MHz):δ 8.09 (d, 2H, H-3 and H-5), 7.85 (d, J 5.2Hz, 1H, H-4), 7.60 (t, J 8.4 Hz, 1H, H-7), 7.50 (d, J 8.4Hz, 1H, H-8), 7.27 (t, J 7.2Hz, 1H, H-6), 4.02 (s, 3H, N_1-CH_3), and 2.98 (s, 3H, C_1-CH_3) ppm.

^{13}C NMR (CD_3OD, 22.5 MHz): δ 143.8 (C-1), 142.9 (C-8a), 137.8 (C-9a, C-3), 130.4 (C-4a), 129.5 (C-7), 122.3 (C-5), 122.2 (C-4b), 120.8 (C-6), 111.1 (C-4), 110.7 (C-8), 32.47 (N_1-CH_3), and 22.72 (C_1-CH_3) ppm.

^{1}H NMR ($CDCl_3$, 90MHz): δ 8.29 (d, J 5.3Hz, 1H, H-3), 7.97 (dd, J 8.4, 1.0Hz, 1H, H-5), 7.64 (d, J 5.3Hz, 1H, H-4), 7.55 (dd, J 8.0Hz, 1Hz, 1H, H-8), 7.46 (t,1H, H-7), 7.23 (t, J 8.0Hz, 1H, H-6), 3.76 (s, 3H, N_1-CH_3), and 2.94 (s, 3H, C_1 - CH_3).

^{13}C NMR ($CDCl_3$, 22.5 MHz): δ141.6 (C-1), 141.1 (C-8a), 135.1 (C-9a), 137.4 (C-3), 128.0 (C-4a), 127.5 (C-7), 120.7 (C-5), 120.5 (C-4b), 119.0 (C-6), 112.1 (C-4), 108.7 (C-8), 31.40 (N_1-CH_3), and 23.0 (C_1-CH_3).

7.2.7.2 1,9-Dimethyl-β-carboline N-oxide 57

To an ice-cooled stirred solution of **56** (190.8 mg, 9.7 x 10^{-4} mole) in $CHCl_3$ (6 ml) was added, *m*-chloroperoxybenzoic acid (0.27 g, 1.6 x 10^{-3} mole, 1.62 eq.) in $CHCl_3$ (4 ml). The solution was stirred for 3 hrs. until the solution cooled down to RT. The yellow reaction mixture was passed through a column of Al_2O_3 (basic) eluted with $CHCl_3$ in order to remove excess *m*-CPBA and any unreacted amines. The N-oxide derivative was eluted with $CHCl_3$:CH_3OH (3:1). The eluate was concentrated under vacuum

yielding a beige solid. The product was purified by column chromatography on silica (Merck 7734) eluting with $CHCl_3$ containing increasing concentrations of CH_3OH. The N-oxide derivative was obtained as a white amorphous solid, m.pt. 183-184°C in 57% yield.

UV (CH_3OH, 1.7 x 10^{-2} mg/ml): λ_{max}317.2 (Σ14,565.5), 261.4 (Σ23,258.4) and 219.4 (Σ13,089.9) nm.

LRFABMS (glycerol matrix): *m/z* 213 (M+H) with a strong signal at *m/z* at 196 (loss of O).

^{1}H NMR (CD_3OD, Varian Unity 400 MHz): δ 8.24 (d, J 6.8Hz, 1H, H-3), 8.16 (d, J 8.0Hz, 1H, H-5), 8.06 (d, J 6.4Hz, 1H, H-4), 7.65 (t, J 5.2Hz, 1H, H-7), 7.64 (d, J 7.2Hz, 1H, H-8), 7.37 (dd, J 8.0, 1.0Hz, 1H, H-6), 4.16 (s, 3H, N_1-CH_3), and 3.12 (s, 3H, C_1-CH_3) ppm.

^{1}H NMR ($CDCl_3$, Varian Unity 400 MHz): δ 8.23 (d, J 6.8Hz, 1H, H-3), 7.99 (d, J 8.0Hz, 1H, H-5), 7.63 (d, J 6.8Hz, 1H, H-4), 7.54 (t, J 8.4Hz, 1H, H-7), 7.42 (d, J 8.4Hz, 1H, H-8), 7.29 (d, J 7.6Hz, 1H, H-6), 4.09 (s, 3H, N_1-CH_3), and 3.07 (s, 3H, C_1-CH_3) ppm.

^{13}C NMR ($CDCl_3$, 22.5 MHz): δ143.5 (C-1), 142.7 (C-8a), 134.8 (C-9a), 131.5 (C-3), 128.3 (C-4a), 127.9 (C-7), 122.6 (C-5), 120.8 (C-4b), 120.8 (C-6), 113.4 (C-4), 109.5 (C-8), 32.6 (N_1-CH_3) and 29.6 (C_1 - CH_3).

7.2.7.3 1-Acetoxymethyl-9-methyl-β-carboline 58

To 57 (4.675 x 10^{-4} mol) was added acetic anhydride (4.7 x 10^{-4} mol, 0.05 g). The yellow solution was refluxed with the resulting red reaction mixture turning to a dark brown after an hour. The product was isolated and purified by column chromatography eluting with $CHCl_3$ with increasing concentrations of CH_3OH affording a yellow amorphous solid in 90% yield.

UV (CH_3OH, 4.2 x 10^{-6} mg/ml): λ_{max}359.2 (Σ20,121.2), 348.8 (Σ19,757.6), 290.4 (Σ55818.2), 264.0 (Σ85,545.4), 238.8 (Σ114,545.4), 210.2 (Σ45,878.8) and 207.2 (Σ45, 939.4) nm.

^{1}H NMR (CD_3OD, Varian Unity 400 MHz): δ 8.33 (d, J 5.6Hz, 1H, H-3), 8.26 (d, J 8.0Hz, 1H, H-5), 8.19 (d, J 5.6Hz, 1H, H-4), 7.74-7.69 (m, H-7 and H-8), 7.37 (t, J 7.6Hz, 1H, H-6), 5.76 (s, 2H, H-10), 4.17 (s, 3H, N_1-CH_3), and 2.18 (s, 3H, H-16, OCOC<u>H</u>$_3$) ppm.

^{1}H NMR ($CDCl_3$, Varian Unity 400 MHz): δ 8.45 (d, J 5.2Hz, 1H, H-3), 8.14 (d, J 8.0Hz, 1H, H-5), 7.99 (d, J 5.2Hz, 1H, H-4), 7.63 (td, J 7.6, 1.0Hz, 1H, H-7), 7.48 (d, J 8.4Hz, 1H, H-8), 7.31 (t, J 7.6Hz, 1H, H-6), 5.71 (s, 2H, H-10), 4.08 (s, 3H, N_1-CH_3), and 2.14 (s, 3H, H-16, OCOC<u>H</u>$_3$) ppm.

^{13}C NMR ($CDCl_3$, 22.5 MHz): δ173.1 (C=O), 140.8 (C-1), 136.1 (C-8a), 134.5 (C-9a), 136.4 (C-3), 129.0 (C-4a), 127.2 (C-7), 120.0 (C-5), 119.4 (C-4b), 118.5 (C-6), 113.6 (C-4), 108.0 (C-8), 64.5 (C-10), 30.2 (N_1-CH_3) and 19.4 (OCO<u>C</u>H$_3$).

7.2.7.4 1-Hydroxymethyl-9-methyl-β-carboline 59

To **<u>58</u>** (2.079 x 10^{-5} mol) was added absolute EtOH and NaOH (2N, 1 ml). The solution was stirred for 1.5 hrs. on a warm (approx. 70°C) hotplate. The reaction mixture was worked up by evaporating the organic solvent. Upon neutralisation with HCl (1N), the 1-hydroxymethyl-9-methyl-β-carboline precipitated out affording a yellow amorphous solid, m. pt. 178-179°C

UV (CH_3OH, 5.9 x 10^{-5} mg/ml): λ_{max}359.6 (Σ2413.7), 346.6 (Σ2356.1), 290.4 (Σ6787.8), 263.6 (Σ7967.6), and 208.8 (Σ2949.6) nm.

^{1}H NMR (CD_3OD, Varian Unity 400 MHz): δ 8.28 (d, J 5.2Hz, 1H, H-3), 8.24 (d, J 7.6Hz, 1H, H-6), 8.13 (d, J 5.6Hz, 1H, H-4), 7.69-7.68 (m,

H-7 and H-8), 7.35 (ddd, J 7.8, 5.6, 2.4Hz, 1H, H-6), 5.24 (s, 2H, H-10), and 4.29 (s, 3H, N_1-CH_3) ppm.

^{13}C NMR (CD_3OD, 22.5 MHz): δ146.1 (C-1), 144.6 (C-8a), 134.5 (C-9a), 137.6 (C-3), 129.0 (C-4a), 129.8 (C-7), 122.4 (C-5), 119.4 (C-4b), 121.0 (C-6), 115.8 (C-4), 110.9 (C-8), 64.8 (C-10), and 32.0 (N_1-CH_3) ppm.

^{1}H NMR ($CDCl_3$, 90 MHz): δ8.36 (d, J 5.3Hz, 1H, H-3), 8.13 (d, J 7.4Hz, 1H, H-5), 7.90 (d, J 5.3Hz, 1H, H-4), 7.62 (td, J 7.7, 1.4Hz, 1H, H-7), 7.52 (d, J8.4Hz, 1H, H-8), 7.29 (dd, J 7.9, 1.1Hz, 1H, H-6), 5.34 (s, 2H, H-10), and 4.08 (s, 3H, N_1-CH_3) ppm.

^{13}C NMR ($CDCl_3$, Varian Unity 100.6 MHz): δ142.0 (C-1), 141.8 (C-8a), 136.5 (C-3), 133.9 (C-9a), 129.1 (C-4a), 128.4 (C-7), 121.5 (C-5), 121.1 (C-4b), 119.9 (C-6), 114.1 (C-4), 109.5 (C-8), 62.0 (C-10), and 32.0 (N_1-CH_3).

7.2.7.5 1-Methyl-β-carboline N-oxide 60

To an ice-cooled solution of **10** (3.165×10^{-5} mol) in $CHCl_3$ was slowly added a solution of *m*-chloroperoxybenzoic acid (7.12 mg) in $CHCl_3$. The reaction mixture was passed through a column of basic alumina with the unreacted amines and *m*-CPBA eluted with $CHCl_3$. The N-oxide derivative was purified by PTLC on silica (Merck 5554) developed in 90% $CHCl_3$ in CH_3OH. The dark blue band under UV_{254} afforded upon concentration a pale yellow solid (85 % yield).

UV ($CHCl_3$, 5.72×10^{-3} mg/ml): λ_{max}321.0 (Σ29,409.7), 255.0 (Σ40694.4), 232.4 (Σ20034.7), 224.2 (Σ20694.4), and 216.0 (Σ23958.3) nm.

LRFABMS (glycerol matrix): *m/z* 199 ($M + H^+$) with a strong tendency to lose oxygen.

^{1}H NMR (CD_3OD, Varian Unity 400 MHz): δ 8.22 (d, J 6.8Hz, 1H, H-3), 8.17 (d, J 7.6Hz, 1H, H-5), 8.07 (d, J 6.8Hz, 1H, H-4), 7.62 (d, J 8.0Hz, H-8), 7.59 (t, J 8.0Hz, 1H, H-7), 7.34 (t, J 8.0Hz, 1H, H-16), and 2.86 (s, 3 H, C_1-CH_3) ppm.

^{13}C NMR (CD_3OD, 22.5 MHz): δ143.8 (C-1), 137.8 (C-8a), 137.3 (C-3), 131.8 (C-9a), 129.5 (C-4a), 129.4 (C-7), 124.1.(C-5), 122.7 (C-4b), 120.8 (C-6), 115.6 (C-4), 113.0 (C-8), and 12.8 (C_1-CH_3) ppm.

^{1}H NMR ($CDCl_3$, 90 MHz): δ 8.78 (br s, indole NH, D_2O exchangeable), 8.21 (d, J 7.2Hz, 1H, H-3), 7.98 (d, J 8.1Hz, 1H, H-5), 7.71 (d, J 7.2Hz, 1H, H-4), 7.50-7.30 (m, 3H, H-6, H-7, H-8), and 2.81 (s, 3H, C_1-CH_3) ppm.

7.2.7.6 1-Acetoxymethyl-β-carboline 61

To **60** (1.56 x 10-5 mole) was added, acetic anhydride (1 eq). The mixture was refluxed in an oil bath for 1 hr. The red coloured solution was cooled to RT. Isolation and purification of the ester was carried out by column chromatography on silica (Merck 7734) eluting first with $CHCl_3$, then with 3% CH_3OH in $CHCl_3$. The major product was obtained as a yellow solid in 31% yield.

LRFABMS (glycerol matrix):*m/z* 241(M+H), 198 (MH-43), 182 (MH-59).

^{1}H NMR ($CDCl_3$, 90 MHz): δ 9.30 (br s, indole NH, D_2O exchangeable), 8.43 (d, J 5.3Hz, 1H, H-3), 8.10 (d, J 7.6Hz, 1H, H-5), 7.94 (d, J 5.3Hz, 1H, H-4), 7.54-7.30 (m, 3H, H-6, H-7, H-8), 5.64 (s, 2H, H-12) and 2.14 (s, 3H, $OCOC\underline{H}_3$) ppm.

^{13}C NMR ($CDCl_3$, 22.5 MHz): δ172.4 (C=O), 140.6(C-1), 135.0 (C-8a), 138.6 (C-3), 130.2 (C-9a), 123.8 (C-4a), 128.8 (C-7), 129.7 (C-5), 121.7 (C-4b) , 120.3 (C-6), 123.8 (C-4), 111.9 (C-8), 65.6 (C-10) and 21.0 ($OCO\underline{C}H_3$).

^{13}C NMR (CD_3OD, 22.5 MHz): δ 143.5(C-1), 142.8 (C-8a), 139.7 (C-9a), 138.1 (C-3), 122.2 (C-4a), 130.0 (C-7), 122.7 (C-5), 125.0 (C-4b), 121.0 (C-7), 116.2 (C-4), 113.0 (C-8), 65.6 (C-10) and 20.7 ($OCO\underline{C}H_3$).

7.2.7.7 1-Acetoxymethyl-9-acetyl-β-carboline 62

To **60** (1.36 x 10^{-4} mole) was added 2 equivalents of acetic anhydride. The mixture was refluxed in an oil bath for 1.5 hrs. The red solution after purification by column chromatography in $CHCl_3$ with increasing concentration of CH_3OH afforded the desired product and the 1-acetomethyl-β-carboline.

UV (CH_3OH, 2.23 x 10^{-2} mg/ml): λ323.2 (ε 4156.7), 283.6 (9955.8), 253.6 (9943.1) and 230.6 (21478.2) nm.

LRFABMS (nitrobenzoic acid): *m/z* 282 (M+H)

^{1}H NMR (CD_3OD, Varian Unity 400 MHz): δ 8.54 (d, J 5.2Hz, 1H, H-3), 8.20 (d, J 6.8Hz, 1H, H-5), 8.10 (d, J 5.2Hz, 1H, H-4), 8.04 (d, J 6.0Hz, H-8), 7.74 (t, J 7.8Hz, 1H, H-7), 7.52 (t, J 7.6Hz, 1H, H-6), 5.50 (s, 2H, H-10), 2.95 (s, 3H, $NCOC\underline{H}_3$), and 2.10 (s, 3H, $OCOC\underline{H}_3$) ppm.

^{13}C NMR (CD_3OD, 22.5 MHz): δ142.8 (C-8a), 139.7 (C-9a), 143.7 (C-3), 131.5 (C-7), 125.1 (C-5), 118.0 (C-4b), 123.0 (C-6), 116.0 (C-4), 115.6 (C-8), 68.1 (C-10), 26.9 ($NCO\underline{C}H_3$) and 20.6 ($OCO\underline{C}H_3$).

^{1}H NMR ($CDCl_3$, 90 MHz): δ 9.26 (br s, indole NH, D_2O exchangeable), 8.54 (d, J 6.3Hz, 1H, H-5), 8.42 (d, J 5.4Hz, 1H, H-3), 81.2 (d, J 8.1Hz, 1H, H-8), 7.95 (d, J 5.4Hz, 1H, H-4), 7.72 (m, 2H, H-6, H-7), 5.64 (s, 2H, H-10), 2.78 and 2.74 (s, 3H, $NCOC\underline{H}_3$, 2:1 isomer), and 2.15 (s, 3H, $OCOC\underline{H}_3$).

7.2.7.8 1-Hydroxymethyl-β-carboline 63

To **62** (1.94 x 10^{-5} mol), in abs EtOH was added, NaOH (2 eq.). The reaction mixture was stirred over a warm (60°C) hotplate for 1.5 hrs. After neutralisation and concentration, a yellow solid was obtained affording the 1-hydroxymethyl-β-carboline.

UV (CH_3OH, 3.2 x 10^{-5} g/ml): λ_{max}348.6 (Σ370.0), 337.2 (Σ3638.6), 288.2 (Σ11,825.5), 249.4 (Σ13601.5), 243.6 (Σ13,688.1) nm.

^{1}H NMR (CD_3OD, 400 MHz):δ 8.25 (d, J 5.2Hz, 1H, H-3), 8.20 (d, J 7.6Hz, 1H, H-5), 8.06 (d, J 5.6Hz, 1H, H-4), 7.62 (d, J 7.6Hz, 1H, H-8), 7.60 (t, J 7.8Hz, 1H, H-7), 7.29 (ddd, J 7.8, 5.6, 2.4Hz, 1H, H-6), and 5.10 (s, 2H, H-10) ppm.

^{13}C NMR (CD_3OD, 22.5 MHz): δ145.1 (C-1), 137.8 (C-8a), 135.4 (C-9a), 137.6 (C-3), 129.4 (C-4a), 129.6 (C-7), 122.5 (C-5), 120.8 (C-4b), 121.0 (C-6), 115.2 (C-4), 112.9 (C-8), and 64.7 (C-10) ppm.

7.2.7.9 1-Methyl-9-acetyl-β-carboline 64

To **10** (2.70 x 10-4 mol) was added acetic anhydride (1 eq.). The reaction mixture was refluxed on an oil bath for 1.5 hrs. Following the same purification as above, the acetyl derivative was obtained. The ^{1}H NMR spectrum showed the occurrence of rotational isomers.

^{1}H NMR (CD_3OD, Varian Unity 400 MHz): δ 8.32 (d, J 5.2Hz, 1H, H-3, major), 8.08 (d, J 5.2Hz, 1H, H-3, minor), 8.04 (d, 1H, H-5, minor), 7.99 (d, J 8.0Hz, 1H, H-5), 7.85 (d, J 8.5Hz, 1H, major), 7.78 (d, J 5.6Hz, 1H, minor), 7.74 (d, J 5.6HZ, 1H, major), 7.58 (td, J 8.0, 1.6Hz, 1H, major), 7.54-7.51 , 7.37 (td, J 7.6,1.0Hz, major), 7.21 (td, J 6.8, 2.4Hz, minor), 2.75 (s, 3H, NCOC$\underline{H}_3$), and 2.59 (s, 3H, C$\underline{H}_3$).

^{1}H NMR ($CDCl_3$, Varian Unity 400 MHz): δ 9.26 (br s, indole NH, D_2O exchangeable), 8.52 (d, J 5.2Hz, 1H, H-3, major), 8.33 (d, J 5.2Hz, 1H,

^{13}C NMR (CDCl3, Varian Unity 100.6 MHz):

Major isomer: δ170.0 (C=O), 146.8 (C-1), 141.8 (C-8a), 134.8 (C-9a), 143.3 (C-3), 133.9 (C-4a), 129.6 (C-7), 123.7 (C-5), 121.9 (C-4b), 121.4 (C-7), 114.7 (C-4), 111.7 (C-8), 25.0 (NCO<u>C</u>H3) and 20.3 (<u>C</u>H3).

Minor isomer: δ170.0 (C=O), 146.8 (C-1), 140.3 (C-8a), 134.7 (C-9a), 138.2 (C-3), 128.1 (C-4a), 128.0 (C-7), 121.7 (C-5), 124.9 (C-4b), 119.8 (C-6), 112.8 (C-4), 111.6 (C-8), 27.1 (NCO<u>C</u>H3) and 20.3 (<u>C</u>H3).

7.3 Experimental Section For Chapter 3

7.3.1 NMR Spectroscopy

^{1}H and ^{13}C NMR, 2-D COSY and Nuclear Overhauser Effect difference spectra were measured in $CDCl_3$ solution at 400 MHz on a Jeol JNM GX-400 NMR spectrometer for solutions in $CDCl_3$ and were referenced relative to TMS, δ0.0. For the COSY spectrum 256 blocks of 1K were collected with 32 scans per block. The data matrix was zero filled once in F_1 to obtain a 512 x 1K matrix prior to Fourier transformation.

7.3.2 Collection of Sample

The sample of *Talauma gitingensis* was obtained from the island of Palawan in Southern Philippines in April 1987. A voucher specimen No. RBM 035 of the plant is kept at the Research Centre for the Natural Sciences, University of Santo Tomas, Manila, Philippines. Identification of the plant was done by R. Madulid and Dr. D. Madulid of the National Museum, Philippines.

7.3.3 Plant Description

Elmer[213] dscribed the plant as a shrub with teret branchlets. The leaves are rigidly chartaceous, alternatingly clustered at the ends of the twigs, spreading in all directions and are shiny deep green above and paler beneath. Their margins are entire and slightly revolute in the dry state, acute to acuminate toward the bluntly rounded end. Leaves are oblong to lanceolately oblong, about 15 cm long without petioles. The fruits are terminal or subterminal; dark green, ovoid, 4 cm long or less, brown when dry,

Figure 49. *Talauma gitingensis (Magnoliaceae)* Plant.

somewhat compressed, wider than their length, attached from the apex to the winged and irregularly growed central axis. (Figure 49).

7.3.4 Extraction and Isolation of Alkaloids

Ground dried leaves of *Talauma gitingensis* (3.1 kg) were exhaustively extracted with 95% EtOH until the leaves gave a negative response with Dragendorff reagent. Upon concentration in vacuo at temp. < 50°, a dark green resinous extract (450 g) was obtained.

The alcoholic extract was partitioned between Et_2O and 1% H_2SO_4. The aqueous layer was basified to pH 9-10 with concentrated NH_3 and extracted with $CHCl_3$. The organic layer was washed once with H_2O, dried over anhydrous Na_2SO_4 and concentrated in vacuo yielding a dark green resinous extract.

The $CHCl_3$ extract was purified by flash chromatography eluting using $CHCl_3$ with increasing CH_3OH concentrations

7.3.4.1 Spectroscopic Data for Tg-3A-1

Tg-3A-1 was isolated by flash chromatography, eluted with $CHCl_3$. The lemon-yellow compound was purified by prep TLC using 10% CH_3OH in $CHCl_3$. Recrystallisation from $CHCl_3$ yielded bright yellow fine needle-like crystals with a mp of 268-270°C (dec.) [282°C, (dec)].[214]

UV (λ_{max}), 247 (Σ14811), 268 (Σ12380), 309 (Σ3952), 415 (Σ5833) nm

IR (Film on KBr disc): υ_{max}2960, 2929, 2859, 1664 (C=O), 1602, 1582, 1490, 1472, 1425, 1367, 1311, 1265, 1233, 1185, 1168, 1125, 1078, 1045, 964, 865 and 728 cm^{-1}.

CIMS:*m/z* 275 (100%)

^{1}H NMR ($CDCl_3$, Bruker 400 MHz): δ 6.39 (s, 2H, -O-CH_2-O-), 7.23 (s,1H, H-3), 7.61 (td,1H, J 8.0, 1.0Hz, H-10), 7.78 (td, 1H, J 8.0,1.0Hz, H-9), 7.90 (d, 1H, J 5.0Hz, H-4), 8.59 (dd, 1H, J 8.0,1.0Hz, H-11), 8.67 (dd, 1H, J 8.0, 1.0Hz, H-8), 8.92 (d, 1H, J 5.0Hz, H-5) ppm.

^{13}C NMR ($CDCl_3$, 100.6 MHz): δ 98.0 (-O-CH_2-O-), 102.0 (C-3), 103.2 (C-11b), 123.0 (C-11c), 124.6 (C-8), 127.4 (C-11), 128.5 (C-9), 131.0 (C-7a), 132.8 (C-11a), 134.0 (C-10), 136.0 (C-3a), 144.2 (C-5), 144.8 (C-6a), 148.0 (C-1), 152.0 (C-2) ppm.

7.3.5 Isolation of the Noraporphine Alkaloids

The $CHCl_3$ extract (58.5 mg) was stirred with Ac_2O (6.0 ml) in Pyridine (2.0ml) at 100° for 3 hrs. The reaction mixture was extracted with Et_2O (4 x 15 ml); washed subsequently with 1N HCl (5 ml) then 1N NaOH (5 ml). The Et_2O layer was washed once with H_2O, dried over anhydrous Na_2SO_4 and concentrated to give the acetylated crude alkaloids as a light brown resinous material.

The acetylated product was chromatographed by flash chromatography on silica eluting with hexane with increasing amount of $CHCl_3$.

Fractions similar by TLC were pooled together and purified by HPLC on μ-porasil using 10% EtOAc/ $CHCl_3$ at 1.0 ml/min and detection at 254 nm.

7.3.5.1 Spectroscopic Data for N-Acetyl-Tg-3A-2

White amorphous solid, mp 227 - 229° (lit. 223-225°C)[215]

$[\alpha]_D^{25}$ = -265° (c= 9 x 10^{-4} g/ml)

HREIMS: Found: M^+ 307.1210, $C_{19}H_{17}NO_3$ requires 307.1208 .

UV ($CHCl_3$): λ_{max}330 (Σ3430), 272 (Σ3310) nm.

IR: υ_{max}2858, 2786,1745, 1649 (C=O, tertiary amide),1575, 1505, 1454, 1422 and 1374 (methylenedioxy group), 1312, 1292, 1229, 1051 and 959 (methylenedioxy group), 780 (Ar-H) and 739 cm^{-1}.

7.3.5.2. Spectroscopic Data for N-Acetyl-Tg-3A-3

White amorphous solid, mp 210 - 211° (lit. 213-214°C)[216]

$[\alpha]_D^{25}$ = -417° (c = 1.5 x 10^{-3} g/ml)

HREIMS: Found: M^+ 337.1312: $C_{20}H_{19}NO_4$ requires 337.1314.

UV ($CHCl_3$):λ_{max}300 (Σ4890) and 205 (Σ1421).

IR: υ_{max}3005, 2927, 2855, 2786, 1647 (C=O, amide), 1612, 1577, 1511, 1466, 1423, 1343, 1295, 1269, 1249, 1123, 1054, 947, 879, 851 and 817 cm^{-1}.

^{1}H NMR ($CDCl_3$, Bruker 400 MHz): δ 8.04 (dd, 1H, J 8.0,1.0Hz, H-11), 6.90 (d,1H, J 2.0Hz, H-8), 6.82 (dd, 1H, J 8.0, 1.0Hz, H-10), 6.54 (s, 0.67H, H-3 Z-form), 6.58 (s, 0.33H, H-3), 6.08 & 5.97 (2d, 2H, J 1.0Hz, -O-CH_2-O-), 5.20 (dd, 0.67H, J 10.0, 4.0Hz, H-6a Z - form), 4.95 (dd, 0.33H, $J_{5ax,4ax}$ = 9.0, $J_{5ax,5eq}$ = 2.0Hz, Ha-5 E - form), 4.69 (dd, 0.33H, $J_{6a,7ax}$ = 14.0, $J_{6a,7eq}$ = 5.0Hz, H-6a E - form), 4.09 (dd, 0.67H, $J_{5ax,4ax}$ = 12.0, $J_{5ax,5eq}$ = 2.0Hz, Ha-5 Z - form), 3.85 (3s, 1H, - OCH_3 at C-9), 3.32 (td, $J_{5eq,4ax}$ = 13.0, $J_{5eq,5ax}$ = 2.0Hz, H_e-5 Z - form), 3.13 (dd, 0.67H, $J_{7ax,6a}$ = 14.0, $J_{7eq,6a}$ = 4.0Hz, H_e-7 Z - form, 0.33H, H_a-7 E - form), 2.78-2.86 (m, 1H, H_a-7 Z-forms, H_e-7, E-form), 2.58-2.77 (m, He-5 E - form, $H_{a,e}$-4 Z & E - forms) and 2.20 and 2.19 (3H, 2s, CH_3 amide) ppm.

Figure 50. *Graptophyllum pictum (Acanthaceae)* Plant.

7.4 Experimental Section For Chapter 4

7.4.1 Collection of Sample

Samples of *Graptophyllum pictum* were collected from Marikina, a suburb of Metro Manila in April 1986. A voucher specimen is deposited with the Research Centre for the Natural Sciences Manila, Philippines. The plant was identified by Mrs Rose Madulid.

7.4.2 Plant Description

Graptophyllum pictum is an erect branched shrub 2 to 3.5 m high, glabrous throughout. The leaves are opposite, entire, oblong to broadly elliptic, narrowed at both ends, about 10-20 cm long and dull purple or green colour and variously mottled with white or gray patches. The inflorescence are 6 to 12 cm in length. The corolla are dull purple or reddish-purple, about 4 cm long (Figure 50).

7.4.3 Isolation of Gp-78

Ground air-dried leaves of *Graptophyllum pictum* (800 g) were extracted exhaustively with 95% EtOH (2.0 l) until negative with Mayer's reagent for alkaloid. On concentration *in vacuo* at temp <50°, a dark green resinous material (174 g) was obtained.

The alcoholic extract was partitioned between Et_2O (1.3 l) and 1% H_2SO_4 (900 ml). The aqueous layer was basified to pH 9-10 with conc NH_3 and extracted with $CHCl_3$ (1500 ml). Evaporation of the dried (anhydrous Na_2SO_4) chloroform extract *in vacuo* afforded the crude basic extract as a green resinous material (2.38 g).

The crude basic extract ($CHCl_3$) was chromatographed by flash column chromatography on silica gel (Merck 7731) gradiently

eluting with hexane, hexane/$CHCl_3$, $CHCl_3$, then MeOH. Similar fractions by tlc were pooled together. The combined fractions eluting in 5% MeOH in $CHCl_3$ were purified by preparative tlc developing first in $CHCl_3$, then in 5% MeOH/$CHCl_3$. The dark blue band (UV_{254}), R_f 0.35, was purified by HPLC using 100% EtOAc at 1.0ml/min to yield Gp-78, 5.08 mg.

7.4.3.1 Spectroscopic Data for Gp-78

A white solid with a mp 117-119°; **HREIMS:** Found: 224.1296, $C_{13}H_{20}O_3$ requires 224.1307; **UV** (CH_3OH): λ_{max} 252 nm (Σ3148); **IR:** υ_{max} 3400 (-OH group), 2970 (C-H stretching for the CH_3 group), 2915 & 2870 (assymmetric stretch for -CH_2-), 1650 (C=O for group α,β- unsaturated ketone), 1380 (>$C(CH_3)_2$), 975 (-CH=CH-C-O) and 800 cm^{-1}; **^{1}H NMR** ($CDCl_3$, 400 MHz, referenced at δ7.25), δ 5.89 (s, 1H, H-6), 5.84 (t, 1H, $J_{8,7}$=16.0, $J_{8,9}$ = 6,0Hz, H-8), 5.79 (dd, 1H, $J_{7,8}$=16.0, $J_{7,9}$=1.0Hz, H-7), 4.41 (quintet,1H, $J_{9,8}$= 6.0, $J_{9,10}$=1.0Hz, H-9), 2.44 (d,1H, J 17.0Hz, H_{ax}-2), 2.24 (d, 1H, J 17.0Hz, H_{eq}-2), 1.89 (d, 3H, J 1.0Hz, H-13), 1.30 (d, 3H, J 6.0Hz, H-10), 1.08 (s, 3H, H-11) and 0.99 (s, 3H, H-12) ppm; **^{13}C NMR** ($CDCl_3$, 100.6 MHz, referenced at δ77.0) δ: 186.0 (C-1), 135.9 (C-2), 129.1 (C-7), 127.0 (C-8), 97.9 (C-3), 79.1 (C-4), 68.0 (C-9), 49.8 (C-6), 41.1 (C-5), 24.1 (C-13), 23.8 (C-10), 22.9 (C_{eq}-11) and 18.8 (C_{ax}-12) ppm.

7.5 Experimental Section For Chapter 5

7.5.1 NMR Spectroscopy

^{1}H NMR spectra were acquired on a Varian Unity 400 spectrometer operating at 400 MHz for protons, with a 5 mm dedicated 1H/19F Varian probe fitted with a deuterium lock circuit and Varian VT temperature control.

^{13}C NMR spectra were acquired on a NMR spectra were acquired on a Varian VXR 500 spectrometer with a 5 mm indirect detection Varian probe fitted with a deuterium lock circuit and Varian VT temperature control.

Attached Proton Test: APT was carried out following the pulse sequence described by Patt *et al.*[217], Rabenstein *et al.*[218], Lecocq *et al.*[219]

7.5.2 2-D NMR Experiments

COSY, TOCSY and ROESY spectrum spectra were acquired on a Varian Unity 400 spectrometer operating at 400 MHz for protons, with a 5 mm dedicated 1H/19F Varian probe fitted with a deuterium lock circuit and Varian VT temperature control.

HMQC and HMBC spectra were acquired either on a Varian 500MHz or a Bruker 500 MHz spectrometers.

Absolute Value COSY: The COSY spectrum was performed using the pulse sequence described by Bax *et al.*[98] A total of 512 blocks of 2048 data points were collected with 16 scans per block. The data matrix was 'zero-filled' once in t_1 to obtain a 1024 x 2048 matrix prior to Fourier transformation.

Total Correlation Spectroscopy: The TOCSY experiment, also known as the Homonuclear Hartmann-Hahn (HOHAHA) experiment was performed using the pulse sequence described by Bax[104]and was acquired in the phase sensitive mode. A total of 64 scans were collected for each of 512 FIDs. The mixing time was set at 80 ms. The data were zero filled as above and multiplied in both dimensions by Gaussian window functions prior to Fourier transformation.

2-D Rotating-Frame NOE (ROESY) Spectroscopy. The ROESY experiment was performed following the pulse sequence described by Kessler.[212] The experiment was performed with a mixing time of 250 ms and the relaxation delay was set at 1.5 s. A total of 512 x 2048 blocks with 32 scan per block were collected. The data were zero filled and processed as described above

Heteronuclear Multiple Quantum Coherence (HMQC) by Indirect Detection:

Spectra of Pandamarilactone-31 and -32 were acquired on a Varian 500 MHz spectrometers operating at 500 MHz while spectra of Pandamarilactone-1 were recorded on a Bruker AMX 500 NMR spectrometer using a 5 mm Inverse ^{1}H/broad band Probe (90_H = 7 μsec, 90_C = 11.4 μsec).

HMQC spectra (Varian 500MHz) of Pandamarilactone-32 and -31 were carried out using the pulse sequence described by Summers *et al.*[179] A total of 256 blocks containing 2048 data points were collected with spectral width of 4400 Hz in the ^{1}H dimension. The delay in the pulse sequence was set at 0.0036s (=1/2J, where J=140 Hz, the one bond ^{1}H-^{13}C J value). The data were zero filled to 2048 x 4096 data points and multiplied in both dimensions by a Gaussian window prior to Fourier transformation.

For HMQC spectra (Bruker AMX 500MHz) of Pandamarilactone-1, Pandamarilactone-2 and Pandamarilactone-32 (repeat), 512 t_1 increments were accumulated into 2048 data points with 32 scans per t_1 increment. The experiments were optimised for J_{H-C} = 135 Hz with interpulse delay of 3 sec. The sample was not spinning during the experiment. Bird sequence with relaxation delay time of 600ms was used to suppress ^1H-^{12}C signals. Phase sensitive experiments were generated by the phase cycling programme, TPPI. Prior to fourier transformation, the initial data matrix of all experiments were zero-filled in each dimension and multiplied by a sine^2-bell function in both the t_1 and t_2 dimensions. The spectra were not symmetrized but the T_1 noise was eliminated by the programme Aurelia.

Heteronuclear Multiple Bond Coherence (HMBC) by Indirect Detection: For Pandamarilactone-32 and -31, a total of 256 blocks containing 2048 data points were collected using the pulse sequence of Summers *et al.*[179] The data were zero filled to 2048 x 4096. The delay in the pulse sequence was set at 0.056s (=1/2J), where J=9Hz is the long range coupling constant of interest. The data were processed in anabsolute value mode.

For Pandamarilactone-1, -2 and -32 (repeat), the pulse sequence by Summers *et al.*[179]was used and the experiment was optimised for J_{LRH-C} = 8.0Hz and the short-range coupling was supressed by Δ = 3.5 msec. An interpulse delay of 5 sec was applied and the sample was not spinning during the experiment.

7.5.3 Isolation of Alkaloids

Pandanus amaryllifolius ground leaves, 2000 g, were extracted exhaustively with 95% EtOH until negative with Mayer's

reagent. The alcoholic extract upon concentration under vacuo yielded a dark green a resinous material, 301.0g.

The alcoholic extract, 110.0 g., was partitioned between Et_2O and 5% H_2SO_4. The organic layer was dried over anhydrous Na_2SO_4, concentrated to give a green resinous extract. The water soluble was alkalinised with concentrated NH_4OH till pH 9 -10 and exhaustively extracted with $CHCl_3$. The $CHCl_3$ soluble fraction afforded a brownish green resinous material, 1.36 g. (1.24%).

Chromatography by tlc on silica developed in 5:1 ratio of $CHCl_3$:CH_3OH and visualised under UV_{254} and Dragendorff spray reagent showed at least five alkaloids, 4 of which appeared as minor components.

Isolation of the major alkaloids and possibly any of the minor alkaloids were carried out by column chromatography (gravity) eluting gradiently in $CHCl_3$ with increasing CH_3OH concentration. The crude alkaloidal fraction, 434.21 mg, gave 4 combined eluates with the first three least polar labelled as Pa-3A-1 (33.42 mg.), Pa-3A-2 (198.52 mg.), Pa-3A-3 (188.06 mg.), respectively.

The chromatogram on SGF_{254} developed in $CHCl_3$:CH_3OH (5:1) showed the fractions labelled as Pa-3A-1 and Pa-3A-2 to be quite clean. The third fraction labelled as Pa-3A-3, however, was observed to be a mixture based on its TLC chromatogram and its ^1H NMR spectrum. Both Pa-3A-2 and Pa-3A-3 showed the presence of a more polar band than any of the three alkaloids as observed from the tlc chomatogram. This polar band appeared as a dark band under UV_{254} and responded positively with Dragendorff reagent.

7.5.3.1 Purification and Spectroscopic Data of Pandamarilactone-1 (Pa-3A-1)

The fraction Pa-3A-1 was purified by PTLC developed in 20% hexane in $CHCl_3$. A dark blue band under UV_{254} was obtained as a light green resin, 7.10 mg. This isolate was further purified by reversed phase HPLC eluting isocratically in 80% CH_3CN in H_2O. A light yellow coloured eluate was obtained after approx. 25.0 min which upon concentration under vacuum yielded a yellow amorphous solid (2.58 mg) labelled as Pandamarilactone-1. On tlc, thiscompound gave an Rf 0.78 ($CHCl_3$:CH_3OH 5:1) or 0.66 ($CHCl_3$:EtOH 9:1)

UV (CH_3OH, 2.58 x 10^{-3}g/ml): λ_{max} 278.4 (Σ423.8), 234.8 (Σ628.9), 211.6 (Σ884.5).

MSFAB (glycerol) : 318 (M+1)

HREIMS : 317.1635 for $C_{18}H_{23}NO_4$ (DBE = 8).

IR (Film on NaCl disc): υ_{max}3392.2, 2921.9, 2852.7, 1764.0, 1695.3, 1455.9, 1379.3, 1262.4, 1056.1, 994.1, 802.1, 757.6 cm^{-1}.

$[\alpha]_D$ -33.0° (1.0 x 10^{-3} g/ml, CH_3OH)

7.5.4. Purification of Pa-3A-3

The third fraction Pa-3A-3 was eluted by column chromatography using $CHCl_3$ with increasing CH_3OH concentration and monitored by tlc. Eluates with similar tlc profile were combined together. These were then purified further by PTLC on SGF_{254} developed twice with $CHCl_3$:EtOH 95:5. Three bands were obtained, with the third alkaloid being the most polar appeared as a bright blue band under UV light.

Finally, Pa-3A-3 was purified by HPLC on reversed phase column using a linear gradient from water to CH_3CN at 1.0 ml/ min

with UV detection set at 254 nm. Two well resolved peaks were obtained after approximately 21.0 and 22.0 min, labelled as Pa-3A-31 and Pa-3A-32 with the latter being the major component.

7.5.4.1 Spectroscopic Data for Pandamarilactone-31 (Pa-3A-31).

colourless solid, m. pt.

MS (HREIMS), 333.1922, $C_{19}H_{27}NO_4$, DBE 8 CI 331

UV (CH_3OH): λ_{max} 294.6 (Σ1.793), 209.8 (Σ1.105)

IR (Film on NaCl disc): υ_{max}3413.2, 2923.4, 2854.1, 2362.6, 2335.3, 1764.5, 1667.5, 1550.5, 1446.6, 1354.0, 1296.4, 1196.6, 1057.5, 801.5, 756.9 cm^{-1}

$[\alpha]_D$ -2.0° (1 x 10^{-3} g/ml, CH_3OH)

7.5.4.2 Spectroscopic Data for Pandamarilactone-32 (Pa-3A-32)

LRFABMS and Electrospray : 299.0

MS (HREIMS) : 299.1521, $C_{18}H_{21}NO_3$ DBE = 9

UV (CH_3OH): λ_{max} 325.4 (A = 0.864), 278.6 (0.939), 230.0 (0.777), and 208.2 (1.040)

IR (Film on NaCl disc) :υ_{max}3413.2, 2923.4, 2854.1, 2362.6, 2335.3, 1764.5, 1667.5, 1550.5, 1446.6, 1354.0, 1296.4, 1196.6, 1057.5, 801.5, 756.9 cm^{-1}

IR ($CHCl_3$ solution): υ_{max}3031.5, 2932.3, 2857.3, 1764.3, 1710.5, 1667.5, 1580.6, 1440.0, 1361.7, 1240.0, 1188.3, 1063.1, and 842.3 cm^{-1}.

$[\alpha]_D$ 0.0°

7.5.5 Pandamarilactone-2 (Pa-3A-2)

Pa-3A-2 was purified initially by column chromatography. However, chromatography by preparative TLC on silica developed in 10% EtOH in $CHCl_3$ provided Pa-3A-2, 32.06 mg. The appearance of another band at a lower Rf than Pa-3A-2.had been observed during the purification of this alkaloid particularly in silica. This band, which gives a positive response with Dragendorff reagent, was later found to be the decomposition product of Pa-3A-2. A 2-D thin layer chromatography on silica showed that Pa-3A-2 is sensitive to acid and breakdowns to a more polar structure. This was further substantiated by the addition of a dilute acid to Pa-3A-2. The disappearance of Pa-3A-2 and the intense colouration with Dragendorff reagent of the more polar compound as observed from its tlc chromatogram suggested a complete conversion to the decomposition product.

Purification by column chromatography on alumina using hexane and $CHCl_3$ afforded Pa-3A-2 with the decomposition product still quite visible. Efforts to isolate a pure Pa-3A-2 failed, hence the structure elucidation of Pa-3A-2 was carried out together with the more polar isolate

LRFABMS: 315

UV (CH_3OH, c=0.02296 g/ml): λ_{max} 275.4 (Σ16408.51)

IR (Film on NaCl disc): υ_{max}3363.5, 2922.8, 2853.6, 2360.6, 2335.8, 1763.8, 1455.3, 1377.9, 1057.9 cm^{-1}

^{1}H NMR ($CDCl_3$, 90 MHz): δ6.96 (q, J1.8Hz, 1H,), 6.92 (q, J1.8Hz, 1H), 5.08 (t, J7.2Hz, 1H), 4.65 (m, J1.8Hz, 1H), 1.89 (m), 1.84 (br s, 1H), 1.80 (t, 1H), 1.79 (br s, 3H), 1.77 (t, 3H), and 1.58 (t, 3H).

7.6 Experimental Section for Chapter 6

7.6.1 Cultivation of the *Ipomoea muricata* Plant

Mature seeds of *Ipomoea muricata* were soaked in water overnight. The swollen seeds were allowed to germinate until about 5 cm in length, afterwhich the seedlings were transferred to individual pots. The plants were kept at a constant temperature of about 25°C in a glasshouse with regular watering. A slow-release fertilizer (Osmocote) was added into the soil to provide nutrients for the plant. Flowers started to bloom after 3 months.

7.6.2 Incorporation Time Determination

One week and two week old seed capsules were collected and ground in a mortar and pestle with the aid of some acid-washed sand. The seed capsules and sand mixture were packed on top of an alumina (neutral) column and extracted with the mixture of EtOH:H_2O:HOAc (90:9:1).[209] The eluate was monitored for alkaloids on tlc using silica (SGF_{254}) developed in 90% $CHCl_3/CH_3OH$ and visualised by UV_{254} and Dragendorff reagent.

7.6.3 Administration of Acetate-Labelled Precursor to *I.muricata*

An aqueous solution of [2-14C] acetate, sodium salt (Amersham, 54mCi/mmol, 1mCi/ml) was injected into one week or two week old seed capsules (40 seed capsules at 4.0 μCi/seed capsule) with a 1.0 ml insulin syringe. The seed capsules were vented by boring an approximately 1 mm diameter hole approximately 1/2 cm deep into the capsule to prevent explusion of injected material. After 3-4 weeks, the brown and dry seed

capsules were collected. The pale brown seeds, 16.0 g, were air dried and ground using a coffee grinder.

7.6.4 Extraction of Ipalbidine and Ipomine from *I. muricata*

The acetate-labelled ground seeds were soaked in 95% EtOH. Extraction was carried out until the alcohol extract was negative with Mayers reagent. The concentrated dark brown alcohol extract, 1.36 g, was partitioned between EtOEt and 5%H_2SO_4. The ether layer yielded a yellow oil, 0.9013 g, upon concentration. The acid layer was basified with concentrated ammonia to pH 9-10 and extracted with ethyl acetate. The EtOAc layer yielded a 58.86 mg of dark brown resinous material on evaporation. TLC of the ETOAc layer was carried out on SGF_{254}, developed in 90% $CHCl_3/CH_3OH$ and visualised in UV_{254} and Dragendorff reagent.

Isolation of the alkaloids from the EtOAc fraction was performed by preparative thin layer chromatography on silica plates (Merck 7731, 2 mm thickness) developed in 30% CH_3OH in $CHCl_3$. The three fluorescent bands under UV_{254} were scraped off, ultrasonicated in EtOAc, filtered and the filtrate concentrated under vacuum. Ipalbidine, the least polar band (R_f =0.58), obtained as a white solid 5.37 mg, was identified by comparison (tlc and ^1H NMR) with an authentic sample. Ipomine identified by comparison (tlc and ^1H NMR) with an authentic sample, was obtained in 6.20 mg yield as a pale yellow solid.

7.6.5 Radioactivity Measurements

(a) Sample Preparation

The different plant extracts and isolates were dissolved in CH_3OH (AR Grade). A 0.1 ml aliquot portion of the solutions were mixed with 3.9 ml OCS (Scintillation Liquid for Organic solvents). The homogenous solutions were kept in the dark for an hour before ^{14}C activity was determined via liquid scintillation counting for 5 minutes (Beckman LS 6000 Series Liquid Scintillation Counter). Average of three readings were reported.

Both ipalbidine and ipomine were purified by column chromatography on silica and elution with $CHCl_3$:CH_3OH:NH_3 (36:6:0.5). Ipalbidine was obtained in 1.85 mg yield while Ipomine yielded 3.00 mg of a yellow solid. The ^{14}C radioactivity was obtained by counting for 10 mins. Average of three readings were reported.

7.6.6 Administration of [U-^{14}C]Tyrosine to *I. muricata*

One week old capsules after flowering were selected. An aqueous solution of universally labelled tyrosine, L-[U-^{14}C] Tyrosine (Amersham, 486mCi/mol, 250μCi/5ml) was injected into a total of 67 seed capsules at a level of 2.5 μCi/seed capsule. The dried capsules containing the pale brown mature seeds of *I. muricata* were collected after 45 days. After air drying for several days, a total of 20.36 gms of seeds were obtained.

The alkaloids were isolated following the same fractionation procedure as mentioned in **6.431** using $CHCl_3$ instead of EtOAc to extract the tertiary alkaloids. The dark brown alcohol extract, 1.64 g. yielded a yellow oily EtOEt extract (1.12 g.) and 46.60 mg of $CHCl_3$

The alkaloids in the $CHCl_3$ fraction (43.80 mg) were isolated and purified by column chromatography on silica, eluting with $CHCl_3$:CH_3OH:NH_3 (36:6:0.5). Ipalbidine (3.45 mg) and Ipomine (2.02 mg) were isolated. Purification by column chromatography using the aforementioned conditions was carried out thrice until radiochemically pure isolates with a constant specific activity were obtained.

The preparation of sample for radioactive counting was carried out as described for the acetate-labelled alkaloids. All the extract and isolates were measured for ^{14}C radioactivity using liquid scintillation counting for 30 mins. Average of all three readings were reported.

APPENDIX 1

TWO DIMENSIONAL NMR SPECTROSCOPY

TWO DIMENSIONAL NMR SPECTROSCOPY

A.1.1 Double Quantum Filtered (DQF) COSY 2-D NMR

In this experiment two 90° pulses separated by time t_1 create double quantum coherence which is followed by a minimal duration fixed delay and then a third 90° pulse that converts the magnetisation back to observable single quantum magnetisation prior to acquisition during t_2.(Diagram 1).[100,101]

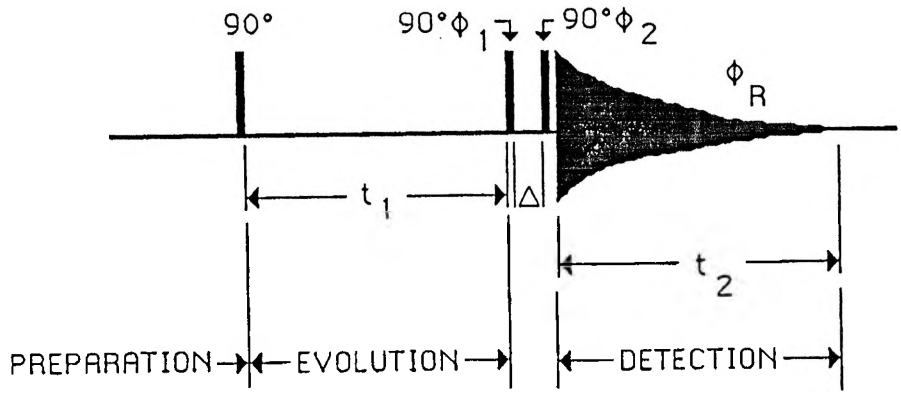

Diagram 1. Pulse Sequence for DQF COSY

A.1.2 Triple Quantum Filtered COSY

The pulse sequence is the same as that for the DQF COSY except that 45° phase shifts are used, instead of 90° phase shifts.[100,101]

A.1.3 Relay COSY

The pulse sequence for RCOSY builds on the pulse sequence for the COSY experiment (Diagram 2).[102]

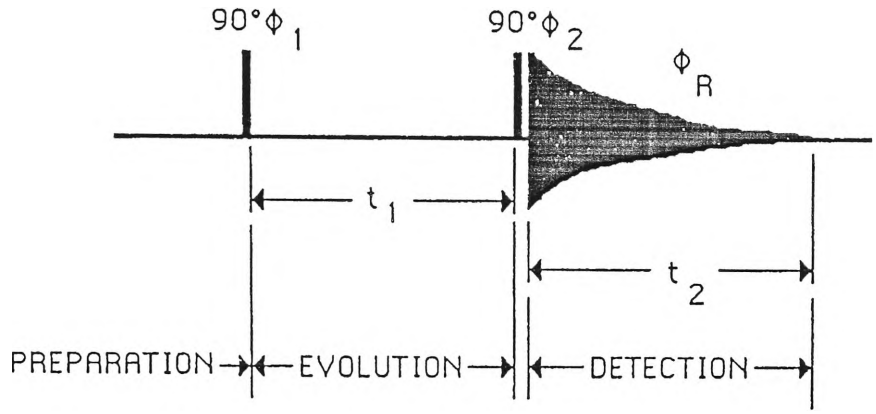

Diagram 2. COSY 90 Pulse Sequence.

In a RCOSY experiment, following the establishment of coherence between mutually coupled protons through the first two 90° pulse of the COSY sequence, magnetisation is then relayed to the next nearest neighbour protons via a mixing period, $-\tau_m-180°-\tau_m-90°-$. The 180° refocusing pulse located midway through the mixing period (after τ_m) serves to eliminate any further chemical shift evolution that would also transpire during the mixing period in the absence of the refocusing pulse (Diagram 3).

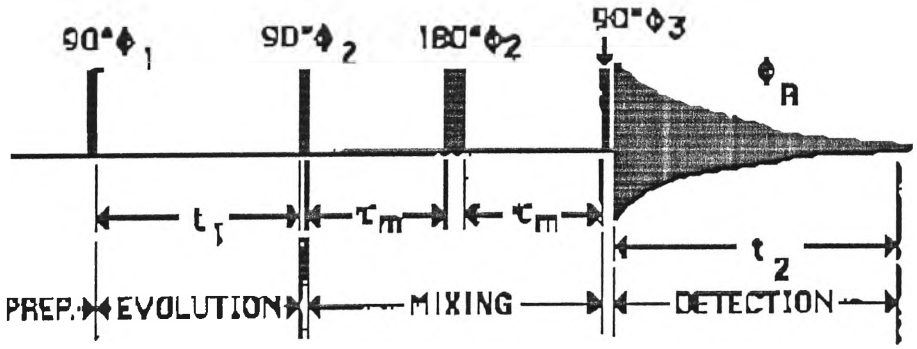

Diagram 3. Relay COSY Pulse Sequence.

The RCOSY responses can be further explained with a 3-spin AMX system where $J_{AX} = 0$. In a COSY experiment, the correlation

between A and M is established via J_{AM} and M and X via J_{MX}. Since $J_{AX} = 0$, no correlation between A and X will be observed in a COSY experiment. However, connectivity between A and X can happen through relayed coherence transfer. This can be observed through the coupling of both A and X to the intermediate M. Experimentally, this is achieved by inserting a mixing time, τ_m, after the establishment of the coherence between the vicinal coupled protons via the first 90° pulse. This mixing time allows the magnetisation to be relayed to the next neighbouring protons. The degree of magnetisation transfer is dependent on the value of J_{MX}. Thus, in setting up a RCOSY experiment, the value of the mixing time, τ_m, is important and an average value is used to cater for the variety of J values in the molecule.

A.1.4 Double Relay COSY

An inclusion of a second mixing period in a RCOSY pulse sequence extends the magnetisation to give the double relay.

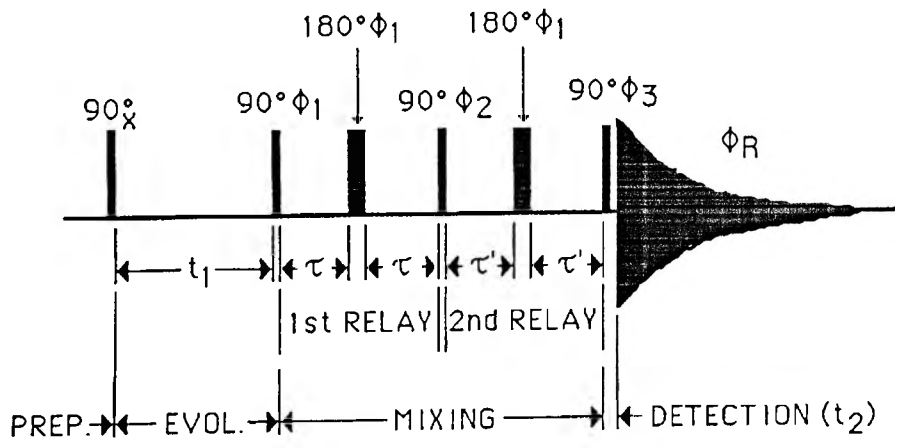

Diagram 4. Double Relay COSY Pulse Sequence.

A.1.5 Total Correlation Spectroscopy (TOCSY)

As shown in Diagram 5, an initial 90° pulse which is phase cycled to suppress axial responses and quadrature phase images, is followed by an evolution time, t_1, incremented in the usual fashion to digitise the second frequency domain. The second 90° pulse common to the COSY pulse sequence is replaced by a mixing interval during which isotropic mixing and hence coherence transfer occurs. The mixing period provides efficient suppression of chemical shift terms with energy matching to allows spin exchange to occur. A variety of sequences of pulses may be applied to satisfy these requirements. The mixing period may consist of a single pulse, a series of pulses of constant phase to provide a spin lock or one of the sequences of phase shifted pulses. The latter, a MLEV-16 pulse train[104] was used in this experiment. The extent of the transfer of coupling is dependent on the length of the mixing intervals. Thus, this experiment is analogous to the multiple-step RELAY experiment. If a sufficient length of mixing interval is used then responses for all members of a spin system, even those without direct coupling, will be observed; hence the basis of the name TOCSY.

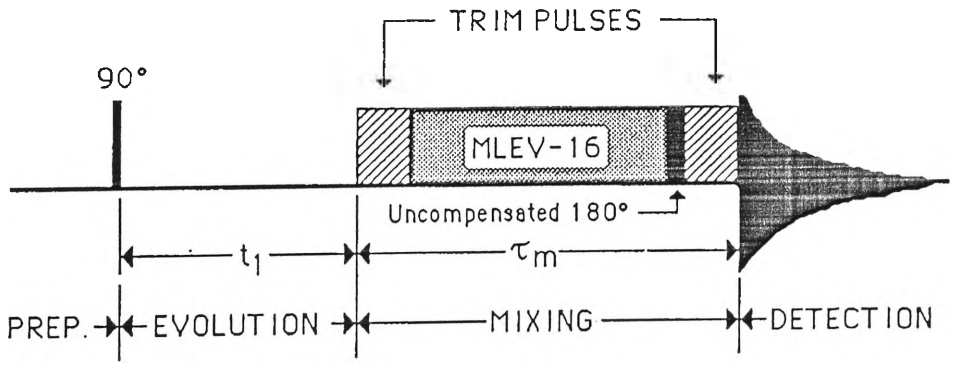

Diagram 5. Total Correlation Spectroscopy Pulse Sequence

A.1.6 Nuclear Overhauser Enhancement Spectroscopy (NOESY) and Rotating-Frame Overhauser Enhancement Spectroscopy (ROESY)

A NOESY experiment provides the dipolar or spatial relationships between protons. Its pulse sequence (Diagram 6) is the same as that used for DQF COSY aside from the introduction of τ_m, thus various coherence transfers maybe present. The occurence of crosspeaks arising from scalar correlation may be observed on the NOESY spectrum which may lead to a misinterpretation of the observed crosspeaks.

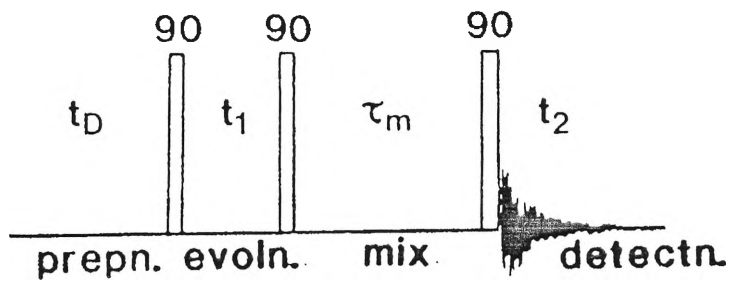

Diagram 6. NOESY Pulse Sequence.

The ROESY or the spin-locked NOE experiment (Diagram 7) is used to provide through-space connectivity between the various networks of coupled protons. However, the occurrence of crosspeaks arising from COSY and HOHAHA (TOCSY) coherence transfer can also be observed. This problem is improved by holding the magnetisation to the xy plane with a so-called spin lock which is actually a continuous irradiation with a radio-frequency field of medium strength. With the spin-locked nOe experiment, nOes are always positive and the crosspeaks due to relayed nOe (from spin A, via M to X) are in-phase with the diagonal peaks and are therefore readily distinguished from

direct nOes which are inverted relative to the diagonal peaks. Also, the scalar correlations can be differentiated from the transverse nOe signals since the nOes are in opposite phase with the COSY and HOHAHA crosspeaks.

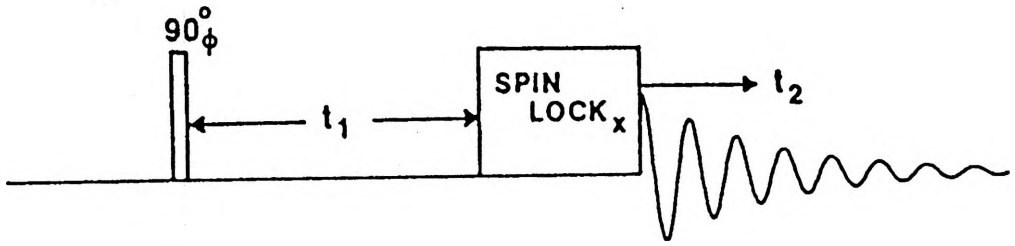

Diagram 7. ROESY Pulse Sequence with spin-locking.

A.1.7. Inverse-Detection Direct Heteronuclear Multiple Quantum Coherence (HMQC)

The pulse sequence (Diagram 8) used in the inverse-detection direct (one-bond) HMQC was based on that described by Summers.[179] The signals from protons bound directly to ^{12}C are first inverted by the BIRD pulse at the beginning of the pulse sequence. This component of magnetisation was allowed to relax longitudinally during the null delay, which was set at 300ms. The

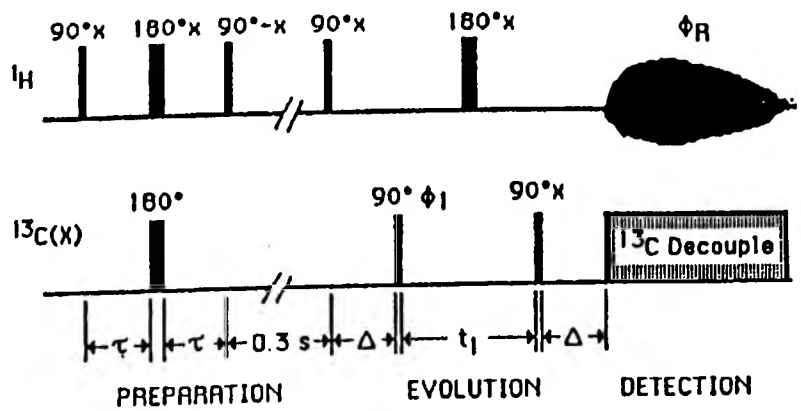

Diagram 8. HMQC Inverse Detection Pulse Sequence.

90° proton pulse, followed by Δ (interpulse delay) later by the 90° carbon pulse, creates heteronuclear multiple quantum coherence that is allowed to evolve during the evolution time period, t_1. The 180° proton pulse midway through the evolution period interchanges zero- and double-quantum coherence terms while simultaneously affording broadband decoupling in F_1. The final 90° carbon pulse converts the evolved multiple quantum coherence into observable single-quantum proton coherence, which is antiphase upon creation.

In principle, the observed ^1H signals are modulated not only in amplitude by the ^{13}C shifts, but also slowly in phase by the homonuclear scalar ^1H coupling.

A.1.8 Inverse-Detection Long Range Heteronuclear Multiple Bond Correlation (HMBC)

The HMQC experiment does not provide assignment information for non-protonated carbon. Also, for the case of exactly overlapping ^1H resonances, the HMQC experiment does not provide the unambiguous ^{13}C resonance assignment. However, couplings between two- and three-bonds can be acquired by long range Heteronuclear Multiple Bond Correlation (HMBC) NMR technique.

Inverse-detected long range HMBC 2-D NMR technique provides structural information unobtainable only a few years ago. This technique provides the means to span heteroatoms and quaternary carbons, thus giving the chemist extremely powerful information that can link structural fragments together through intervening quaternary carbons.

The pulse sequence used for the HMBC experiment is that described by Summers[179] and is shown in Diagram 9.

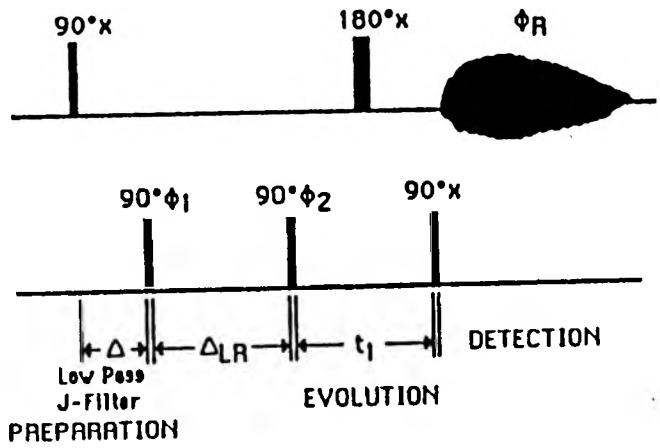

Diagram 9. HMBC Inverse Detection Pulse Sequence.

The first 90° ^{13}C pulse, applied at time Δ_1 ($=1/2^1J_{CH}$) after the first 90° proton pulse, serves to suppress one-bond correlation in the 2D spectrum. This 90° ^{13}C pulse generates heteronuclear multiple-quantum coherence for protons directly attached to ^{13}C, which is removed from the spectrum by alternating the phase of the pulse along the + axis, without changing the phase of the receiver. The second 90° ^{13}C pulse, applied at time Δ_2 later, creates the multiple bond, multiple-quantum coherence of interest. In principle the optimum choice of Δ_2 is $1/2^nJ_{CH}$, where $^nJ_{CH}$ is the long-range coupling constant of interest.

A.1.10 Attached Proton Test (APT)

The Attached Proton Test experiment is related to the refocused INEPT experiment in which a multiplicity selection effected via a spin echo is preceded by a polarization transfer from protons to carbon. The pulse sequence for APT used in this work is shown in Diagram 10.

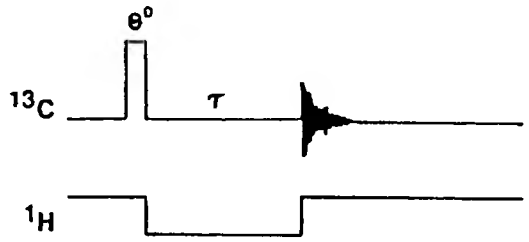

Diagram 10. Attached Proton Test with Delayed Acquisition.

APPENDIX 2

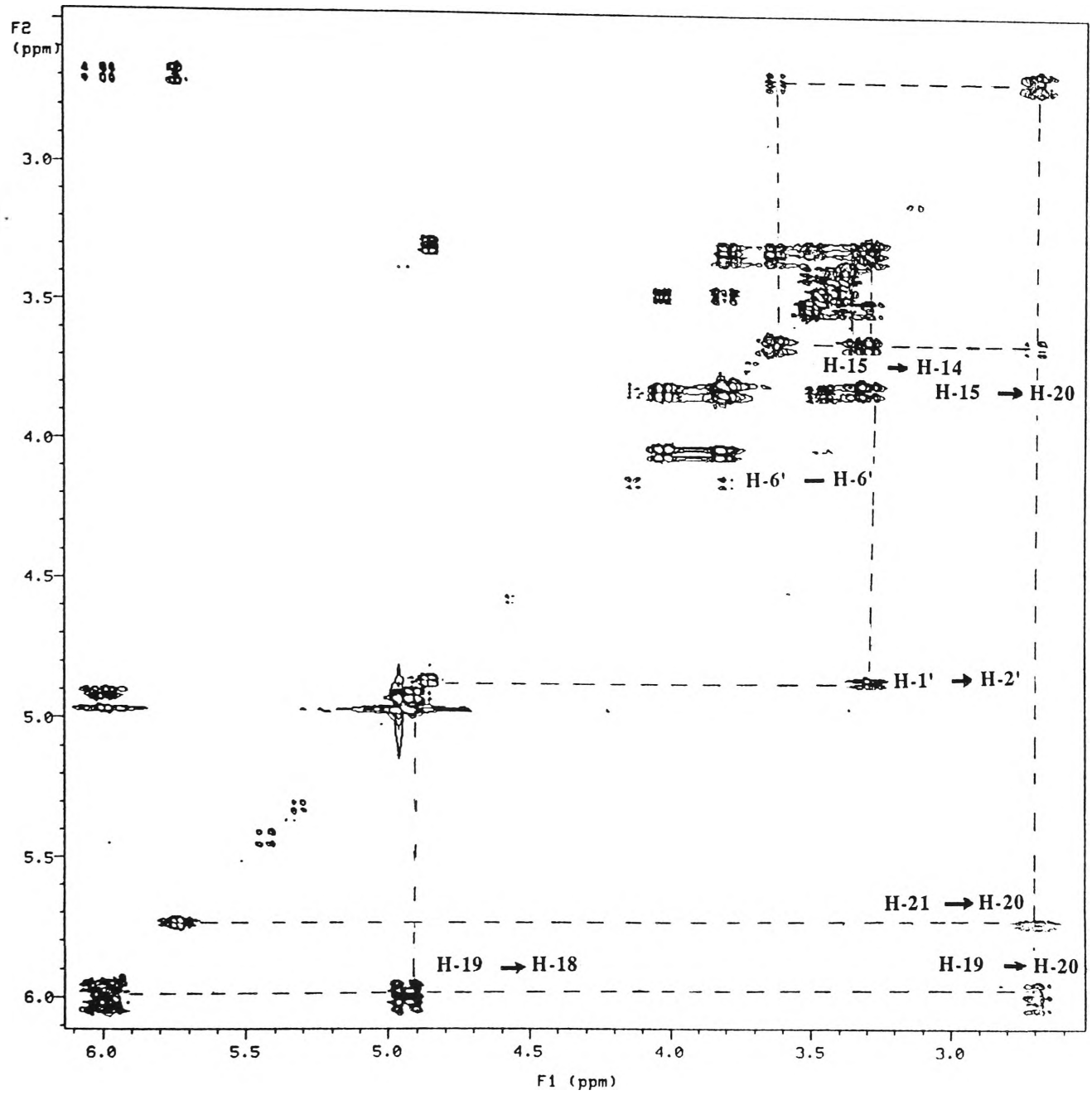

Appendix 2.1. ^{1}H-^{1}H COSY NMR Spectrum of Oa-4A-1 [400 MHz, CD_3OD, referenced relative to δ3.35].

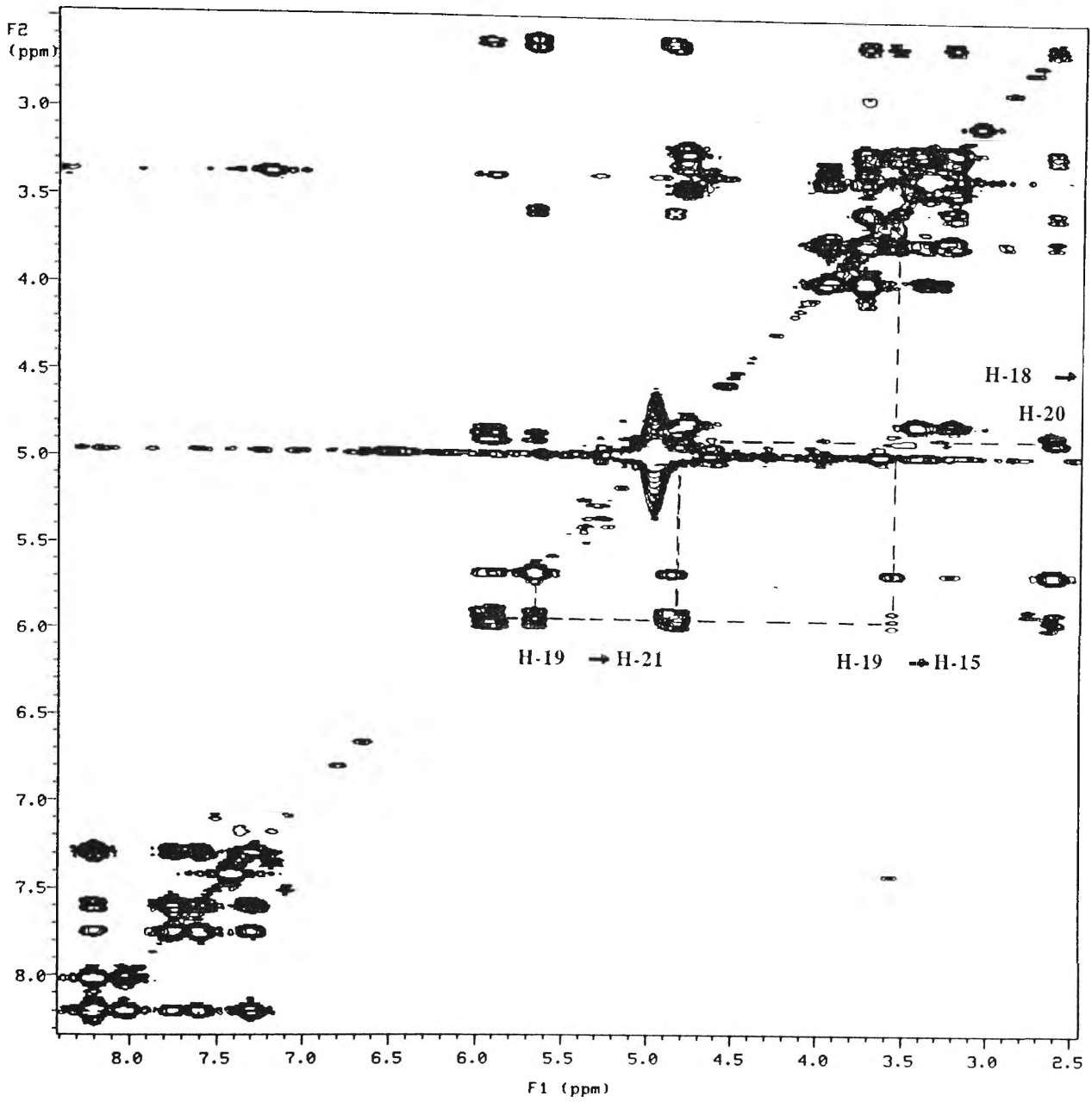

Appendix 2.2. 2RCOSY NMR Spectrum of Oa-4A-1 [400 MHz, CD_3OD, referenced relative to δ3.35].

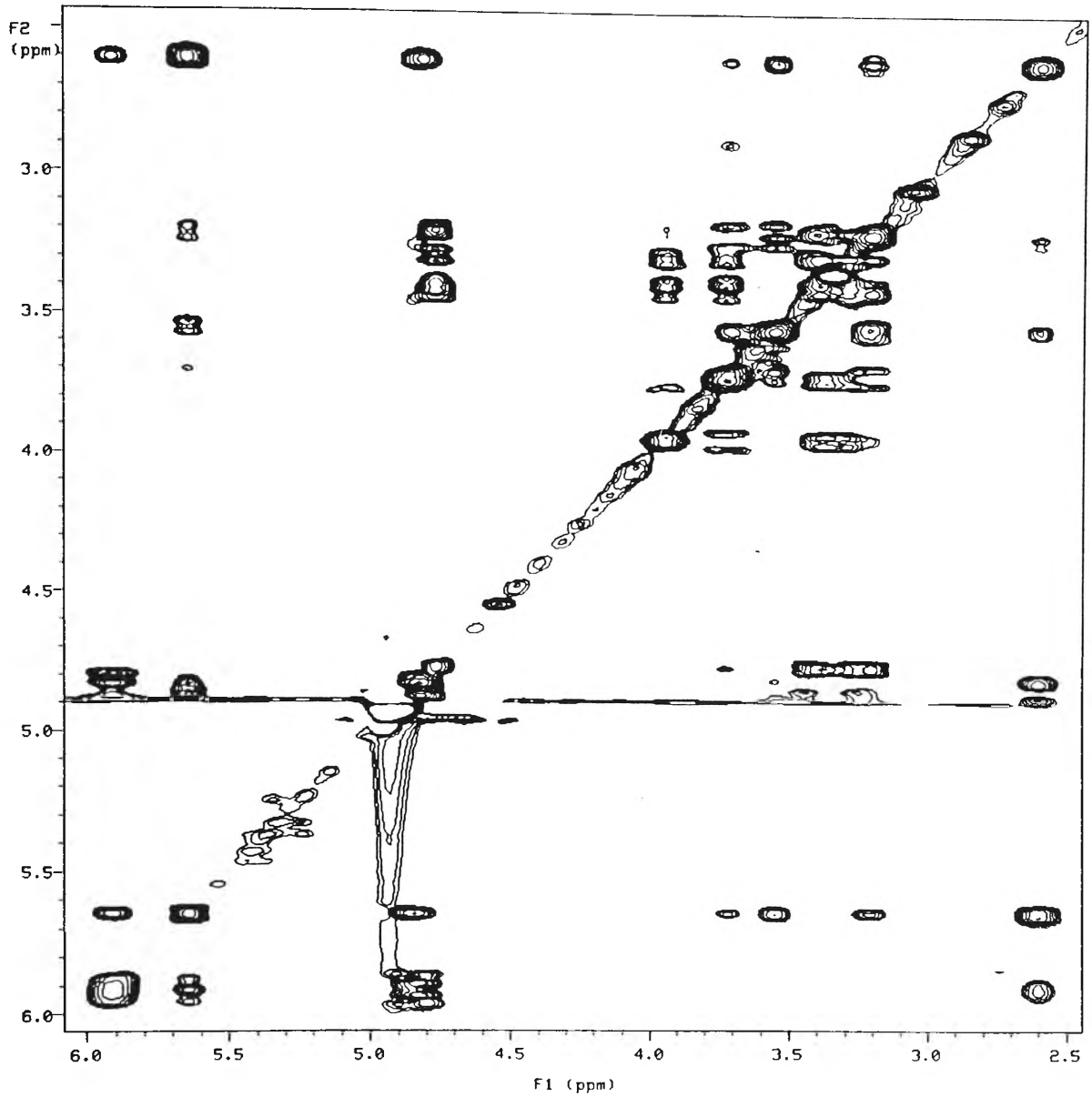

Appendix 2.3. TOCSY NMR Spectrum of Oa-4A-1 [400 MHz, CD_3OD, referenced relative to δ3.35].

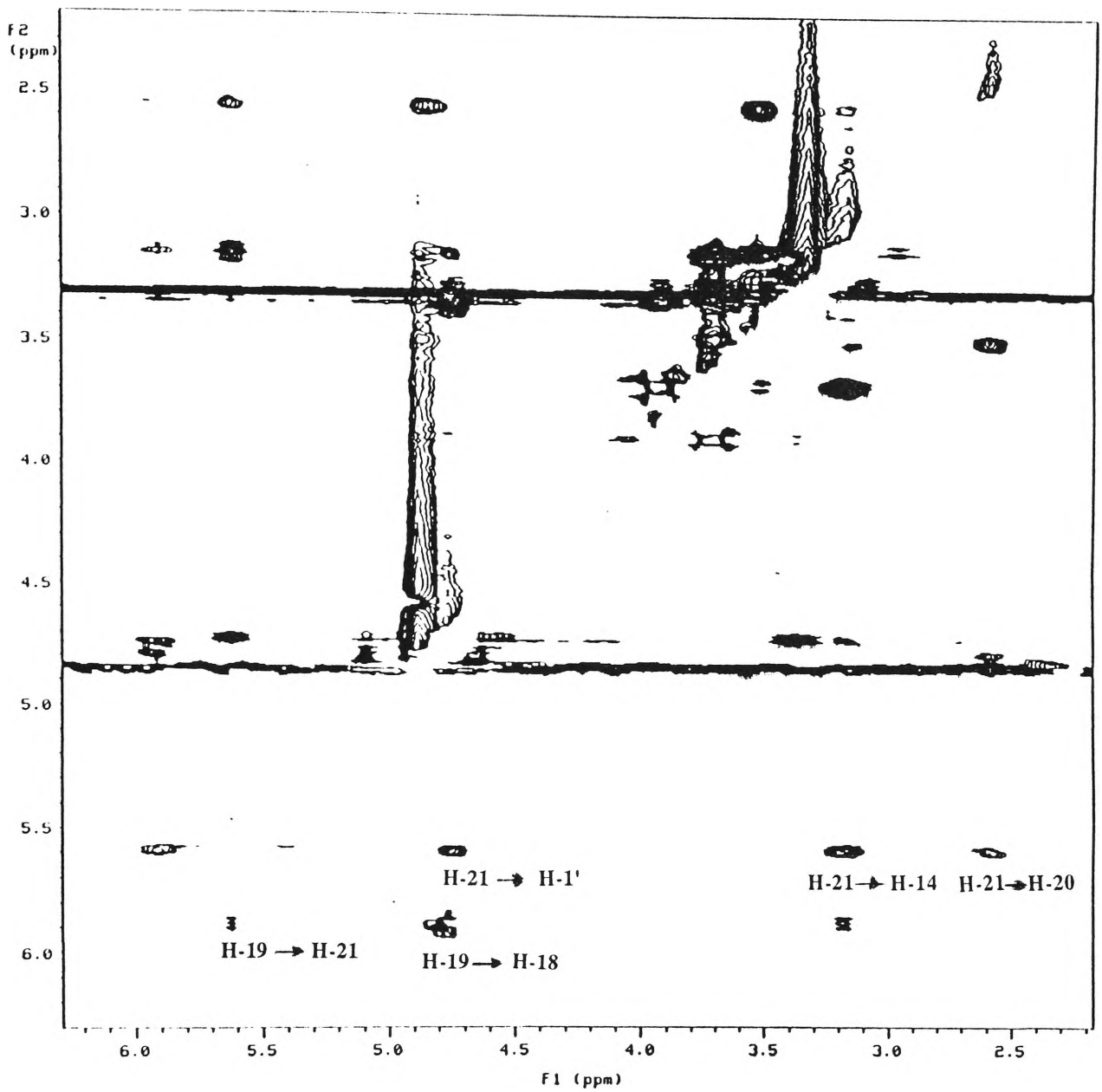

Appendix 2.4. NOESY NMR Spectrum of Oa-4A-1 [400 MHz, CD_3OD, referenced relative to δ3.35].

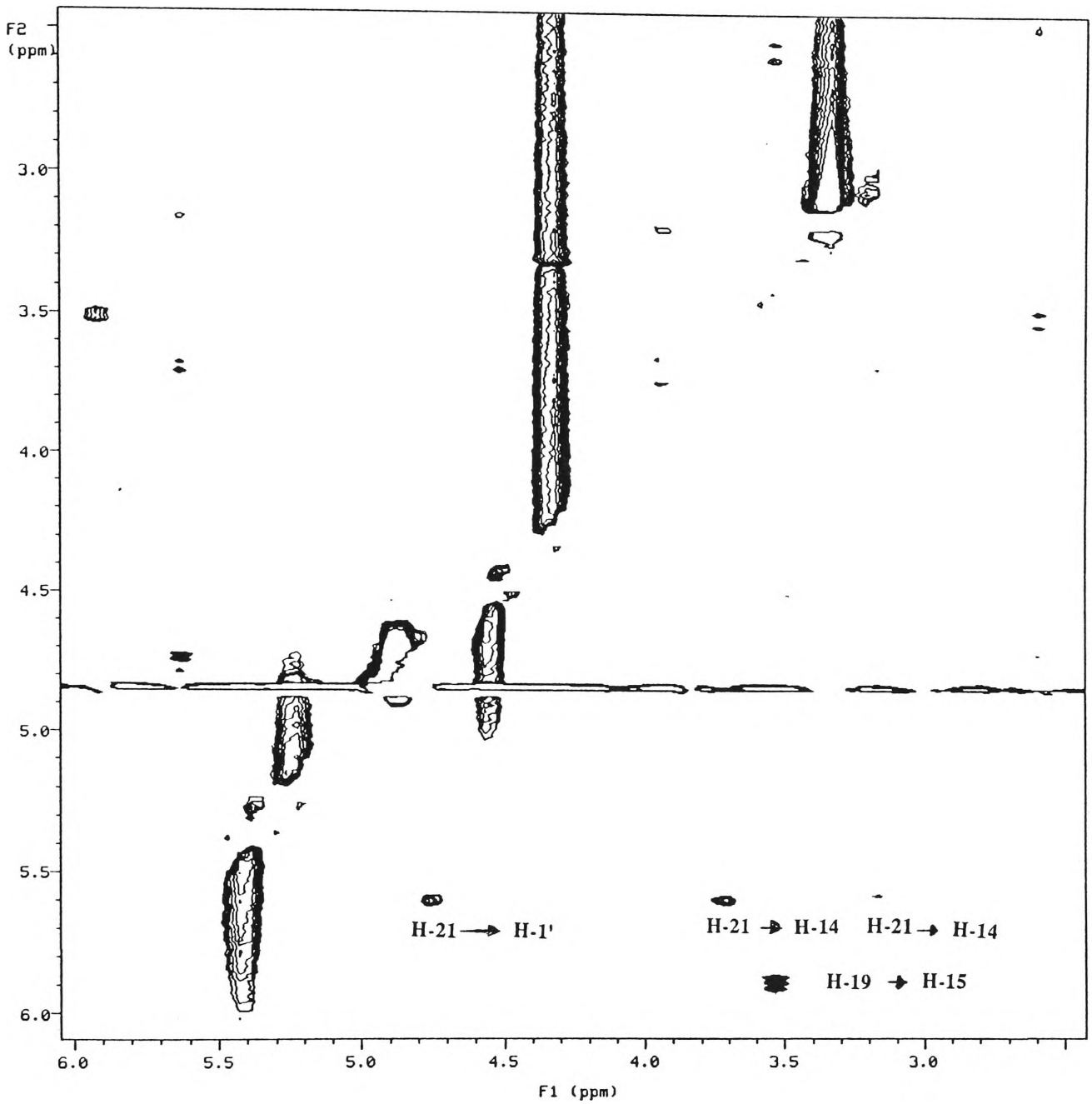

Appendix 2.5. ROESY NMR Spectrum of Oa-4A-1 [400 MHz, CD_3OD, referenced relative to δ3.35].

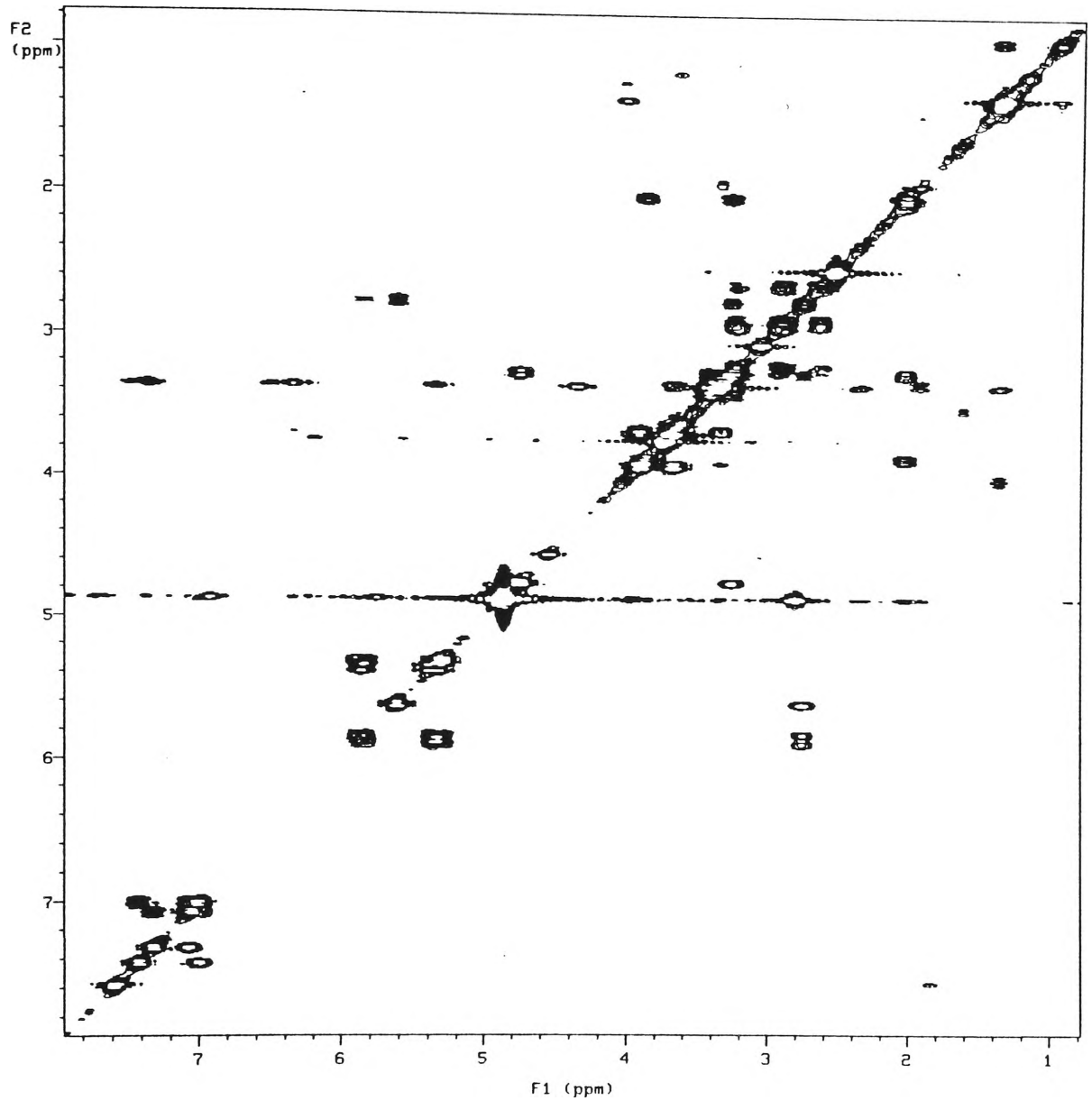

Appendix 2.6. ^{1}H-^{1}H COSY NMR Spectrum of Oa-WS-Me-II [400 MHz, CD_3OD, referenced relative to δ3.35].

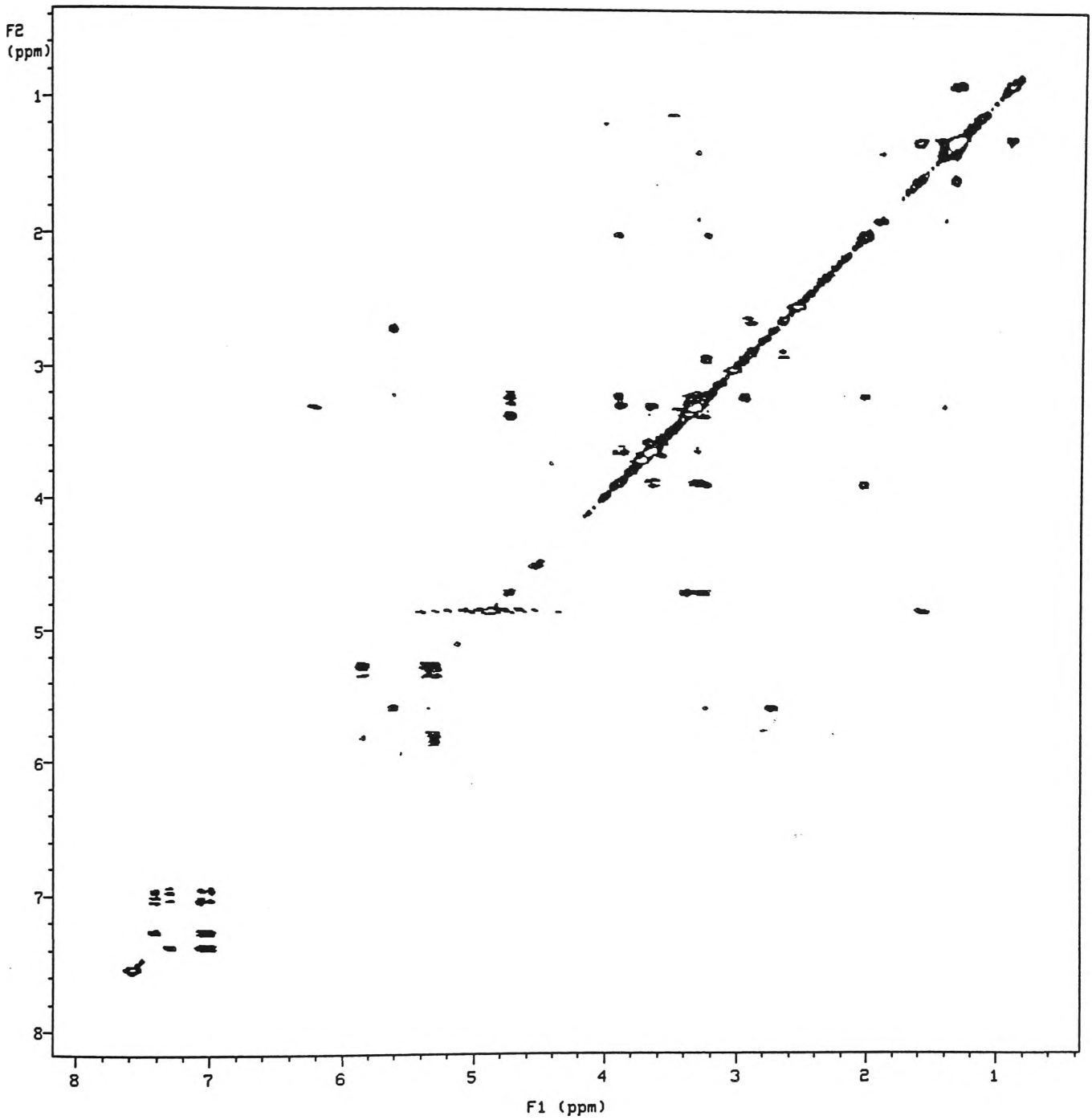

Appendix 2.7. TOCSY NMR Spectrum of Oa-WS-Me-II [400 MHz, CD_3OD, referenced relative to δ3.35].

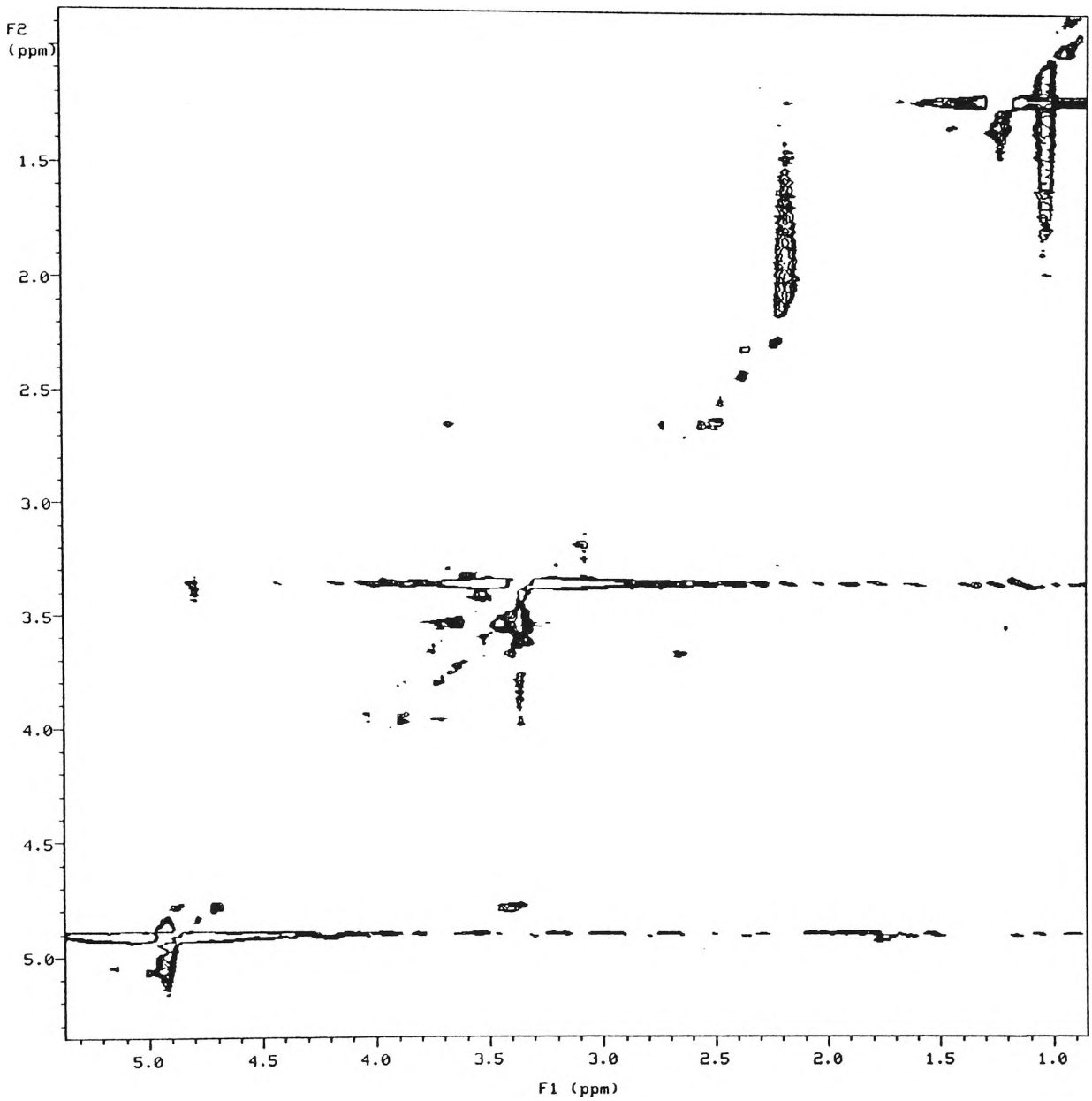

Appendix 2.8. ROESY NMR Spectrum of Oa-WS-Me-II [400 MHz, CD_3OD, referenced relative to δ3.35].

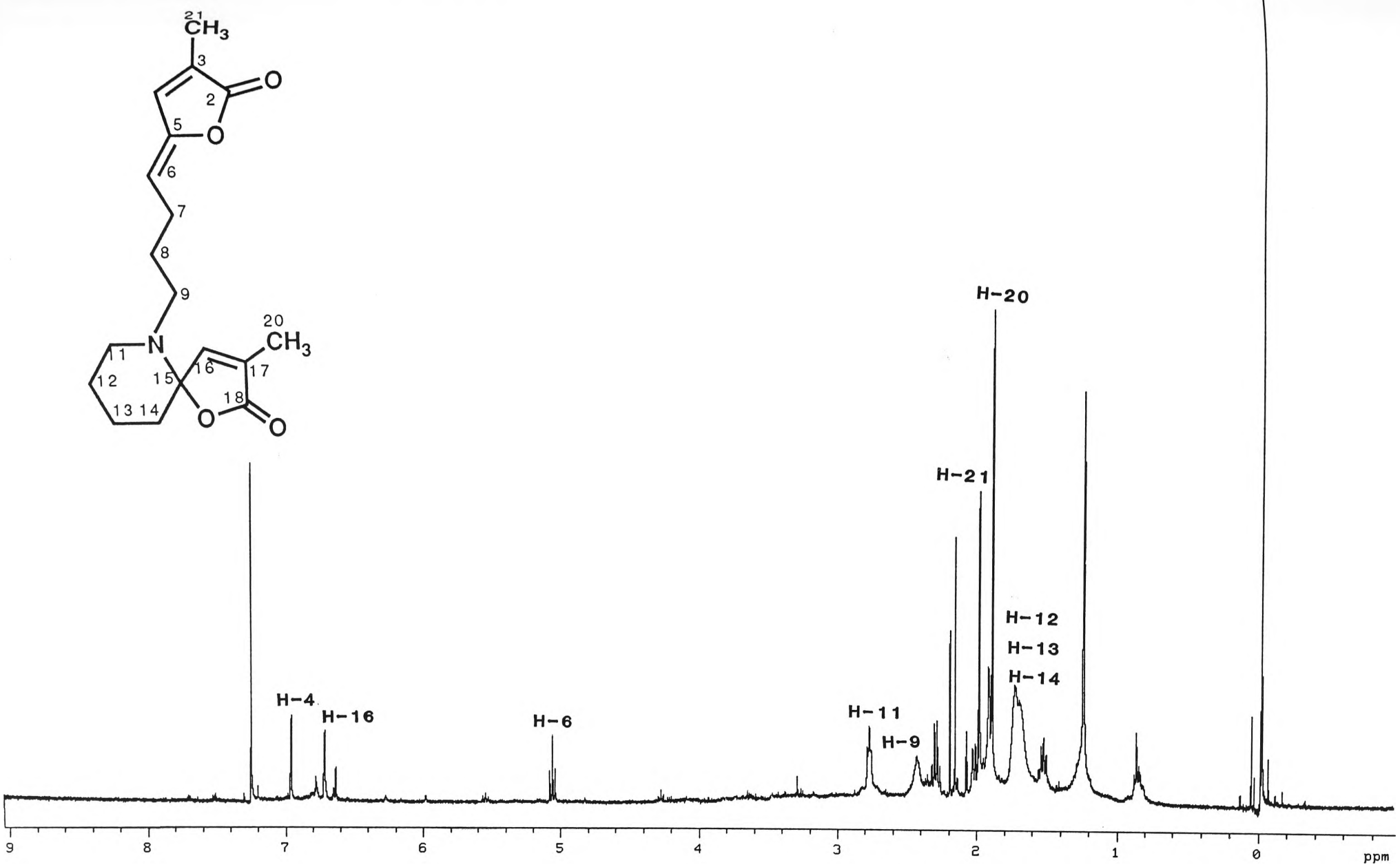

Appendix 2.9. ^{1}H NMR Spectrum of Pandamarilactone-1 [400 MHz, $CDCl_3$, referenced at δ7.25].

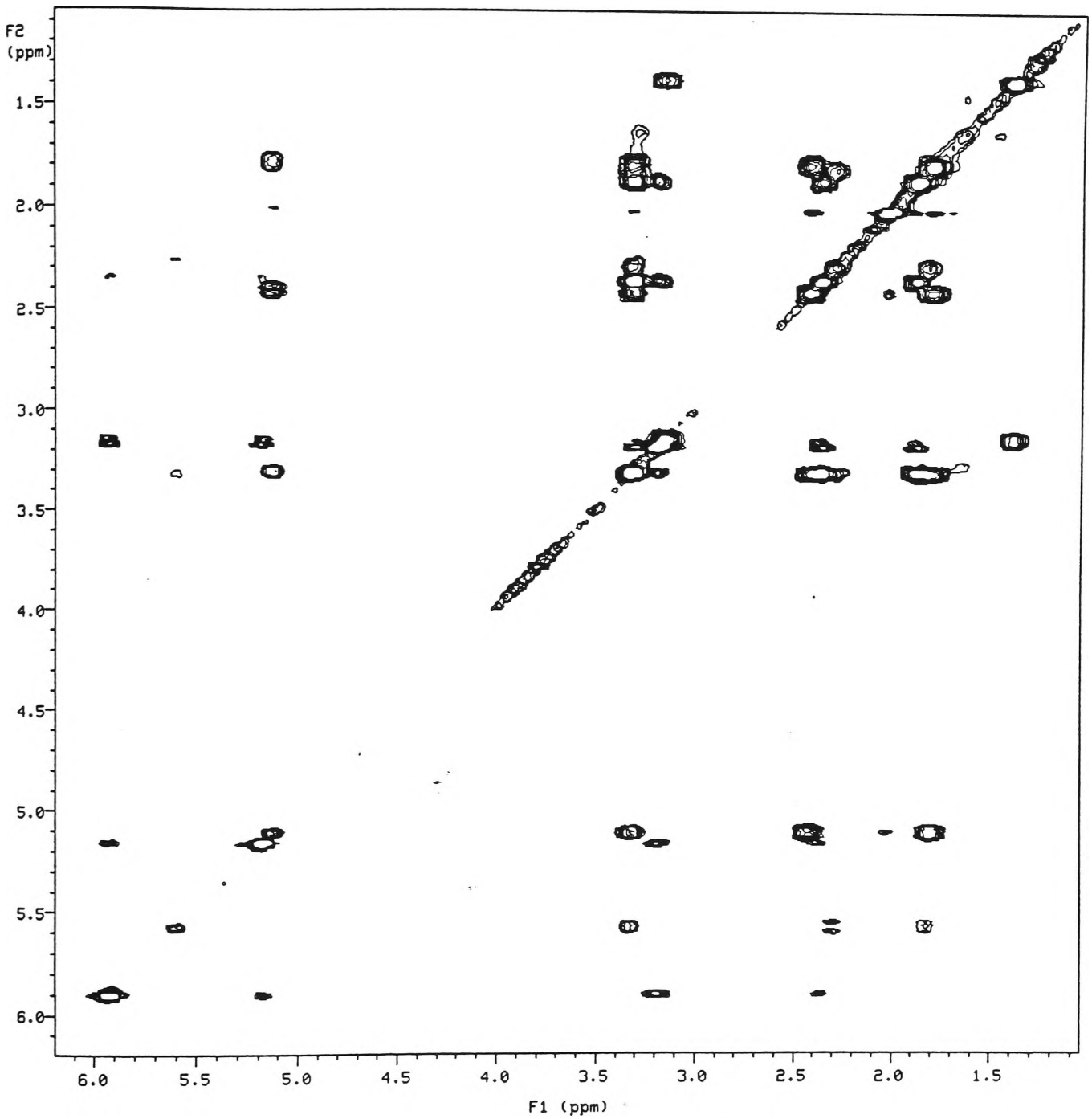

Appendix 2.10 TOCSY NMR Spectrum of Pandamarilactone-32 [400 MHz, CD_3OD, referenced at δ3.35].

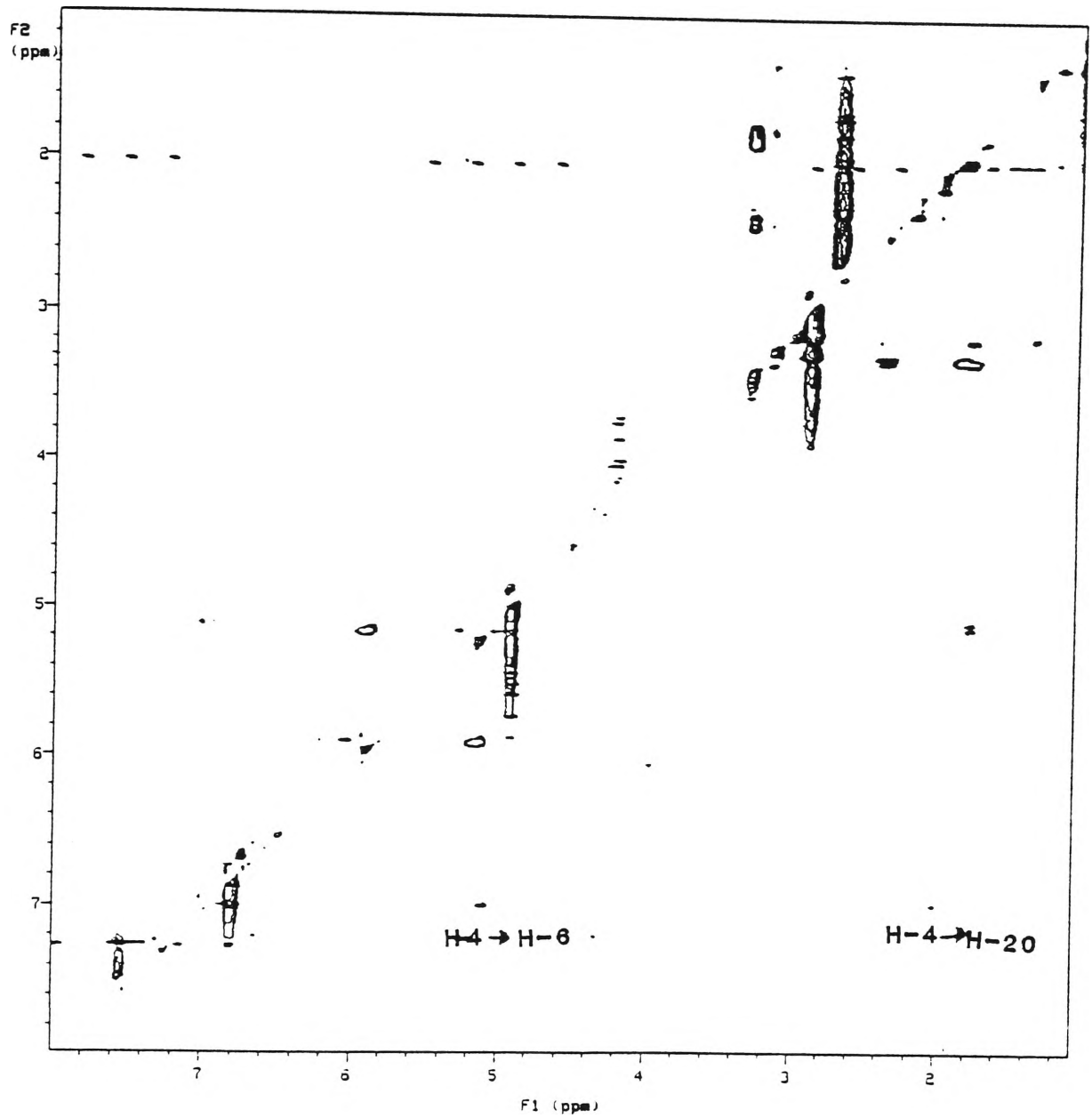

Appendix 2.11 ROESY NMR Spectrum of Pandamarilactone-32 [400 MHz, CD_3OD, referenced at δ3.35].

APPENDIX 3
CALCULATIONS

A3.1 Circular Dichroism

$$CD = \Delta\Sigma = h \times S / 3.2982 \times C \times 10^4 \times l$$ where,

$\Delta\Sigma$ = dichroic absorption

h = height in mm

S = m^o/cm

c = mole/dm^3 or mole/liter

l = cell path in cm

A3.2 Biosynthesis Studies

$$\% \text{ Incorporation} = \frac{\text{Amount of } ^{14}C \text{ recovered}}{\text{Amount of } ^{14}C \text{ Incorporated}} \times 100$$

$$\text{Dilution Factor} = \frac{\text{Specific Activity of Precursor in } \mu Ci/mmole}{\text{Specific Activity of Product in } \mu Ci/mmole} \times \text{Number of Labelled Sites}$$

REFERENCES

1. Bu'Lock, J. D., (1965) Biosynthesis of Natural Products, McGraw-Hill, Maidenhead.
2. Geissman, T. A. and Crout, D. H. G., (1969) Organic Chemistry of Secondary Plant Metabolism. Freeman, Cooper and Company, U.S.A.
3. Herbert, R. B., (1981) The Biosynthesis of Secondary Metabolites, Chapman & Hall, London and N. Y.
4. Mann, J., (1978) Secondary Metabolism, Clarendon Press, Oxford.
5. Haslam, E., (1985) Secondary Metabolism, Clarendon Press, Oxford.
6. Luckner, M., (1972) Secondary Metabolism in Plants and Animals, Academic Press, New York.
7. Swain, T., (1974) Biochemical Evolution in Plants. In: Comprehensive Biochemistry (Florkin, M and Stotz, E. H. eds), Vol 29A, Elsevier, Amsterdam.
8. Whittaker, R. H., (1970) The Biochemical Ecology of Higher Plants. In: Chemical Ecology (Sandheimer, E. and Simeone, J. B. eds) Academic Press, New York.
9. Lee, H. J. and Waller, G. R., (1972) *Phytochem.* **11**, 965.
10. Fairbairn, J. W. and Suwal, P. N.,(1962) *Phytochem.* **1**, 38.
11. Fairbairn, J. W. and Wassel, G. M., (1964) *Phytochem.* **3**, 253.
12. Fairbairn, J. W. and Wassel, G. M., (1967) *J. Chem. U. A. P.* **10**, 275.
13. Skursky, L. Burleson, D. and Waller, G. R., (1969) *J. Biol. Chem.* **244**, 3238.
14. Barz, W. and Hoesel, W., (1979) Recent Advances in Phytochemistry. In: Biochemistry of Plant Phenolics (van

Sumere, C, Swain, T and Harborne, J. B. eds.) Vol 12, Plenum Press, N. Y., p.339.

15. Seigler, D. S., (1977) Primary Role for Secondary Compound. In: Biochemical Systematics and Ecology Vol.5, p.195.
16. Robinson T., (1973) *Phytochem. Bull.* **6**, 5.
17. Fraenkel, G. S., (1959) *Science* **125**, 1466.
18. Robinson, T., (1974) *Science*, **184**, 430.
19. Mothes, K., (1966) *Naturwissen Schaffen* **53**, 317-23.
20. Hegnauer, R., (1966) Comparative Phytochem. of Alkaloids. In: Comparative Phytochem. (Swain, T. ed) pp.211-30 Academic Press, New York.
21. Hughes, D. W. and Genert, K., (1973) " Alkaloids" In Phytochemistry: The Process and Products of Photosynthesis (Miller, L. P. ed.) Vol. 1 Van Nostrand Reinhold Co. New York. p.118-170.
22. Manske, R. H. F., The Alkaloids: Chemistry and Physiology Academic Press, New York.
23. Haslam, E., (1974) "*Shikimate Pathway*", Butterworths, London.
24. Farnsworth, N. R., (1966) *J. Pharm. Sci.* **55**, 225.
25. De Leon, G. V., Arambulo, A. S., Bernal-Santos, R. M. and Javier, E., (1966) *Acta Med. Phillipina*, **3**, 121.
26. Popp. F. D., Wefer, J. M., Rosen, G. and Noble, A. C., (1967). *J. Pharm. Sci.* **56**, 1195.
27. Le Men, J and Taylor, W. I., (1965) *Experientia*, **21**, 508.
28. Mothes, K., (1966) *Lloydia* **29**,156.
29. Hegnauer, R., (1963) in "Chemical Plant Taxonomy (Swain, T. ed.). Academic Press, N. Y., p.389.

30. Cordell, G. A., (1981) Introduction to Alkaloids: A Biogenetic Approach, John Wiley and Sons, N. Y.

31. Dalton, D., (1979) The Alkaloids: The fundamental Chemistry, A Biogenetic Approach, Marcel Dekker, Inc.

32. Ohmoto, T. and Koike, K., (1988) *Shoyakugaku Zasshi*, **42**(2), 160.

33. Al-allaf, T. A. K., Ayoub, M. T. and Rashan, L. J., (1990) *J. Inorg. Biochem.*, **38**, 47.

34. Pezzuto, J., Lau, P., Luh, Y., Moore, P., Wogan, G. and Hecht, S., (1980) *Proc. Nat'l Acad. Sci. USA*, **77**, 427.

35. Leavitt, R., Legauerent, C., Nevert, D. and Pelkonen, O., (1977) *Biochem. Biophys. Res. Comm.* **79**, 1167.

36. Rashan, L. J., (1990) *Fitoterapia*, **56**, 153.

37. Ho, B. T., McIsaac, W. M., Walker, K. E. and Estevez, V., (1968) *J. Pham. Sci.* **57**(2), 269.

38. McIsaac, W. M. and Estevez, V., (1966) *Biochem. Pharmacol.*, **15**, 1625.

39. Kernack, W. O., Perkin, W. N. and Robinson, R., (1921) *J. Chem. Soc.*, **119**, 1602.

40. Hopkins, F. G. and Cole, S. W., (1903) *J. Physiol.* **29**, 451.

41. Fischer, O., (1901) Festschrift Zum 80. Geburtstag des Prinzregenten Luitpold, Erlangen.

42. Spath, E., (1920), *Monatsh*, **41**, 401.

43. Spath, E., (1919) *Monatsh*, **40**, 351.

44. Asahina, Y. and Osada, S., (1926) *J. Pharm. Soc. Japan*, **63**, 534.

45 Hahn, G. and Gudjons, H. F., (1938) *Ber.* **71**, 2175.

46. Spath, E. and Ledener, E., (1930) *Ber.* **63**, 120.

47. Tatsui, G., (1928) *J. Pharm. Soc. Japan*, **48**, 453.

48. Menshikov, G. P., Gunevitch, E. L. and Samsonova G. A., (1950) *J. Gen. Chem.* USSR, **20**, 1927.

49. Ungenack, F., DiPierro, M., Weber, R. and Cook, J. M., (1981) *J.Org. Chem.*, **46**, 164.

50. Perkin Jr., W. H., and Robinson, R., (1919) *J. Chem. Soc.* **115**, 933.

51. O'Donovan, D. G. and Kenneally, M. F., (1967) *J. Chem. Soc. C*, 1109.

52. Slaytor, M. and MacFarlane, I. J., (1968) *Phytochem.*, **7**, 605.

53. Stolle, K. and Groger, O., (1968) *Arch. Pharm (Weinheim)* **301**, 561.

54. Kompis, I., Hesse, M. and Schmid, H., (1971) *Lloydia*, **34**(2), 269.

55. Battersby, A. R., Binks, R., Lawrie, W., Parry, G. V. and Webster, B. R., (1963). *Proc. Chem. Soc. London*, 369.

56. Battersby, A. R., Binks R., Lawrie, W., Parry, G. V. and Webster, B. R., (1965) *J. Chem. Soc.*, 7459.

57. Stolle, K., Groger, D. and Mothes, K., (1965) *Chem. Ind. (London),* 2065.

58. Barton, D. H. R., Kirby, G. W., Prager, R. H., and Wilson, E. M., (1965) *J. Chem. Soc.*, 3900.

59. Kutney, J. P., Bick, J. F., Nelson, V. R., Stuart, K. L. and Bose, A. K., (1970) *J. Amer. Chem. Soc.*, **92**, 2174.

60. Battersby, A. R., Brown, R. T., Kapil, R. S. Plunkett, A. O. and Taylor, J. B., (1966) *J.C.S Chem. Comm.*, 46.

61. McCapra, F., Money T., Scott, A. I. and Wright, I. G., (1965) *Chem. Comm.*, 537.

62. Arigoni, D. and Goeggel, H., (1965) *Chem. Comm.* 538.

63. Battersby, A. R., Burnett, A. R., and Parsons, P. G., (1969) *J. Chem. Soc (C)* 1193.

64. Stockigt, J. and Zenk, H. M., (1977) *JCS Chem. Comm.* 646.

65. Treimer, J. F. and Zenk, H. M., (1978) *Phytochem.* **17**, 227.

66. Stockigt, J. and Zenk, H. M., (1977) *FEBS Letters* **79**, 233.

67. Stockigt, J., (1979) *Phytochem.* **18**, 965.

68. Battersby, A. R., Lewis, N. G. and Trippett , J. M., (1978) *Tetrahedron Letters* 4849.

69. Scott, A. I., Lee, S. I., DeCapite, P., Culver, M. G. and Hutchinson, C. R., (1977) *Heterocycles* **7**, 979.

70. Brown, R. T., Leonard, J. and Sleigh, S. K., (1978) *Phytochem.* **17**, 899.

71. Agarwal, K. P. and Dhar, M. M., (1959) *Journal of Scientific and Industrial Research (India)* **18B**, 114-115.

72. Tafur, S., Nelson, J. D., DeLong, D. C. and Svoboda, G. H., (1976) *Llyodia* **39**(4), 261.

73. Wall, M. E., Wani, M. C., Cook, C. E., Palmer, K. H. McPhail, A. T. and Sim, G. A., (1966) *J. Am. Chem. Soc.*, **88**, 3888.

74. Agawal, J. S. and Rastogi, R. P., (1973) *Indian J. Chem.* **11**,969.

75. Becker, Y. and Olshevsky U., (1973) *Israel J. Med. Sci.* **9**, 1578.

76. Horwitz, S. B., (1975) Camptothecin in Sartollei, A. C. and D. G. Johns, Antineoplastic and Immunosuppressive Agents Part II. Springer- Verlag, N. Y., p.649.

77. Fujita E. and Sumi, A., (1967)*Yakugaku Zasshi* **87**, 1153.

78. Aimi, N., Tsuyuki, T., Murakami, H., Sakai, S. and Haginiwa, J., (1985) *Tetrahedron Letters*, **26**,(43), 5299.

79. Aimi, N., Murakami, H., Tsuyuki, T., Nishiyama, T. , Sakai, S. and Haginiwa, J., (1986) *Chem. Pharm. Bull.* **34**(7), 3064.

80. Aimi, N., Tsuyuki, T., Murakami, H., Seki, H., Nishiyama, T., Haginiwa, J., Sajai, S., (1986) Tennen Yuki Kagobutsu Toronkai Koen Yoshishu 28th, 12-136.

81. Phillipson, J. D., Hemingway, S. R. and Ridsdale, C. E., (1982) *J. Nat. Prod.* **45**, 145.

82. Hemingway, S. R. and Phillipson, J. D., (1980) "Indole and Biogenetically Related Alkaloids" ed. by J. D. Philipson and M. H. Zenk, Academic Press, London , p.63.

83. Stuart, K. L. and Woo-Ming, R. B., (1974) *Tetrahedron Letters*, 3853.

84. McLean S. and Murray, D. G., (1970) *Can. J. Chem.*, **48**, 867.

85. Adeoye, A. O. and Waigh, R. D., (1983) *Phytochem.* **22**, 2097.

86. Rahman, A. and Basha, (1983) "Biosynthesis of Indole Alkaloids, Clarendon Press, Oxford, p.156 and the references cited therein.

87. Aimi, N., Nishimura, M., Miwa, A., Hoshino, H., Sakai, S. and Haginiwa, J. (1989) *Tetrahedron Letters* , **37**,4991.

88. Cai, J. C. and Hutchinson, C. R., "The Alkaloid XXI" (A. Brossi ed.), Academic Press, N. Y., p.101.

89. Carte, B. K., DeBrosse, C., Eggleston, D., Hemling, M., Mentzer, M., Poehland, B., Troupe, N., Westlay, W., and Hecht, S. M., (1990) *Tetrahedron*, **46**, 2747.

90. Aimi, N., Hoshimo, H., Nishimura, M., Sakai, S. and Haginiwa, J. (1990) *Tetrahedron Letters,* **3**, (36), 5169.

91. Yaegashi, T., Sawada, S., Okigima, S., Miyasaka, S., Mutai, M., Furuta, T. and Yokokura, T., (1989) Japan Kokai Tokyo Koho

92. Weiss, G., Koreeda, M. and Nakanishi, K., (1973) *JCS Chem. Comm.*, 565.

93. Welti, D. H., (1985) *Magnetic Resonance in Chemistry* **23**(10), 872.

94. Crouch, R. C. and Martin, G. E., (1991) *Journal of Magnetic Resonance*, **92**, 189.

95. Hermansson, K., Kenne, L. Rukunga, G. M. and Samuleson, G., (1990) *Phytochemi.* **29**(2), 513.

96 Pretsch, E., Seibl J., Simon, W and Clerc, T., Tables of Spectral Data for Structures Determination of Organic Compounds. Second Edition, Springer Verlag Berlin, 1989, p. C210.

97. Levesque, J. Pousset, J. L. and Cave, A., (1975) *C. R. Acad. Sci. Paris* C, **280**, 593.

98. Bax A., Freeman, R. and Morris, G. A., (1981) *J. Magn. Reson.*, **42**, 164.

99. Bodenhausen, G., Freeman, R., Niedenmeyer, R. and Turner, D. L., (1977) *J. Magn. Reson.*, **26**, 133-164.

100. Piatini, U., Sorensen, O. W., and Ernst, R.R., (1982) *J. Amer. Chem. Soc.*,**104**, 6800.

101. Rance, M., Sorensen, O. W., Bodenhausen, G. Wagner, G., Ernst, R. R. and Wuthrich, K., (1983) *Biochem. Biophys. Res. Comm.*,**117**, 479.

102. Wagner, G., (1983). *J. Magn. Res.*, **55**, 151.

103. Eich, G., Bodenhausen G., R. R. Ernst, (1982) *J. Am. Chem. Soc.*, **104**, 3731.

104. Bax, A. and Davis, D. G., (1985) *J. Magn. Reson..*, **65**, 355.

105. States, D. J., Haberkorm, R. A. and Ruber, D. J., (1982) *J. Magn. Reson..*,**48**, 286.

106. Levesque, J., Jacquesy, R. and Foucher, J. P., (1982) *Tetrahedron*, 38, 1417.

107. Bothner-By, A. A., Stephens, R. L., Lee, J. M. Warren C. D.,and Jeanloz, R. W. (1984) *J. Amer. Chem. Soc..*, **106**, 811.

108. Dietrich, W., Rudel, C. H. and Neumann, M., (1991) *J. Magn. Reson..*, **91**, 1.

109. Neuhaus, D. and Williamson, M., The Nuclear Overhauser Effect In Structural and Conformational Analysis, VCH Publisher, Inc., U. K. 1989.

110. Le Men, J., (1964), *Lloydia*, 463.

111. Morita, H., Ichihara, Y., Takeya, K., Watanabe, K., Itokawa, H. and Motidome, M., (1989), *Planta Medica*, **55**, 288.

112. Coune C. and Angenot L., (1978), *Planta Medica*, **34**, 53.

113. Leclerq, J. and Angenot L., (1984), *Planta Medica* , **50**, 457.

114. Stockigt, J., (1979) *Phytochem.*, **18**, 965.

115. De Bruyn, A., Zhang, W. and Budinsky, M., (1989), *Magnetic Resonance in Chemistry*, **27**, 935.

116. Crabb, T. A., (1978) Accounts of Nuclear Magnetic Resonance of Alkaloids, Vol. 8 in: Annual Reports on NMR Spectroscopy.

117. BLackstown, W. P., Brown, R. T., Lee, K. G., (1971), *JCS Chem. Comm.*, 910.

118. Blackstown W. P., Brown, R. T., Chapple, C. L. and Frase, S. B., (1972) *JCS Chem. Comm..*,1006.

119. Ho, B. T., McIsaac, W. M., Walker, K. E. and Estevez, V., (1968), *J. of Pharm. Sciences*, **57**(2),269.

120. Craig, J. C. and Purushothaman, K. K. (1970), *J. Org. Chem.*, **35** (5), 1721.

121. Bodalski, R. and Katrizky, A. R., (1968), *Phys. Org. J. Chem. Soc. (B)*, 831.

122. Traynelis, U. J. and Martello, R. F., (1958), *J. Amer. Chem. Soc.*, **80**, 6590.

123. Shamma, M. and Slusarchyk, W. A., (1963) *Chemical Reviews,* **63**, 59.

124. Manske, R. H. F. and Holmes, H. L. eds., (1954), The Alkaloids, Vol IV, Academic Press, New York.

125. Shamma, M., (1972) The Isoquinoline Alkaloids: Chemistry and Pharmacology, Academic Press, N. Y., p.194.

126. Pelletier, S. W., (1970) The Chemistry of Alkaloids, Van Nostrand Reinhold Company, N. Y., p.42.

127. Robinson, R. and Sugasawa, S., (1932), *J. Chem. Society,* London, p.789.

128. Brochmann-Hanssen, E., Fu, C. C. and Misconi, L. Y., (1971), *J. Pharm. Sci.,* **60**, 1880.

129. Barton, D. H. R., Bhakuni, D. S., Chapman, G. M. and Kirby, G. W., (1966), *Chem. Communication*, p.259: *J. Chem. Soc (C)* 1967, p. 2134.

130. Shamma, M. and Salgar, S. S., (1974), in The Alkaloids (Specialist Periodical Reports, J. E. Saxton (ed.) The Chemical Society, Burlington House, London, p.197.

131. Goldberg, L. I., Somneville, P. F. and McNay, J. L., (1968), *J. Pharmacol. Exp. Ther.,* **163**, 188.

132. Barnett, A. and Fiove, J. W., (1971) ,*Eur. J. Pharmcol.,* **14**, 206.

133. Manske, R. H. F. (ed), (1973), The Alkaloids, Vol XIV, Academic Press, N. Y., p.226.

134. Taylor, W. I., (1961), *Tetrahedron*, **14**, 42.

135. Hooker, J. D., "The Flora of British India", Vol. 1, L. Reeve, London, p.39.

136. Pallares, E. S. and Garza, H. M., (1948), *Archives Biochem.,* **16**, 275.

137. Kametani, T., Terasawa, H., Ihara, M, and Iriarte, J., (1975), *Phytochem.*, **14**, 1884.

138. Talapatra S. K., Mukhopadhyay, S. K., Talapatra, B., (1977), *J. Indian Chem. Soc.*, **54**, 790.

139. Plantinet, C., Sevenet, T., Chan, K. C. and Bruneton J., (1985), *Ann. Pharmaceutiques Francaise* , **43**(2), 189.

140. Hoffmann, J. J., Torrance S. T., Wiedhopf, R. M. and Cole, J. R., (1977), *J. of Pharm. Sci.*, **66**, (6), 883.

141. Economic Botany, **18**, 270 (from Williaman, J. J. and Hui-Lin Li, Alkaloid-Bearing Plants and their Contained Alkaloids).

142. Merill, E. D., An Enumeration of Philippine Flowering Plants. Bureau of Printing, Manila, 1926.

143. Briggs, L. H., Colebrook, L. D., Fales, H. M. and Wildman, W. C., (1957), *Analytical Chemistry*, **29**, (6), 904.

144. Buchanan, M. A. and Dickey, E.E., (1960), *J. Org. Chem,* **25**,1389.

145. Williams, D. H. and Fleming I., Spectroscopic Methods in Organic Chemistry (4th Edition), McGraw-Hill Publishing, New York.

146. La Planche, L. A. and Rogers, M. T., (1963) *J. Amer. Chem. Soc.*, **85**, 3728.

147. Achenbach, H., Renner, C. and Addae-Mensah, I., (1982), *Liebigs Ann. Chem.*,1623.

148. Santos, A. C., (1930), *Philippine J. Sci.*, **43**, 561.

149. Fraenkel, G., Cava, M. P. and Dalton, D. R., (1967), *J. Amer. Chem. Soc.*, **89**, 329.

150. Schmultz, J., (1959), *Helv. Chim. Acta*, **42**, 335.

151. De Padua, L., Lugod, G. and Pancho, J., Handbook on Philippine Medicinal Plants, Vol 2. (Documentation and Information

Section, Office of the Director Research, University of the Philippines, Los Banos, 1978) .

152. Ozaki, Y., Sekita, S., Setsuko, S. and Masatoki, H. (1989) *Chem. Pharm. Bull.*, **37**, (10), 2799.

153. Aimi, N., Hoshino, H., Nishimura, M., Sakai, S. and Haginiwa, J., (1990),*Tetrahedron Letters* , **31**, (36), 5169.

154. Crews, P. and Kho-Wiseman, E., (1978), *Tetrahedron Letters,* No. 28, 2483.

155. Pousset, J. and Poisson, J., (1969),*Tetrahedron Letters,* No.15, 1173.

156. Galbraith, M. N. and Horn, D. H. S., (1972), *J.C.S. Chemical Communications.*,113.

157. Galbraith, M. N. and Horn, D. H. S., (1973), *J.C.S. Chemical Communications*, 566.

158. Weiss, G., Koreeda, M. and Nakanishi, K., (1973), *J.C.S. Chemical Communications*, 565.

159. Aimi, N., Hoshino, H., Nishimura M., Sakai, S., Haginiwa, J., (1990), *Tetrahedron Letter,* **31**(36), 5269.

160. Farnsworth, N. R., Pilewski, N. A. and Draus, F. J., (1962), *Lloydia (Journal of Natural Product),* **25**, 312.

161. Willis, J. C., 'A Dictionary of the Flowering Plants and Ferns' 8th edn, University Press, Cambridge, 1973.

162. Stone, B. C., (1976), *Phil. J. Biol*, **5**, 1.

163. Burkill, I. H., A Dictionary of the Economic Products of the Malay Peninsula, Ministry of Agriculture and Cooperatives, K. L., (1966).

164. Wu, L., Tan, J., Chen., H., Xie, C, and Pu, Q., (1987), *Zhongcaoyao,* **18**(9), 391.

165. Macleod, A. J. and Pieris, N. M., (1982), *Phytochem.*, **21**, 1653.

166. Jadot, J., Casimir, J. and Loffet, A., (1967), *Biochimica Et Biophysica Acta* ,**136**, 79.

167. Arthur Bell, E., Meier, L. K. and Sorensen, H., (1981), *Phytochem,.* **20**(9), 2213.

168. Buttery, R. G., Juliano, B. O. and Ling, L. C., (1983), *Chem. & Ind.*, 478.

169. Amarasingham, R. D., Bisset, N. G., Millard, A. A. and Woods, M. C., (1968), *Econom. Bot.*, **18**, 270.

170. Aguinaldo, A. M., Claustro, A. L., Recio, B. V., Cadelina, N. B. and Guevara, B. Q., (1984), *Acta Manilana*, **23**, 39.

171. Virtanen A. I. and Hietala, P. K., (1955), *Acta Chem. Scand.*, **9**, 175.

172. Fowden, L. and Steward, F. C., (1957), *Ann. Botany N. S.*, **21**, 53.

173. Hatanaka, S., (1962), *Acta Chem. Scand.*, **16**, 513.

174. Fowden, L., (1970), Progress in Phytochemistry (Reinhold, L. and Liwschitz, Y., eds), Vol.2, p.203. John Wiley, New York.

175. Meier, L. K. and Sorensen, H., (1979), *Phytochem.*, **18**, 1173.

176. Meier, L. K., Olsen, O. and Sorensen, H., (1979), *Phytochem.*, **18**, 505.

177. Olsen, O. and Sorensen, H., (1980), *Phytochem.*, **19**, 1712.

178 Bryne, L. T., Guevara, B. Q., Patalinghug, W. C., Recio, B. V., Ualat, C. R. and White, A. H., "The X-ray Crystal Structure of (+)-Pandamarine, the Major Alkaloid of *Pandanus amaryllifolius*", Unpublished Report.

179. Summers, M. F., Marzilli, L. G. and Baz, A., (1986), *J. Amer. Chem. Soc.*, **108**, 4285.

180. Fenn, J. B., Mann, M., Meng, C. K., Wong, S. F., Whitehouse, C. M., (1990), *Mass Spectrometry Reviews*, **9**, 37.

181. Zeisberg, R. and Bohlman, F., (1974), *Chem. Ber.*, **107**, 3800.

182. Virtanen, A. I. and Berg, A. M., (1955) *Acta Chem. Scand.*, **9**, 553.

183. Steward, F. C., Wetmore, R. H. and Pollard, J. K., (1955), *Am. J. Botany*, **42**, 946.

184. Grobbelaar, N., Pollard, J. K. and Steward, F. C., (1955), *Nature*, **175**, 703.

185. Jadot, J., Casimir, J, and Loffet, A., (1967), *Biochim. Biophys. Acta*, **136**, 79.

186. Larsen, P.O. and Kjaer, A., (1960) ,*Biochim. Biophys. Acta*, **38**, 148.

187. Alderweireldt, F., Jadot, J., Casimir, J. and Loffet, A., (1967), *Biochim. Biophys. Acta* ,**136**, 89.

188. Blake, J., and Fowden L., (1964), *Biochem. J.*, **92**, 136.

189. Nulu, J. R. and Bell, E. A., (1972), *Phytochem.*, **11**, 2573.

190. Dardene, G. A., Bell, E. A., Nulu, J. R. and Cone, C., (1972), *Phytochem.*, **11**, 791.

191. Peterson, P. J. and Fowden, L., (1972), *Phytochem.*, **11**, 663.

192. Hesse, M., Alkaloid Chemistry, John Wiley and Sons, New York 1978, p.46,49.

193. Herbert, R. B., Jackson, F. B. and Nicolson, I. T., (1976), *JCS Chem. Comm.*, 865.

194. Herbert, R. B., Jackson, F. B. and Nicolson, I. T., (1984), *J. Chem. Soc. Perkin Trans. I*, 825.

195. Mulchandani, N. B., Iyer, S. S. and Bhadeka, L. P., (1971), *Phytochem.*, **10**, 1047.

196. Mulchandani, N. B., Iyer, S. S. and Bhadeka, L. P., (1969), *Phytochem.*, **8**, 1931

197. Harris, C. M., Schneider, M. J. Ungemach, F. S., Hill, J. E. and Harris, T. M., (1988), *J. Amer. Chem. Soc.*, **110**(3), 940.

198. Gourley, J. M., Heacock, R. H., McInnes, A. G., Nikolin, B. and Smith D. G., (1969), *Chem. Comm.*, 709.

199. Ikhiri, K., Koulodo, D. D. D., Garba, M., Mamane, S., Ahond, A., Poupat, C. and Potier, P., (1987), *J. Natural Prod.*, **50**, 152.

200. Dawidar, A. M. Winternitz, F. and Johns, S. R., (1977), *Tetrahedron*, **33**, 1733.

201. Liu, Z., Lu, R. and Xu, F., (1987), *Acta Chim. Sinica (Huaxue Xuebao)* , **45**, 514.

202. Cannon. J. R. and Guevara, B. Q. (1988) *Acta Manilana* **37**, 51.

203. Govindachari, T. R., Sidhaye, A. R. and Viswanathan, N., (1970), *Tetrahedron*, **26**, 3829.

204. Iida, H., Watanabe, Y. and Kibayashi, C., (1983), *Chem. Lett.*, **8**,1195.

205. Liu, Z., Ren-rong, L., Qi, C. and Hai, H., (1985), *Acta Chimica Sinica*, No.**3**, 262.

206. Cragg, J. E., Hedges, S. H. and Herbert, R. B., (1981), *Tetrahedron Letter* , **22**(22), 2127.

207. Hedges, S. H. and Herbert R. B., (1979), *J. Chem. Research (S)*, **1**,410.

208. Claustro, A. L. and Guevara, B. Q. (1978) *Acta Manilana* **17**(27), 16.

209. Clarke, E. G C. and Hawkins, A. E., (1961), Forensic Science Society Journal (Great Britain), 1: 120.

210. Herbert, R. B., The Biosynthesis of Secondary Metabolites, 2nd Ed., Chapman & Hall, London, 1981.

211. Barber, J. Garson, M. J. and Staunton J., (1981), *J. Chem. Soc. Perkin Trans I.*, 2584.

212. Kessler, H., Griesinger, C., Kerssebaum, R., Wagner, K. and Ernst., R. R., (1987), J. Am. Chem. Soc., **109**, 607.

213. Elmer, A. D. E., Leaflet of Philippine Botany, Vol 4, Manila, Philippines, 1912.

214. Buchanan, M. A. and Dickey, E. E., (1960), *J. Org. Chem.*, **25**, 1389.

215. Casagrande, C. and Merotti, G., (1970), *Farmaco, Ed. Sci.*, **25**, 799.

216. Johns, S. R., Lamberton, J. A. and Sioumis, A. A., (1968), *Aust. J. Chem.*, **21**, 1383.

217. Patt, S.I. and Schoolery, N., (1982), *J. Magn. Reson.*, **46**, 535 .

218. Rabenstein, D. and Nakashima, T., (1979) *Anal. Chem.*, **51**, 1465/A .

219. Lecocq, C. and Lellem, J., (1981), *J. Chem. Soc. Chem. Comm.*, 150.

PUBLICATIONS

1. Nonato, M. G., Garson, M. J., Truscott, R. J. W. and Carver, J. A. "^{1}H-NMR Assignments of Anonaine and Xylopine Derivatives from *Talauma gitingensis*" *J. Nat. Prod.* **53**(6), 1623 (1990).
2. Nonato, M. G., Garson, M. J., and Truscott, R. J. W. "Blumenol A from *Graptophyllum pictum*" *ACGC Chemical Research Communications*, in press.

CONFERENCES/SEMINARS

1. 11th National Conference RACI Organic Chemistry Division, 3-7 July 1989, James Cook University, Townsville. Poster presented: "The Natural Product Chemistry of Philippine Flowering Plants".
2. University of Wollongong Second Research Student Open Day, August 1989. Poster presented: "The Natural Product Chemistry of Philippine Flowering Plants".
3. University of Wollongong Third Research Student Open Day, August 1990. Poster presented: "Blumenol A from *Graptophyllum Pictum*".
4. RACI One-Day Organic Chemistry Symposium- NSW Branch, November 27, 1990, University of Wollongong. Presented a paper entitled, "Alkaloids of *Ophiorrhiza acuminata*".
5. 12th National Conference RACI Organic Chemistry Division, 9-13 July 1991, University of Queensland, Brisbane. Poster Presented: "Alkaloids from a Philippine Medicinal Plant *Ophiorrhiza acuminata*".

6. University of Wollongong Fourth Research Student Open Day, August 1991. Poster Presented: "Alkaloids from a Philippine Medicinal Plant *Ophiorrhiza acuminata*".